UNIVERSITE MONTPELLIER I - UFR de MEDECINE

THESE

Pour l'obtention du grade de

DOCTEUR

Ecole doctorale : Sciences Chimiques et Biologiques pour la Santé (CBS2)

Discipline : Physiologie Cardiovasculaire

Présentée par :

Lucas ANDRE

LE 17 Décembre 2010

Couplage excitation-métabolisme-contraction dans le cœur sain et insuffisant : mécanismes physiopathologiques, influence d'une pollution atmosphérique et stratégies préventives

Thèse dirigée par : Dr Sylvain Richard

Co-dirigée par : Dr Olivier CAZORLA

Jury :

Parini Angelo, MD, PhD, Professeur de Physiologie (Inserm U858-Toulouse)

Rochette Luc, PhD, Professeur de Physiologie (EA 2979-Dijon)

Mercier Jacques, MD, PhD, Professeur de Médecine (ERI25- Montpellier)

Obert Philippe, PhD, Professeur de Physiologie (EA4278-Avignon)

Cazorla Olivier, PhD, Chargé de Recherche (Inserm U637-Montpellier)

Richard Sylvain, PhD, Directeur de Recherche (Inserm U637-Montpellier)

Remerciements

Liste des abréviations

Introduction Générale.....p 1

Introduction.....p 3

I. Le Myocarde.....p 3

1. Anatomo-physiologie
2. Cycle cardiaque
3. Biomécanique cardiaque
4. Automatisme cardiaque
5. Electrocardiogramme
6. Circulation coronaire
7. Métabolisme cardiaque

II. Le Cardiomyocyte.....p 12

1. Architecture intracellulaire
    - 1.1. Généralités
    - 1.2. Sarcolemme
    - 1.3. Réticulum sarcoplasmique
    - 1.4. Système contractile
2. Couplage excitation-contraction
    - 2.1. Excitation
    - 2.2. Contraction
        - 2.2.1. Régulation par la longueur : loi de Frank-Starling
        - 2.2.2. Régulation neurohormonale
    - 2.3. Relaxation
3. Couplage excitation-métabolisme-contraction
4. Homéostasie redox
    - 4.1.Production d'espèces oxygénées réactives
    - 4.2. Systèmes antioxydants
    - 4.3. Rôle des ROS et concept de stress oxydant
5. Régionalisation des propriétés cardiaques cellulaires

III. L'insuffisance cardiaque.....p 28

1. Contexte épidémio-économique
2. Physiopathologie
    a. Remodelage électrophysiologique

2.2. Remodelage de l'homéostasie calcique
2.3. Remodelage des propriétés de la machinerie contractile
2.4. Remodelage métabolique et dysfonction mitochondriale

IV. Pollution atmosphérique au monoxyde de carbone.....p 35
1. Sources de CO
2. Epidémiologie des effets de la pollution au CO sur le système cardiovasculaire
3. Propriétés physico-chimiques du CO

V. Stratégies préventives.....p 38
1. Exercice physique
2. Thérapies antioxydantes

VI. Objectifs de thèse.....p 40

Matériels et méthodes.....p 41

I. Populations.....p 41

II. Insuffisance cardiaque ischémique.....p 41

III. Exposition à un stress environnemental : Pollution atmosphérique au monoxyde de carbone.....p 42

IV. Stratégies préventives et thérapeutiques.....p 43
1. Exercice physique
2. Traitement pharmacologique antioxydant : Supplémentation en N-acetylcystéine

V. Etudes in vivo sur cœur entier.....p 44
1. Evaluation des propriétés morphologiques et fonctionnelles par échocardiographie
2. Mesure de l'activité électrocardiographique

VI. Etudes *in-vitro* sur cardiomyocytes isolés.....p 45
1. Isolement cellulaire
2. Mesure de la signalisation calcique intracellulaire et de la variation de longueur des sarcomères
3. Mesure des Sparks calciques
4. Mesure de la charge en Ca^{2+} du RS
5. Mesure de l'homéostasie en NADH cellulaire
6. Mesure de la production de ROS mitochondriale

7. Evaluation des propriétés contractiles des myofilaments
8. Solutions

VII. Etudes biochimiques.....p 53
1. Analye des protéines du métabolisme mitochondriale
2. Analyse des protéines de la signalisation calcique (RyR2, Serca, PLB, FKBP12.6)
3. Analyse des protéines contractiles (TnI, MLC2, MHC)
4. Mesure de l'activité enzymatique de la PKA

VIII. Statistiques.....p 57

Résultats.....p 58

1ère partie : Altérations du Couplage excitation-métabolisme-contraction dans l'IC ischémique : mécanismes physiopathologiques et stratégies préventives

I. Implication des ROS dans l'arythmogénicité de l'insuffisance cardiaque ischémique : rôle de la voie PKA et effet d'un traitement chronique antioxydant.....p 58
1. Introduction
2. Article 1
3. Conclusion

II. Altération mitochondriale et dysfonction contractile dans l'insuffisance cardiaque ischémique : implication de la voie PKA.....p 59
1. Introduction
2. Article 2
3. Conclusion

III. Prévention du phénotype arythmique dans l'insuffisance cardiaque ischémique par l'exercice physique à travers une amélioration du métabolisme mitochondriale L'exercice

physique réduit les phénomènes arythmiques dans l'IC ischémique : rôle de la mitochondrie.....p 62
1. Introduction
2. Article 3
3. Conclusion

Conclusion Partie I.....p 63

2ème partie : Effet d'une pollution au monoxyde de carbone sur le couplage excitation-métabolisme-contraction de populations saines et insuffisantes cardiaques

III. Effet d'une pollution au monoxyde de carbone sur la fonction cardiaque globale et cellulaire.....p 65
1. Introduction
2. Article 4
3. Conclusion

IV. Effet d'une pollution au monoxyde de carbone sur la susceptibilité cardiaque à l'ischémie-reperfusion.....p 66
1. Introduction
2. Article 5
3. Conclusion

V. Implication des ROS dans le phénotype arythmique consécutif à une exposition chronique au monoxyde de carbone....p 67
1. Introduction
2. Article 6
3. Conclusion

VI. Effet d'une pollution au monoxyde de carbone dans l'insuffisance cardiaque ischémique et prévention des effets délétères par l'exercice physique.....p 70
1. Introduction
2. Article 7
3. Conclusion

Conclusion Partie II.....p 71

Conclusion générale.....p 73

Annexes.....p 75

Bibliographie.....p 76

Coup de cœur

Le cœur a ses raisons que la raison ne connait point… Ce doctorat est le fruit d'un long travail où raison et connaissance ont grandi sous l'impulsion de différentes personnes auxquelles je voudrais adresser, de tout cœur, ma très grande reconnaissance :

A Sylvain Richard avec qui la science devient un art,

> En m'accueillant à l'U637, tu m'as permis de découvrir et d'apprécier un univers nouveau et plutôt chouette. Trouve ici ma sincère reconnaissance pour m'avoir donné tous les moyens nécessaires à la réalisation de ce projet, m'avoir conseillé pour son orientation, et pour m'avoir soutenu jusqu'à son éclosion.

A Olivier Cazorla et tous ses postulats,

> Tu m'as formé et encadré pendant toutes ces années. Reçois ici l'expression de ma sincère reconnaissance pour ta disponibilité, ta pédagogie, et tes précieux conseils qui m'ont permis d'apprendre sur la science et sur moi-même.

A Alain Lacampagne et sa culture scientifique de la gagne,

A Jérémy Fauconnier et ses chants déjantés,

A Cyril Reboul qui sait rendre la science cool,

A Philippe Obert, et sa structuration scientifique exemplaire

A Greg Meyer et Julien Boissière, et leur rigueur légendaire

A Fares Gouzi qui concilie culture et science avec frénésie

A l' ERI25 / INSERM U637 et toutes ses vedettes,

> Particulièrement à Patrice, Jérôme, Valérie, Romain, Ludo, Maurice, Gilou, Christine, Guillermo, Younss et Santiago. A travers vos individualités, vous avez contribué à la réalisation de ce projet.

A l'INRA UMR866 et Christine Feillet-Coudray pour leur amabilité

A ma famille, et son soutien de folie !

A mes amis, toujours au top et pleins de vie !

A la coloc' parisienne et la ferveur au 56 cours de Vincennes

Au sport, un état d'esprit, des valeurs d'abord !

Aux voyages, qui apprennent au moins autant que l'avancée en âge

Aux soirées à Montpellier et leurs rythmes endiablés

A la musique, aux rythmes folkloriques, éclectiques et dynamiques

A Snežana

Poljubime u oko dragićino

« L'imagination est plus importante que le savoir »

Albert Einstein

Liste des abréviations

ADP	Adenosine diphosphate
ATP	Adenosine triphosphate
Ca^{2+}	Calcium
Cat	Catalase
CEC	Couplage excitation-contraction
CICR	Ca^{2+}-induced Ca^{2+} release
FKBP12.6	FK506 Binding Protein
GPx	Glutathion peroxydase
H_2O_2	Peroxyde d'hydrogène
HbCO	Carboxyhémoglobine
HO_2	Radical perhydroxyle
IC	Insuffisance cardiaque
MLC-2	Chaine légère de myosine type 2
NAC	N-acetylcystein
NCX	Echangeur Na^+/Ca^{2+}
NOS	Nitrogen oxygen species
$O2^{-}$	Radical Superoxyde
$ONOO^-$	Péroxynitrite
CO	Monoxyde de carbone
DHPR	Récepteurs à la Dihydropyridine
ECG	Electrocardiogramme
EMC	Excitation-métabolisme-contraction
ENDO	Couche sous-endocardique
EPI	Couche sous-épicardique
FFT	Transformée rapide de Fourrier
Pi	Phosphate inorganique
PKA	Protéine Kinase A
PLB	Phospholamban
PMI	Post myocardial infarcted
RO	Radical alkoxyle
RO_2	Radical peroxyle
ROS	Reactive Oxygen Species
RS	Réticulum sarcoplasmique
RyR	Récepteurs à la Ryanodine
SERCA	Sarco/endoplasmic reticulum Ca^{2+}-ATPase
SOD	Superoxyde dismutase
TnC	Troponine C
TnI	Troponine I

Les maladies cardio-vasculaires représentent la première cause de mortalité dans le monde. L'OMS estime à 17,1 millions le nombre de décès imputables aux maladies cardio-vasculaires, soit 29% de la mortalité mondiale totale [1]. Plus de 82% des décès ont lieu dans des pays à revenu moyen ou faible. D'ici à 2030, près de 23,6 millions de personnes mourront d'une maladie cardio-vasculaire (cardiopathie ou accidents vasculaires cérébraux principalement). En France, ces pathologies représentent la deuxième cause de mortalité après les cancers, à l'origine de 180 000 décès par an (soit 32% des décès, tous âges confondus). Le développement de l'arsenal thérapeutique au cours des dernières années a permis d'améliorer la qualité de vie et le pronostic vital des patients atteints de cardiopathie. D'autre part, les progrès thérapeutiques ont permis de freiner la progression de la maladie, mais surtout de mieux prévenir le risque cardiovasculaire et par conséquent de réduire la survenue d'accidents cardiovasculaires. D'après les projections épidémiologiques, les maladies cardiovasculaires, notamment d'origine ischémique, devraient néanmoins rester les premières causes mondiales de décès, le taux de progression le plus important devant toucher la région de la méditerranée orientale ; l'Asie du Sud-Est devrait compter le plus grand nombre de décès.

Cet état des lieux épidémiologique illustre donc des insuffisances concernant à la fois la prévention, mais également la prise en charge du risque cardiovasculaire. Une meilleure compréhension des mécanismes physiopathologiques, ainsi qu'une amélioration de la détection des facteurs de risque cardiovasculaire permettraient une optimisation des traitements cardiovasculaires.

Dans ce contexte, la première partie de ce travail de thèse s'est intéressée à la compréhension des mécanismes physiopathologiques de l'IC ischémique, pathologie cardiovasculaire la plus fréquente, à travers l'exploration des processi cellulaires assurant la cohérence fonctionnelle cardiaque. L'activité du myocarde, assurant l'irrigation sanguine des différents territoires tissulaires et organiques, repose sur un couplage spatio-temporel des activités électriques, métaboliques et mécaniques cardiaques. Ce couplage excitation-métabolisme-contraction, caractérisé par une adaptation des activités électriques et métaboliques en fonction de la demande mécanique en condition physiologique, est particulièrement sensible à l'ischémie myocardique. En effet, suite à un accident ischémique cardiaque, une profonde détérioration des activités électriques, métaboliques et mécaniques cellulaires a été mise en évidence de manière isolée pour chacune des trois composantes. Ces

altérations retentissent à l'échelle de l'organe et sont responsables d'une défaillance cardiaque globale et chronique au long cours. Cet état d'IC se caractérise par l'incapacité du cœur à assurer le débit sanguin nécessaire à l'irrigation des différents territoires. **La première partie de ce travail de thèse repose sur une investigation des relations entre activités électriques, métaboliques et mécaniques dans le cœur sain et le cœur insuffisant cardiaque afin d'envisager des stratégies préventives améliorant le pronostic vital et les caractéristiques morpho-fonctionnelles cardiaques au décours d'un infarctus.**

Les pathologies cardiovasculaires sont multifactorielles. Différents facteurs de risque permettant de prédire le risque de survenue d'un accident cardiovasculaire ont été identifiés : l'âge, le sexe et les antécédents familiaux sont les facteurs non modifiables ; le tabagisme, l'hypertension artérielle, le diabète, l'hypercholestérolémie, la sédentarité et l'obésité sont les facteurs pouvant être la cible de modifications. Les facteurs environnementaux, bien que non considérés dans l'évaluation du risque cardiovasculaire à l'heure actuelle, ont été, ces dernières années, l'objet d'attentions particulières. Le myocarde est en effet une structure particulièrement sensible à ces facteurs, notamment la pollution atmosphérique : de nombreuses études épidémiologiques rapportent des corrélations entre variation de la qualité de l'air ambiant et accidents cardiovasculaires. Parmi les agents polluants, le monoxyde de carbone (CO) semble être impliqué de façon majeure dans les dysfonctions cardiaques consécutives aux épisodes de pollution atmosphérique. **La seconde partie de ce travail de thèse s'est alors intéressée à l'étude du remodelage du couplage excitation-métabolisme-contraction dans un contexte de pollution au monoxyde de carbone dans le cœur sain, ainsi qu'aux répercussions d'une telle exposition sur le myocarde soumis à un accident ischémique, afin de déterminer si la pollution atmosphérique peut être considérée comme un facteur de risque cardiovasculaire potentiel.**

Ce travail de thèse vise donc à améliorer la compréhension du fonctionnement cardiaque en conditions normale et pathologique, ainsi que dans un contexte de pollution atmosphérique au CO, *via* l'étude de la plasticité du couplage excitation-métabolisme-contraction ; afin d'améliorer la prophylaxie du risque cardiovasculaire global.

Introduction

I. Le myocarde

1. Anatomo-physiologie

Le cœur est le moteur principal et le point de départ de la circulation sanguine. Son rôle est d'assurer l'hémodynamique, c'est à dire la pression nécessaire à la circulation du sang afin d'approvisionner continuellement les muscles en oxygène et en nutriments pour la production d'énergie. Le myocarde est un muscle strié semblable aux muscles squelettiques. Le myocarde est enfermé dans un sac fibreux (le péricarde) rempli d'un liquide aqueux qui sert de lubrifiant aux mouvements du cœur. Ce sac fibreux porte le nom de péricarde. La face interne du cœur est tapissée d'une mince couche de cellules conjonctives: l'endocarde.
Situé dans la cavité thoracique, le cœur humain est divisé longitudinalement en deux moitiés ; chacune étant constituée de deux cavités différentes : les oreillettes et les ventricules. On distingue alors le cœur droit du cœur gauche, séparés l'un de l'autre par une cloison parfaitement étanche : le septum interventriculaire.

Les cavités de l'oreillette et du ventricule de chaque moitié du cœur communiquent entre elles, étant simplement séparées l'une de l'autre par les valvules auriculo-ventriculaire. Ces valvules permettent au sang de circuler de l'oreillette vers le ventricule (sens antérograde) et évitent tout reflux rétrograde. La valvule du cœur droit est appelée tricuspide (trois valves), et celle du cœur gauche mitrale ou bicuspide (deux valves). Ces valves sont amarrées aux parois ventriculaires par des cordages tendineux portés par de puissantes excroissances pariétales, les piliers du cœur ou muscles papillaires. Lorsque le sang circule de l'oreillette vers le ventricule, les valvules s'abaissent sous l'effet de la charge du sang de part et d'autre des valvules. A l'inverse, lorsque les ventricules se contractent, les valvules se ferment sous l'effet de l'augmentation de la pression du sang dans les ventricules, interdisant ainsi au sang de refluer dans les oreillettes. Le mouvement mécanique des valvules est strictement passif et ne dépend que de la différence de pression entre les oreillettes et les ventricules.

Ainsi, à partir du cœur droit, le sang est éjecté dans l'artère pulmonaire qui remonte directement aux poumons et, à partir du cœur gauche, dans l'aorte qui distribue le sang à tous les organes. L'ouverture des deux ventricules sur l'artère pulmonaire et sur l'aorte est aussi protégée par les valvules pulmonaire et aortique qui empêchent le reflux du sang dans les

ventricules au cours de la phase de repos des ventricules. A l'entrée des oreillettes, il n'existe pas de valvule car la contraction des oreillettes comprime les veines à leur point de pénétration dans celles-ci.

Environ 70% du sang arrivant dans les oreillettes passe directement dans les ventricules avant qu'elles ne se contractent. La contraction simultanée des oreillettes chasse le reste du sang dans les ventricules sous jacents. Presque immédiatement après la contraction auriculaire, les ventricules se contractent et éjectent le sang dans le circuit artériel.

2. Cycle cardiaque

L'activité cardiaque est cyclique puisque chaque partie du myocarde est successivement en activité puis au repos. On parle d'alternance systole / diastole. Le cycle cardiaque débute par la systole auriculaire (droite et gauche) permettant le remplissage des ventricules. Le remplissage ventriculaire est réalisé en fait en deux phases : une première de remplissage passif au cours de laquelle le sang provenant des oreillettes passe directement dans les ventricules ; et une phase de remplissage actif où la contraction simultanée des oreillettes chasse le reste du sang dans les ventricules sous jacents. La relaxation des ventricules facilite cette étape agissant comme une pompe aspirante. Après fermeture des valves auriculo-ventriculaires, la systole ventriculaire permet l'éjection du sang dans le système pulmonaire et systémique de façon simultanée. Ensuite, les valves sigmoïdes se referment, le ventricule se relâche : c'est la diastole. La répétition successive de ces phases de systole et diastole s'intègre au sein d'une biomécanique particulière.

3. Biomécanique cardiaque

L'efficacité contractile cardiaque repose sur une architecture complexe et hétérogène au sein de la paroi ventriculaire gauche. En effet, un gradient transmural de contraction assure un débit cardiaque optimal. Ce gradient repose sur la disparité qui existe entre la paroi interne sous-endocardique (ENDO) et la paroi externe sous-épicardique (EPI): l'orientation des fibres est de -60° dans l'EPI et atteint +60° dans l'ENDO [2]. Cette architecture hétérogène confère au myocarde une activité contractile différentielle dans le temps et dans l'espace. En effet, l'éjection du sang dans les conduits aortique et pulmonaire est assurée par la contraction

successive de différentes zones cardiaques : la contraction des couches internes sous-endocardiques précède celle des couches externes sous-épicardiques.

Cet enchaînement spatio-temporel entraine un mouvement de torsion du myocarde de la base vers l'apex, à l'origine de l'efficacité contractile cardiaque. Cette biomécanique cardiaque résulte d'une propagation ordonnée et progressive de l'activité électrique, elle-même orchestrée par un automatisme cardiaque.

4. L'automatisme cardiaque

Le cœur a la particularité d'être un organe myogénique, c'est-à-dire qu'il génère lui-même l'influx électrique nécessaire à son activité globale. La succession des évènements et le synchronisme cœur droit/cœur gauche sont assurés par la distribution anatomique de cellules myocardiques particulières : les cellules du tissu nodal (ou de Keith et Flack), situées dans la paroi postérieure de l'oreillette droite, et les cellules du nœud auriculo-ventriculaire, dans la partie supérieure de la cloison interventriculaire. Ces cellules sont dénuées d'activité mécanique contractile mais, produisent spontanément, à intervalles réguliers, un signal électrique qui stimule les cellules voisines. L'automaticité et la rythmicité normale du cœur sont imposées par le nœud sinusal car la fréquence des dépolarisations spontanées des cellules composant le sinus est plus élevée que celle du nœud-auriculo ventriculaire. Ce tissu nodal joue le rôle d'un pacemaker, véritable chef d'orchestre de l'activité électrique cardiaque. L'onde se propage simultanément dans les deux oreillettes et permet leur contraction en bloc. Elle atteint ensuite le nœud auriculo-ventriculaire, seul point conducteur situé entre les oreillettes et les ventricules. L'onde dépolarisante est alors transmise, avec un court temps de latence, au niveau des ventricules *via* le faisceau de His. Il se subdivise en deux branches, dans chaque ventricule, qui se ramifient en un réseau de Purkinje sous-endocardique. La contraction ventriculaire se produit ainsi quelques fractions de seconde après celles des oreillettes, compte tenu du temps de propagation de l'onde de dépolarisation. La conduction rapide assurée par ces fibres spécialisées, ainsi que leur distribution étendue, entraînent une dépolarisation plus ou moins simultanée de toutes les cellules ventriculaires droites et gauches ; ce qui assure une contraction unique et coordonnée.

La fréquence de contraction cardiaque est sous la dépendance de la fréquence de dépolarisation du nœud sinusal, véritable chef d'orchestre du cœur qui possède une capacité de dépolarisation autonome puisque les cellules nodales ne présentent pas de potentiel de repos stable. La membrane se dépolarise lentement jusqu'à un certain seuil à partir duquel se

déclenche un nouveau potentiel d'action (PA), conduit par le faisceau de His et les fibres de Purkinje aux différents territoires ventriculaires, afin de transmettre la dépolarisation et entraîner la contraction des différentes zones cardiaques dans un ordre hiérarchisé et intangible.

La cohérence de l'activité électrique cardiaque repose sur l'existence d'une période réfractaire, c'est-à-dire une durée consécutive à la dépolarisation cardiaque pendant laquelle aucune stimulation additionnelle ne peut avoir lieu, contrairement au muscle squelettique qui est capable de présenter le phénomène de sommation des contractions jusqu'à l'obtention d'une tétanisation. Dans le muscle cardiaque, la période réfractaire absolue est presque aussi longue que la contraction ce qui interdit toute autre sommation avant la fin de la première. Ce phénomène évite alors une tétanie cardiaque qui empêcherait le remplissage et donc l'activité de pompe cardiaque.

5. Electrocardiogramme

L'électrocardiogramme (ECG) est l'enregistrement, au cours du temps, des fluctuations de potentiel de l'ensemble des tissus cardiaques successivement en activité. L'asynchronisme de la stimulation des différentes parties (oreillettes puis ventricules), les différences de masse des parois et les directions variables des voies de conduction et de la propagation de l'activation (de l'endocarde vers l'épicarde) se somment ; ce qui confère à l'ECG un tracé en trois phases (Figure 1).

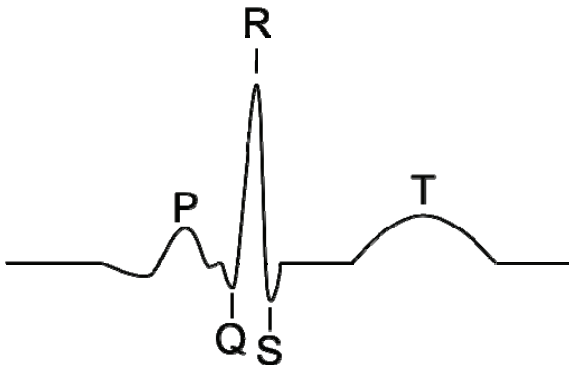

Figure 1 : Ondes P, Q, R, S et T observées sur un tracé ECG normal

La première, l'onde P, traduit l'activation auriculaire, rapidement suivie (<200 ms selon la fréquence cardiaque) par un complexe d'ondes dites rapides, étiquetées Q, R, et S, témoin de

l'activation des ventricules. Enfin, une onde lente, l'onde T, qui traduit la repolarisation ventriculaire.

6. Troubles du rythme cardiaques

Les arythmies sont des troubles du rythme cardiaque naturel visibles par des anomalies du tracé ECG. Les arythmies prennent la forme d'une accélération (tachycardie) ou d'un ralentissement (bradycardie) de la fréquence de repos (60 à100 battements par minute) ; ou encore de l'addition ou de la suppression de battements, par rapport au tracé physiologique régulier. Une arythmie peut être «supraventriculaire», si le dysfonctionnement provient de l'oreillette ou «ventriculaire».

Certaines arythmies n'ont que peu de signification au plan médical. Les arythmies les plus fréquentes, ou extrasystoles, qui affectent surtout les personnes âgées sont généralement bénignes. La caféine et le stress peuvent augmenter la fréquence des extrasystoles. Certaines personnes peuvent présenter, occasionnellement, des battements surnuméraires, ou palpitations, qui ne nécessiteront pas de traitement. D'autres arythmies (par exemple dans le cas de fibrillation ventriculaire) peuvent être rapidement fatales si elles ne sont pas traitées immédiatement. Certaines arythmies sont cliniquement significatives, mais sont traitées chirurgicalement ou par l'implantation d'un pacemaker artificiel.

La survenue d'épisodes arythmiques en période de récupération après un test d'effort a été cliniquement rapportée comme étant un prédicteur fort du risque de décès cardiovasculaire à moyen terme [3]. Ainsi, toute apparition d'un phénotype arythmique chez une personne à priori saine doit alerter le cardiologue et l'inciter à procéder à une recherche exhaustive des différents facteurs cardiovasculaires afin d'adapter une stratégie préventive optimale.

7. Circulation coronaire

Le cœur ne reçoit pas directement son irrigation des cavités cardiaques, mais il possède son propre système circulatoire : la circulation coronaire. Comme il n'existe aucun réseau circulatoire entre les chambres cardiaques et le tissu musculaire cardiaque, l'apport en nutriments se fait par les artères coronaires droites et gauches qui prennent naissance à la base de l'aorte juste au-dessus des valvules aortiques [4]. A cet endroit, le sang est déjà oxygéné. Ces artères épousent la surface du cœur et se divisent rapidement en un réseau capillaire dense dans tout le myocarde. Une fois les échanges effectués, le sang quitte le ventricule droit par

les veines cardiaques antérieures qui aboutissent à l'oreillette droite et, le ventricule gauche par le sinus coronarien. L'extraction en oxygène par le myocarde à partir du réseau artériel est plus importante que celle du muscle squelettique. Cependant, lors d'un stress, le myocarde ne peut au mieux que quadrupler le débit coronaire ; contrairement au muscle squelettique qui peut multiplier son débit par 30. Cette moindre augmentation de l'approvisionnement en O_2 explique la sensibilité accrue du cœur aux perturbations de l'irrigation coronaire.

8. Métabolisme du myocarde

Le myocarde a besoin d'une grande quantité d'adénosine triphosphate (ATP) par jour afin d'assurer son activité, alors que son stock intrinsèque (~10 mM) ne lui permet que quelques contactions. D'autre part, le myocyte doit pouvoir changer instantanément son métabolisme, en fonction des apports réglés par l'alimentation, l'exercice ou les conditions physiopathologiques [5]. Différentes voies métaboliques sont alors sollicitées pour répondre aux besoins énergétiques. Le cœur est parfois décrit comme un « omnivore métabolique » capable de produire de l'énergie à partir d'une grande variété de substrats. Le myocarde fonctionne uniquement en aérobiose en utilisant 5 sources d'énergie:

- les acides gras représentant 60% à 65% de l'énergie
- le glucose représentant 15 % à 20%
- le lactate représentant l0% à 15%: après transformation en pyruvate, le lactate entre dans le cycle de Krebs:
- les corps cétoniques
- les acides aminés

La glycolyse ou voie d'Embden-Meyerhof-Parnas est la principale voie métabolique d'utilisation des hexoses, notamment du glucose. Elle se déroule dans le cytoplasme de la cellule. Le passage du glucose (6 atomes de carbone) vers 2 pyruvates (3 atomes de carbone) se fait au décours d'une succession de 10 réactions biochimiques. L'énergie libérée par ce processus est utilisée pour former de l'ATP.

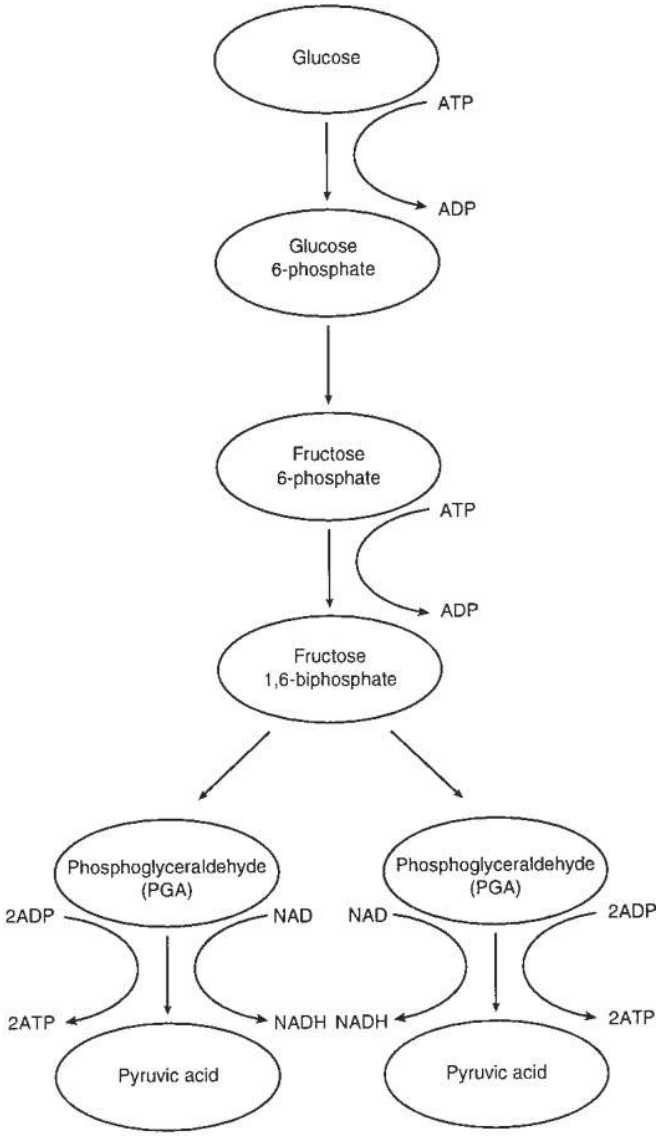

Figure 2 : Cascade de réactions composant la glycolyse. Adapté de [6]

La première partie de la glycolyse consiste en une activation du glucose qui utilise 2 ATP. On parle de phase préparatoire. Dans une deuxième partie, une production d'ATP a lieu, remboursant ainsi la dette liée à la phase d'activation et produisant de nouveaux ATP. On parle de phase productrice d'énergie.

Les lipides sont dégradés sous forme d'acides gras qui vont alors subir le processus de β-oxydation. La première étape a lieu dans le cytoplasme, au niveau de la membrane externe mitochondriale où est située l'acylCoA synthétase, enzyme permettant la formation de acylcoenzyme A. Cet AcylCoA pénètre alors dans la mitochondrie où il est déshydrogéné par l'acylCoA déshydrogénase puis hydraté pour former du β-hydroxyacylCoA. Le β-

hydroxyacylCoA est à son tour déhydrogéné puis hydraté ; ce qui conduit à la formation d'acétylCoA qui sera utilisé par le cycle de Krebs, et d'acylCoA qui pourra subir à nouveau la β-oxydation. L'AcetylCoA est donc au centre d'un carrefour métabolique puisqu'il est le produit commun des premières étapes de dégradation des glucides et lipides. La dégradation de l'acétylCoA est assurée par les enzymes du cycle de Krebs.

Point de convergence de plusieurs réactions du catabolisme cellulaire, le cycle de Krebs correspond à une série de réactions biochimiques dont la finalité est de produire des intermédiaires énergétiques qui serviront à la production d'ATP dans la chaîne respiratoire (Figure 2). Il s'agit d'un cycle car le dernier métabolite, l'acide oxaloacétique, est aussi impliqué dans la première réaction. Le cycle peut se résumer à l'oxydation de 2 carbones en CO_2 ; l'énergie dégagée par ces réactions génère de l'ATP, des électrons, du NADH, et du FADH, qui pourront être métabolisés par la chaine respiratoire pour former de l'ATP. Il se déroule dans la matrice de la mitochondrie.

La citrate synthase, première enzyme du cycle, permet d'initier le cycle de réaction à travers la transformation de l'acétylCoA en citrate (figure 2).

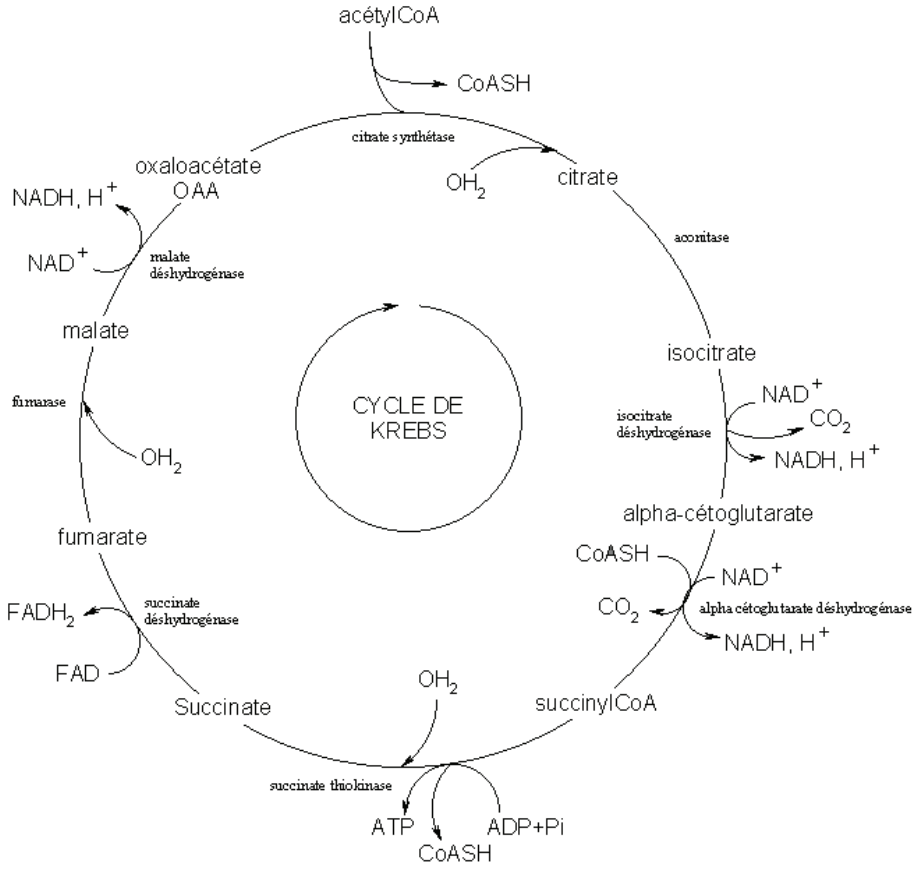

Figure 2 : Cycle de Krebs D'après [7]

La chaine respiratoire est la voie finale d'oxydation des substrats énergétiques. Les molécules de NADH produites par la β-oxydation ainsi que par le cycle de krebs sont oxydées par le complexe I de la chaine respiratoire. Elle est constituée d'un ensemble complexe de protéines membranaires de la mitochondrie qui servent à réoxyder les coenzymes NADH et ubiquinone (CoQ) qui ont été réduits en particulier au cours du cycle de Krebs. Cette réoxydation s'accompagne de la création d'un gradient transmembranaire de protons. Ce gradient est une forme de stockage de l'énergie contenue dans les coenzymes, qui dérive elle-même de l'énergie contenue dans les molécules dégradées au cours du catabolisme. Le gradient de proton va servir à fabriquer de l'ATP, molécule énergétique universellement utilisable, au niveau de l'ATP synthase, une protéine membranaire mitochondriale.
Le gradient électrochimique de protons, de part et d'autre de la membrane mitochondriale interne, est créé par l'expulsion de protons vers l'espace intermembranaire. Cette expulsion est couplée au transfert des électrons dans les complexes I, III et IV. L'utilisation de ce gradient par l'ATP synthétase (complexe V) pour la phosphorylation des molécules d'ADP en ATP assure le couplage de la chaine des oxydoréductions à la production d'ATP. L'ATP est ensuite transportée vers l'espace intermembranaire par le translocateur des nucléotides adényliques, puis vers le cytosol par le *voltage dependent anion chanel* (canal anionique voltage-dépendant). L'ATP peut être également immédiatement utilisée dans l'espace intermembranaire par la créatine kinase qui synthétise la créatine phosphate, forme chimique de stockage et de transfert d'énergie.

Ce qui conditionne la résistance du cœur à l'agression, ce n'est pas sa capacité à disposer d'un stock d'ATP, mais son aptitude à maintenir fonctionnelles les voies métaboliques permettant de faire face à toute évolution de la demande. En condition physiologique, les sources principales d'énergie proviennent de la β-oxydation des acides gras, du glucose et du lactate. Le rapport entre la consommation d'oxygène et la synthèse d'ATP dépend du substrat utilisé : la quantité d'oxygène consommé pour produire une molécule d'ATP sera supérieure avec les acides gras qu'avec le glucose. Le myocarde a la propriété particulière de multiplier sa consommation d'oxygène par un facteur de 3 à 5, en fonction du travail, sans variation notable des concentrations des composés riches en énergie (ATP et phosphocréatine). Cela implique une régulation complexe reposant sur des mécanismes cellulaires complexes (Chapitre II.3.). La caractéristique essentielle de la régulation du métabolisme cardiaque est la relation stricte qui existe entre le travail cardiaque

et la consommation en oxygène, montrant par là qu'il existe un lien entre la production d'ADP par les ATPases et la synthèse d'ATP par la mitochondrie.

Même au repos, le cœur est un grand consommateur d'oxygène et extrait environ 70 à 80% de l'oxygène de la circulation coronaire. Contrairement aux muscles squelettiques qui peuvent assurer leur métabolisme en anaérobiose, le cœur s'en remet presque exclusivement au métabolisme aérobie. Pour cela, les cellules cardiaques présentent une concentration élevée de mitochondries, et sont donc bien équipées pour utiliser le catabolisme des lipides mais aussi du glucose et de l'acide lactique produit lors de la glycolyse anaérobie par le tissu musculaire.

II. Le cardiomyocyte

1. Architecture intracellulaire

1.1. Généralités

L'ultrastructure cardiaque est un système complexe résultant de l'association intégrée et coordonnée de différents types cellulaires : les fibroblastes qui forment le tissu conjonctif, les cellules endothéliales tapissant l'endocarde et les coronaires, les cellules musculaires lisses (artères et veines), les terminaisons nerveuses du système sympathique et parasympathique, et les cellules contractiles excitables : les cardiomyocytes. Ces derniers représentent prés de 75% du volume total de l'organe. Ce sont des cellules musculaires striées caractérisées en microscopie optique par une alternance de bandes claires (bandes I : isotropes) et sombres (bandes A : anisotropes). Cette striation est le reflet d'un assemblage particulier et dense de protéines contractiles organisées en sarcomère. Cette disposition est à l'origine de l'activité mécanique de l'organe.

La morphologie du cardiomyocyte est cylindrique et atteint en moyenne 10 à 25 µm de diamètre et 100 µm de long. Au sein du myocarde, les cardiomyocytes sont solidement et étroitement liés entre eux par des jonctions adhérentes (*tight junction*) et communicantes (*gap junction*). Ces jonctions permettent le couplage mécanique, électrique et chimique intercellulaire, et donc la synchronicité de l'activité cardiaque : on parle de *syncitium* cardiaque.

L'organisation architecturelle intracellulaire repose sur l'agencement de différents organites, entourés d'une double couche lipidique : la membrane plasmique du cardiomyocyte ou sarcolemme.

1.2. Sarcolemme

Le sarcolemme est une bicouche phospholipidique amphipatique, composée principalement de lipides, de protéines et de glucides. Cette structure constitue un maillage intercellulaire, qui permet la cohésion intracardiaque au cours des fortes contraintes exercées lors d'un cycle cardiaque. L'une des fonctions essentielles du sarcolemme est de maintenir, contrôler et réguler l'homéostasie calcique intracellulaire. La présence d'un réseau d'invaginations membranaires transversales, ou système tubulaire transverse (tubules T), permet la conduction de l'influx électrique vers le centre de la cellule. Localisé au milieu des bandes I (stries Z définies ci-après), il représente entre 30 et 50 % de la surface membranaire des cardiomyocytes ventriculaires [8]. L'accolement étroit des tubules T avec le RS fonctionnel (diades) constitue le lieu privilégié d'échange entre les milieux intra et extracellulaires, ce qui est accentué par la présence de nombreuses protéines membranaires (récepteurs, canaux ioniques, pompes, échangeurs…).

1.3. Réticulum sarcoplasmique

Le réticulum sarcoplasmique (RS), forme spécialisée du réticulum endoplasmique, est le pivot de la régulation des mouvements de Ca^{2+} intracellulaire. Ce réseau de tubes étanches a pour fonction principale le stockage du Ca^{2+} intracellulaire, par le biais de la calséquestrine. Cette réserve de Ca^{2+} joue un rôle dynamique fondamental dans la régulation de l'homéostasie calcique et dans le couplage excitation-métabolisme contraction. La membrane du RS est tapissée de protéines régulant les flux de Ca^{2+} : les récepteurs à la ryanodine cardiaque (RyR-2) permettent la libération de Ca^{2+} du réticulum, tandis que les protéines Serca cardiaques (Serca-2a) recaptent le Ca^{2+} qui a été libéré.

1.4. Système contractile

Le système contractile occupe environ 60 % du volume de la cellule [9]. L'unité contractile de la cellule musculaire est le sarcomère. Il est caractérisé par une striation

résultant de l'alternance de bandes I et A. Chaque bande I est traversée en son milieu par une ligne sombre appelée strie Z (pour *Zwischensheibe*). La bande A, quant à elle, est traversée par une bande plus claire, la bande H (pour *Hensen*), elle-même divisée en son centre par la ligne M (pour *Mittlemembran*) plus sombre. La zone délimitée par deux stries Z, soit deux hémi-bandes I encadrant une bande A, forme l'unité élémentaire de la contraction : le sarcomère. Ce jeu d'ombre et de lumière, caractérisant les cellules musculaires striées, est la conséquence de l'interpénétration de filaments protéiques fins et épais formant les myofibrilles [10].

Le filament épais est constitué de 300 à 400 molécules de myosine qui s'assemblent selon le grand axe du filament. Chaque molécule de myosine est un hexamère formé de 2 chaînes lourdes (MHC pour *Myosin Heavy Chain*) associées à 4 chaînes légères (MLC pour *Myosin Light Chain*). Il existe 2 types de chaînes légères : la MLC-1 (chaîne légère essentielle) et la MLC-2 (chaîne légère régulatrice). L'extrémité C-terminale des MHC s'enroule en hélice α et forme la queue de la myosine. Elle est reliée en sous-fragment flexible (S2) à la tête globulaire formée par la partie N-terminale (sous-fragment S1) associée aux 4 chaînes légères (2 par tête). Chaque tête possède un site de fixation à l'actine et une activité [10].

Les filaments fins, rattachés au niveau des lignes Z par des protéines du cytosquelette, sont constitués de :

- L'actine : macromolécule double brin d'actine filamenteuse (polymère d'actine globulaire ou actine-G, 42 kD). Elle doit son nom à sa capacité d'activer les Mg-ATPases des têtes de myosine lui faisant face. Il existe plusieurs isoformes d'actine : α-sarcomériques, β et γ.
- La tropomyosine (Tm) : protéine filamenteuse, formée d'homo ou hétérodimère de sous-unité α et β. L'expression de ces deux isoformes dépend de l'espèce (α prédominant chez les rongeurs et β chez les gros mammifères) ainsi que du territoire cardiaque considéré (oreillette ou ventricule).
- La troponine (Tn): protéine constituée de 3 sous-unités : (i) la TnI dite inhibitrice, fixée à l'actine ; (ii) la TnC qui possède 3 sites de fixation d'affinité variable pour le Ca^{2+}, (iii) la TnT qui fixe la Tm. En absence de Ca^{2+}, la TnI inhibe l'effet activateur de l'actine sur l'activité ATPasique de la myosine, en masquant le site d'association de l'actine et de la myosine.

- La tropomoduline : protéine jouant un rôle dans le développement et la croissance à travers l'assemblage de monomère d'actine [11]. En présence de l'actine-F, elle se fixe à la tropomyosine.

Enfin, la titine constitue le troisième système de myofilament du muscle strié [12]. Elle représente prés de 10% de la masse des myofibrilles. Au sein du sarcomère ; elle peut être subdivisée en deux parties distinctes : une zone dite extensible, du fait de son interaction avec les filaments fins et épais, au niveau de la strie Z et de la bande A, et une zone dite extensible dans la bande I. Cette dernière, relativement libre, possède trois segments principaux : un segment PEVK riche en proline (P), glutamate (E), valine (V) et lysine (K) ; un segment formé d'une succession de type d'immunoglobuline encadrant le segment PEVK [13], et un troisième segment composé de séquences unique N2A et/ou N2B [14]. La titine a un rôle primordial dans la rigidité cellulaire ; elle est également majoritairement responsable de la force dite passive (force développée durant le remplissage, au cours de la diastole). Cette force, proportionnelle au niveau d'étirement, est la conséquence directe de l'allongement de la zone dite extensible. La titine agit comme un élastique moléculaire qui, outre son rôle dans la rigidité cellulaire, limite le degré d'extension des cellules lors de la diastole, permet le retour à la longueur de repos des cellules en fin de systole, et maintient le centrage des filaments au cours de la contraction [14].

2. Couplage excitation-contraction

La contraction du myocarde résulte de la contraction coordonnée de chacune des cellules du muscle cardiaque. A l'échelle cellulaire, l'activité contractile est régie par le couplage excitation-contraction. Ce couplage regroupe l'ensemble des processi assurant la transformation du stimulus électrique (potentiel d'action) en un signal intracellulaire qui engendre la contraction de la cellule. Il inclut l'ensemble des événements se produisant entre la dépolarisation membranaire (genèse du potentiel d'action) et la contraction cellulaire. On peut y distinguer trois phases:

- L'excitation qui correspond à la dépolarisation membranaire
- La contraction
- La relaxation qui est le retour de la cellule musculaire à l'état de *repos physiologique*.

2.1. Excitation

Le stimulus princeps du couplage excitation-contraction cardiaque est une dépolarisation transitoire de la membrane cellulaire des myocytes, qui traduit l'activation coordonnée de courants ioniques entrants et sortants qui se superposent de manière complexe au cours du temps. Ce processus d'excitation résulte de la genèse spontanée d'un potentiel d'action par les cellules du nœud sino-atrial : l'ouverture de canaux sodiques (Na^+) voltage – dépendants augmente la perméabilité membranaire au Na^+ entrainant une entrée de Na^+ dans le sens de son gradient électrochimique, générant alors une dépolarisation rapide.

L'arrivée du potentiel d'action sur le sarcolemme provoque l'ouverture de canaux calciques voltage-dépendants de type L (appelés aussi canaux à la dihydropyridine, DHPR, en raison de leur affinité pour cette molécule) permettant l'entrée d'un courant entrant $I_{Ca,L}$. Ces canaux sont couplés aux récepteurs à la ryanodine (RyR) situés en vis à vis sur la membrane du RS, réservoir en Ca^{2+} de la cellule musculaire (Figure 2). L'isoforme de RyR cardiaque (RyR-2) possède une extrémité N-terminale cytoplasmique sur laquelle viennent interagir de nombreuses protéines régulatrices. Ainsi viennent se fixer sur la portion cytosolique de chaque sous-unité : la FKBP12.6 (*FK506 Binding Protein*) ; la sous-unité catalytique et régulatrice de la PKA, la mAKAP ; la phosphatase 1 (PP1) et la phosphatase 2A (PP2A) (Marx SO, 2000). Le FKBP12.6 stabilise le RyR2, favorisant ainsi des cycles ouverture/fermeture du canal synchronisé [15].

Il existe un couplage ionique entre DHPR et RyR2, de telle sorte que les ions Ca^{2+} entrant via DHPR (courant $I_{Ca,L}$) se fixent sur les RyR2, provoquant leur ouverture synchronisée et, ainsi, la libération massive du Ca^{2+} contenu dans le RS [15]. Ce mécanisme de « Calcium Induced Calcium Release » (CICR) traduisant cette libération transitoire de Ca^{2+} par le RS en réponse à une activation des canaux à la ryanodine via I_{CaL} (Figure 2), représente l'élément moteur du CEC et fournit la quantité calcique suffisante pour la contraction [15].

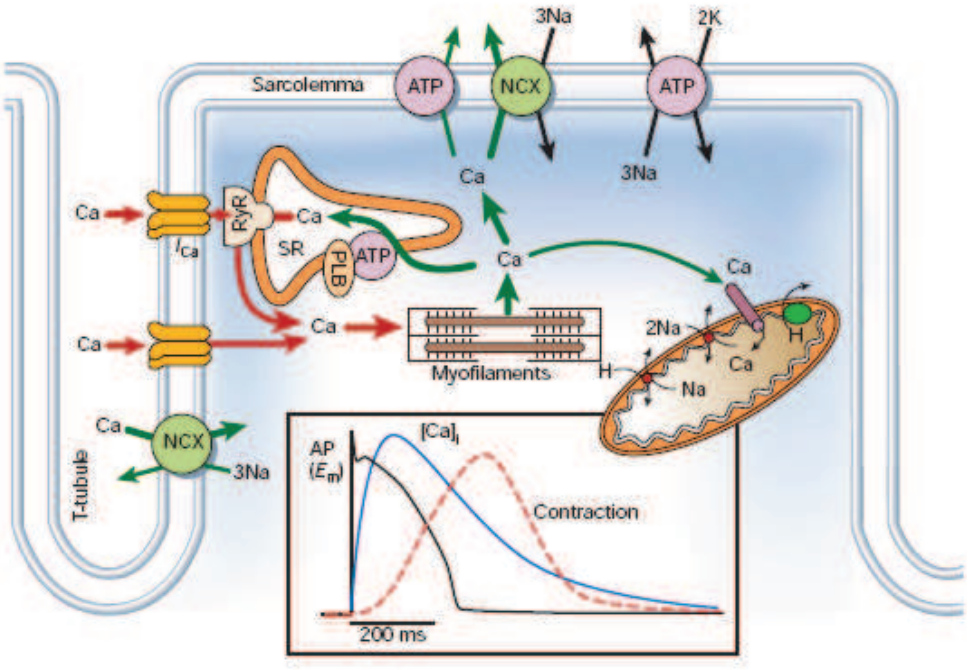

Figure 3 : Couplage excitation-contraction. D'après [15]

Le transitoire calcique est alors la résultante de la somme des évènements unitaires locaux de libération du Ca^{2+} au niveau de la dyade ou jonction entre membrane sarcolemmale, tubules T et RS. Ce signal calcique transitoire dépend des propriétés du signal électrique le précédant, ainsi que de l'organisation structurale intracellulaire, notamment la stœchiométrie DHPR/RyR-2(Bers, Nature, 2002).

2.2. Contraction

La contraction cellulaire est assimilée à un développement de force résultant d'un raccourcissement cellulaire (diminution de la longueur des sarcomères).

Le mécanisme moléculaire de la contraction est unanimement expliqué par la théorie des filaments glissants. Ce glissement des filaments d'actine sur les filaments de myosine résulte de la formation de ponts actomyosine (interaction entre les têtes globulaires de myosine et actine) dans la zone de recouvrement des filaments fins et épais. Cette interaction active l'ATPase de la myosine et, l'énergie libérée par l'hydrolyse de l'ATP est rapidement convertie en énergie mécanique permettant le pivotement de la tête de myosine capable d'exercer une traction sur les filaments fins. La force développée par le myocarde est donc directement proportionnelle au niveau de recouvrement des filaments fins et épais ainsi qu'au nombre de ponts actomyosine formés.

Les ponts actomyosine oscillent entre deux états (faiblement ou fortement attachés) en fonction de la fixation de l'ATP, de son hydrolyse et de la libération de phosphate inorganique (Pi). On distingue ainsi des ponts d'actomyosine faibles (ne produisant pas de force) caractérisés par une oscillation rapide entre les états attaché et détaché. On distingue également des ponts forts, responsables de la force produite, et caractérisés par une fréquence d'oscillation lente entre les états attaché et détaché (l'état attaché prédomine). Le passage d'un pont faible à un pont fort se fait lors de la libération de Pi. Lorsqu'une nouvelle molécule d'ATP se lie à la myosine, une dissociation myosine / actine s'opère et un nouveau cycle peut démarrer.

La nature des isoformes des différentes protéines contractiles et régulatrices et leur état de phosphorylation, ainsi que la force unitaire développée par un pont ou les cinétiques de transition d'un état à l'autre, vont ainsi influencer la production de force et/ou les cinétiques de contraction/ relaxation [16].

La contraction du cardiomycoyte est initiée par la libération massive de Ca^{2+} intracellulaire qui induit un changement conformationnel du complexe troponine / tropomyosine [17]. En effet, lorsque la concentration en Ca^{2+} libre intracellulaire est faible (10^{-7} M), la TnC ne lie pas le Ca^{2+}. Dans cette configuration, la TnI se lie au complexe actine-tropomyosine (Tm) et inhibe les interactions fortes entre l'actine et la myosine. Lorsque la concentration en Ca^{2+} atteint la micromole, le Ca^{2+} se fixe sur le site II de la partie N-terminale de la troponine C (TnC), à l'origine d'une cascade de changements conformationnels nécessaires et suffisants pour permettre la formation des ponts forts et la génération de la force. Le changement de conformation de la TnC affaiblit l'interaction entre la TnI et l'actine-Tm et renforce les interactions TnI-TnC mais aussi TnC-TnT. Cette cascade démasque le site de fixation de la myosine sur l'actine sur lequel peut venir se fixer le sous-fragment S de la myosine. La force développée par un cardiomyocyte est donc en partie corrélée à la concentration en Ca^{2+} libre dans le voisinage des myofilaments. Cette corrélation suit une relation sigmoïdale décrite par une équation de Hill. Cela signifie que la fixation de Ca^{2+} sur la TnC répond à un principe de coopérativité : plus il y a de ponts formés, plus la TnC est affine pour le Ca^{2+}, et donc plus de ponts se forment [18]. La force maximale est atteinte lorsque le maximum de ponts actomyosine est formé. Cependant, il est estimé qu'uniquement 25% des ponts actomyosine génèrent une force à chaque battement cardiaque. Il existe donc une réserve importante de ponts pouvant être utilisés ou recrutés en fonction des besoins.

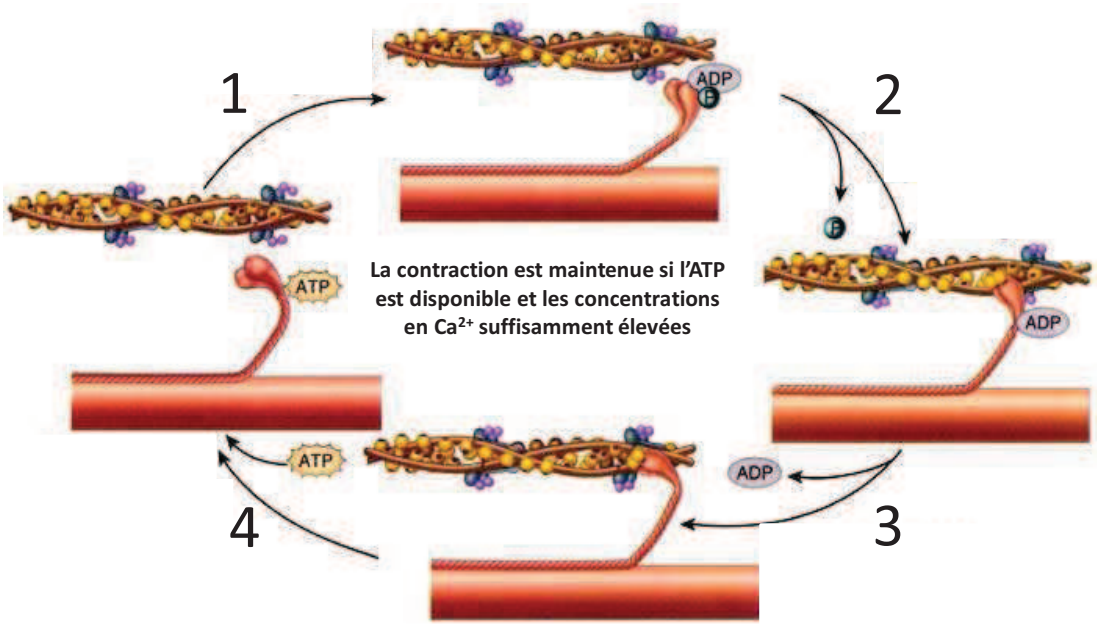

Figure 4 : Interactions actine/myosine au cours d'un cycle cardiaque D'après [19]

La figure 4 représente les différentes positions et réactions successives de la myosine au cours d'une contraction. L'étape 1 caractérise la position initiale retrouvée suite à l'hydrolyse de l'ATP. L'étape 2 correspond au relargage du phosphate inorganique (Pi) qui augmente l'affinité de la myosine pour l'actine, induisant ainsi la formation d'un pont fort. Lors de l'étape 3, le relargage de l'ADP induit un mouvement de la tête de myosine d'environ100 Å. Enfin, lors de l'étape 4, l'occupation du site catalytique par l'ATP induit une baisse de l'affinité des têtes de myosine aux filaments d'actine induisant ainsi leur détachement et il retrouve ainsi leur position initiale (étape 1)

La force de contraction cardiaque est régulée soit de manière « externe » *via* le système neurohormonal, soit de manière « intrinsèque » en fonction des variations de volume au cours du remplissage des ventricules.

2.2.1. Régulation par la longueur : loi de Frank-Starling

Lors de la diastole, le remplissage sanguin entraine une déformation des parois ventriculaires, permettant d'emmagasiner de l'énergie élastique. Cette déformation (stress pariétal) est transmise aux myofibrilles et modifie leurs propriétés contractiles. La puissance mécanique ventriculaire est alors directement modulée par le volume télédiastolique : plus le

remplissage cardiaque est important, notamment en raison d'un retour veineux accru, plus l'énergie élastique emmagasinée dans le mur ventriculaire sera forte, plus la force active développée par chaque cellule sera importante et, par conséquent, plus la force contractile du battement cardiaque suivant sera importante. Cette relation pression / volume, ou loi de Frank-Starling, est une propriété intrinsèque du myocarde que l'on retrouve au niveau cellulaire à travers la relation tension-longueur. La courbe tension-longueur cardiaque résulte d'une sensibilisation au Ca^{2+} de myofilaments induite par l'étirement. Cette sensibilisation au Ca^{2+} est sous-tendue par différents mécanismes soumis à controverse. D'une part, l'augmentation de l'affinité Ca^{2+}/TnC permet de faciliter le nombre de ponts actine/myosine. D'autre part, une régulation *via* l'espacement interfilamentaire permet module le nombre de ponts forts qui peuvent se former : au cours d'un étirement, le volume de la cellule cardiaque reste constant ; par conséquent, l'allongement de la cellule suivant son axe longitudinal (allongement des sarcomères) est associé à une diminution de son épaisseur et de sa largeur. Cette réduction de la section de la cellule comprime les myofilaments, diminuant ainsi l'espace séparant la myosine de son site de fixation sur l'actine. Suite à un étirement, le rapprochement des filaments fins et épais augmente la probabilité de formation des ponts d'actomyosine. Cependant, ce mécanisme de régulation interfilamentaire reste très controversé [20]. La titine et son action sur la tension passive participerait également à la régulation de la sensibilisation au Ca2+ des myofilaments induite par l'étirement. Enfin, l'état de phosphorylation des protéines myofilamentaires, notamment de la TnI et de la MLC-2, participe à la modulation de la loi de Frank-Starling à l'échelle cellulaire [21].

2.2.2. Régulation neurohormonale

Le système nerveux n'intervient pas dans la genèse de l'activité électrique cardiaque, mais il régule cependant la contraction myocardique. Ainsi, la stimulation des nerfs sympathiques entraine la dépolarisation du nœud sinusal, et augmente la fréquence cardiaque. Les nerfs sympathiques, à l'origine de libération de catécholamines, se distribuent non seulement au niveau du nœud sinusal, mais aussi à toutes les cellules du cœur. Cette libération de catécholamines exerce un effet positif sur l'intensité (effet inotrope) et la fréquence (effet chronotrope) de contraction, ainsi que sur la vitesse de relaxation (effet lusitrope). La stimulation des nerfs parasympathiques produit l'effet inverse aux nerfs sympathiques. Le seuil du potentiel d'action est atteint plus lentement et la fréquence cardiaque diminue. Les fibres inhibitrices circulent dans le nerf vague dont les corps cellulaires sont situés dans le

centre cardio-inhibiteur du tronc cérébral. Les nerfs sympathiques agissent par libération d'acétylcholine. A l'état de repos, l'influence parasympathique est dominante et la fréquence cardiaque chez un sujet normal est largement inférieure à 100 pulsations minutes. Ce système est qualifié de frein vagal.

Les neurones sympathiques et parasympathiques se terminent sur le nœud sinusal et sur le nœud auriculo-ventriculaire ce qui rend la totalité du myocarde sous la dépendance d'un des deux systèmes. Ainsi, l'activité intégrée et coordonnée des deux systèmes permet la régulation de l'inotropisme (force développée par le myocarde), du bathotropisme (excitabilité), du chronotropisme (fréquence de dépolarisation) et du lusitropisme (relaxation) cardiaque.

2.3. La relaxation

La relaxation correspond au retour du sarcomère à sa longueur initiale. La diminution rapide de la concentration en Ca^{2+} permet la relaxation du myocyte. La recapture du Ca^{2+} dans le RS s'effectue par des pompes calciques appelées SERCA (sarco/endoplasmic reticulum Ca^{2+}-ATPase). Elles assurent le transport actif de Ca^{2+} vers la lumière du RS à raison de deux ions Ca^{2+} par molécule d'ATP hydrolysée. Le gène Serca-2, exprimé dans le cœur, donne naissance à trois isoformes : Serca-2a, 2b et 2c. Cependant, dans le cardiomyocyte, Serca-2a est la principale forme exprimée. L'activité Serca-2a est régulée par la phosphorylation d'une protéine associée, le phospholamban (PLB). Le PLB est un homopentamère qui, lorsqu'il est déphosphorylé, se lie au domaine cytoplasmique et inhibe l'activité de l'ATPase.
La seconde voie permettant l'élimination du Ca^{2+} cytosolique implique l'échangeur Na^{+} / Ca^{2+} (NCX). La stœchiométrie de NCX (3 ions Na^{+} pour 1 ion Ca^{2+}) lui confère un caractère électrogène qui contribue activement aux variations de potentiel membranaire.

Selon l'espèce, 80 à 90% du Ca^{2+} systolique est recaptuéé dans le RS par les Serca-2a. Les 10 à 20% restants sont extrudés de la cellule, majoritairement par le NCX. Ainsi Serca-2a contrôle la relaxation, le niveau de charge du RS et la concentration en Ca^{2+}. Plusieurs mécanismes sont impliqués : l'inactivation dépendante du Ca^{2+}, selon laquelle le Ca^{2+} libéré viendrait se fixer sur le RyR-2 et l'inactiver, « l'usure stochastique » d'après la théorie du contrôle local selon laquelle la fermeture d'un DHPR induit une diminution localisée de Ca^{2+} qui, en cascade, est à l'origine de la fermeture des RyR-2. Enfin, la déplétion en Ca^{2+} du RS diminuerait la probabilité d'ouverture des RyR-2, induisant ainsi leur fermeture synchronisée.

Une autre structure intervient dans les mouvements calciques : la mitochondrie. Bien que minoritaire en condition physiologique, son rôle est indispensable pour assurer le couplage entre activité mécanique contractile et énergétique. Elle joue un rôle pivot afin de coupler la production d'énergie en réponse à la demande mécanique contractile.

3. Couplage excitation-métabolisme-contraction

Longtemps ignoré dans la description du processus de régulation de la contraction cellulaire, la mitochondrie est le carrefour de la signalisation cellulaire et de la production d'énergie. Son rôle est d'assurer la production énergétique afin de subvenir à l'activité mécanique cardiaque. Elle est considérée comme la « centrale énergétique » de la cellule. C'est dans la mitochondrie que se déroulent les deux dernières phases de la respiration cellulaire : le cycle de Krebs (dans la matrice) et la chaîne de transport d'électrons (au niveau de la membrane interne).

Le cardiomyocyte est une véritable usine qui fonctionne à flux tendu, puisque les stocks d'ATP intracellulaire de quelques mM (environ 5 μmol/g ATP) sont juste suffisants pour assurer la fonction contractile pendant environ une minute. Le renouvellement perpétuel des stocks d'ATP est alors indispensable pour permettre à la machinerie contractile et aux différentes protéines consommatrices d'ATP de fonctionner. Ce couplage entre la demande énergétique émanant de l'activité mécanique et l'apport énergétique par l'activité mitochondriale est régulé par un ion ubiquitaire : le Ca^{2+}. Outre sa participation au couplage excitation-contraction, l'entrée de Ca^{2+} dans la mitochondrie joue un rôle énergétique majeur en régulant différents processi intra-mitochondriaux[22]. La mitochondrie intègre les mouvements de Ca^{2+} à travers les RyR-mitochondriaux, et le canal à Ca^{2+} uniporteur, à chaque cycle systole/ diastole afin d'adapter la production d'ATP face à la demande des protéines intervenant dans le couplage excitation-contraction, notamment les myosines et serca-2A [23]. Dans la matrice mitochondriale, le Ca^{2+} a joue un rôle important dans la régulation énergétique en activant l'ATPase F1/FO (responsable de la catalyse de l'ATP en ADP et phosphate inorganique) [24], l'adénine nucléotide translocase (protéine régulant les échanges ATP/ADP à travers la membrane interne mitochondriale) [25] ainsi que plusieurs déshydrogénases dans le cycle de Krebs, notamment la pyruvate déshydrogénase [26 27], la 2-cétoglutarate (α-cétoglutarate) déshydrogénase, et la déshydrogénase isocitrate liée au NAD^+ [28 26].

Le NADH est un donneur d'électrons de la chaîne respiratoire, considéré comme un reflet de l'état énergétique des mitochondries [29]. Lors d'une augmentation de la charge de travail, le Ca^{2+} cytosolique augmente et entraine alors une augmentation du Ca^{2+} mitochondrial responsable d'une activation plus importante des déshydrogénases dans le cycle de Krebs, ce qui entraine une augmentation de la production de NADH [30]. Ce mécanisme régulé par le Ca^{2+} est essentiel pour ajuster la production énergétique lors d'une surcharge de travail. L'augmentation du travail cardiaque s'accompagne d'une augmentation de la respiration mitochondriale, laquelle consomme du NADH et contribue donc à diminuer sa concentration cytosolique. Dans un état d'équilibre entre la demande et l'approvisionnement énergétique, le NADH est maintenue à un niveau stable : l'augmentation de production de NADH stimulée par la surcharge calcique cytosolique temporaire est compensée par une utilisation plus importante de ce NADH par la chaine respiratoire, aboutissant à une production plus importante d'ATP [29]. Cette autorégulation, qui fait intervenir le Ca^{2+} intracellulaire, permet d'éviter une déplétion des stocks d'ATP pouvant causer des dommages cellulaires en inhibant la fonction musculaire, ou provoquer l'apoptose ou la nécrose [31 32]. Une accumulation de preuves indique que la mitochondrie capture du Ca^{2+} à chaque cycle systole/diastole [33 34 35]. Ainsi, des transitoires calcique d'origine mitochondriale auraient lieu lors du CEC. Cependant, la cinétique de ces mouvements de Ca^{2+} trans-mitochondriaux sont mal connus [36]. La capture du Ca^{2+} par la mitochondrie, afin de maintenir les niveaux de NADH lors d'une augmentation de charge de travail, repose principalement sur le canal uniporteur calcique et l'extrusion cellulaire via l'échangeur Na^{+}/Ca^{2+} [37].

Le Ca^{2+} est alors l'élément intracellulaire pivot assurant la régulation énergétique au sein d'un couplage complexe des activités électriques, métaboliques et mécaniques : l'entrée de Ca^{2+} par les DHPR détermine la quantité de Ca^{2+} qui sera libérée par les RyR-2. Le Ca^{2+} libéré par les RyR-2 entraine la contraction musculaire, de manière dose-dépendante (l'intensité du raccourcissement cellulaire étant directement proportionnel à la quantité de Ca^{2+} libéré), et informe les messagers mitochondriaux de l'évolution de la demande énergétique.

4. Homéostasie redox

4.1. Production d'espèces oxygénées réactives

Il existe des imperfections dans la chaine respiratoire. En effet, 2 à 5% de l'O_2 consommé est transformée en espèces oxygénées réactives (ROS pour *reactive oxygen species*). Un ROS est une espèce chimique neutre, chargée, caractérisée par un électron libre dit « célibataire » sur son orbite externe. Les ROS sont des espèces chimiques très réactives ayant une durée de vie extrêmement courte car ils cherchent à « rapparier » leur électron célibataire.

Parmi ces radicaux libres on retrouve le radical superoxyde ($O_{2\cdot}^-$), le radical perhydroxyle (HO_2), le radical hydroxyle (OH), le radical peroxyle (RO_2) et le radical alkoxyle (RO), ainsi que des formes non radicalaires comme le peroxyde d'hydrogène (H_2O_2). Le radical $O_{2\cdot}^-$ a une durée de vie de l'ordre de quelques secondes, qui lui permet de diffuser au-delà de son lieu de production [38]. La toxicité du radical $O_{2\cdot}^-$ est directe, via une action délétère sur les constituants cellulaires, mais aussi indirecte car il peut former d'autres ROS ou réagir avec le NO pour former des espèces réactives oxygénées azotées (NOS pour *nitrogen oxygen species*) telles que le peroxynitrite ($ONOO^-$) [39]. Le $ONOO^-$ est un puissant oxydant dont la demi-vie est plus longue que celle de l'$O_{2\cdot}^-$. Celui-ci peut franchir les membranes cellulaires et provoquer notamment l'oxydation et/ou la nitration de nombreuses cibles protéiques ainsi que la péroxydation des lipides membranaires [39]. Les ROS et NOS sont ainsi capables d'endommager tous les types de composants cellulaires :

- Les acides nucléiques : l'attaque radicalaire est responsable d'altérations structurelles et de lésions directes (brèches) sur la molécule d'ADN. Ces lésions peuvent être à l'origine d'une altération de la synthèse protéique voire conduire à la mort de la cellule.
- Les protéines : la toxicité des ROS vis-à-vis des acides aminés peut entrainer des modifications structurales ou catalytiques des protéines.
- Les hydrates de carbone : Les ROS peuvent induire une modification des récepteurs membranaires en agissant sur les oligosaccharides membranaires.
- Les lipides membranaires : la peroxydation lipidique d'origine radicalaire a été largement étudiée. Les altérations des lipides membranaires peuvent conduire à des modifications de la perméabilité et du potentiel de membrane, à un dysfonctionnement mitochondrial, à une surcharge calcique (liée à des variations de perméabilités ioniques) et à l'inactivation d'enzymes membranaires [39].

Les ROS sont la conséquence inévitable de la consommation d'O_2 par l'organisme. Leur production est permanente et physiologique. La notion d'homéostasie redox renvoie à la capacité du système oxydo/réduction (redox) cellulaire à conserver son équilibre de fonctionnement en dépit des contraintes extérieures. Au cours de la vie, le cardiomyocyte est soumis à des « stress » aigus (pratique d'une activité physique, état de stress…) ou chronique (exposition environnemental, pathologies chroniques…) qui influencent les processi mitochondriaux, notamment la respiration mitochondriale et donc la production de ROS. Le cardiomyocyte met alors en place une autorégulation afin de restaurer le plus rapidement les variations du système redox. Des systèmes intrinsèques cellulaires permettent de maintenir les ROS à faible concentration, et éviter ainsi toute perturbation de l'homéostasie redox : ce sont les systèmes antioxydants.

4.2. Systèmes antioxydants

L'organisme est doté de systèmes de défense très efficaces contre la production des ROS. Les molécules contrôlant cette production sont désignées par le terme « antioxydants » et caractérisent toute substance qui, présente à faible concentration par rapport à celle du substrat oxydable, retarde ou inhibe significativement l'oxydation de ce substrat [40]. On peut distinguer deux catégories d'antioxydants : les défenses antioxydantes enzymatiques et non enzymatiques. Parmi les défenses antioxydantes non enzymatiques on retrouve notamment la vitamine E et A, l'acide ascorbique, le coenzyme Q10 et la cystéine. Bien que certaines études aient mis en avant l'intérêt de ces antioxydants, les défenses de type enzymatique sont reconnues comme étant les plus performantes, notamment au cours du syndrome d'ischémie-reperfusion. Il existe 3 enzymes antioxydantes principales : la superoxyde dismutase (SOD), la glutathion peroxydase (GPx) et la catalase (CAT) qui vont agir en synergie afin de défendre l'organisme contre une production excessive de ROS.

- la SOD : est une métalloenzyme qui catalyse la dismutation du radical $O_2^{\cdot -}$ en H_2O_2. Le peroxyde d'hydrogène ainsi formé n'est pas un radical libre, car tous ses électrons sont appariés, mais c'est malgré tout un intermédiaire réduit toxique qui possède une durée de vie relativement longue (quelques minutes). Comme le radical $O_2^{\cdot -}$, il possède la capacité de diffuser loin de son site de production et peut également traverser les membranes. Cette enzyme est présente chez pratiquement tous les

organismes vivants et procurent un système de défense essentiel à leur survie en milieu aérobie [41].

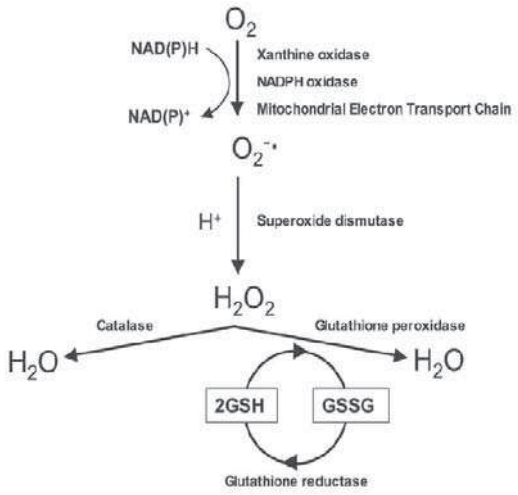

Figure 5 : Prise en charge des ROS par les enzymes antioxydantes. Adapté de [42]

- La GPx : est une enzyme capable de détoxifier le peroxyde d'hydrogène et d'autres hydroperoxydes. Le substrat de la GPx est le glutathion. La GPx va réduire les hydropéroxydes en H_2O ou en alcool, tandis que le glutathion réduit (GSH) est transformé en glutathion oxydé (GSSH) [43].
- La CAT : est une enzyme héminique capable de transformer le peroxyde d'hydrogène en eau et en oxygène moléculaire. La réaction catalysée par cette enzyme est une dismutation du peroxyde d'hydrogène [42].

4.3. Rôle des ROS et concept de stress oxydant

L'équilibre existant entre production et élimination de ROS permet de maintenir l'intégrité de la cellule. En effet, bien que qualifié d'imperfection de la chaine respiratoire, la production de ROS est essentielle à l'activité cellulaire. Notamment, les ROS sont impliquées dans diverses voies de signalisation régulant la transcription génique [44], mais également la contraction musculaire. En effet, il a été montré qu'une réduction trop importante de la quantité de ROS intracellulaire entraine des altérations du fonctionnement myofilamentaire, à l'origine d'une réduction des performances contractiles [45]. Un état d'oxydation basal permet en fait d'assurer les flux ioniques intracellulaires à l'origine du processus contractile.

Le concept de stress oxydant renvoie à une perturbation de l'homéostasie redox en faveur d'une accumulation excessive de ROS. Cet état de surcharge oxydative est rencontré lorsque les ROS sont produits soit de manière trop importante, notamment en raison de dysfonctions de la chaine respiratoire [46] [47] [48] ou de surcharge calcique mitochondriale, soit lorsqu'ils ne peuvent être complètement neutralisés en raison d'une défaillance des systèmes antioxydants (en condition pathologique). Les ROS exercent alors des effets délétères sur leurs différentes cibles.

5. Régionalisation des propriétés cellulaires cardiaques

L'efficacité du débit cardiaque repose sur un gradient transmural de contraction à travers le mur ventriculaire gauche (Voir chapitre I.3). Cette hétérogénéité transmurale des propriétés contractiles observées *in vivo* sur cœur entier résulte d'une disparité endo/epicardique dans le fonctionnement du couplage excitation-métabolisme contraction. Il a en effet été rapporté une contraction supérieure en intensité et en vélocité dans l'ENDO par comparaison à l'EPI [49]. Cette hétérogénéité transmurale contractile résulte d'une contraction plus importante des cardiomyocytes issus de l'ENDO par rapport à ceux issus de l'EPI [50]. La contraction d'un cardiomyocyte résulte de l'intégration simultanée des mouvements intracellulaires de Ca^{2+} et des propriétés de la machinerie contractile. Il a été rapporté une plus grande quantité de Ca^{2+} libérée dans l'ENDO par comparaison à l'EPI. Cette libération calcique accrue est associée à une sensibilité des myofilaments au Ca^{2+} supérieure [21]. La supériorité contractile de l'ENDO est sous-tendue par une distribution disparate des protéines du CEC au sein du myocarde. En effet, les DHPR sont présents en quantité plus importante dans l'ENDO par rapport à l'EPI permettant un courant entrant $I_{Ca,L}$ supérieur, et entrainant alors une stimulation plus importante des RyR-2 (dont le nombre et la fonction ne semblent pas varier entre les deux régions), et donc une libération de Ca^{2+} augmentée [51]. D'autre part, l'ENDO est plus riche en Serca-2a, ce qui permet une recapture optimal des grandes quantités de Ca^{2+} libérées en diastole, et donc une reformation complète des stocks en Ca^{2+} du RS à chaque cycle cardiaque [50]. La présence en quantité importante de Serca-2a dans l'ENDO participe également au lusitropisme supérieur dans cette région par rapport à l'EPI [52]. Enfin, au niveau des myofilaments, l'ENDO possède des MLC-2 dans un état plus phosphorylé par comparaison à l'EPI lorsque les cardiomyocytes sont étirés ; ce qui participe à accroitre la sensibilité au Ca^{2+} des myofilaments dans cette région [21].

L'hétérogénéité transmurale des propriétés contractiles, caractérisée par une activité mécanique plus importante dans l'ENDO, implique une distribution disparate des propriétés métaboliques au sein de la paroi ventriculaire gauche. En effet, la perfusion myocardique [4], la consommation en oxygène [53], et le métabolisme oxydatif [54] sont supérieurs dans l'ENDO par rapport à l'EPI, et permettent donc une production plus importante d'ATP afin de répondre à la demande énergétique supérieure de l'ENDO.

Cette construction hétérogène du couplage EMC à travers le mur ventriculaire gauche, associée à la disposition complexe dans l'espace des structures conjonctives permettant la transmission des forces, assure une biomécanique cardiaque efficace.

III. L'Insuffisance cardiaque

1. Contexte épidémio-économique

L'insuffisance cardiaque (IC) chronique est définie comme l'incapacité du cœur à assurer, dans des conditions normales, le débit sanguin nécessaire aux besoins métaboliques et fonctionnels des différents organes. Elle représente l'une des principales causes de morbidité et mortalité au XXIe siècle. Le pronostic de cette maladie, moins bon que celui de la plupart des cancers [55], est sombre, puisqu'un patient sur cinq décède dans l'année qui suit le diagnostic, et le taux de décès à 5 ans est de plus de 50%. L'IC affecte au moins 6,5 millions de personnes en Europe, et 5 millions aux Etats-Unis [56] [57]. En France, environ 500 000 personnes présentent une IC (dont un tiers sont âgées de moins de 70 ans) ; on dénombre environ 120 000 nouveaux cas et 32 000 décès chaque année. Elle représente la première cause de mortalité d'origine cardiovasculaire dans les pays industrialisés. La prévalence globale de l'IC est en augmentation du fait du vieillissement de la population, ainsi que des améliorations du traitement des épisodes coronaires aigus à la phase aiguë et en prévention secondaire. Au-delà des considérations humaines liées à la mortalité, l'IC a un coût économique important ; 85 à 93 % des coûts sont imputables aux hospitalisations. Environ 3,5 millions de consultations et 150 000 hospitalisations pour IC sont recensées chaque année. La durée moyenne de séjour est de 11 jours. Les dépenses liées à l'IC représentent plus de 1 à 2 % des dépenses médicales totales [58], faisant de l'IC un problème majeur de santé publique. Ce syndrome progressif apparaît dans la phase finale de la plupart des maladies cardiaques et se manifeste par une détérioration de la fonction contractile du cœur. Une forme prédominante,

l'IC ischémique, est provoquée initialement par un accident aigu, l'infarctus du myocarde suite à une occlusion d'une artère coronaire, entrainant une nécrose du muscle cardiaque (zone infarcie). En effet, l'ischémie puis la réponse inflammatoire entraine la perte rapide et irréversible des cardiomyocytes. Une cicatrice fibreuse akinétique, peu ou avasculaire, remplace une portion entière de myocarde contractile. De manière à compenser cette perte cellulaire, le myocarde pathologique augmente le travail des myocytes des zones non affectées. Cette surcharge de travail est impliquée dans l'apparition progressive d'une phase de décompensation myocardique, au cours de laquelle les changements morphologiques, biochimiques, électrophysiologiques et structuraux, qualifiés de « remodelage » [59], entrainent une perte de cohérence dans le fonctionnement du myocarde.

2. Physiopathologie

Le myocarde IC subit un profond remodelage morpho-fonctionnel caracérisé notamment par une hypertrophie ventriculaire gauche associé à une fraction d'éjection inférieure à 50%. Cette dysfonction fonctionnelle systolique s'accompagne de troubles de la relaxation, notamment d'un remplissage passif (par diffusion du sang de l'oreillette gauche vers le ventricule gauche) dégradé. La physiopathologie de cette dysfonction fonctionelle myocardique emprunte à un profond remodelage des activités électriques, métaboliques et mécaniques.

2.1. Remodelage électrophysiologique

Les paramètres électrophysiologiques intracardiaques subissent un profond remodelage au cours de l'IC. L'allongement de la durée du PA est un phénomène clairement établi, retrouvé dans les modèles d'IC, y compris chez l'homme [60] [61]. Cet allongement résulte d'une altération de la balance des courants dépolarisants et repolarisants. Le courant sodique rapide, responsable de la phase 0 de dépolarisation du PA n'est pas modifié dans les modèles expérimentaux d'IC ou chez l'humain [62]. En ce qui concerne le courant entrant $I_{Ca,L}$, des données controversées sont rapportées dans la littérature. Certains auteurs rapportent une augmentation [63], d'autres une diminution [64] ou aucune modification [65]. La diversité des modèles animaux utilisés, le stade d'étude de l'IC ainsi que les conditions expérimentales

employées (isolement cellulaire, sélection des cellules) pourraient expliquer la disparité des résultats.

Parmi les courants sortants ou repolarisants, I_{to} joue un rôle important dans la phase 1 de la repolarisation du PA. Ce courant est rapporté comme étant diminué au cours de l'IC [61] [62]. Enfin, le courant rectifieur I_{K1} est diminué au cours de l'IC [66].

2.2. Remodelage de l'homéostasie calcique

Un profond bouleversement du cyclage du Ca^{2+} a lieu au cours de l'IC. Les caractéristiques du transitoire calcique sont largement altérées ; ces modifications se traduisent par une augmentation des concentrations en Ca^{2+} diastolique. Cette surcharge calcique diastolique fait suite à une fuite de Ca^{2+} en diastole. En effet, bien qu'aucune modification du niveau d'expression des RyR-2 n'ait été rapportée en condition pathologique [67], une dysfonction de ce canal est caractéristique de l'IC ischémique. La protéine régulatrice du canal, le FKBP12.6, qui maintient le canal fermé en diastole est dissociée du RyR-2 dans la pathologie ischémique. Ce découplage protéique est à l'origine d'un fonctionnement stochastique du RyR-2 et augmente alors sa probabilité d'ouverture en diastole (Lenhart, JCI, 2008). Cette ouverture incontrôlée des RyR-2 pendant la diastole engendre une véritable fuite de Ca^{2+} du RS, perturbant alors le relâchement complet du cardiomyocyte et empêchant ainsi le repompage correct du Ca^{2+} dans le RS [68]. Cette libération anarchique de Ca^{2+} en diastole est à l'origine de contractions ectopiques et phénomènes arythmiques cardiaques (Lehnart SE, PNAS, 2006). D'autre part, le ralentissement de la relaxation cellulaire associée à la surcharge calcique diastolique limite le remplissage cardiaque en diastole et participe, par la relation de Frank-Starling (l'étirement des parois ventriculaires en systole suite au remplissage sanguin, permet d'emmagasiner de l'énergie élastique qui est restituée lors de la systole entrainant alors une contraction efficace), à la réduction de la force de contraction ventriculaire.

Les mécanismes sous-jacents à la dissociation de FKBP12.6 du RyR-2 sont soumis à controverse. En effet, il a été initialement proposé que l'hyperactivation β-adrénergique chronique associée à l'IC était responsable d'une activation accrue de la PKA, laquelle phosphorylait le RyR-2 sur le site Ser^{2808} PKA-dépendant en diastole [69] (Figure 6). Des *sparks* Ca^{2+} ou « étincelles calciques », traduisant des dysfonctions unitaires et localisées de canaux RyR-2, étaient alors observées localement dans le cardiomyocyte au niveau des RyR-2 altérés. Ces *sparks* Ca^{2+} se somment dans le temps et l'espace et aboutissent à une surcharge calcique cytosolique pendant la diastole. La Ca^{2+} calmoduline Kinase serait également

impliquée dans l'hyperphosphorylation du RyR-2 associée à l'IC (Wehrens XH, circ res, 2004 ; Kushnir A, PNAS, 2010 ; Chelu MG, JCI, 2009). Récemment, un second mécanisme a été proposé comme étant responsable du dysfonctionnement des RyR-2 impliquant une modification de l'environnement redox intracellulaire. En effet, le stress oxydatif ainsi que la nitrosylation associés à l'IC altèreraient également l'interaction RyR-2/FKBP12.6, entrainant alors une libération anarchique de Ca^{2+} dans le cytosol [70 71 72]

Malgré l'augmentation de $I_{Ca,L}$ rapportée par certains auteurs, la réduction de libération de Ca^{2+} chez les populations IC est clairement admise, illustrant ainsi une origine des défaillances de libération de Ca^{2+} liée aux RyR-2 plutôt qu'aux caractéristiques électrophysiologiques. En fait, il a été rapporté à la fois des troubles de libération de Ca^{2+} par le RS, liés notamment à la fuite de Ca^{2+} en diastole, qui déplète les stocks internes du RS et empêche de conserver une quantité de Ca^{2+} suffisante pour les contractions successives.

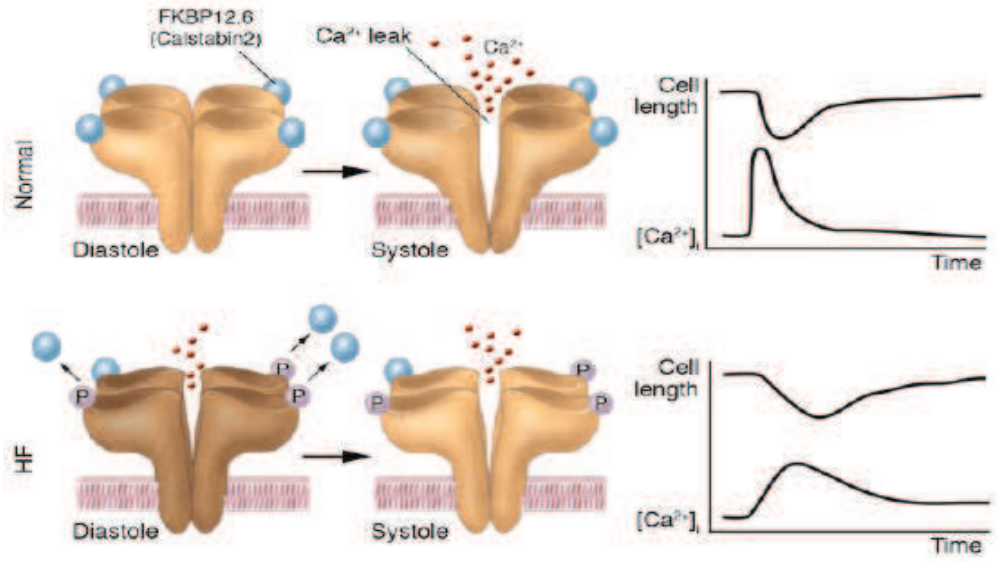

Figure 6 : Dissociation de FKBP12.6 par hyperphosphorylation PKA-dépendante des RyRs dans l'IC (HF). La fuite calcique engendrée en diastole provoque des perturbations de la signalisation calcique et des propriétés mécaniques. D'après Yano *et al*., 2005 [68]

2.3. Remodelage des propriétés de la machinerie contractile

Les propriétés de la machinerie contractile subissent un profond remodelage au cours de l'IC. La diminution de la sensibilité au Ca^{2+} des myofilaments, à l'origine d'une réduction des performances contractiles globales, est retrouvée de manière unanime sur des modèles murins mais fait débat chez l'homme [73]. La sensibilité au Ca^{2+} des myofilaments est régulée principalement par l'état de phosphorylation des différentes protéines constitutives des myofilaments, notamment la TnI, la TnC et les chaines légères de myosines (MLC-2). Au cours de l'IC, l'hyperphosphorylation chronique PKA-dépendante entrainerait une phosphorylation de la TnI sur le site PKA (Wolff et al. 1996; Cazorla et al. 2006). Cette phosphorylation serait alors à l'origine d'une réduction de la sensibilité au Ca^{2+} des myofilaments. La diminution de sensibilité au Ca^{2+} des myofilaments est normalement associée à un lusitropisme positif en raison d'une affinité Ca^{2+}/TnC plus faible. Cependant, le cœur en IC est caractérisé par des troubles de relaxation. L'efficacité de la relaxation repose d'une part sur la dissociation du Ca^{2+} des protéines contractiles, mais également sur l'élimination du Ca^{2+} intracellulaire. En fait, la dissociation rapide du Ca^{2+} de la TnC est contrebalancée par la surcharge Ca^{2+} diastolique, ce qui empêche une relaxation correcte des cardiomyocytes.

D'autre part, la loi de Frank-Starling, qui associe l'étirement des fibres cardiaques à une augmentation de la puissance contractile, est également affectée par la pathologie. En effet, l'étirement de préparations cardiaques est associé à un plus faible inotropisme (Cazorla, Faseb, 2005). Ces troubles contractiles, traduisant des anomalies d'adaptation cardiaque à l'exercice, lorsque l'augmentation du retour veineux s'accompagne normalement d'une potentialisation de la contractilité myocardique, résultent d'une réduction de la phosphoryaltion des MLC-2 (Cazorla, Faseb, 2005). Enfin, le cœur IC est caractérisé par une modification de l'expression des chaines lourdes de myosine. En effet, une modification de l'expression des chaines lourdes de myosine au profit ches chaines β intervient au cours de l'IC afin d'économiser la fonction contractile. Les chaines β sont plus efficientes que des chaines α permettant alors pour une dépense énergétique plus faible. Cependant, la surexpression des chaines β est associée à un ralentissement des cinétiques de contraction et relaxation [74].

2.4. Remodelage métabolique et dysfonction mitochondriale

L'activité métabolique subit également de profondes modifications au cours de l'IC. En effet, un déséquilibre entre l'offre et la demande en ATP a lieu au cours de la pathologie. Différentes études rapportent que l'origine des troubles métaboliques serait liée aux dysfonctions contractiles. En effet, une altération de l'efficacité contractile caractérisée par une demande énergétique plus importante pour réaliser une même contraction [75] [76, 77] a lieu lors de l'IC. Ce remodelage métabolo-contractile résulterait d'un changement conformationnel de certaines protéines de structure et de fonction musculaire, telles que la troponine T [78] [79], à l'origine d'altérations de l'interaction acto-myosine, en faveur d'un coût énergétique supérieur [80]. Ainsi, un cycle cardiaque consomme plus d'ATP en condition pathologique ; une augmentation de la production d'ADP a alors lieu, et contribue à réduire les ponts d'union acto-myosine [81]. La créatine kinase qui catalyse la conversion de la créatine en phosphocréatine, impliquant la conversion de l'ATP en ADP est réduite au cours de l'IC. Parallèlement, une diminution ou un maintien des concentrations en ATP a été rapporté au cours de l'IC [82]. Ces réductions concomitantes participent à limiter les capacités du myocarde IC à répondre à un inotropisme positif lors d'une surcharge de travail (stress, exercice physique) [83]. D'autre part, la respiration mitochondriale est diminuée dans le myocarde défaillant [84], sous-tendue par une réduction de l'activité des complexes I à IV de la chaîne respiratoire [85] [86]. Cette dysfonction mitochondriale est associée à une élévation de la production de ROS [46] [48] [87], qui vont à leur tour amplifier les altérations mitochondriales, notamment le monoxyde d'azote en se fixant sur la cytochrome c-oxydase (complexe IV) à la place de l'oxygène [88].

Enfin, le myocarde IC est caractérisé par une modification dans l'utilisation des substrats énergétiques. En effet, dans des conditions normales, l'oxydation des acides gras et du glucose couvre environ 65% et 30% des apports énergétiques cardiaques, respectivement [89]. Au cours de la pathologie, une réduction de l'utilisation des acides gras, associée à une augmentation simultanée de la consommation de glucose ont lieu [90]. Une partie substantielle du glucose exogène est alors converti en lactate au lieu d'être oxydé au cours de la pathologie [91]. Bien que considéré comme un intermédiaire métabolique et un substrat cardiaque de second plan, le lactate joue cependant un rôle cardio-toxique en altérant des protéines impliquées dans la signalisation et le contrôle de la régulation cardiaque [92].

Les mécanismes à l'origine de ces troubles métaboliques impliqueraient d'une part des altérations de la perfusion coronaire [93]. En effet, au cours de l'IC, un remodelage morpho-fonctionnel du réseau coronaire a lieu, caractérisé par une altération des de la vasomotricité au profit d'une vasoconstriction chronique [94]. A l'inverse, les capacités de vasodilatation, notamment impliquant l'endothélium, sont altérées. Ces dysfonctions à l'origine d'une réduction de la perfusion coronaire empêche alors un fonctionnement oxydatif mitochondrial correct, et pourrait alors expliqué le recours aux substrats glucidiques en priorité dans le cœur IC. En plus des troubles de l'oxydation des lipides, le myocarde pathologique est caratérisé par une altération du transport des lipides du milieu extracellulaire vers le sarcoplasme. L'entrée d'cides gras dans le cardiomyocyte est régie par des transporteurs spécifiques : les FAT/CD36. Il semblerait que ces transporteurs soient réduits au cours de la pathologie, contribuant alors à limiter le métabolisme oxydatif des lipides et au profit d'une dégradation glucidique [95].

Enfin, une altération de l'homéostasie en Ca^{2+} mitochondrial est retrouvée dans le myocarde IC. Le Ca^{2+} mitochondrial permet la stimulation de différentes enzymes impliquées dans la phosphorylation oxydative. Une élévation des concentrations en Ca^{2+} mitochondriale au cours de la pathologie pourrait alors contrecarrer les altérations métaboliques caractéristiques de la maladie, notamment la moindre oxydation des lipides. L'augmentation artificielle des concentrations en Ca^{2+} mitochondrial chez des cœurs IC permet de restaurer le couplage entre demande et fourniture d'ATP (Liu, O'rourke, Circ res, 2008). Cependant, une surcharge Ca^{2+} mitochondriale est à l'origine d'une production exacerbée de ROS et favorise la nécrose des cardiomyocytes [34]. Bien que non consensuelle à l'heure actuelle, l'implication des troubles de l'homéostasie en Ca^{2+} dans les perturbations métaboliques te contractiles cardiaques au cours de l'IC semble tangible.

Au cours de l'IC, les activités électriques, mécaniques et métaboliques subissent donc des altérations majeures qui retentissent à l'échelle de l'organe par un profond remodelage morpho-fonctionnel. Cependant, la plasticité de ces activités a été étudiée de manière isolée les unes par rapport aux autres. L'intégration des trois dimensions excitation métabolisme et contraction au sein d'une même unité (couplage) permettrait alors une meilleure compréhension du remodelage cellulaire au cours de l'IC. Ainsi, la première partie du travail de thèse s'est intéressée à l'exploration des propriétés du couplage EMC dans le cœur sain et insuffisant cardiaque.

IV. Pollution atmosphérique au monoxyde de carbone

1. Epidémiologie des effets de la pollution au CO sur le système cardiovasculaire

Le système cardiovasculaire est une structure malléable capable de modifier ses propriétés morphologiques et fonctionnelles en réponse à un stress exogène. Cette plasticité cardiaque est notamment sensible aux facteurs environnementaux, particulièrement la pollution atmosphérique. Au cours de cette dernière décennie, la prolifération d'enquêtes épidémiologiques impliquant la pollution atmosphérique dans la dégradation de la fonction cardiaque et dans la précipitation des risques de survenue d'accidents cardiovasculaires [96] [97] [98], en particulier chez des personnes fragilisées par une pathologie chronique [99] [100] [101], suggèrent un rôle majeur de ce stress environnemental dans la pathogenèse des maladies cardiovasculaires. Parmi les agents polluants, le CO est souvent associé, dans les enquêtes épidémiologiques, avec la fréquentation des services de cardiologie et l'accroissement du taux de mortalité cardiovasculaire [102] [103]. Notamment, une étude rapporte une relation linéaire significative entre pollution citadine au CO et mortalité cardiovasculaire [104]. Les populations à risque, notamment les insuffisants cardiaques, présentent une sensibilité exacerbée au CO [105], gaz libéré à partir de sources multiples et d'une manière qui peut être quotidienne (fumée de cigarette, gaz d'échappements de véhicules motorisés...). Le CO est connu pour accroître certains des facteurs de risque de l'IC [103]: augmentation de la viscosité sanguine, tachycardies ventriculaires, et diminution de la variabilité du rythme sinusal [106]. Il est classiquement rapporté qu'une exposition chronique au CO, à des doses similaires à celles rencontrées chez le fumeur (500ppm), exacerbe le remodelage morphologique cardiaque délétère des patients insuffisants cardiaques [107], et provoque une survenue accrue des accidents cardiovasculaires (arythmies, infarctus) chez ces populations à risque [108].

Le CO est présent en très faible concentration dans l'environnement. Cependant, il peut atteindre des concentrations plus importantes dans certaines zones particulièrement polluées. En effet divers travaux ont pu mettre en évidence des taux moyens de CO urbains de l'ordre de 20 à 40 ppm dans des environnements urbains pollués avec des pics pouvant aller jusqu'à 170 ppm [109] [110].

Les principales données de la littérature, qui concernent les effets cardiovasculaires du CO, sont issues de travaux en toxicologie [111] [112], pour lesquels les taux de CO utilisés sont très

supérieurs (500 ppm) à ceux habituellement rencontrés lors des pollutions citadines (20-80 ppm). Pour des doses non létales, les effets du CO sont principalement expliqués par sa fixation à l'hémoglobine dont l'affinité est 200 à 250 fois supérieure à celle pour l'oxygène, réduisant alors les capacités de transport de l'oxygène.

2. Propriétés physico-chimiques du CO

Le CO est un gaz inodore, incolore, insipide, non irritant, non suffocant, inflammable et potentiellement détonant [113]. Il diffuse rapidement dans le milieu ambiant d'où son danger potentiel dans un milieu fermé. Dans le milieu biologique, il se lie facilement par coordination au fer divalent ou au cuivre des hémoprotéines, ce qui rend sa capacité de solubilisation plus grande dans le sang que dans d'autres liquides. Le CO réagit avec plusieurs hémoprotéines, notamment l'hémoglobine, mais aussi la myoglobine, le cytochrome p450, le cytochrome c-oxydase (a3) et à moindre importance avec l'hydroxypéroxydase [114].

Concernant l'hémoglobine, le CO a une affinité pour l'hémoglobine 240 à 250 fois plus grande que l'O2. Le CO forme alors avec l'hémoglobine la carboxyhémoglobine (HBCO) et empêche un transport correct de l'oxygène par la protéine. L'HbCO induit également un déplacement de la courbe de dissociation de l'oxyhémoglobine vers la gauche, traduisant un accroissement de l'affinité de l'oxygène pour l'hémoglobine [114]. Cette altération hémodynamique entrainant une moindre diffusion de l'O_2 aux cardiomyocytes s'accompagne d'une hypoxémie tissulaire liée à la fixation du CO à la myoglobine cardiaque et aux cytochromes mitochondriaux, altérant ainsi la chaine de transport d'électrons, et entrainant une réduction de l'utilisation de l'O_2 par les cardiomyocytes [115]. Ces hypoxémies sanguine et tissulaire associées au CO contribuent certainement à aggraver l'ischémie myocardique rapportée chez des patients coronariens [116].

Concernant la myoglobine, l'affinité pour le CO est 40 fois plus grande que pour l'O2 [113]. Cette liaison empêche une utilisation correcte par les cardiomyocytes de l'O2.

Concernant le cytochrome p450, une enzyme intervenant dans les complexes terminaux de la chaîne respiratoire mitochondriale, le CO empêche le fonctionnement normal de la chaîne respiratoire mitochondriale, altérant alors l'oxydation des substrats énergétiques et générant un stress oxydatif [114].

Ainsi, les effets du CO seraient médiés par l'hypoxémie et/ou les troubles mitochondriaux associés.

3. Sources de CO

L'évaluation du CO intra-organique repose sur la mesure de l'HbCO. Elle reflète les taux de CO circulants, c'est-à-dire le CO issu de sources exogènes et endogènes. Concernant l'origine exogène du CO, la concentration atmosphérique en CO est toujours inférieure à 0,0001 %. Ce taux est plus élevé en milieu urbain qu'en rural [117]. Les principales sources exogènes de production de CO sont variables :

- les fumées échappées par les moteurs de véhicules
- le dysfonctionnement des appareils de chauffage et de production d'eau chaude utilisant tout combustible organique (fuel, butane, essence, charbon..)
- les fumées d'incendie,
- les intoxications professionnelles (industrie minière, métallurgique, chimique).
- Le tabagisme passif : la fumée de cigarette est en fait un vaste cocktail de substances nocives, parmi lesquelles le CO est présent en quantité importante.

La production de CO endogène est issue soit de la dégradation hémique (70%) [118], soit de l'oxydation des molécules organiques. Le CO endogène a longtemps été considéré exclusivement comme un déchet de la dégradation hémique. Toutefois il est désormais considéré comme un précurseur de fonctions physiologiques essentielles [118].

Un taux basal de 1 à 3% d'HbCO est classiquement retrouvé chez des personnes non fumeurs sans pathologie apparente [119]. La production de CO endogène est minime par rapport aux taux exogènes et n'influence donc pas le niveau d'HbCO, excepté chez des populations présentant des pathologies inflammatoires chroniques. Par conséquent, il est considéré que la mesure du taux d'HbCO chez des populations saines est un index du degré d'exposition de ces populations aux CO environnants [120].

V. Stratégies préventives

La prévention du risque cardiovasculaire est un enjeu majeur de santé publique. Différentes actions médico-politiques œuvrent à l'éducation thérapeutique du grand public afin de favoriser une prise de conscience des risques cardiovasculaires. Ainsi, les programmes nutrition-santé, les actions faisant la promotion de l'activité physique visent notamment à prévenir le risque cardiovasculaire en incitant les citoyens à modifier leurs modes de vie. L'objectif des actions mises en place est de prévenir les facteurs de risque cardiovasculaires modifiables que sont le tabagisme, les dyslipidémies, l'hypertension artérielle, le diabète et l'obésité, à travers la promotion de mesures hygiéno-diététiques. Parmi les approches préventives naturelles conseillées, les thérapies antioxydantes et l'exercice physique s'avèrent particulièrement efficaces.

2.5. Thérapies antioxydantes

L'implication du stress oxydatif dans la physiopathologie de l'IC est maintenant clairement admise. D'autre part, l'exposition en milieu pollué est également associée à la genèse d'un stress oxydant. Le recours à des thérapies antioxydantes se justifie alors afin de prévenir les altérations ROS-dépendantes. Différentes études ont alors évalué les effets de traitements antioxydants chroniques tels que des supplémentations en polyphénols, β-carotène (provitamines A), acide ascorbique (vitamine C), tocophérol (vitamine E) et lycopène. Bien que non consensuels, ces travaux rapportent en majorité des effets bénéfiques des supplémentations antioxydantes pour la prévention du risque d'accident cardiovasculaire chez des populations saines [121] [122] [123] et coronariennes [124]. Les bénéfices des traitements antioxydants reposent sur la neutralisation des ROS et des marqueurs inflammatoires tels que le TNF [125] et par conséquent des oxydations des différentes protéines cibles. D'autre part ces stratégies s'avèrent efficaces pour améliorer la fonction endothéliale des artères et donc favoriser une meilleure perfusion cardiaque [126]. Parmi les traitements antioxydants, l'administration de N-acétylcystéine NAC a été particulièrement étudiée. Le NAC est un acide aminé produit par le corps, qui stimule la production de glutathion. Le glutathion est un tripeptide, formé par la condensation d'acide glutamique, de cystéine et de glycine : γ-L-Glutamyl-L-cystéinylglycine. Le groupement amine de la cystéine se condense avec la fonction acide carboxylique en γ de l'acide glutamique. La plupart des cellules en contiennent

une concentration élevée. On le représente de manière simplifiée par GSH (forme réduite) ou GSSG (forme oxydée), la fonction thiol lui conférant ses principales propriétés biochimiques, notamment son action comme puissant antioxydant. Un traitement au NAC permet notamment de maintenir une fonction cardiaque normal lorsque le cœur est exposé à des agents inflammatoires tels que le TNF-α [127].

2.6. Exercice physique

L'IC a été longtemps une contre-indication formelle à l'exercice physique. Pour comparaison, les bétabloquants étaient également dénigrés pendant des années avant de devenir incontournables avec une réduction reconnue de près de 30 % de la mortalité à long terme [128]. L'intégration de patients présentant une altération majeure de la cinétique ventriculaire gauche dans les programmes de réentraînement n'est cependant pas nouvelle, mais la démonstration par des études randomisées contrôlées d'un bénéfice fonctionnel ne date que de la dernière décennie. La réadaptation, qui reste cependant encore insuffisamment proposée aux patients coronariens (on estime qu'en France, moins de 20 % des infarctus récents bénéficient d'un réentraînement physique secondaire) reste encore balbutiante dans l'IC, en raison des insuffisances de structures existantes mais aussi des réticences du corps médical face à des patients fragiles, souvent âgés et présentant des handicaps associés. La réadaptation a pour objectif d'améliorer la capacité fonctionnelle et donc l'autonomie des insuffisants cardiaques [129, 130]. Les symptômes de l'IC (dyspnée d'effort et fatigabilité musculaire) ne sont pas uniquement le fait de l'hypertension pulmonaire et de l'insuffisance de la perfusion musculaire. La réduction prolongée de l'activité associée à un état grabataire amplifié au cours du temps entraîne une amyotrophie anatomique et fonctionnelle qui à son tour incite au repos, et donc à l'exacerbation des dysfonctions cardiaques. Ce cercle vicieux de déconditionnement doit être évité le plus précocement possible afin de placer le myocarde dans une dynamique de reconditionnement. Les muscles respiratoires déconditionnés ne supportent plus l'excès de travail que leur impose l'hyperventilation. Le dérèglement neurohormonal provoque une vasoconstriction qui s'oppose à la perfusion musculaire. L'entraînement physique peut améliorer considérablement ces dysfonctionnements. Ainsi, l'exercice physique est fréquemment utilisé à des fins thérapeutiques et préventives dans le cas de pathologies cardiaques. Ses effets bénéfiques sur l'ultrastructure cardiaque et sur les propriétés des myocytes cardiaques sont largement documentés dans la littérature [131 132] et lui

ont valu une attention particulière dans les maladies du cœur liées à des perturbations cellulaires.

Cette stratégie de réhabilitation cardiaque a clairement fourni la preuve de son succès. Outre l'amélioration des propriétés fonctionnelles cardiaques, l'exercice physique augmente la qualité de vie des patients insuffisants, ainsi que leur performance physique et leur capacité aérobie [133] [134] [135]. Or, l'amélioration de la capacité aérobie se traduit par une amélioration des paramètres endothéliaux (vasodilatation), mitochondriaux, et cardiaques (augmentation de la taille des cardiomyocytes, de leur raccourcissement et potentialisation des cinétiques de contraction et relaxation) et contribue alors à limiter le risque cardiovasculaire [136].

D'autre part, le réentraînement à l'effort des populations pathologiques n'est plus une hérésie scientifique puisqu'il a été prouvé qu'il ne laissait pas transparaître l'ombre d'une potentielle dangerosité vitale. En effet, l'exercice n'augmente pas la mortalité ; au contraire, il contribue à prolonger le pronostic vital des patients IC. L'exercice a donc une valeur prophylactique bien établie. Son action protectrice dans l'IC repose sur le partage de cibles communes entre l'IC et l'exercice, mais dans un mode inversé. Notamment, le pattern de changement du cycle calcique et des propriétés contractiles suite à un entraînement est l'inverse des phénomènes néfastes rencontrés chez des populations IC : l'exercice physique améliore ce que la pathologie détériore [132]. En effet, la pratique régulière et modérée de l'exercice physique permet de rétablir les altérations de l'homéostasie calcique, les troubles myofilamentaires et les perturbations métaboliques chez les patients IC. Ces effets sont notamment médiés par une réduction de l'hyperactivation β-adrénergique et un rétablissement de l'homéostasie redox [137]. Il est donc légitime d'envisager le réentraînement comme moyen potentiel de prévention et de réversion des altérations du couplage EMC chez des populations IC ou exposées en milieu pollué.

VI. Objectifs de thèse

L'objet de ce travail de thèse a été d'étudier le couplage E-M-C du cœur sain et du cœur pathologique afin de comprendre l'origine des dysfonctions contractiles rapportées dans l'insuffisance cardiaque ischémique ainsi que chez des populations exposées à une pollution atmosphérique de type urbaine. Une fois les mécanismes caractérisés, l'objectif était

d'identifier de potentielles stratégies thérapeutiques limitant le remodelage cardiaque délétère au cours de l'IC et/ou d'une exposition en milieu pollué.

Matériel et Méthodes

I. Populations

Les maladies cardiovasculaires constituent des pathologies multifactorielles complexes qui sont difficiles à étudier chez l'homme en raison du caractère invasif des procédés méthodologiques. Les modèles murins sont d'un grand intérêt pour obtenir rapidement un nombre important d'échantillons et permettent des études physiologiques complètes sur des populations génétiquement uniformes très bien caractérisées. C'est pourquoi, les différentes études de ma thèse ont été réalisées sur des rats males Wistar (Charles River, Arbresle, France), en accord avec les directives du ministère français de l'agriculture et les conventions européennes sur l'utilisation et le conditionnement des animaux de laboratoire.

II. IC ischémique

L'IC était obtenue par occlusion chirurgicale de l'artère coronaire gauche (rats PMI, pour *Post* Myocardial Infarction), à l'âge de 5 semaines. Après anesthésie par injection intra-péritonéale d'un mélange xylazine (50 mg/kg) kétamine (15 mg/kg), les rats étaient intubés puis ventilés mécaniquement. Une fois l'animal stabilisé, une thoracotomie gauche était réalisée, et l'artère coronaire antérieure gauche ligaturée (fil à suture 6-0) au niveau de son segment proximal. Le changement de couleur du myocarde ainsi que la survenue immédiate d'une dyskinésie validait le caractère complet de l'occlusion. La ligature de l'artère coronaire gauche induisait alors une ischémie irréversible et localisée dans le territoire inférieur du ventricule gauche. La cage thoracique était ensuite refermée et les pressions intra-thoraciques rééquilibrées. Les rats étaient alors placés dans une cage individuelle jusqu'à leur réveil, puis en cage collective pour une période de récupération *post*-opératoire de 15 jours en environnement sain. Bien que l'anthropisation des données déduites de l'animal ne puisse être systématique, ce modèle d'infarctus du myocarde reproduit assez fidèlement les

caractéristiques phénotypiques de l'IC ischémique humaine (REF). La même opération était réalisée pour la population contrôle (rats Sham), toutefois sans ligature de l'artère coronaire. Les animaux étaient sacrifiés 12 semaines après l'intervention chirurgicale afin d'explorer l'activité cardiaques de rats en IC réelle. En effet, 12 semaines post-infarctus les mécanismes compensateurs initiaux, notamment la compensation β-adrénergique, disparaissent et laissent place à la phase décompensée de l'IC. Des mesures échocardiographiques avait préalablement permis d'évaluer la reproductibilité de la ligature ainsi que la sévérité de l'IC au sein du laboratoire.

III. Exposition à un stress environnemental : Pollution atmosphérique au monoxyde de carbone

L'Organisation Mondiale de la Santé a déterminé les seuils d'exposition au CO au delà desquels la santé de l'individu peut être altérée. Des expositions à 9 particules par million (ppm) pendant 8 heures constituent des limites à ne pas dépasser. Cependant, il existe des périodes de la journée, en milieu urbain, où ces concentrations sont largement dépassées. En effet, différentes enquêtes portant sur la qualité de l'air rapportent des concentrations de CO avoisinants ou dépassants les 50 ppm dans des lieux tels que les garages, le métro, les parkings souterrains, les péages d'autoroute, les tunnels ou encore les carrefours lors d'embouteillage [138]. L'exposition au CO a été testée sur une population saine, ainsi que sur une population de rats fragilisés par une occlusion coronaire. Les rats étaient placés dans un environnement pollué au CO, simulé à l'aide d'un caisson étanche, relié par un débitmètre et une électrovanne à une bouteille de gaz comprimé. Le système d'électrovanne permettait de contrôler l'entrée de CO en fonction des temps d'exposition voulus et de la concentration souhaitée. Pendant 4 semaines, les animaux (Sham-CO et PMI-CO) étaient exposés durant toute la phase nocturne de leurs différents séjours expérimentaux, à une concentration continue de 30 ppm, complétée par cinq pics d'une heure à 100 ppm déclenchés par ouverture réglée d'un système d'électrovanne. Pendant la phase diurne, une concentration de 0 ppm de CO était maintenue (Figure 7). La valeur moyenne d'exposition quotidienne au CO de 30 ppm (7 heures à 30 ppm, 5 pics d'une heure à 100 ppm, et 12 h à 0 ppm) restait en deçà des valeurs moyennes d'exposition au CO (50 ppm) estimées par le ministère français de l'écologie, du développement et de l'aménagement durable. Les rats étaient soumis à un cycle de luminosité

12h/12h et bénéficiaient d'un accès libre à l'eau ainsi qu'aux denrées alimentaires pendant toute la durée du protocole.

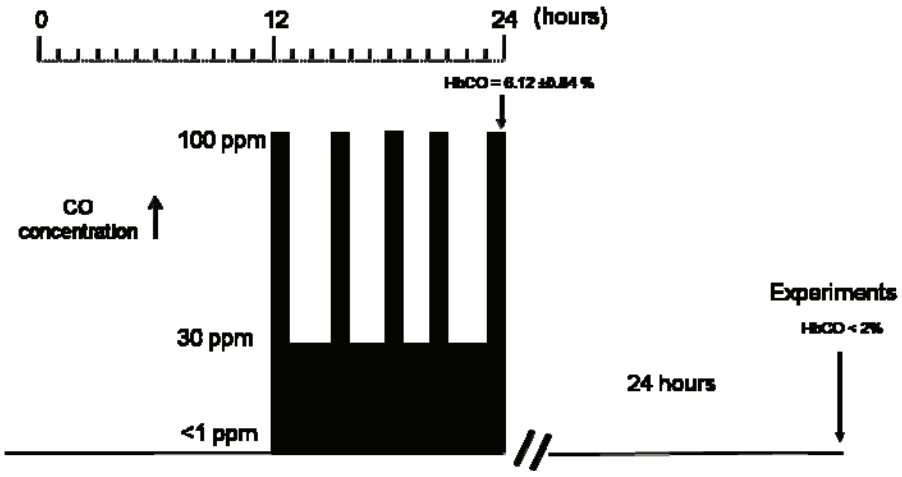

Figure 7 : Protocole d'exposition au CO

IV. Stratégies préventives et thérapeutiques

1. Exercice physique

Afin d'évaluer les effets potentiellement protecteurs de l'exercice physique, les rats ont été soumis à un protocole de course sur tapis roulant [50]. Huit semaines après la ligature coronaire, les animaux couraient sur tapis roulant à 16-18m/min, 5 jours/semaine, et 50 min/jour pendant 4 semaines. Le volume et l'intensité d'entraînement ont été incrémentés progressivement pendant la première semaine et une familiarisation des animaux avec le dispositif d'entraînement a été réalisée pendant deux jours précédents le protocole.

2. Traitement pharmacologique antioxydant au N-acétylcystéine

Les effets potentiellement protecteurs d'un traitement antioxydant ont été évalués chez différentes populations de rat à l'aide d'une supplémentation en N-acétylcystéine (NAC-Sigma). Le NAC était administré dans l'eau de boisson (75 mg / jour / animal) pendant 4 semaines [125]. Afin d'éviter toute dégradation de la molécule en solution, le breuvage était changé tous les deux jours.

V. Etudes *in vivo* sur cœur entier

1. Evaluation des propriétés morphologiques et fonctionnelles par échocardiographie

Les paramètres morpho-fonctionnels cardiaques ont été mesurés à l'aide d'une sonde haute fréquence (12 MHz) permettant l'acquisition d'image de qualité fine chez le rat. L'épaisseur des parois cardiaques ainsi que les dimensions du ventricule gauche ont été utilisées comme index de morphologie du myocarde. La fraction de raccourcissement du ventricule gauche, les vitesses de contraction du myocarde et le VTIAO (*Velocity time integral* - index de la vitesse du flux sanguin mesuré par Doppler TDI) ont été utilisés comme index fonctionnel du myocarde.

2. Mesure de l'activité électrocardiographique

Les enregistrements Holter ECG ont été effectués chez l'animal éveillé et libre de ses mouvements à l'aide d'un système télémétrique. Un capteur électrocardiographique (Data Sciences International, St Paul, MN, USA) était implanté sous anesthésie générale en position intra-péritonéale chez les rats 1 semaine avant l'acquisition ECG. Deux électrodes reliées au capteur étaient alors fixées en position sous-cutanée. L'électrode positive était fixée à l'apex du cœur, et la seconde dans la partie scapulaire du cœur. Le signal était enregistré continuellement sur une période de 24 heures. L'acquisition du signal était réalisée à l'aide du logiciel EMKA (ECG 1.50). La fréquence cardiaque, les intervalles PR, QRS, QT et QT corrigé (formule de Bazett), ainsi que la variabilité sinusale (dispersion des intervalles RR) ont été calculés. Les phénomènes arythmiques étaient détectés manuellement sur l'enregistrement de 24 heures. Ces mêmes paramètres ont été mesurés pendant une période de 2 heures consécutive à un *bolus* en isoprotérénol (1 $mg.kg^{-1}.min^{-1}$) afin d'évaluer les caractéristiques électrophysiologiques des différentes populations en condition de stress.

VI. Etudes *in-vitro* sur cardiomyocytes isolés

1. Isolement cellulaire :

La procédure d'isolement cellulaire suivait celle habituellement réalisée dans le laboratoire [21]. Brièvement, une thoracotomie était réalisée sur rat anesthésié par injection intra-péritonéale de pentobarbital sodique (40 mg/kg), après pesée de l'animal. Le cœur était prélevé, pesé sur une balance précise à 0,001 g (Modèle TE612, Sartorius, France), puis canulé sur un système de perfusion rétrograde Langendorff perfusé à 37° C. le cœur est alors perfusé par le système coronaire avec une solution physiologique de rinçage dépourvue de Ca^{2+}. Après un rinçage de 5 minutes permettant d'éliminer le sang du cœur et de fragiliser les jonctions intercellulaires, le cœur était ensuite perfusé pendant 15 minutes (20-25 minutes pour les cœurs de rat PMI) avec une solution enzymatique contenant de la collagénase de type A (0,8 mg/mL de solution Hanks-Hepes, Worthington Freehold, NJ, U.S.A), afin de digérer la matrice extracellulaire. Le dispositif expérimental utilisé est présenté figure 8. Le cœur était alors enlevé de la canule. Les 2 oreillettes étaient découpés, et le cœur placé dans une solution sans Ca^{2+}. Les couches externes sous-épicardiques et internes sous-endocardiques étaient disséquées puis les cellules extraites mécaniquement après agitation avec une pipette (P5000). La préparation était filtrée (Nylon 250 mesh) pour éliminer les tissus non dissociés, et les cellules étaient incubées pendant 15 minutes à 37° C durant lesquelles la concentration en Ca^{2+} est augmentée progressivement jusqu'à 1 mM. Les cellules reposaient alors 1 heure dans cette solution physiologique à 1 mM Ca^{2+}.

Pour la dissociation cellulaire, la solution tampon Hanks-HEPES contenait (en mM) : NaCl 117 ; KCl 5,7 ; $NaHCO_3$ 4,4 ; KH_2PO_4 1,5 ; $MgCl_2$ 1,7 ; HEPES 21 ; glucose 11,7 ; taurine 20 ; pH 7,15 ajusté avec NaOH. La remontée progressive des cellules en Ca^{2+}, ainsi que la technique d'imagerie calcique, utilisait cette même solution ajustée à différentes [Ca^{2+}].

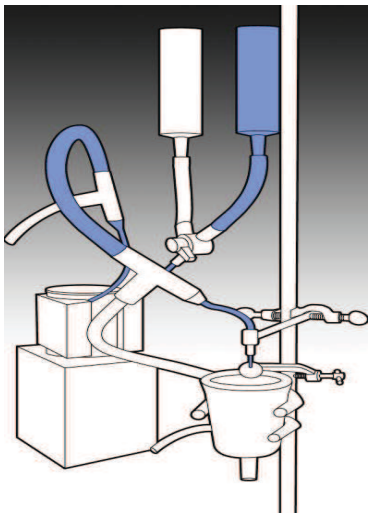

Figure 8 : Système de perfusion utilisé pour l'isolement des cardiomyocytes de rat (d'après Ait-Mou, thèse, 2008)

2. Mesure de la signalisation calcique intracellulaire et de la variation de longueur des sarcomères

La technique d'imagerie calcique permettait d'étudier le couplage entre la quantité de Ca^{2+} cytosolique mesurée à l'aide de sonde fluorescente et la contractilité de cardiomyocytes intacts en condition isotonique.

Les cellules étaient chargées avec un indicateur calcique ratiométrique fluorescent, l'Indo-1AM pendant 30 minutes (50 000 cellules / µL d'Indo). La forme acétoxyméthylester (AM) de la sonde permet de traverser la membrane. Les estérases cytosoliques hydrolysent la fonction ester, rendant alors l'Indo hydrophile et sensible au Ca^{2+}. Après excitation de la sonde à 360 nm, la forme libre de l'Indo-1 émet une fluorescence à 480 nm alors que la forme liée au Ca^{2+} émet à 405 nm. Ainsi, quand la concentration intracellulaire augmente, l'amplitude du pic à 480 nm diminue, alors que celle du pic à 405 nm augmente. Le rapport F405/F480 reflète alors la $[Ca^{2+}]_i$ dans une gamme de concentration de 5 nM à 30 µM, en minimisant les artefacts de mouvement. Les cellules étaient placées dans une cuve contenant la solution physiologique à 1,8 mM Ca^{2+}, et stimulées électriquement par des électrodes de platine. La longueur des sarcomères et la concentration en Ca^{2+} étaient mesurées en temps réel à l'aide du système IonOptix (Boston, USA). La sonde était excitée par une lampe Xénon 75 W (XBO 75, 14 V) à 360 nm. Les signaux de fluorescence étaient collectés par deux photomultiplicateurs (PM1, PM2, Hamamatsu R1104). L'acquisition et l'analyse des transitoires calciques étaient réalisées grâce au logiciel IonOptix.

La mesure de la longueur des sarcomères repose sur une propriété structurale intrinsèque des cardiomyocytes : l'alternance régulière des bandes claires (isotropes) et sombres (anisotropes) des protéines contractiles (actine et myosine). Cette alternance peut être assimilée à une fonction périodique de l'espace, analysée par une fonction mathématique : la transformée de Fourrier rapide (FFT). Cette fonction permet de transformer un signal périodique pur (de périodicité T) en une raie de fréquence dont la valeur fondamentale est 1/T. L'analyse fréquentielle des sarcomères par la FFT donne un spectre de fréquences dont la valeur fondamentale est inversement proportionnelle à la distance moyenne entre deux sarcomères. L'acquisition et la mesure de la longueur des sarcomères étaient réalisées à l'aide du logiciel IonOptix. L'analyse de la longueur des sarcomères s'effectuait à l'intérieur d'une fenêtre d'acquisition dont la position était choisie de telle sorte que l'on puisse avoir le maximum de sarcomères. L'analyse de l'image numérisée était effectuée toutes les 20 ms, durée inférieure à la durée moyenne de contraction des cellules cardiaques à température ambiante (22° C) qui est de plusieurs centaines de millisecondes. La résolution de la mesure de la longueur des sarcomères était de ± 7 nm.

Divers paramètres étaient analysés sur le transitoire calcique et le raccourcissement cellulaire. La fraction de raccourcissement cellulaire était mesurée par le pourcentage de variation de la longueur des sarcomères lors de la stimulation. L'amplitude du transitoire calcique, reflet de la quantité de Ca^{2+} libérée à chaque stimulation, était mesurée par la différence entre le pic du transitoire et le niveau basal.
Les vitesses de contraction et de relaxation cellulaire étaient calculées par la dérivée de la meure des sarcomères par rapport au temps. La dérivée de la décroissance du transitoire Ca^{2+} par rapport au temps était utilisée comme index de la vitesse d'élimination du Ca^{2+} cytosolique, c'est-à-dire de l'activité intégrée des pompes SERCA, NCX et mitochondriales.

La mesure simultanée de la fraction de raccourcissement et de l'amplitude du transitoire calcique nous permettait alors d'établir un lien entre la quantité de Ca^{2+} libérée et la contractilité des cellules intactes, définissant le gain du couplage excitation-contraction.

3. Mesure des sparks calciques

Les sparks Ca^{2+} correspondent aux unités de libération de Ca^{2+} par un petit réseau de RyR-2. Afin de mesurer cette activité, les cellules étaient chargées avec l'indicateur Fluo 4-AM (5 µM Invitrogen inc., France) pendant 20 minutes à température ambiante. La

fluorescence était enregistrée grâce à un microscope confocal inversé Zeiss LSM 510, à l'aide d'un objectif 63X à eau. Les images confocales étaient analysées par ligne de balayage le long de l'axe cellulaire. La fréquence d'acquisition par ligne était fixée à 1.54 ms par ligne; 512 pixels x 3000 lignes. Les images étaient alors analysées à l'aide du logiciel Image j (National Institutes of Health [disponible sur http://rsb.info.nih.gov/ij]) suivant la méthode décrite par Picht et al [139]. La fréquence des sparks Ca^{2+} était calculée pour chaque cardiomyocyte par le nombre de sparks enregistré sur 10 images successives enregistrées à différents endroits sur la cellule.

4. Mesure de la charge en Ca^{2+} du RS

Le contenu en Ca^{2+} du RS était mesuré sur cellules intactes chargées en Fluo-4. Après 5 minutes de stimulation électrique, une perfusion rapide en caféine (20mM) était utilisée afin de provoquer la libération massive des stocks en Ca^{2+} du RS.

5. Mesure de l'homéostasie en NADH cellulaire

Le NADH est un donneur d'électrons de la chaîne respiratoire, considéré comme un reflet de l'état énergétique des mitochondries [29]. L'autofluorescence endogène du NADH cellulaire était mesurée par microscopie confocale (Zeiss LSM 510NLO) à l'aide d'un objectif 25X à eau. Les cellules étaient stimulées électriquement à l'aide de 2 électrodes en platine. L'autofluorescence NADH était enregistrée au repos et après stimulation électrique. Pour chaque cellule, la valeur de fluorescence était obtenue après soustraction du bruit de fond mesurée dans l'environnement proche de la cellule.

6. Mesure de la production de ROS mitochondriale

Les cardiomyocytes isolés étaient chargés avec l'indicateur MitoSox Red (5 µM Invitrogen inc., France) pendant 15 minutes à température ambiante, afin d'évaluer la production d'anion superoxyde $O_2^{\cdot -}$. La fluorescence cellulaire était mesurée à l'aide du microscope confocal inversé Zeiss LSM 510NLO à l'aide d'un objectif 25X à eau. Pour chaque cellule, la valeur de fluorescence était obtenue après soustraction du bruit de fond mesurée dans l'environnement proche de la cellule.

7. Evaluation des propriétés contractiles des myofilaments

Les propriétés intrinsèques de la machinerie contractile étaient évaluées dans des conditions isométriques par la technique de micromécanique sur cellules pelées, comme précédemment réalisé au laboratoire (Cazorla *et al*., 1999). Le pelage des cellules permettait de perforer la membrane plasmique, le réticulum sarcoplasmique et les mitochondries, afin de contrôler la concentration interne en Ca^{2+}, et de s'intéresser uniquement aux propriétés de la machinerie contractile, indépendamment des autres composantes intracellulaires.

Après la dissociation cellulaire, les cellules intactes étaient incubées pendant 5 minutes à température ambiante et sous légère agitation, en présence d'une solution intracellulaire relaxante (milieu interne dépourvu de Ca^{2+} : composition au chapitre 2.4) contenant 0,3 % de Triton-X 100 (détergent utilisé pour le pelage cellulaire) ; 0,04 mM de leupeptine ; 0,01 mM d'E64. La leupeptine et l'E64 sont des anti-protéases protégeant la titine durant la procédure de pelage de sa dégradation par des protéases endogènes. Les cardiomyocytes étaient ensuite centrifugés à 1000 tours / min pendant 30 sec à 4° C. Le culot était lavé avec la solution relaxante. Les myofilaments ainsi obtenus étaient conservés à 4° C pendant toute la journée d'expérience.

La technique de micromécanique repose sur le collage des deux extrémités d'un cardiomyocyte pelé à des pointes piézo-résistantes (Figure 9) (AE801 sensor, Memscap, Crolle, France). Ces pointes sont préalablement enduites d'une colle optique à polymérisation aux UV (NOA 63, Norland Products Inc., Brunswick Nord, NJ). Avant chaque collage, un mélange eau / BSA était déposé pendant quelques minutes dans une boite de culture (Cellstar, Greiner Labotchnik, US) afin de limiter l'adhésion des cellules au fond de la boite. Avant chaque utilisation, les pointes étaient nettoyées (solution de soude 10 N pendant plusieurs minutes jusqu'à dissolution de la colle polymérisée du précédent collage), puis rincées à l'eau distillée, et déshydratées dans l'éthanol afin de favoriser l'efficacité du collage. La cellule était collée aux deux extrémités à des micro-pointes inoxydables (diamètre d'environ 20 µm). L'une des pointes était fixée sur une fine tige de verre, elle-même collée à une jauge de contrainte (modèle AE 801, Sensornor, Horten, Norvège). Celle-ci permettait de mesurer la tension isométrique développée par la cellule lors de la perfusion d'une solution activatrice (tension active). La jauge de contrainte était reliée à un amplificateur, et les signaux bruts étaient enregistrés sur un ordinateur (système IonOptix), filtrés (10 Hz) puis visualisés sur un traceur papier (Modèle Grass Dash IV 7400, Astro-Med Inc., West Warwick, USA) et

enregistrés sur un ordinateur. L'autre pointe était fixée à une tige de verre reliée à un système piézoélectrique (Modèle P-244.27, Physick Instruments, Waldbronn, Allemagne). Cette pointe était utilisée comme point fixe lors de la mesure de la tension développée par la cellule lors des contractions.

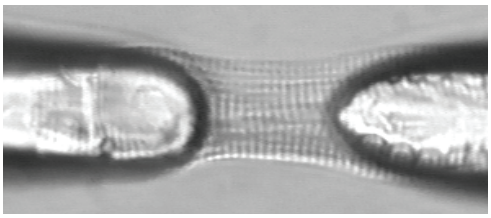

Figure 9 : Attachement du cardiomyocyte à deux pointes piézorésistives, l'une étant reliées à un capteur de tension

L'installation était placée sous un microscope inversé (Nikon Diaphot 300) sur lequel était montée une lampe au mercure 100 W (Modèle HB-10104AF, Nikon) qui permettait de transmettre les *flash* ultra-violets aux pointes (miroir dichroïque 400 nm, filtre d'excitation 330-380 nm). Une caméra CCD placée sur le microscope permettait de mesurer la longueur des sarcomères. L'ensemble du dispositif était monté sur une table antivibratoire (Micro-G, TMC, Peabody, USA) et recouvert par une cage de Faraday tapissée à l'intérieur d'une couche de mousse et fermée par un tissu noir. La cage permettait de diminuer le bruit électrique et la mousse d'absorber les vibrations qui pourraient être transmises aux pointes par le sol ou l'air. Pendant toute la durée d'expérience sur cellule isolée, la longueur des sarcomères était contrôlée avant et pendant les contractions. Ceci permettait de travailler toujours à la même longueur de sarcomère et de tester les effets de l'étirement sur les propriétés mécaniques de cellules pelées (sensibilité au Ca^{2+}). Pour cela, les cellules étaient positionnées tout d'abord à une longueur de sarcomère de repos de 1,9 µm puis étirées à 2,3 µm. Ces longueurs de sarcomère correspondent à la gamme de travail physiologique maximale observée *in situ* [21]. L'évaluation des propriétés actives des myofilaments à deux longueurs de sarcomère permettait d'étudier l'incrémentation de la sensibilité au Ca^{2+} induite par l'étirement.

Cette technique permettait l'étude de la relation entre la quantité de Ca^{2+} et la force générée par les myofilaments. Le système de perfusion était approché à proximité de la cellule pelée attachée. Il permettait de soumettre la cellule à des solutions contenant différentes concentrations en Ca^{2+}. Un ensemble de 9 seringues, contenant les solutions pCa (pCa = - log

[Ca^{2+}]) par mélange des solutions relaxante (pCa9) et activatrice (pCa4,5), permettait la perfusion de solutions avec une concentration croissante en Ca^{2+}(Figure 10A).

Les expériences avaient lieu à température ambiante (20-24° C) et la longueur des sarcomères était contrôlée en permanence par le logiciel IonOptix. L'étirement était réalisé manuellement en utilisant les micromanipulateurs (MO-103 Narishige, Charenton, France), et contrôlé par la transformée rapide de Fourrier.

Les tensions développées par la cellule au cours de l'expérience étaient visualisées sur un traceur papier, permettant la détermination de la tension développée à l'état stable par chaque cellule au cours de la perfusion des différentes pCa et aux deux longueurs de sarcomère (Figure 10A). La tension développée était ensuite normalisée par rapport à la tension isométrique maximale, classiquement obtenue à pCa5. Les cellules qui ne maintenaient pas 80% de la tension maximale initiale ou qui ne présentaient pas un « pattern » de striations visibles étaient éliminées. La force développée par le cardiomyocyte était normalisée par la section cellulaire.

La relation entre tension et pCa était lissée selon l'équation suivante :

$$Tension = \frac{\left[Ca^{2+}\right]^{n_H}}{\left(K + \left[Ca^{2+}\right]^{n_H}\right)}$$

Où K est la constante d'affinité, nH est le coefficient de Hill. K permet de déterminer la pCa50, concentration en Ca2+ (pCa) nécessaire pour développer 50% de la tension maximale, à partir de la relation : pCa50= - (log K) / nH. La détermination de la courbe qui rend compte au mieux des points expérimentaux (lissage) était réalisée à l'aide du logiciel Origin 7.5 (Figure 10B).

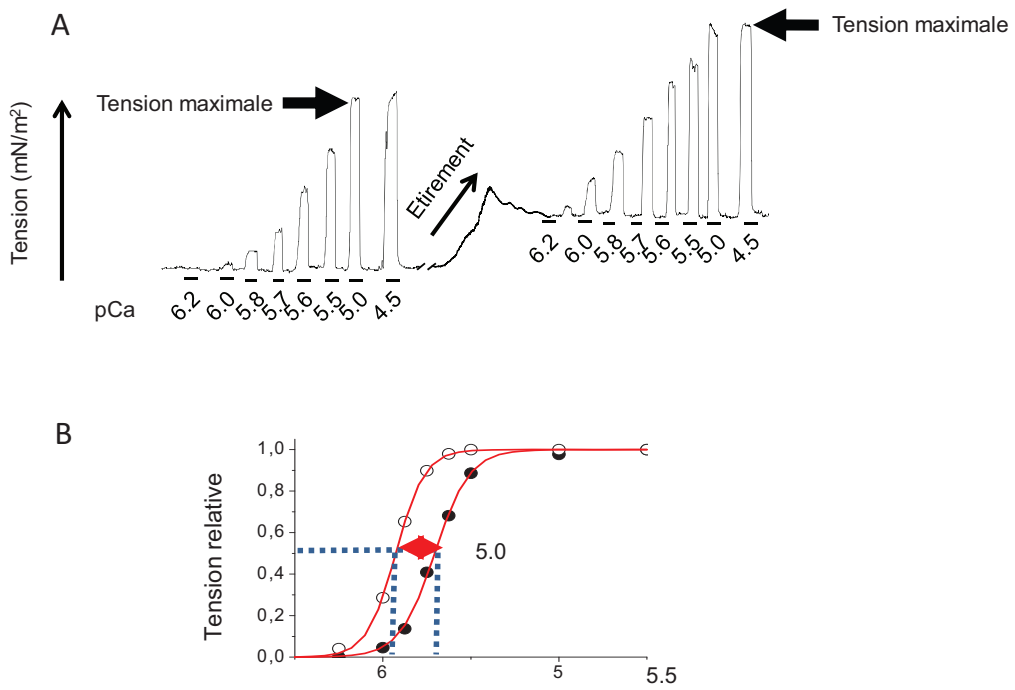

Figure 10 : A : Tracé de la force développée par la cellule en réponse aux différentes concentrations en Ca^{2+} ; B : Courbe Tension relative-pCa lissée

8. Solutions

Pour la mesure de force cellulaire en micromécanique, les solutions activatrices étaient préparées quotidiennement en mélangeant les solutions relaxantes (pCa9) et activatrices maximales (pCa4,5), contenant :

Solutions (mM)	Relaxante	Activatrice
Imidazole	30	30
K-acétate	58	58
Mg-Acétate	7.5	7.5
Na_2 ATP	3.3	3.3
Créatine P	12	12
K_2 EGTA	10	0.04
CaK_2 EGTA	0.04	10
Dithiotreitol	0.3	0.3

Des inhibiteurs de protéases (Leupeptin 0,04 mM et E64 [trans-epoxysuccinyl-1-leucine-guanidobutylamide] 0,01 mM) sont ajoutés, et le pH est ajusté à 7,1 avec KOH.

VII. Etude biochimique

Afin d'apporter un rationnel moléculaire aux modifications des paramètres physiologiques observées dans les différentes études, des analyses biochimiques des protéines impliquées dans le couplage excitation-métabolisme-contraction ont été réalisées.

1. Analyse des protéines du métabolisme mitochondrial

L'analyse du métabolisme mitochondrial par l'auto-fluorescence NADH a été complétée par la mesure des activités des complexes I et IV de la chaine de transport d'électrons mitochondriale. L'activité du complexe I était évaluée par la mesure de la réduction du 2, 6–dichlorophenolindophenol par les NADH déshydrogénase, à 600nm (37°C) {Janssen, 2007 #71}. La mesure du complexe IV a été réalisée par la mesure de l'activité de la cytochrome-c oxydase (COX) selon la méthode de Wharton and Tzagoloff [140]: l'oxydation du cytochrome-c était suivie par spectrophotométrie. La citrate synthase (CS) était mesurée par suivi de la fluorescence émise par l'acide 5,5'-dithiobis-2-nitrobenzoic cause par la déacetylaction de l'acetyl-CoA. La CS était utilisée comme index du nombre de mitochondries présentes dans le cardiomyocyte. Ainsi, les activités des complexes I et IV de la chaine de transport d'électrons étaient normalisées par rapport à l'activité de la CS.

Le statut antioxydant cellulaire a été établi par la mesure des activités des enzymes antioxydantes : catalase et Superoxyde dismutase (SOD). La catalase était mesurée selon la méthode décrite par Beers and Sizer [141]. La mesure de SOD était mesurée selon la méthode décrite par Marklund *et al.* [142].

2. Analyse des protéines de la signalisation calcique (RyR2, Serca, PLB)

Les altérations du cyclage du Ca^{2+} des cardiomyocytes observées dans les différentes études traduisent un remodelage biochimique des protéines impliquées dans les mouvements de Ca^{2+} intracellulaire. Ce remodelage est caractérisé par des variations de l'expression

(quantité et/ou isoformes) et des modifications post-traductionnelles (phosphorylation). Ainsi, le RyR2 et son état de phosphorylation, la Serca ainsi que le PLB étaient évalués sur culot de cellules congelé.

Les échantillons étaient solubilisés dans un tampon de lyse (en M : Tris 0,05, NaCl 0,2, b-glycérophosphate 0,02, EDTA 0,002, DTT 0,05, NaF 0,05, benzamidine 0,01, Na3VO4 0,0002, leupeptine 0,04, E64 0,01, PMSF 0,0005, 1% (v/v) Triton X100, pH 7.4). Les échantillons étaient maintenus dans cette solution 30 min à 4°C. Après dosage par *Reducing agent Compatible Detergent Compatible* (RC DC) le volume correspondant à 50 mg de protéine était prélevé de chaque échantillon et mixé pendant 15 min à 37°C avec une solution Laemmli-urée (en M : Tris-base 0,05, SDS 3% (w/v), urée 8, thio-urée 2, DTT 0,075, EGTA 0,001, EDTA 0,001,benzamidine 0,01, Na3Vo4 0,0002, b-glycérophosphate 0,02, NaF 0,05, leupeptine 0,04, E64 0,01, PMSF 0,0005, bleu de bromophénol). Les protéines étaient ensuite séparées sur un gel gradient (2-20 % SDS PAGE), 30 min à 70 V puis 1 heure à 150 V (Tableau 1).

	2%	20%
H2O	3,88	1,117
Acryl/Bis acryl 40 % (29/1)	0,27	2,5
Fairbanks (10 X)	0,50	0,50
Glycérol 100 %	0,25	0,75
SDS 20 %	0,025	0,025
APS 20 %	0,020	0,010
Temed	0,006	0,004

Tableau 1: Composition du gel intégrait les éléments suivants : (en mL)

L'immunodétection a été réalisée à l'aide d'anticorps secondaires couplés à la peroxydase et d'un kit de révélation ECL plus (Amersham Pharmacia, Little Chalfont Buckinghamshire, Angleterre). L'intensité de la fluorescence était acquise par une caméra CCD (Kodak image station 2000R). L'intensité des bandes était alors analysée en utilisant le logiciel Kodak1D 3.6 (Kodak, NY, USA). Le taux d'expression des protéines était normalisé par rapport à la calséquestrine (protéine cardiaque stable en réponse à divers stimuli) et le taux de phosphorylation des protéines était normalisé par rapport aux taux de leurs formes non phosphorylées.

3. Analyse des protéines contractiles (TnI, MLC2)

Afin de se replacer dans les conditions expérimentales des expériences de micromécanique, l'évaluation des protéines sarcomériques a été étudiée à partir de cœurs pelés (perfusion avec la solution relaxante contenant 1% de Triton X100). Des lambeaux de tissus ont été disséqués sous loupe binoculaire afin de suivre l'orientation des fibres. Les effets de l'étirement des fibres pelés sur les modifications protéiques étaient évalués sur des lambeaux de tissus étirés pendant 1 minute à une longueur correspondant à une longueur de sarcomère de 2,3 µm. Les différents tissus étaient alors congelés dans l'azote liquide et conservés à -80°C.

3.1. Analyse de la MLC-2 :

La procédure d'extraction de la MLC-2 suivait celle habituellement réalisée au laboratoire (Cazorla et al. 2005). Les tissus préalablement congelés étaient placés sur la glace dans une solution contenant 10 % d'acide Tri-Chloro-Acétique (TCA), dans laquelle ils étaient homogénéisés à l'aide d'un mixer (modèle PRO200, PRO scientific Inc, Oxford). Cette solution permettait le maintien de l'état de phosphorylation des protéines lors des différentes étapes du processus de solubilisation des échantillons. La suspension ainsi obtenue était centrifugée 10 min à 10 000 g à 4°C. Le culot était rincé trois fois avec une solution froide d'acétone contenant 10 mM de DTT. Après séchage, le culot était solubilisé 1 heure dans un tampon urée fraîchement préparé et contenant en mM (urée 0,008, Tris 10, glycine 20, DTT 10, sucrose saturé, ethylenediaminetetraacetic acid (EDTA) 0,2, PMSF 0,5, NaF 5). La quantité de protéine contenue dans chaque échantillon était dosée selon la méthode de Lowry (Lowry et al. 1951) en utilisant un kit RC DC dédié à cet effet (#500-120, biorad, USA). Les différentes formes de MLC-2 étaient alors séparées selon leurs charges sur un mini-gel (1,5 mm d'épaisseur) 10 % urée (Tableau 2).

Réactifs	
H2O	2.65 mL
Acryl/Bis acryl 40 % (29/1)	2.47 mL
Tampon gel urée	0.84 mL
Glycérol 100 %	3.96 mL
APS 20 %	30 µL
Temed	8 µL

Tableau 2: Composition du gel Urée 10 %

20 µg de protéines étaient ensuite déposés dans les puits du gel et migraient pendant 2 heures à 400 Volts. Les protéines étaient ensuite transférées dans un milieu semi-sec (1heure à 70 mA/mini gel) sur une membrane en nitrocellulose (Protran, Schleichen and Schuele, Dassel, Allemagne). La MLC-2 était détectée par un anticorps spécifique (1:200, Coger SA, Paris, France) ; la distinction entre la forme non phosphorylée et la forme phosphorylée est possible grâce à la différence de charge entre ces deux formes. Ainsi la forme phosphorylée ayant une charge négative supplémentaire migre plus loin sur le gel que la forme non phosphorylée.

Le degré de phosphorylation de la TnI était évalué sur des tissus solubilisés avec une solution contenant en M : Tris 0,05, NaCl 0,2, b-glycérophosphate 0,02, EDTA 0,002, DTT 0,05, NaF 0,05, benzamidine 0,01, Na3VO4 0,0002, leupeptine 0,04, E64 0,01, PMSF 0,0005, 1% (v/v) Triton X100, pH 7.4). 50 µg de proétines était déposé sur des gels 4-20% (Tableau 2). La TnI et sa forme phosphorylée par la PKA sur le Site $Ser^{23/24}$ étaient détectées à l'aide d'anticorps spécifiques.

4. Mesure de l'activité enzymatique de la PKA

L'activité de la PKA a été mesurée à l'aide d'un kit non-radioactif (Assay designs, France). Les tissus étaient mélangés à l'ATP pendant 90 minutes. L'incubation avec un anticorps spécifique de la PKA pendant une heure précédait la mesure de l'absorbance à 450 nm.

VIII. Statistiques

Les données sont présentées sous forme de moyennes ± SE. L'analyse statistique des résultats a été effectuée à l'aide du logiciel Statview 5.0. (Abacus concept, inc, Berkeley, CA). Les effets de la pathologie, de l'exposition au CO, de la régionalisation intra-cardiaque, et l'interaction des trois facteurs sont examinés par une ANOVA à 3 facteurs bimodaux. Les tests *Post-Hoc* de Bonferroni ont permis d'identifier les différences significatives *a posteriori*. Des tests de Chi2 ont été utilisés afin de comparer les différences de pourcentage (notamment dans les études 2, 3 et 5 pour comparer le pourcentage de cellules arythmiques). Le seuil de probabilité d'hypothèse nulle inférieur à 0.05 a été retenu comme significatif. Pour plus de clarté, seuls les résultats des tests *Post-Hoc* ont été présentés.

Résultats

1ère partie : Altérations du Couplage excitation-métabolisme-contraction dans l'IC ischémique : mécanismes physiopathologiques et stratégies préventives

I. Implication des ROS dans la perturbation de l'homéostasie calcique et dans l'arythmogénicité associée à l'IC ischémique : rôle de la voie PKA et effet d'un traitement chronique antioxydant

1. Introduction

Les arythmies ventriculaires sont une cause majeure de mort subite et sont responsables d'environ 50% des décès chez les patients souffrants d'IC [143]. Le récepteur de la ryanodine cardiaque (RYR-2) joue un rôle central dans le déclenchement de ces évènements arythmiques [144 145]. En effet, la dissociation de la protéine régulatrice du canal, le FKBP12.6, entraine une libération anarchique de Ca^{2+} par le récepteur à la ryanodine, laquelle est responsable de contractions désordonnées et incontrôlées des cardiomyocytes [69]. Deux mécanismes distincts ont été proposés à l'heure actuelle pour expliquer la dissociation du complexe RyR-2/FKBP12.6 : l'hyper-phosphorylation, notamment par une hyperactivation de la protéine kinase A (PKA) [69], et l'oxydation/nitrosylation par les espèces oxygénées réactives (ROS) du RyR2. D'autre part, certains auteurs ont rapporté que les ROS pouvaient directement activer la protéine kinase A dans certains tissus comme le cerveau, entrainant alors la phosphorylation de ses protéines cibles [146]. L'objectif de cette première étude a alors été de déterminer si la production excessive de ROS associée à l'IC ischémique pouvait activer la PKA dans les cardiomyocytes et entrainer des perturbations du RyR-2

2. Article 1 - Soumis pour publication

ROS contribute to PKA-dependent RyR2 phosphorylation and trigger ventricular arrhythmias in ischemic heart failure

Running title: ROS-induced PKA-dependent RyR2 phosphorylation

Lucas Andre[1]*, Jeremy Fauconnier[1] *, Valérie Scheuermann[1], Christine Feillet-Coudray[2], Gilles Fouret[2], Sylvain Richard[1], Andrew R. Marks[3], Olivier Cazorla[1] and Alain Lacampagne[1]

[1]INSERM, U-637, F-34295 Montpellier, France. Université MONTPELLIER 1, UFR de Médecine, F-34295 Montpellier, France
[2]INRA UMR866, Différenciation cellulaire et croissance, 34060 Montpellier, France.
[3]Clyde and Helen Wu Center for Molecular Cardiology, Department of Physiology & Cellular Biophysics, Columbia University College of Physicians & Surgeons, New York, NY, USA

*Contributed equally to this work

Corresponding author:
Alain Lacampagne
Inserm U637 Physiopathologie Cardiovasculaire
CHU Arnaud de Villeneuve
34295 Montpellier, France
Phone: +33 467 41 52 44
Fax: +33 467 41 52 42
alain.lacampagne@inserm.fr

Key words: Oxidative stress, ectopic Ca^{2+} transient, calstabin2

Number of words: 5499

Abstract:

During ischemic heart failure (HF), defects in ryanodine receptor (RyR2) function promote the occurrence of ventricular arrhythmic events. Here we aimed to determine whether and how HF related redox imbalance could be involved in this arrhythmogenicity. Twelve weeks after myocardial infarction (MI) in rats the generation of superoxide anion ($O_2^{\cdot-}$), evaluated by confocal microscopy using MitoSOX Red dye, was significantly increased over sham operated animals. The activities of both superoxide dismutase and catalase were decreased as well as the activities of both complexes I and IV of the mitochondrial electron transport chain. Incubation of MI cardiomyocytes for 45 min with the antioxidant N-Acetyl Cysteine (NAC) normalized the HF-associated Ca^{2+} handling defects (i.e. decreased Ca^{2+}-sparks frequency, decreased SR Ca^{2+} load and systolic Ca^{2+} release). The occurrence of spontaneous Ca^{2+} waves was also reduced by NAC incubation. The MI-associated Ca^{2+} signaling defects were closely linked with increased PKA activity, PKA-dependent RyR2 phosphorylation and calstabin2 (FKBP12.6) depletion from RyR2 macromolecular complex. Chronic treatment of MI rats with NAC for 4 weeks prevented Ca^{2+} handling defects and RyR2 dysfunction, normalized PKA activity and reduced *in vivo* arrhythmic events. Impaired redox balance during HF affects PKA-mediated RyR2 phosphorylation, thereby contributing to Ca^{2+} handling disturbances and arrhythmias. A therapeutic strategy aimed at improving redox imbalance may provide beneficial anti-arrhythmic effects by preventing PKA-dependent RyR2 phosphorylation and calstabin2 depletion.

Abbreviations

CPVT	Catecholaminergic Polymorphic Ventricular Tachycardia
CS	Citrate synthase
DAD	Delayed After Depolarization
EC	Electrocardiogram
FKBP	FK506 Binding protein
Fluo-3-AM	4-(6-Acetoxymethoxy-2,7-dichloro-3-oxo-9-xanthenyl)-4'-methyl-2,2'-(ethylenedioxy)dianiline-N,N,N',N'-tetraacetic acid tetrakis(acetoxymethyl) ester
HF	Heart Failure
HRV	Heart Rate Variability
MI	Myocardial Infarction
NAC	N-Acetyl Cysteine
PKA	Protein kinase A
PVB	Premature Ventricular Beat
ROS	Reactive Oxygen Species
RyR2	Cardiac ryanodine receptor
SDNN	standard deviation of normal-to-normal intervals
SOD	Superoxide dismutase
SR	Sarcoplasmic Reticuum
VA	Ventricular Arrhythmias

Introduction

Ventricular arrhythmias are a major cause of sudden cardiac death that account for ~50% of deaths in patients with heart failure (HF) (Cohn *et al.*, 1986). The cardiac ryanodine receptor (RyR2) macromolecular complex is now recognized as a central actor in triggering HF-associated ventricular arrhythmogenesis (Farr & Basson, 2004; Wehrens *et al.*, 2004). Indeed, disruption of the RyR2/calstabin2 (also known as FKBP12.6) complex promotes diastolic sarcoplasmic reticulum (SR) Ca^{2+} leak and subsequent delayed after depolarisations (DADs) (Pogwizd *et al.*, 2001). Protein kinase A (PKA)-dependent RyR2 phosphorylation (Marx *et al.*, 2000; Wehrens *et al.*, 2003) and redox modification of RyR2 (Yano *et al.*, 2005; Zissimopoulos *et al.*, 2007; Terentyev *et al.*, 2008) are known to contribute to HF-associated RyR2 dysfunction. Although both mechanisms have been propose to increase SR Ca^{2+} leak in chronic HF, it is not clear whether redox modification and PKA-phosphorylation pathways are independent mechanisms. Moreover, the role of PKA mediated RyR2 phosphorylation in the regulation of calcium handling remains extremely controversial.

Ca^{2+} signalling requires ATP and depends on cardiac metabolic properties. It is now accepted that failing hearts exhibit oxidative stress and defective energy metabolism (Neubauer, 2007). Reactive oxygen species (ROS) are known to modify the phosphorylation status of proteins notably through activation of PKA (Rhee *et al.*, 2000; de Lamirande & O'Flaherty, 2008). We thus hypothesized that, in ischemic HF, ROS production activates PKA leading to RyR2 PKA phosphorylation and subsequent impairment of RyR2 function and, thereby, Ca^{2+} handling. Our results show that HF associated-metabolic defects lead to a redox imbalance that affects RyR2 function *via* a PKA-dependent pathway. Chronic (4 weeks) *in vivo* treatment with an anti-oxidant (N-Acetyl Cysteine, NAC) reduced PKA-dependent RyR2 phosphorylation as well as PKA-activity and ventricular arrhythmias.

Methods

Animals

The investigations conformed to the *Guide for the Care and Use of Laboratory Animals* published by the US National Institute of Health (NIH Publications No. 85-23, revised 1996) with the approval of French Agriculture Department. Male Wistar rats (5 weeks old, Charles River) were randomly assigned to left coronary artery ligation in order to induce myocardial infarction (MI rats) or to sham-operated procedure (Sham rats) (Cazorla *et al.*, 2005). Eight weeks after MI, 15 rats (MI-NACc) were chronically treated with NAC (Sigma) administered in the drinking water (75 mg/day per animal) for 4 weeks (Bourraindeloup *et al.*, 2004). Experiments were performed 12 weeks post-ligature. The HF state of rats was assessed by Doppler-echocardiography. A group of Sham rats was treated by "rycal" S107 (0.25 g/L of drinking water, for 7 days before sacrifice), an orally available specific RyR Ca^{2+} release channel stabilizer that inhibits depletion of calstabin2 from the RyR2 complex. (Fauconnier *et al.*)

ECG Recording and analysis

Rats were implanted with radio transmitters for ECG telemetry (Data Sciences International, Minnesota, USA). Surface ECG was recorded for a 24 h period, 12 weeks after MI. ECG signals were manually analyzed to identify and count spontaneous arrhythmic disorders. Heart rate variability was also analyzed. The mean (RR) and standard deviation (SDNN) of all normal RR intervals were calculated. Ventricular arrhythmias were also measured after isoproterenol (2.5 mg.kg-1, IP) performed for each animal during a period of 2 hrs.

Cell isolation

Single left ventricular cardiomyocytes were isolated by enzymatic digestion (Mou *et al.*, 2009). Briefly, hearts were quickly removed and mounted on a Langendorff apparatus. The heart was perfused

with a Ca^{2+}-free solution (in mM : NaCl 117, KCl 5.7, $NaHCO_3$ 4.4, KH_2PO_4 1.5, $MgCl_2$ 1.7, HEPES 21, glucose 11, taurine 20, pH 7.2 adjusted with NaOH) followed by perfusion with a collagenase IV enzymatic solution (Worthington, USA). The infarct and boarder zones were discarded. Small pieces of left ventricular tissues were dissociated and the Ca^{2+} concentration was gradually increased to 1 mM.

Measurement of mitochondrial ROS production

Isolated cardiomyocytes were loaded with MitoSOX Red (5 µM Invitrogen inc., France) for 15 min at room temperature, followed by washout, to evaluate mitochondrial $O_2^{\cdot-}$ production (Fauconnier *et al.*, 2007). Fluorescence images were recorded using a Zeiss LSM 510 inverted confocal microscope with an x25 lens (H_2O immersion, NA=0.8). Confocal images were obtained at 5-min intervals by excitation at 488 nm. Emitted light was measured at 583 nm. MitoSOX Red fluorescence was collected at rest and after 5 min stimulation at 0.5 HZ. For each cell, resting fluorescence value was obtained after subtracting background noise measured outside the cell and set to 100%.

Ca^{2+} imaging in intact cardiomyocytes

Cardiomyocytes were loaded for 30 min at room temperature (22 ± 2°C) with Indo-1 AM (10 µM Invitrogen inc., France) in order to monitor intracellular Ca^{2+}. Cells were field stimulated at 0.5 Hz (20 V, 1 ms), and simultaneously illuminated at 305 nm using a xenon arc bulb light. Indo-1 fluorescence was recorded at 405 nm and 480 nm (IonOptix system, Hilton, USA). Spontaneous SR Ca^{2+} waves were analyzed during a rest period of 30 s following a pacing period of 1 min at 0.5 Hz.

For Ca^{2+}-sparks analysis, myocytes were loaded with Fluo-4 AM (5 µM Invitrogen inc., France) for 20 minutes at room temperature. Fluorescence images were recorded using a Zeiss LSM 510 inverted confocal microscope (63X H_2O immersion objective, NA= 1.2). Confocal images were obtained by line scanning along the long axis, with focus in the middle of the cell at two different places. Line scan rate was set to 1.54 ms per line; 512 pixels x 3000 lines. Stored confocal images were analyzed with Image J (National Institutes of Health [available at http://rsb.info.nih.gov/ij]) according to the methods described by Picht et al (Picht *et al.*, 2007). Ca^{2+}-sparks frequency was calculated for each cardiomyocyte as the number of sparks recorded on 10 successive images collected at different line location. The SR Ca^{2+} content was measured in intact cardiomyocytes loaded with Fluo-4. After 5 minutes of electrical stimulation at 0.5 Hz, rapid perfusion of caffeine (20 mM) was used to induce full release of Ca^{2+} from the SR.

Determination of mitochondrial enzymatic activities in cardiomyocytes

After cell lysis in hypotonic buffer (phosphate buffer 8 mM, pH 7.4), catalase activity was measured according to the procedure described by Beers and Sizer (Beers & Sizer, 1952) and total superoxide dismutase (SOD) was measured as described by Marklund (Marklund, 1976). Protein levels in cell homogenates were measured using the Bradford technique (Bradford, 1976). Citrate synthase (CS) activity was measured by following the color of 5-thio-2-nitrobenzoic acid (Srere, 1970). Complex I of the electron transport chain (ETC) was evaluated by measuring the reduction of 2, 6– dichlorophenolindophenol by the NADH dehydrogenase at 600 nm (37°C) (Janssen *et al.*, 2007). Complex IV of the ETC was estimated by determining the oxidation of cytochrome-c oxidase (Cyt-c oxidase) activity (Wharton, 1978).

Protein Analysis

Proteins were separated using 2-20 % SDS-PAGE and blotted onto a nitrocellulose membrane (Protran, Schleichen and Schuele, Dassel, Germany). Membranes were incubated overnight at 4°C with the following primary antibodies: anti-RyR2 (Covalab, France), anti-Phospho Ser^{2809}-RyR2 (A010-30, Badrilla, UK), anti-calstabin (BD biosciences**,** Le Pont de Claix, France). RyR2 levels were expressed relative to calsequestrin content (PA1-913, ABR, USA) on the same membrane. Immunodetection was carried out using the ECL Plus system (Amersham Pharmacia, Little Chalfont Buckinghamshire, England).

RyR2 was immunoprecipitated by incubating 250 mg of homogenate with anti-RyR antibody in 0.5 ml of a modified RIPA buffer (in mM: Tris·HCl 50, NaF 5.0, Na_3VO_4 1.0; pH 7.4, 0.9% NaCl 0.5% Triton X-100, and protease inhibitors) for 1 h at 4°C. The samples were incubated with protein A Sepharose beads (Amersham Pharmacia) at 4°C for 1 h, after which the beads were washed three times with RIPA buffer. Proteins were separated with SDS-PAGE gel (4-20% gradient) and transferred onto nitrocellulose membranes for 2 h at 200 mA (SemiDry transfer blot; Bio-Rad). After incubation with blocking solution (Li-Cor Biosciences) to prevent nonspecific antibody binding and a wash in Tris-buffered saline with 0.1% Tween-20, membranes were incubated for 1-2 h at room temperature with primary antibodies anti-calstabin (1:2,500 in blocking buffer).

PKA activity was measured using a non-radioactive PKA activity assay kit according to manufacturer recommendations (Assay designs, France).

Statistical analysis

Data were analyzed using a one-way or 2-way ANOVA between groups. When significant interactions were found, a Bonferroni post-hoc test was applied with $p < 0.05$ (Statview 5.0). For spatio-temporal properties of Ca^{2+}-sparks, statistical comparison of population parameters between groups was conducted using a nonparametric Kruskal-Wallis test. Data were presented as mean±SE.

Results

Mitochondrial function is altered in HF

Mitochondrial $O_2^{\cdot-}$ production was measured, using MitoSOX Red (Fauconnier *et al.*, 2007), after pacing the cardiomyocytes for 5 minutes at 0.5 Hz. Mitochondrial ROS production was higher in MI rats than in sham rats (27±5 % *vs* 12±4 %, respectively; *p<0.05) (Fig. 1A). Oxidative stress results from an imbalance between pro-oxidant activities and antioxidant defense buffering ROS. We thus evaluated the antioxidant enzyme activities, SOD which converts $O_2^{\cdot-}$ to H_2O_2, and catalase which converts H_2O_2 to H_2O. Both SOD and catalase activities were reduced in HF rat hearts (Fig. 1B) potentially accounting for the higher susceptibility to oxidative stress in HF. ROS production may also be increased under conditions of inefficient oxidative metabolism, mainly due to reduced complex I (Pitkanen & Robinson, 1996; Ide *et al.*, 1999). We measured mitochondrial metabolic parameters to determine whether mitochondrial dysfunction could account for HF-associated abnormal ROS production. The reduced redox carriers NADH and $FADH_2$ are oxidized in the inner membrane of mitochondria by complexes (I-IV) of the ETC. The electron transfer of both NADH and FADH2 generates a proton motive force driving ATP synthesis via the terminal complex (complex V) (Stanley *et al.*, 2005).

Complex I and IV activities were normalized to CS activity, an index of mitochondrial content. CS activity, as well as normalized complex I and IV, were decreased in MI rats (Fig. 1C).

Role of oxidative stress on abnormal Ca^{2+} release in HF

Oxidative stress is known to disturb Ca^{2+} handling (Zima & Blatter, 2006). In order to determine whether ROS affect RyR2 function in HF, we measured spontaneous Ca^{2+}-sparks, as an index of diastolic Ca^{2+} leak, before and after incubating cardiomyocytes with the non specific antioxidant NAC (20 mM) for 1 hour. Ca^{2+}-sparks frequency was higher in MI rats than in sham animals (Fig. 2A). Acute *in vitro* incubation with NAC for 1 hour restored normal Ca^{2+}-sparks frequency, suggesting involvement of ROS-mediated SR Ca^{2+} leak during HF. We thus evaluated whether a chronic *in vivo* antioxidant treatment could prevent this RyR2 dysfunction. Rats treated with NAC for 4 weeks (75 mg/day per animal) had a Ca^{2+}-sparks frequency similar to sham animals suggesting a normalization of SR Ca^{2+} leak by an antioxidant treatment.

Increased diastolic SR Ca^{2+} leak is known to reduce SR Ca^{2+} content and to promote cytosolic Ca^{2+} overload. In accordance, diastolic Ca^{2+} was increased (Fig. 2C) and SR Ca^{2+} load was reduced

(Fig. 2E) in MI rats. In addition, peak Ca^{2+} transient was decreased (Fig. 2D). When failing cardiomyocytes were incubated with NAC for 1 hour, diastolic free Ca^{2+} was reduced whereas Ca^{2+} transient amplitude and SR Ca^{2+} load were restored to values similar to that obtained in sham rats (Fig. 2B-E). Moreover, chronic NAC treatment totally prevented all MI-associated Ca^{2+} handling alterations (Fig. 2).

Taken together these results indicate that antioxidant treatment prevented impaired RyR2 function and Ca^{2+} handling in MI rats. Increased Ca^{2+}-sparks activity and diastolic [Ca^{2+}] are known to promote arrhythmic events in cardiomyocytes (Hove-Madsen *et al.*, 2004)' (Fauconnier *et al.*). We thus evaluated whether ROS-dependent impairment of Ca^{2+} handling in MI cardiomyocytes resulted in ectopic Ca^{2+} transients and/or Ca^{2+} waves. Fig. 2F shows Ca^{2+} transients in ventricular myocytes paced at 0.5 Hz. Spontaneous Ca^{2+} waves triggered after electric pacing interruption were observed in 21% of Sham and 36% of MI cardiomyocytes. This is consistent with higher triggered activity and DADs in HF. Acute NAC treatment corrected this arrhythmic phenotype, supporting the concept of ROS-induced Ca^{2+} waves in HF. The chronic administration of NAC also completely prevented the HF-associated Ca^{2+} waves.

ROS-induced PKA phosphorylation of RyR2

Leaky RyR2 and subsequent DADs have been attributed to calstabin2 depletion from the RyR2 macromolecular complex (Pogwizd *et al.*, 2001). Consistently, RyR2 was found to be depleted from calstabin2 in MI rats (Fig. 3A). Acute NAC treatment of MI myocytes partially prevented this depletion, supporting the hypothesis of a ROS-mediated dissociation of calstabin2 from the RyR2 complex [10]. Given that PKA-dependent RyR2 phosphorylation has been linked to calstabin2 dissociation and that ROS can activate PKA (Brennan *et al.*, 2006) we sought to determine whether ROS-dependent activation of PKA contributes to RyR2 PKA phosphorylation. RyR2 was PKA hyperphosphorylated in MI rats (Fig. 3B). Acute *in vitro* (MI-NACa) and chronic *in vivo* (MI-NACc) NAC treatment prevented this hyperphosphorylation. PKA activity was then measured in different cardiac tissues to determine whether MI-induced RyR2 hyperphosphorylation was associated with an increased PKA activity. In MI rats, the PKA activity was increased compared to Sham animals (Fig. 3C). Acute treatment with NAC restored PKA activity toward Sham level. In addition, chronic NAC treatment decreased PKA activity in MI rats to a level lower than that seen in Sham animals (Fig. 3C).

In order to determine whether ROS are directly responsible for PKA activation, we also measured PKA activity in sham tissue incubated for 20 min with hydrogen peroxide H_2O_2 (0.1 mM). PKA activity was significantly increased following acute incubation with H_2O_2 (Fig. 3C) thus supporting the hypothesis of a direct ROS-dependent PKA activation (Brennan *et al.*, 2006). Furthermore, RyR2 was hyperphosphorylated on serine 2809 (Fig. 3D) known as a PKA dependant phosphorylation site and calstabin2 depleted (Fig. 3E) in Sham tissue incubated with H_2O_2. When myocytes were pre-incubated with NAC for 1 hour, the effects of H_2O_2 on RyR2 phosphorylation and calstabin2 depletion were abolished, thus confirming the buffering effect of NAC (Fig. 3D-E). We then performed the same experiment with cardiac samples from sham animal treated with S107, a well described stabilizer of RyR2/calstabin2 complex (Fauconnier *et al.*, ; Bellinger *et al.*, 2008). Chronic treatment of Sham rats with S107 did not affect RyR2 phosphorylation status and RyR2/calstabin2 complex interaction (Fig. 3D, E). Subsequent treatment of these myocytes with H_2O_2 increased PKA-dependent RyR2 phosphorylation without modifying the calstabin2/RyR2 ratio. Altogether, these results suggested that PKA activity is increased during oxidative stress and may account in part for the ROS-dependent RyR2 dysfunction in MI rats.

ROS contribute to Isoproterenol-induced alterations of Ca^{2+} handling

The functional consequences of isoproterenol (ISO, 10 nM) stimulation on ROS production, RyR2 function, and PKA activity were then evaluated in sham and MI rat myocytes. Application of ISO (Fig. 4A) increased ROS production in both Sham and MI myocytes. Of note, as shown in Fig. 1A, ROS levels were higher in MI than in Sham cardiomyocytes. In both conditions, incubation of the cardiomyocytes with NAC reduced the level of ROS, as expected for an antioxidant. Furthermore,

under NAC treatment ROS production before and after ISO stimulation of MI myocytes were normalized to Sham levels (Fig. 4A). We then evaluated the PKA activity in Sham cardiomyocytes under ISO stimulation (Fig. 4B). The typical increased PKA activity under ISO stimulation was lowered in cardiomyocytes incubated in NAC. Taken together, these results suggest that part of the ISO effects are mediated by ROS. Given that ISO increases ROS production and that ROS increases SR Ca^{2+} leak, we evaluated the functional consequence of ISO on RyR2 by measuring spontaneous diastolic Ca^{2+}-sparks frequency under ISO treatment (Fig. 4C). Ca^{2+}-sparks frequency was significantly increased in MI compared to sham cardiomyocytes. This increase was fully abolished by an acute (MI-NACa) or chronic (MI-NACc) treatment demonstrating the role of ROS elevation in ISO elicited RyR2 activity (Fig. 4C).

The increase in Ca^{2+}-sparks frequency under ISO stimulation was associated with the triggering of Ca^{2+} waves. This was, again, abolished by chronic NAC treatment (Fig. 4D). To quantify the propensity of ISO stimulation to trigger spontaneous Ca^{2+} waves, we calculated the percentage of cardiomyocytes exhibiting spontaneous Ca^{2+} waves during the first 30 s of ISO perfusion. ISO increased the percentage of Ca^{2+} wave in MI cells and this again was partially abolished by an acute NAC treatment and fully abolished by a chronic treatment.

Chronic NAC treatment prevents electrophysiological disturbances *in vivo*

Surface ECGs were recorded and analyzed in conscious rats from the sham, MI and MI-NACc groups. The basal heart rate was increased in MI rats (Fig. 5A). This was prevented by chronic NAC treatment. When the animals were challenged with isoproterenol (1 $mg.kg^{-1}$ i.p.), the heart rate in both groups was increased but the difference between sham and MI rats was abolished, reflecting a weaker response to β-adrenergic stimulation in MI rats (Fig. 5A). Surprisingly, chronic NAC treatment increased the heart rate of MI rats during ISO challenge, suggesting an increased cardiac reserve to β-adrenergic stimulation compared to Sham and MI rats. Although the PR duration was similar in the three groups, the QRS, QT and QTc intervals were prolonged in MI rats compared to sham (Table 1). All these prolongations were not affected by NAC treatments (Table 1). The standard deviation of normal-to-normal intervals (SDNN), an estimate of overall heart rate variability (HRV), was decreased in MI rats (Fig. 5B). Chronic NAC treatment partially prevented this HRV decrease. Increased heart rate and decreased HRV are usually associated with an increased occurrence of arrhythmic events. The number of premature ventricular beats (PVB) at rest and after ISO challenge was estimated. MI rats displayed a 64% increase in the number of PVB at rest, which was amplified under conditions of ISO stimulation (Fig. 5C). Chronic NAC treatment abolished occurrence of PVB both at rest and after ISO stimulation (Fig. 5C). Accordingly, sustained ventricular tachycardia, absent in shams, were detected in 80% of MI rats and only 40% of MI-NACc rats.

Discussion

This study highlights the major impact of ROS production on Ca^{2+} handling in an experimental rat model of HF. We showed that during HF: (i) mitochondrial abnormality were associated with an imbalance of the redox state, which altered Ca^{2+} handling; (ii) ROS increased PKA activity; (iii) ROS induced phosphorylation of RyR2 on serine 2809; (iii) β-adrenergic stimulation promoted ROS production that amplified PKA-dependent phosphorylation of RyR2, (iv) chronic antioxidant treatment with NAC normalized PKA activity as well as Ca^{2+} handling disturbances and prevented ventricular arrhythmias (VA) during HF.

Thus, this study identifies a new pathway involving ROS production and leading to defective RyR2 function, subsequent Ca^{2+} handling disturbance and related ventricular arrhythmias in HF. Moreover, this study provides new insight regarding to the potential consequence of PKA mediated RyR2 phosphorylation. It may be proposed that this phosphorylation become deleterious for the channel only in case of a redox imbalance.

As previously reported (Neubauer, 2007), the mitochondrial oxidative capacity in cardiomyocytes from failing MI rats is weaker due to reduced electron transport chain activity. Decreased oxidative phosphorylation, mainly attributed to defects in complex I, is associated with increased superoxide anion production (Pitkanen & Robinson, 1996; Ide *et al.*, 1999). As a consequence, the metabolic defects of failing hearts are associated with elevated ROS production after cell stimulation. In the present study, as in others (Hill & Singal, 1997; Sawyer & Colucci, 2000; Giordano, 2005), the imbalance in ROS homeostasis during HF may result from a reduced respiratory chain capacity and also from a decrease in oxidative defenses (SOD and catalase).

Increased ROS levels lead to dysfunction of numerous cardiac proteins (Stadtman, 1992; Takimoto & Kass, 2007; Wang *et al.*, 2008). Among potential targets, RyR2 is particularly sensitive to redox modulation (Zima & Blatter, 2006). In the present study, we demonstrate indeed that SR Ca^{2+} leak in MI rats was corrected by acute NAC treatment, thus supporting further the notion that ROS alter RyR2 open probability (Yan *et al.*, 2008). To date, the mechanisms underlying the ROS-induced RyR2 alterations have been attributed to a direct modification of RyR2 (Terentyev *et al.*, 2008; Yan *et al.*, 2008; Belevych *et al.*, 2009). However, ROS can also inhibit protein phosphatase activity (Rhee *et al.*, 2000) and activate PKA (O'Flaherty *et al.*, 2006; de Lamirande & O'Flaherty, 2008), thus modifying protein phosphorylation status. We established here that ROS contribute to PKA-dependent RyR2 phosphorylation. We also provide further evidence that, in HF, abnormal increases in ROS levels activate PKA leading to chronic RyR2 phosphorylation, depletion of calstabin2 from the RyR2 macromolecular complex and SR Ca^{2+} leak (Marx *et al.*, 2000; Wehrens *et al.*, 2004; Lehnart *et al.*, 2008).

Cumulative evidence indicates that the RyR2 redox state modifies calstabin2 binding affinity (Zissimopoulos *et al.*, 2007; Terentyev *et al.*, 2008), which leads to SR Ca^{2+} leak. Thus, direct ROS-induced redox modification, as well as ROS-induced PKA activation, may act in synergy to dissociate calstabin2. Although the present study was designed to specifically address the effect of ROS on the PKA-dependent regulation of RyR2, one cannot exclude ROS activation of CamKII and CamKII-dependent RyR2 phosphorylation (Howe *et al.*, 2004), (Erickson *et al.*, 2008). This remains to be examined.

In addition to the SR Ca^{2+} leak, ROS also contributed to decreased systolic Ca^{2+} release in MI rats. Indeed, recovering normal diastolic RyR2 activity prevents SR Ca^{2+} depletion, thereby preserving appropriate conditions for an optimal systolic Ca^{2+} release.

Diastolic Ca^{2+} overload is a major substrate for oscillations of the cellular membrane potential and triggering of delayed after depolarisations (DAD) (Ter Keurs & Boyden, 2007). Ca^{2+} overload leads to the activation of a Na^{+}/Ca^{2+} exchanger-mediated transient depolarizing inward current I_{ti} and reduction of the inward rectifier potassium current I_{K1} favoring the occurrence of DADs (Pogwizd *et al.*, 2001; Fauconnier *et al.*, 2005). Scavenging excessive ROS production reduced SR Ca^{2+} leak and ectopic Ca^{2+} transients through a normalization of RyR2 function as previously reported (Terentyev *et al.*, 2008). These results are also in line with recent work showing a decline of Ca^{2+} alternans with reducing agents in a canine MI model of sudden cardiac death (Belevych *et al.*, 2009). Furthermore, under isoproterenol stimulation, the cellular pro-arrhythmic phenotype was worsened. Indeed, we provide evidence that ISO increases ROS production leading to increased RyR2 PKA phosphorylation and SR Ca^{2+} leak.

However, we also show that part of the ISO effects is mediated by ROS. Thus, ISO may activate PKA through multiple pathways: a direct activation involving the G-protein / adenylate cyclase pathway and an indirect activation mediated by ROS (O'Flaherty *et al.*, 2006; de Lamirande & O'Flaherty, 2008). Nevertheless, our results suggest that RyR2 phosphorylation on serine 2809 under ISO stimulation requires the presence of ROS to activate PKA.

The cross-talk between ROS and PKA may represent a key aspect of HF pathophysiology since failing hearts are characterized by a basal hyper-adrenergic state. During conditions of stress, the adrenergic activation is intensified leading to increased ROS production which in turn aggravates PKA activation and subsequent effects, notably RyR2 mediated SR Ca^{2+} leak. This could explain, in part,

the occurrence of sudden cardiac death during or after stress in HF patients or in other pathologies such as catecholaminergic Polymorphic Ventricular Tachycardia (CPVT) (Lehnart *et al.*, 2004).

There is growing evidence attributing a beneficial role of antioxidant treatment to reduced HF progression and risk of sudden cardiac death (Yano *et al.*, 2005; Mochizuki *et al.*, 2007; Epstein, 2008; Hare *et al.*, 2008). The present study demonstrates that a chronic antioxidant treatment with NAC for 4 weeks mitigated the development of a pathological phenotype in MI rats. Indeed, chronic NAC treatment prevented all MI-associated Ca^{2+} handling defects associated with a decrease of PKA activity, reduced arrhythmic events and increased heart rate variability measured *in vivo*. In addition, the high propensity of MI rats to trigger ventricular arrhythmias (VA) under ISO challenge was also prevented by NAC treatment, thus protecting against sudden cardiac death. Part of the beneficial effects of chronic NAC treatment could be mediated by a reduction of the sympathetic hyperinnervation observed in MI rats (Lee *et al.*). Nevertheless, the beneficial effects of acute NAC treatment on cardiomyocytes demonstrate a direct effect on ROS scavenging. Ideally, a clinical approach addressing the consequences of both chronic β-adrenergic activation and oxidative stress could be optimal to improve cardiac function and decrease arrhythmia during HF.

In conclusion, altered mitochondrial metabolism promotes oxidative stress which impairs RyR2 function through a ROS mediated PKA-dependent phosphorylation of the channel. A therapeutic strategy improving redox imbalance may provide beneficial effects that reduce arrhythmias in ischemic HF through prevention of ROS-induced RyR2 PKA phosphorylation on serine 2809 and depletion in calstabin2.

Author contributions :

The experiments were performed at “Inserm U637/Physiopathologie Cardiovasculaire”, CHU Arnaud de Villeneuve and at “INRA UMR866/Différenciation cellulaire et croissance”, Montpellier, France. J.F., O.C., A.L. were involved in the conception and design of the experiments. Collection, analysis and interpretation of data was performed by L.A., J.F., V.S.,C.F.C., G.F., O.C., A.L. Drafting the article or revising it critically for important intellectual content was done by L.A., J.F., S.R., A.M.R., O.C., A.L.

Acknowledgments

We would like to thank J. Thireau for his help in ECG recording and analysis and B. Petrof for helpful comments on the manuscript. SR, JF, OC, AL are CNRS scientists. This work was supported by the “Institut de la Santé et de la Recherche Médicale” (Inserm), “Région Languedoc Roussillon” and the Leducq Foundation, CAERUS transatlantic network of excellence. A.R.M. is a consultant for ARMGO Pharma, Inc, a start-up company targeting RyR2 to treat HF and cardiac arrhythmias, and is the recipient of funding from the National Institutes of Health (HL 061503, HL 067849, HL 056180 and HL 083418).

References

Beers RF, Jr. & Sizer IW. (1952). A spectrophotometric method for measuring the breakdown of hydrogen peroxide by catalase. *J Biol Chem* 195, 133-140.

Belevych AE, Terentyev D, Viatchenko-Karpinski S, Terentyeva R, Sridhar A, Nishijima Y, Wilson LD, Cardounel AJ, Laurita KR, Carnes CA, Billman GE & Gyorke S. (2009). Redox modification of ryanodine receptors underlies calcium alternans in a canine model of sudden cardiac death. *Cardiovasc Res* 84, 387-395.

Bellinger AM, Reiken S, Dura M, Murphy PW, Deng SX, Landry DW, Nieman D, Lehnart SE, Samaru M, LaCampagne A & Marks AR. (2008). Remodeling of ryanodine receptor complex causes "leaky" channels: a molecular mechanism for decreased exercise capacity. *Proc Natl Acad Sci U S A* 105, 2198-2202.

Bourraindeloup M, Adamy C, Candiani G, Cailleret M, Bourin MC, Badoual T, Su JB, Adubeiro S, Roudot-Thoraval F, Dubois-Rande JL, Hittinger L & Pecker F. (2004). N-acetylcysteine treatment normalizes serum tumor necrosis factor-alpha level and hinders the progression of cardiac injury in hypertensive rats. *Circulation* 110, 2003-2009.

Bradford MM. (1976). A rapid and sensitive method for the quantitation of microgram quantities of protein utilizing the principle of protein-dye binding. *Anal Biochem* 72, 248-254.

Brennan JP, Bardswell SC, Burgoyne JR, Fuller W, Schroder E, Wait R, Begum S, Kentish JC & Eaton P. (2006). Oxidant-induced activation of type I protein kinase A is mediated by RI subunit interprotein disulfide bond formation. *J Biol Chem* 281, 21827-21836.

Cazorla O, Szilagyi S, Le Guennec JY, Vassort G & Lacampagne A. (2005). Transmural stretch-dependent regulation of contractile properties in rat heart and its alteration after myocardial infarction. *Faseb J* 19, 88-90.

Cohn JN, Archibald DG, Ziesche S, Franciosa JA, Harston WE, Tristani FE, Dunkman WB, Jacobs W, Francis GS, Flohr KH & et al. (1986). Effect of vasodilator therapy on mortality in chronic congestive heart failure. Results of a Veterans Administration Cooperative Study. *N Engl J Med* 314, 1547-1552.

de Lamirande E & O'Flaherty C. (2008). Sperm activation: role of reactive oxygen species and kinases. *Biochim Biophys Acta* 1784, 106-115.

Epstein JA. (2008). Currying favor for the heart. *J Clin Invest* 118, 850-852.

Erickson JR, Joiner ML, Guan X, Kutschke W, Yang J, Oddis CV, Bartlett RK, Lowe JS, O'Donnell SE, Aykin-Burns N, Zimmerman MC, Zimmerman K, Ham AJ, Weiss RM, Spitz DR, Shea MA, Colbran RJ, Mohler PJ & Anderson ME. (2008). A dynamic pathway for calcium-independent activation of CaMKII by methionine oxidation. *Cell* 133, 462-474.

Farr MA & Basson CT. (2004). Sparking the failing heart. *N Engl J Med* 351, 185-187.

Fauconnier J, Andersson DC, Zhang SJ, Lanner JT, Wibom R, Katz A, Bruton JD & Westerblad H. (2007). Effects of palmitate on Ca(2+) handling in adult control and ob/ob cardiomyocytes: impact of mitochondrial reactive oxygen species. *Diabetes* 56, 1136-1142.

Fauconnier J, Lacampagne A, Rauzier JM, Vassort G & Richard S. (2005). Ca2+-dependent reduction of IK1 in rat ventricular cells: a novel paradigm for arrhythmia in heart failure? *Cardiovasc Res* 68, 204-212.

Fauconnier J, Thireau J, Reiken S, Cassan C, Richard S, Matecki S, Marks AR & Lacampagne A. Leaky RyR2 trigger ventricular arrhythmias in Duchenne muscular dystrophy. *Proc Natl Acad Sci U S A*.

Giordano FJ. (2005). Oxygen, oxidative stress, hypoxia, and heart failure. *J Clin Invest* 115, 500-508.

Guo T, Cornea RL, Huke S, Camors E, Yang Y, Picht E, Fruen BR & Bers DM. Kinetics of FKBP12.6 binding to ryanodine receptors in permeabilized cardiac myocytes and effects on Ca sparks. *Circ Res* 106, 1743-1752.

Hare JM, Mangal B, Brown J, Fisher C, Jr., Freudenberger R, Colucci WS, Mann DL, Liu P, Givertz MM & Schwarz RP. (2008). Impact of oxypurinol in patients with symptomatic heart failure. Results of the OPT-CHF study. *J Am Coll Cardiol* 51, 2301-2309.

Hill MF & Singal PK. (1997). Right and left myocardial antioxidant responses during heart failure subsequent to myocardial infarction. *Circulation* 96, 2414-2420.

Houser SR. Does protein kinase a-mediated phosphorylation of the cardiac ryanodine receptor play any role in adrenergic regulation of calcium handling in health and disease? *Circ Res* 106, 1672-1674.

Hove-Madsen L, Llach A, Bayes-Genis A, Roura S, Rodriguez Font E, Aris A & Cinca J. (2004). Atrial fibrillation is associated with increased spontaneous calcium release from the sarcoplasmic reticulum in human atrial myocytes. *Circulation* 110, 1358-1363.

Howe CJ, Lahair MM, McCubrey JA & Franklin RA. (2004). Redox regulation of the calcium/calmodulin-dependent protein kinases. *J Biol Chem* 279, 44573-44581.

Ide T, Tsutsui H, Kinugawa S, Utsumi H, Kang D, Hattori N, Uchida K, Arimura K, Egashira K & Takeshita A. (1999). Mitochondrial electron transport complex I is a potential source of oxygen free radicals in the failing myocardium. *Circ Res* 85, 357-363.

Janssen AJ, Trijbels FJ, Sengers RC, Smeitink JA, van den Heuvel LP, Wintjes LT, Stoltenborg-Hogenkamp BJ & Rodenburg RJ. (2007). Spectrophotometric assay for complex I of the respiratory chain in tissue samples and cultured fibroblasts. *Clin Chem* 53, 729-734.

Lee TM, Lai PY & Chang NC. Effect of N-acetylcysteine on sympathetic hyperinnervation in post-infarcted rat hearts. *Cardiovasc Res* 85, 137-146.

Lehnart SE, Mongillo M, Bellinger A, Lindegger N, Chen BX, Hsueh W, Reiken S, Wronska A, Drew LJ, Ward CW, Lederer WJ, Kass RS, Morley G & Marks AR. (2008). Leaky Ca2+

release channel/ryanodine receptor 2 causes seizures and sudden cardiac death in mice. *J Clin Invest* 118, 2230-2245.

Lehnart SE, Wehrens XH, Kushnir A & Marks AR. (2004). Cardiac ryanodine receptor function and regulation in heart disease. *Ann N Y Acad Sci* 1015, 144-159.

Marklund S. (1976). Spectrophotometric study of spontaneous disproportionation of superoxide anion radical and sensitive direct assay for superoxide dismutase. *J Biol Chem* 251, 7504-7507.

Marx SO, Reiken S, Hisamatsu Y, Jayaraman T, Burkhoff D, Rosemblit N & Marks AR. (2000). PKA phosphorylation dissociates FKBP12.6 from the calcium release channel (ryanodine receptor): defective regulation in failing hearts. *Cell* 101, 365-376.

Mochizuki M, Yano M, Oda T, Tateishi H, Kobayashi S, Yamamoto T, Ikeda Y, Ohkusa T, Ikemoto N & Matsuzaki M. (2007). Scavenging free radicals by low-dose carvedilol prevents redox-dependent Ca2+ leak via stabilization of ryanodine receptor in heart failure. *J Am Coll Cardiol* 49, 1722-1732.

Mou YA, Reboul C, Andre L, Lacampagne A & Cazorla O. (2009). Late exercise training improves non-uniformity of transmural myocardial function in rats with ischaemic heart failure. *Cardiovasc Res* 81, 555-564.

Neubauer S. (2007). The failing heart--an engine out of fuel. *N Engl J Med* 356, 1140-1151.

O'Flaherty C, de Lamirande E & Gagnon C. (2006). Reactive oxygen species modulate independent protein phosphorylation pathways during human sperm capacitation. *Free Radic Biol Med* 40, 1045-1055.

Picht E, Zima AV, Blatter LA & Bers DM. (2007). SparkMaster: automated calcium spark analysis with ImageJ. *Am J Physiol Cell Physiol* 293, C1073-1081.

Pitkanen S & Robinson BH. (1996). Mitochondrial complex I deficiency leads to increased production of superoxide radicals and induction of superoxide dismutase. *J Clin Invest* 98, 345-351.

Pogwizd SM, Schlotthauer K, Li L, Yuan W & Bers DM. (2001). Arrhythmogenesis and contractile dysfunction in heart failure: Roles of sodium-calcium exchange, inward rectifier potassium current, and residual beta-adrenergic responsiveness. *Circ Res* 88, 1159-1167.

Rhee SG, Bae YS, Lee SR & Kwon J. (2000). Hydrogen peroxide: a key messenger that modulates protein phosphorylation through cysteine oxidation. *Sci STKE* 2000, PE1.

Sawyer DB & Colucci WS. (2000). Mitochondrial oxidative stress in heart failure: "oxygen wastage" revisited. *Circ Res* 86, 119-120.

Srere PA. (1970). An eclectic view of metabolic regulation: control of citrate synthase activity. *Adv Enzyme Regul* 9, 221-233.

Stadtman ER. (1992). Protein oxidation and aging. *Science* 257, 1220-1224.

Stanley WC, Recchia FA & Lopaschuk GD. (2005). Myocardial substrate metabolism in the normal and failing heart. *Physiol Rev* 85, 1093-1129.

Takimoto E & Kass DA. (2007). Role of oxidative stress in cardiac hypertrophy and remodeling. *Hypertension* 49, 241-248.

Ter Keurs HE & Boyden PA. (2007). Calcium and arrhythmogenesis. *Physiol Rev* 87, 457-506.

Terentyev D, Gyorke I, Belevych AE, Terentyeva R, Sridhar A, Nishijima Y, de Blanco EC, Khanna S, Sen CK, Cardounel AJ, Carnes CA & Gyorke S. (2008). Redox modification of ryanodine receptors contributes to sarcoplasmic reticulum Ca2+ leak in chronic heart failure. *Circ Res* 103, 1466-1472.

Wang W, Fang H, Groom L, Cheng A, Zhang W, Liu J, Wang X, Li K, Han P, Zheng M, Yin J, Wang W, Mattson MP, Kao JP, Lakatta EG, Sheu SS, Ouyang K, Chen J, Dirksen RT & Cheng H. (2008). Superoxide flashes in single mitochondria. *Cell* 134, 279-290.

Wehrens XH, Lehnart SE, Huang F, Vest JA, Reiken SR, Mohler PJ, Sun J, Guatimosim S, Song LS, Rosemblit N, D'Armiento JM, Napolitano C, Memmi M, Priori SG, Lederer WJ & Marks AR. (2003). FKBP12.6 deficiency and defective calcium release channel (ryanodine receptor) function linked to exercise-induced sudden cardiac death. *Cell* 113, 829-840.

Wehrens XH, Lehnart SE, Reiken SR, Deng SX, Vest JA, Cervantes D, Coromilas J, Landry DW & Marks AR. (2004). Protection from cardiac arrhythmia through ryanodine receptor-stabilizing protein calstabin2. *Science* 304, 292-296.

Wharton DC. (1978). Purification of electron-transfer components from Pseudomonas. *Methods Enzymol* 53, 646-661.

Yan Y, Liu J, Wei C, Li K, Xie W, Wang Y & Cheng H. (2008). Bidirectional regulation of Ca2+ sparks by mitochondria-derived reactive oxygen species in cardiac myocytes. *Cardiovasc Res* 77, 432-441.

Yano M, Okuda S, Oda T, Tokuhisa T, Tateishi H, Mochizuki M, Noma T, Doi M, Kobayashi S, Yamamoto T, Ikeda Y, Ohkusa T, Ikemoto N & Matsuzaki M. (2005). Correction of defective interdomain interaction within ryanodine receptor by antioxidant is a new therapeutic strategy against heart failure. *Circulation* 112, 3633-3643.

Zima AV & Blatter LA. (2006). Redox regulation of cardiac calcium channels and transporters. *Cardiovasc Res* 71, 310-321.

Zissimopoulos S, Docrat N & Lai FA. (2007). Redox sensitivity of the ryanodine receptor interaction with FK506-binding protein. *J Biol Chem* 282, 6976-6983.

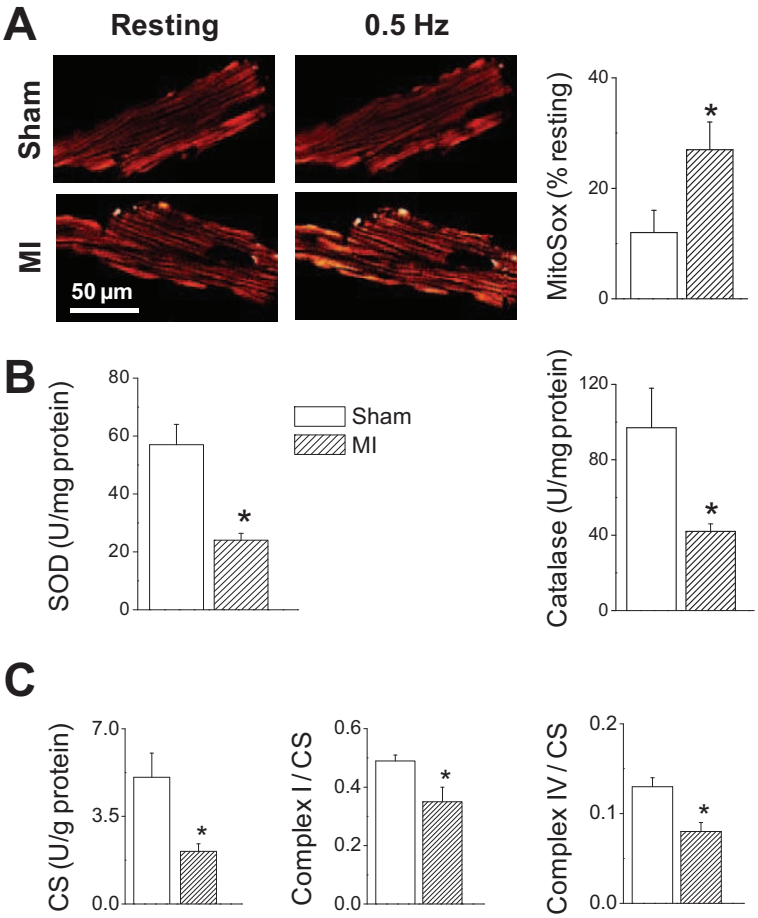

Figure 1: Altered mitochondrial metabolism results in increased oxidative stress in MI rats. A: Typical images (left panel) and averaged data (right panel) of MitosoxRed fluorescence in cardiomyocytes from Sham and MI rats at resting state, and after 5 minutes of 0.5 Hz stimulation (32-40 cells / 4 hearts, data are expressed relative values to the resting state). **B**: SOD and catalase activities in cardiomyocytes from Sham and MI rats (5 hearts). * P<0.05 *vs.* Sham. **C**: Citrate syntase (CS), complex I and IV activities in cardiomyocytes from Sham and MI rats (5 hearts).

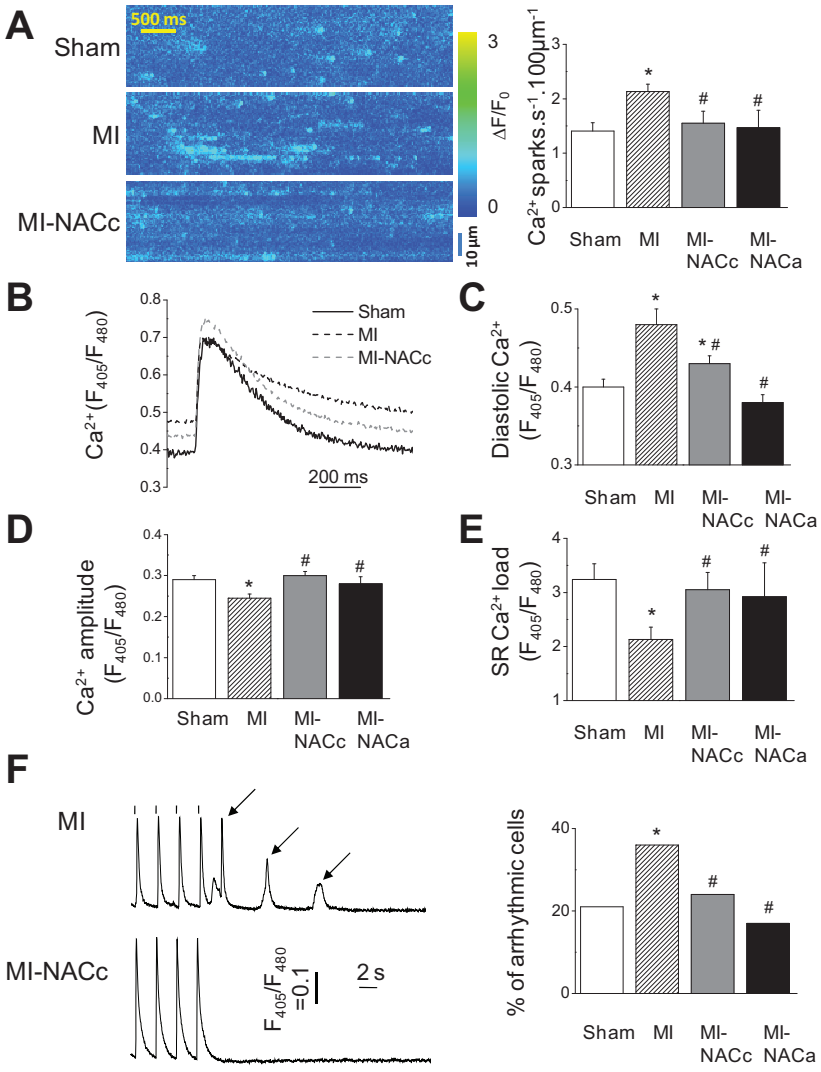

Figure 2: ROS provoked Ca^{2+} handling impairments and Ca^{2+} waves in MI cardiomyocytes. A: Typical images (left panel) and averaged data (right panel) of Ca^{2+}-sparks in Sham, MI, MI-NACa and MI-NACc (25-33 cells / 3-4 hearts). **B**: Representative traces of indo-1 Ca^{2+} transient in cardiomyocytes paced at 0.5 Hz. Averaged data of diastolic Ca^{2+} (**C**), Ca^{2+} transient amplitude (**D**) and caffeine-pulsed SR Ca^{2+} load (**E**) of Sham, MI, MI-NACa and MI-NACc cardiomyocytes (35-50 cells / 4-5 hearts). **F**: Typical time courses of Ca^{2+} signals showing early after depolarisations in MI rats. After pacing interruption, MI cells show Ca^{2+} waves consistent with DADs whereas the MI-NACc cardiomyocytes remain silent. **G**: Averaged data of arrhythmic cells of Sham, MI, MI-NACa and MI-NACc cardiomyocytes (35-50 cells / 4-5 hearts). * P<0.05 *vs.* Sham; # P<0.05 *vs.* MI.

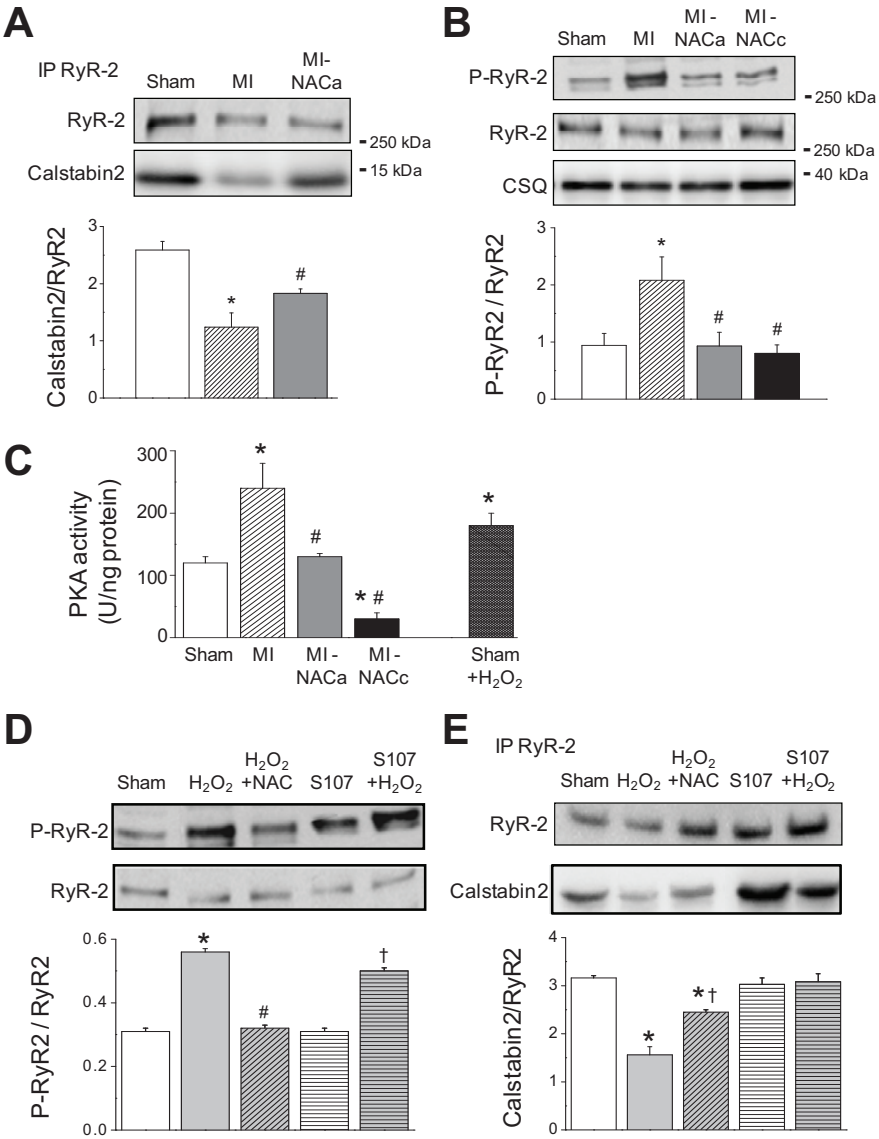

Figure 3: ROS-induced PKA-dependent RyR2 hyperphosphorylation **A:** Typical immunoblot showing calstabin2 and RyR2 after immunoprecipitation of RyR2 (top) and averaged data of calstabin2/RyR2 ratio in Sham, MI and MI-NACa cardiomyocytes (bottom). **B:** Representative Western blot images showing calsequestrin (CSQ), RyR2 and P-RyR2 abundance in cardiomyocytes of Sham, MI, MI-NACa and MI-NACc cardiomyocytes (top) and averaged data of Ser^{2809} RyR2 phosphorylation normalized to total RyR2 content (bottom) (n=5 hearts). **C:** PKA activity measured in cardiac tissue of Sham incubated or not with H_2O_2, MI, MI-NACa and MI-NACc hearts (n=5 hearts). **D:** Western blot analysis of RyR2 and P-RyR2 abundance in cardiomyocytes of Sham, Sham incubated with H_2O_2, Sham incubated with H_2O_2 and NAC, S107 treated sham samples and S107 treated sham samples incubated with H_2O_2 (top) and averaged data of Ser^{2809} RyR2 phosphorylation normalized to total RyR2 content (bottom). **E:** Typical immunoblot blot showing calstabin2 and RyR2 after immunoprecipitation of RyR2 (left) and averaged data of calstabin2/RyR2 ratio (right) in the same experimental condition as for panel D. * P<0.05 *vs.* Sham; # P<0.05 *vs.* MI, † P<0.05 *vs.*H_2O_2.

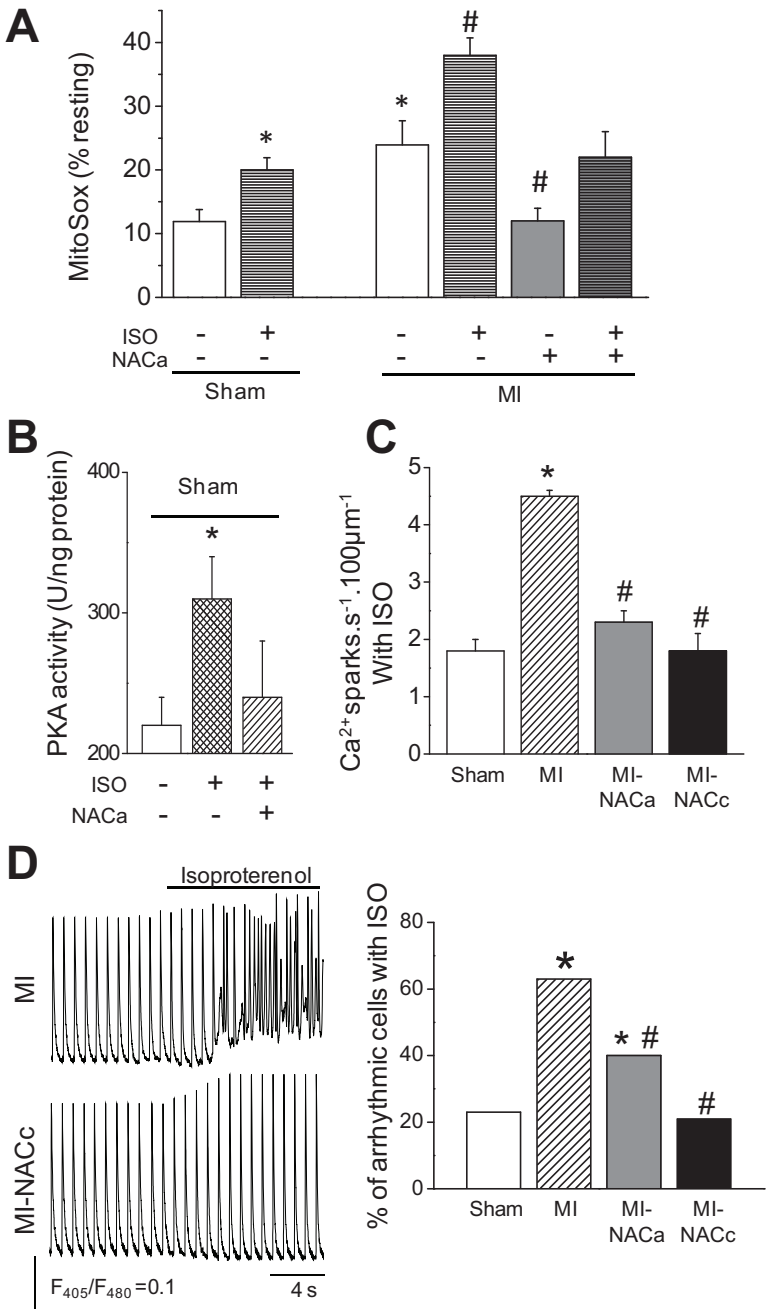

Figure 4: Cross-talk between Isoproterenol and ROS in cardiomyocytes **A**: Effect of ISO perfusion (10 nM) on Mitosox Red fluorescence measured in sham and in MI cardiomyocytes, before and after NAC incubation (20 mM for 1 hour). * P<0.05 *vs.* Control; # P<0.05 *vs.* ISO; † P<0.05 *vs.* NAC. **B:** PKA activity measured in Sham cardiomyocytes, after ISO perfusion (10 nM) and after NAC incubation (20 mM for 1 hour). * P<0.05 *vs.* Control. **C**: Diastolic spontaneous Ca^{2+}-sparks frequency after ISO perfusion (10 nM) in Sham, MI, MI-NACa and MI-NACc cardiomyocytes. * P<0.05 *vs.* Control; # P<0.05 *vs.* MI. **D**: Effect of ISO on Ca^{2+} transients from cardiomyocytes isolated from MI and MI-NACc rats. Rapidly after ISO perfusion, MI cardiomyocytes display stochastic Ca^{2+} transient whereas MI-NACc cardiomyocytes remain silent. **E**: Percentage of arrhythmic Sham, MI, MI-NACa and MI-NACc cardiomyocytes (25-32 cells / 4 hearts). * P<0.05 *vs.* Control; # P<0.05 *vs.* MI.

Figure 5

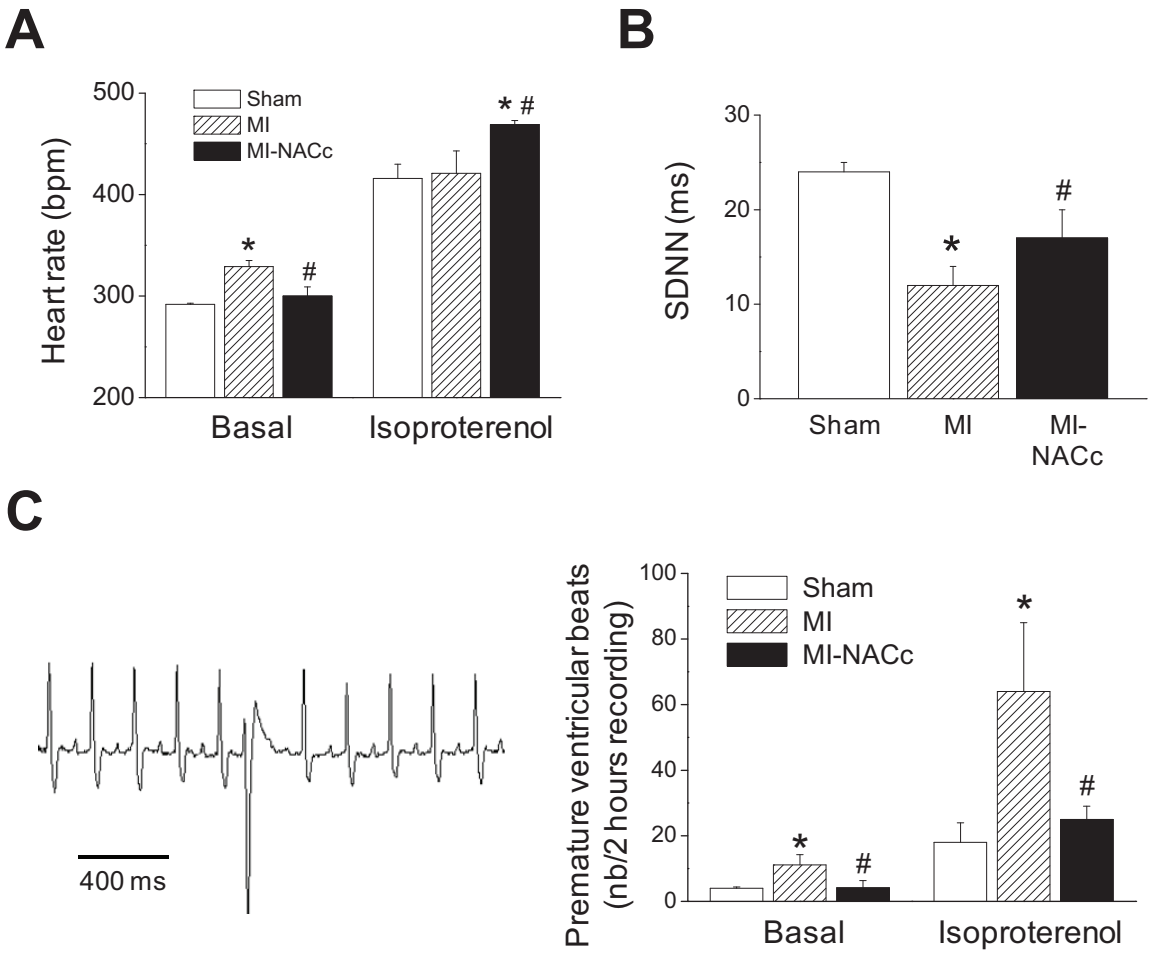

Figure 5: Chronic NAC treatment prevents HF-associated electrophysiological alterations *in vivo.* A: Heart rate under basal condition and after injection of ISO (1mg/kg i.p.) **B:** Standard deviation of the normal RR intervals (SDNN) in basal condition (n=9 rats in each group). **C:** Representative example of ventricular ectopic beat occurring during ECG recordings in MI rats (left panel). Analysis of the occurrence of arrhythmic events at rest and after acute challenge with ISO (right panel); * P<0.05 *vs.* Sham; # P<0.05 *vs.* MI.

3. Conclusion

Cette étude met en évidence l'implication des ROS dans l'arythmogénicité associée à l'IC ischémique. Douze semaines après un infarctus du myocarde, les évènements arythmiques associés à l'IC ischémique résultent d'altérations mitochondriales responsables de la genèse d'un stress oxydatif. Les ROS activent alors la protéine kinase A entrainant la phosphorylation du RyR-2 et la fuite de Ca^{2+} à travers le canal. Ainsi, les deux mécanismes (modifications redox et phosphorylation PKA-dépendante du RyR-2) ne sont pas indépendants mais sont unis dans une même voie d'action. Cette première étude réconcilie alors les deux théories proposées (phosphorylation et oxydation/nytrosilation du RyR-2) pour expliquer la dysrégulation du RyR-2 à l'origine d'une libération anarchique de Ca^{2+} et des évènements arythmiques. Cette étude légitime alors le recours aux traitements antioxydants dans l'IC ischémique afin de réduire la concentration en ROS et par conséquent les dysfonctions du RyR-2 et la genèse d'évènements arythmiques. Bien qu'encore controversés dans la prise en charge des patients IC, les traitements antioxydants permettent de réduire les marqueurs inflammatoires impliqués dans la pathogenèse de l'IC et réduisent le stress oxydatif associé, limitant alors les attaques oxydatives protéiques [125].

Les troubles de l'homéostasie redox associés à la dysfonction mitochondriale semblent donc jouer un rôle dans la genèse de phénomènes arythmiques au cours de l'IC, en activant la voie PKA. Les autres cibles protéiques de la PKA, notamment au niveau myofilamentaire, pourraient également subir des modifications à l'origine de dysfonctions contractiles. L'étude 2 s'est alors intéressée aux conséquences régionalisées des dysfonctions mitochondriales sur le fonctionnement myofilamentaire, ainsi qu'aux répercussions sur l'activité contractile à l'échelle de l'organe.

II. Implication des ROS dans la dysfonction contractile associée à l'IC ischémique : rôle de la voie PKA et effet d'un traitement chronique antioxydant

1. Introduction

Dans des conditions physiologiques, un gradient transmural de contraction à travers la paroi ventriculaire gauche assure une biomécanique cardiaque optimale permettant au cœur de

se contracter de façon efficace. En effet, l'ENDO se contracte de manière plus importante que l'EPI, en raison d'une distribution hétérogène des propriétés du coupage excitation-métabolisme contraction, caractérisée notamment par une consommation en oxygène, une libération de Ca^{2+} et une sensibilité des myofilaments au Ca^{2+} supérieures dans l'ENDO par rapport à l'EPI. L'IC ischémique est caractérisée par une homogénéisation des propriétés contractiles au sein de la paroi ventriculaire gauche, en raison d'altérations du couplage excitation-contraction localisées principalement dans l'ENDO. Par ailleurs, des altérations métaboliques mitochondriales, caractérisées notamment par une production excessive de ROS accompagne le développement de l'IC. La précédente étude a montré que les ROS étaient à l'origine d'une activation de la voie PKA, aboutissant à l'hyperphosphorylation du RyR-2 puis au déclenchement de phénomènes arythmiques. L'objectif de cette étude a été de déterminer si des dysfonctions mitochondriales régionalisées pouvaient être à l'origine du nivellement des propriétés contractiles au sein du ventricule gauche, impliquant la phosphorylation PKA-dépendante induite par les ROS des protéines contractiles.

2. Article 2 - Soumis prochainement pour publication

Regionalized ROS production depresses contractile function in ischemic heart failure: preventive effect of a chronic antioxidant therapy

Lucas Andre[1], Jeremy Fauconnier[1], Cyril reboul[2], Christine Feillet-Coudray[3], Gilles Fouret[3], Sylvain Richard[1], Alain Lacampagne[1] and Olivier Cazorla[1]

[1]INSERM, U-637, F-34295 Montpellier, France. Université MONTPELLIER1, UFR de Médecine, F-34295 Montpellier, France
[2] EA-4278, Université Avignon et des Pays de Vaucluse, UFR Sciences, F-84000 Avignon, France.
[3]INRA UMR 866, Unité Différentiation Cellulaire et Croissance, 34060 Montpellier, France

Correspondence to :
Olivier CAZORLA
Inserm U637 Physiopathologie Cardiovasculaire
CHU Arnaud de Villeneuve
34295 Montpellier, France
Phone : +33 467 41 52 44
Fax : +33 467 41 52 42
olivier.cazorla@inserm.fr

Key words: heart failure, mitochondria, oxidative stress, PKA, cardiac heterogeneity

Abstract :

Ischemic heart failure (HF) is characterized by regionalized contractile alterations resulting in loss of transmural contractile gradient across left ventricular free wall. We aimed to determine whether mitochondrial dysfunction could be involved in the HF contractile defects. Twelve weeks after left coronary artery ligation (MI), the NADH homeostasis measured in cardiomyocytes isolated from sub-endocardial (ENDO) and sub-epicardial (EPI) was altered only in ENDO layer compared with sham rats, and correlated with decreased activity of both complex I and IV of the electron transport chain. The generation of superoxide anion ($O_2^{\cdot -}$), evaluated by MitosoxRed dye, was increased two fold in ENDO layer of MI rats, and was associated with decreased antioxidant activity of both superoxide dismutase and catalase. Incubation of cardiomyocytes with the antioxidant N-acetylcystein (NAC) for 1 hour restored most of the cell shortening in ENDO layer of MI rats without affecting EPI layer, by restoring the Ca^{2+} homeostasis (decreased diastolic Ca^{2+} overload and increased Ca^{2+} transient amplitude) and the properties of the contractile machinery properties (Ca^{2+} sensitivity evaluated on skinned cardiomyocyte). We show that the beneficial effect of NAC is mediated by a reduction of PKA activity that is increased during HF, in particular by preventing the hyperphosphorylation of proteins such as troponin I and the ryanodine receptor . Chronic treatment with NAC (for 4 weeks) improved *in vivo* contractility by improving excitation-contraction coupling in ENDO layer. In conclusion regionalized HF-associated mitochondrial dysfunction is responsible of ROS production in ENDO layer which contribute to the loss of transmural contractile gradient and global contractility mediated by PKA activation.

Introduction

Under physiological conditions, heart displays a transmural contractile gradient across left ventricle (LV) due to higher contractility of sub-endocardial (ENDO) layer when compared to sub-epicardial (EPI) layer [1]. This contractile gradient results from transmural excitation-contraction coupling (ECC) heterogeneity with longer action potential [2,3], higher sarcoplasmic reticulum (SR)-Ca^{2+} release [4] and higher myofilament Ca^{2+} sensitivity [5] in ENDO *vs* EPI layers. ECC requires vast amount of ATP and depends on cardiac metabolic properties, which are also differentially distributed across LV free wall. Indeed, ENDO layer is characterized by greater perfusion [6], oxygen consumption [7] and oxidative metabolism [8] than EPI layer.

Heart failure (HF) is a syndrome characterized by the inability of the cardiac pump to provide sufficient cardiac output. Pathogenesis implies morpho-functional remodeling including contractile and metabolic disorders [9] as well as electro-mechanical alterations resulting in loss of transmural left ventricular contraction heterogeneity [10] due to reduced contractility mainly localized in ENDO layer [4, 5]. On the other hand, the failing heart displays altered mitochondrial function characterized by disturbed metabolism [11,12] and abnormal reactive oxygen species (ROS) production [13,14]. It is well documented that ROS alter ECC proteins [15] and contribute to the HF-associated contractile defects. On the other hand, ROS have been shown to activate directly PKA leading to phosphorylation of PKA substrates [16]. In the present study we aimed to determine: (i) whether transmural mitochondrial dysfunction could be responsible for contractile defects in ischemic heart failure and (ii) whether chronic antioxidant treatment of HF animals could improve heart function. The results indicated that HF associated-mitochondrial troubles were exclusively localized in ENDO layer where a ROS overproduction negatively affected ECC through a PKA-dependent pathway. A chronic antioxidant treatment improved global cardiac function through recovering of HF-associated contractile machinery and Ca^{2+} homeostasis alterations.

Materials and Methods

Animals

The investigations were carried out in agreement with the *Guide for the Care and Use of Laboratory Animals* published by the US National Institute of Health (NIH Publications No. 85-23, revised 1996) and with the approval of French Agriculture Department. Male Wistar rats (5 weeks old, Charles River) were randomly assigned to left coronary artery ligation in order to induce myocardial infarction (MI rats) or to sham-operated procedure (Sham rats) [5]. 8 weeks after MI, 15 rats (MI-NACc) were chronically treated with N-Acetyl Cysteine (NAC) (Sigma) administered in their drinking water (75 mg/ day per animal) for 4 weeks [17]. Experiments were performed 12 weeks post-ligature.

Echocardiographic Investigation

Regional and global cardiac morphology and function remodelling of rat hearts was assessed by Doppler-echocardiography [4].

Cell isolation

Single left ventricular myocytes were isolated by enzymatic digestion as previously described [18]. Briefly, hearts were quickly removed and mounted on a Langendorff apparatus. The heart was perfused with a Ca^{2+}-free solution (in mmol/L : NaCl 117, KCl 5.7, $NaHCO_3$ 4.4, KH_2PO_4 1.5, $MgCl_2$ 1.7, HEPES 21, glucose 11, taurine 20, pH 7.2 adjusted with NaOH) followed by perfusion with a collagenase IV enzymatic solution (Worthington). The infarct zone and boarder zone were discarded. Small pieces of ventricular tissues from the inner free wall ENDO layer and from the outer free wall EPI layer were dissociated and the Ca^{2+} concentration was gradually increased to 1 mM Ca^{2+}.

Measurement of mitochondrial NADH

The endogenous auto fluorescence of mitochondrial NADH was measured using two-photon excitation at 720 nm and its emission recorded at λem=450-485 nm. Fluorescence images were recorded in X-Y mode using a Zeiss LSM 510NLO inverted two-photon confocal microscope with an x25 lens (H_2O immersion, Numerical Aperture, NA=0.8). Cells were paced at 0.5 Hz using two platinum electrodes placed in each side of the Petri dish. NADH fluorescence was collected at rest and after 5 min stimulation. For each cell, resting fluorescence value was obtained after subtracting background noise measured outside the cell and set to 100%.

Measurement of mitochondrial ROS production

Isolated cardiomyocytes were loaded with MitoSOX Red (5 µM Invitrogen inc., France) for 15 min at room temperature, followed by washout, to evaluate mitochondrial $O_2^{\cdot-}$ production [19]. Fluorescence images were recorded using a Zeiss LSM 510 inverted confocal microscope with an x25 lens (H_2O immersion, NA=0.8). Confocal images were obtained at 5-min intervals by excitation at 488 nm. Emitted light was measured at 583 nm. MitoSOX Red fluorescence was collected at rest and after 5 min stimulation. For each cell, resting fluorescence value was obtained after subtracting background noise measured outside the cell and set to 100%.

Ca^{2+} transient and cell shortening in intact cardiomyocytes

Cells were loaded for 30 min at room temperature with Indo-1 AM (10µM Invitrogen inc., France) in order to monitor intracellular Ca^{2+}. Cells were field stimulated at 0.5 Hz (20V, 1 ms), and simultaneously illuminated at 305 nm using a xenon arc bulb light. Sarcomere length (SL) and Indo-1 fluorescence emitted at 405 nm and 480 nm were simultaneously recorded using IonOptix acquisition software (IonOptix system, Hilton, USA).

Force measurement in permeabilized cardiomyocytes

Isometric force was measured in single permeabilized cardiomyocytes [5]. Force was normalized to the cross-sectional area measured by imaging (IonOptix system). The relationship between Ca^{2+} activated force and internal Ca^{2+} concentration was measured at 2.3 µm SL and was fitted with a modified Hill equation. In some experiments, permeabilized cardiomyocytes were incubated with a recombinant catalytic subunit of protein kinase A (PKA, Sigma) for 50 min at room temperature [20].

Determination of antioxidant activities in cardiomyocytes
After cell lysis in hypotonic buffer (phosphate buffer 8mM, pH 7.4), catalase activity was measured according to the method of Beers and Sizer [21] and total superoxide dismutase (SOD) was measured according to the method of Marklund [22]. Protein levels in cell lysates were measured by the Bradford technique.

Determination of mitochondrial enzymatic activities in cardiomyocytes
After cell lysis in hypotonic buffer (phosphate buffer 8mM, pH 7.4), citrate synthase (CS) activity was measured according to Srere [23]: the activity of the enzyme was measured by following the color of 5-thio-2-nitrobenzoic acid generated from 5,5'-dithiobis-2-nitrobenzoic acid present in the reaction of citrate synthesis, and caused by the deacetylation of Acetyl-CoA.
Complex I of the electron transport chain (ETC) was evaluated through measurement of the reduction of the 2 ,6 – dichlorophenolindophénol by the NADH dehydrogenase at 600 nm (37°C) [24]. Complex IV of the ETC was measured through the measure of the cytochrome-c oxidase activity according to Wharton and Tzagoloff [25]: oxidation of reduced cytochrome-c was followed by spectrophotometry.

Protein Analysis
Proteins were separated using 4-20 % SDS-PAGE and blotted onto a nitrocellulose membrane (Protran, Schleichen and Schuele, Dassel, Germany). Membranes were incubated overnight at 4°C with the following primary antibodies: ryanodine receptor type 2 (RyR-2) antibody (Covalab, France), phospho Ser^{2809}-RyR-2 antibody (Badrilla, UK), troponin I (TnI) and phospho Ser^{22}/Ser^{23} -TnI (Hytest, Finland). RyR-2 and TnI levels were expressed relative to calsequestrin content (Cat # PA1-913, ABR, USA) on the same membrane. Immunodetection was carried out using the ECL Plus system (Amersham Pharmacia, Little Chalfont Buckinghamshire, England). PKA activity was measured using a non-radioactive PKA activity assay kit (Assay designs, France). Tissue extracts were mixed with ATP for 90 minutes. Phosphospecific and anti-rabbit antibody were consecutively added before measuring the absorbance at 450 nM.

Statistical analysis
Data were analyzed using one-way or 2-way ANOVA between groups. When significant interactions were found, a Bonferroni post-hoc test was applied with $P< 0.05$ (Statview 5.0). Data are presented as mean±SEM.

Results

Transmural mitochondrial metabolism
Mitochondria are the primary ATP provider in cardiomyocyte *via* the conversion of food fuels to usuable energy, in order to match energy demand and supply. Both fatty acid and carbohydrate metabolism converge at the Krebs cycle, with the generation of reduced redox carriers NADH and $FADH_2$. Once forming, NADH and $FADH_2$ are oxidized in the inner membrane of mitochondria by complexes (I-IV) of the ETC where their electron transfer generate a proton motive force driving ATP synthesis *via* the terminal complex (complex V)

[26]. We measured NADH autofluorescence after 5 minutes of 0.5 Hz stimulation in both ENDO and EPI layers, as an index of the oxidative metabolism [27,28,29]. In Sham rats, NADH autofluorescence decreased after stimulation suggesting NADH oxidation. The decrease of autofluorescence was higher in ENDO layer than in EPI layer (55 ± 3% *vs* 36 ± 7%, respectively; $p<0.05$) reflecting a transmural gradient of metabolism (Figure 1A). NADH oxidation was significantly smaller in failing cardiomyocytes originating from the ENDO layer (33 ± 7%) compared with sham cells. No significant modification was observed for the EPI layer. Most notably, the physiological transmural metabolic state disappeared in rats with HF due to leveling of ENDO toward EPI values (Figure 1A).
NADH autofluorescence reflects the balance between NADH production by tricarboxylic acid cycle and NADH oxidation within the ETC. We evaluated whether NADH accumulation in ENDO layer of MI rats could be attributed to reduced ETC activity. Complex I and IV (Cyt-c Oxydase) activities were measured and normalized to citrate synthase (CS) activity, an index of mitochondrial content. A transmural gradient of CS activity was observed in Sham rats with higher activities in ENDO layer (Figure 1B) suggesting a higher mitochondrial content in this layer. In HF rats, CS activity was decreased only in ENDO layer to the level of EPI cells. Complex I and IV activities were both significantly higher in ENDO layer in Sham rats when compared to EPI layer (Figure 1B). In HF rats, the two ETC complexes were decreased only in ENDO layer to the level of EPI cells. All together, those results indicate that the transmural gradient of mitochondrial metabolism in sham rats disappeared during HF due to altered oxidative capacity localized in ENDO layer.

Regionalized ROS production
Under conditions of inefficient oxidative metabolism mainly due to reduced complex I activity, ROS production may be increased [30,31,32]. We next measured mitochondrial $O_2^{\cdot-}$ production after 5 minutes stimulation using MitoSOX Red, which is targeted to the mitochondria and increases its fluorescence when oxidized [19]. In sham animals, No regional differences were observed for ROS production in normal conditions (Figure 1C). Rats with HF produced significantly more mitochondrial ROS after stimulation in ENDO layer when compared to Sham rats (27±5% *vs* 12±4%, respectively). EPI layer was not affected by the pathology, indicating the development of a transmural gradient in mitochondrial ROS production in rats with HF (Figure 1C). Oxidative stress results from an imbalance between pro-oxidant activities and antioxidant defenses buffering ROS. We thus evaluated antioxidant enzyme activities: SOD which converts O_2^{-*} to H_2O_2, and catalase which converts H_2O_2 to H_2O. Both SOD and catalase activities were higher in ENDO layer compared to EPI layer in sham rats (Figure 1D). In failing hearts, both SOD and catalase activities were reduced only in ENDO layer (Figure 1D). Taken together, those results indicate that, during HF, ENDO layer produces more ROS, partly due to reduced antioxidative defenses leading to an higher susceptibility to oxidative stress.

Effects of regionalized ROS production on contractility
Oxidative stress may affect Ca^{2+} handling [15] and myofilament properties [33] in cardiomyocytes originated from failing ENDO layer. In order to determine whether ROS production could be responsible for the alterations of contractility previously reported in HF myocytes [4], we measured cell shortening after incubating cardiomyocytes with the ROS-scavenger, N-acetylcystein (NAC, 20 mM) for 1 hour. As previously observed [4], there was a LV transmural gradient of cell shortening due to higher contractility of cardiomyocyte originated from

ENDO layer in sham animals (Figure 2A and 2B). This gradient disappeared in MI rats due to decreased cell shortening exclusively in ENDO layer (Figure 2A and 2B). The contractile alterations were associated with lengthening of both contraction and relaxation kinetics in ENDO layer (Figure 2B). Incubation with NAC restored the transmural gradient of contractility in MI rats by recovering partially cell shortening in ENDO layer (+23% in cell shortening), without affecting EPI layer (Figure 2A and 2B). NAC treatment restored significantly contraction and relaxation velocities only in ENDO layer but to a modest extent. Those results suggest a ROS-dependent component in the alterations of contractility in the failing ENDO cardiomyocytes.

Effects of regionalized ROS production on Ca^{2+} cycling

Force development of cardiomyocyte depends on myofilament Ca^{2+} sensitivity and the amount of Ca^{2+} released by the sarcoplasmic reticulum (SR). We thus evaluated the Ca^{2+} transient characteristics. In sham rats, the Ca^{2+} transient amplitude was significantly higher in ENDO than EPI layer (0.29 ± 0.01 F405/F480 *vs* 0.23 ± 0.01, respectively) (Figure 3A and 3B). This transmural gradient for Ca^{2+} release disappeared in failing hearts due to reduced Ca^{2+} transient amplitude in ENDO layer. The MI-induced SR Ca^{2+} release troubles in ENDO cells were associated with an increased in diastolic Ca^{2+} and a slowing of Ca^{2+} transient decay (Tau) (Figure 3B). NAC treatment reversed this MI-induced abnormalities in Ca^{2+} handling only in ENDO layer (Figure 3A and 3B). These results indicate that altered Ca^{2+} handling exclusively in ENDO is partly mediated by increased ROS production in this layer.

We then assessed the properties of the contractile machinery in single permeabilized cardiomyocytes (Figure 4). In sham rats, as previously described [5,4], a transmural gradient for myofilament Ca^{2+} sensitivity as indexed by pCa_{50} was observed due to higher pCa_{50} in ENDO cells compared to EPI cells (5.99 ± 0.03 *vs* 5.89 ± 0.03, respectively) (Figure 3C and 3D). HF decreased myofilament Ca^{2+} sensitivity and maximal active tension only in ENDO layer ($p<0.05$) toward values obtained in EPI layer (Figure 3D). NAC treatment prior permeabilization reversed the MI-induced abnormalities in contractile machinery properties observed in ENDO cells by restoring pCa_{50} and maximal active tension. These results suggest a ROS-dependent alteration of myofilament properties in MI ENDO cells. Myofilaments from EPI layer were not affected by NAC treatment.

PKA-mediated ROS alterations during HF

HF-associated myofilament Ca^{2+} desensitization is usually associated to a PKA-dependent phosphorylation of contractile proteins [34]. Given that ROS have been shown to activate PKA [35], we sought to explore whether the ROS-dependent ECC alterations reported in our study could be attributed to PKA activation. We thus incubated permeabilized myofilaments with a recombinant catalytic subunit of PKA. PKA incubation normalized all three groups to the same pCa_{50} in both ENDO and EPI layer (Figure 4A). This result suggests that the differences in pCa_{50} observed before PKA incubation was due to PKA activation. Notably, the failing myofilaments previously incubated with NAC displayed the same pCa_{50} than the failing myofilament, after PKA incubation. This result supports the hypothesis that the beneficial effects of NAC were mediated through a decreased PKA activity in ENDO layer. This is further supported by the measurement of PKA activity in cardiac tissue that significantly increased by 101 % in the ENDO layer of HF rats (Figure 4B). NAC restored completely the level of PKA activity in HF ENDO layer. Surprisingly, PKA activity was also significantly

increased in the EPI layer of HF rats but to a lower extent compared with ENDO layer (+ 33 %) (Figure 4B). NAC also reversed the PKA activation in EPI layer (Figure 4B).
We then evaluated the phosphorylation status of two proteins involved in HF-associated ECC defects and modulated by PKA: TnI and RyR2. TnI, a regulatory protein of the myofilaments, was hyperphosphorylated in failing cardiomyocytes only in ENDO layer on the PKA site (Figure 4C). NAC treatment prevented the HF-associated PKA-dependent TnI hyperphosphorylation. RyR2, playing a key role in Ca^{2+} homeostasis regulation, was also hyperphosphorylated in ENDO layer of HF rats on the PKA site and was normalized by NAC treatment (Figure 4C). In EPI layer, no modification was observed (Figure 4C) suggesting that the weak PKA activation in this layer was not sufficient to phosphorylate the target proteins.
Taken together, the results indicate that the ROS production in failing ENDO cardiomyocytes activates PKA which then modulates the protein phosphorylations involved in ECC; acute treatment of failing cardiomyocytes with ROS scavenger can prevent these alterations.

Effects of chronic antioxidant treatment on contractile gradient in MI rats
Next, we evaluated the effect of a chronic antioxidant treatment with NAC administered in the drinking water (75 mg/ day per animal) for 4 weeks on the contractile properties of rats with heart failure. Treatment was started 8 weeks after MI, when most of the morphological remodelling and heart failure were established. *In vivo*, contractile function investigated by echocardiography was largely deficient in HF animals as indexed by the decreases in end-systolic strain (-72%) and aortic velocity time integral (-38%) compared with sham animals (Figure 5B). Chronic NAC treatment improved end-systolic strain (-25% *vs* sham) and restored aortic velocity time integral (Figure 5B). In addition NAC treatment restored a transmural gradient of velocity shortening that was abolished in MI animals suggesting a regional improvement of contractility (Figure 5B). NAC treatment had minor effects on cardiac remodeling induced by MI (Table 1). At the cellular level, chronic treatment with NAC restored the HF-induced alterations in cardiomyocyte shortening, Ca^{2+} transient amplitude and myofilament Ca^{2+} sensitivity observed in ENDO layer (Figure 5C). It is interesting to note that EPI cardiomyocytes were also affected by chronic NAC treatment with significant increases in cell shortening, Ca^{2+} transient amplitude and myofilament Ca^{2+} sensitivity.
We previously showed that the hyper-activation of PKA during HF could be normalized by an acute treatment with NAC (Figure 4B). After chronic treatment with NAC, we observed a significant decreased PKA activity in myocytes isolated from both EPI and ENDO layers in MI rats (Figure 6A). The reduction of PKA activity was however more pronounced in ENDO layer with an activity lower than in sham animals. As a consequence, we observed a decreased PKA-dependent phosphorylation of both TnI and RyR2 in ENDO layer of chronically treated MI rats (Figure 6B). No change was observed for TnI and RyR2 phosphorylation in EPI layer (Figure 6B).

Discussion

This study highlights the impact of transmural mitochondrial dysfunction and ROS production on ECC in heart failure. We demonstrated that 12 weeks after MI: (1) transmural gradient of metabolic properties disappeared in HF due to preferential alterations in ENDO layer; (2) the metabolic disorders were associated with a regionalized oxidative stress

responsible for decreasing contractility through a PKA-dependent pathway affecting both myofilament Ca^{2+} sensitivity and systolic Ca^{2+} release in ENDO layer; (3) chronic antioxidant treatment of MI animals improved *in vivo* cardiac function, restored a transmural gradient of contractility across left ventricular free wall, and recovered the cellular cardiac function.

Regional mitochondrial dysfunction in HF

In physiological conditions, ≈ 2% of ATP is consumed at each heart beat essentially by the myosin ATPase of the contractile machinery allowing efficient ejection fraction [36,37]. However, the coupling between metabolic and contractile properties is heterogeneous across LV since whole heart efficiency is driven by a transmural contractile gradient from epicardial to endocardial layer. Indeed, the subendocardial layer displays higher myocardium strain rate, circumferential shortening and velocities compared to the subepicardial layer [1], thus requiring higher metabolism [38]. We provide here direct evidence that the higher contractile demand of ENDO layer is correlated with higher NADH oxidation resulting from greater electron transport chain activity. It has been shown that the higher rate of metabolic activity in ENDO layer requires greater oxygen extraction [39,40]. However, in failing heart, the myocardial blood flow and oxygen delivery are more severely affected in the inner sub-endocardial layer compared to the outer sub-epicardial layer [41,42]. This regionalized ischemia may thus avoid sufficient oxygen extraction and subsequent NADH oxidation and could then explain the altered mitochondrial metabolism in ENDO layer of failing hearts. Impairment of electron transport chain activity, mainly defects in complex I, promote superoxide anion production [30,31,32]. As a consequence, we show that the metabolic defects in ENDO layer of failing hearts are associated with elevated ROS production after cell stimulation. Both increased ROS production linked to disturbed metabolism and decreased antioxidant defences have been proposed to explain the HF-associated oxidative stress [43,44,45]. In our study, reduced respiratory chain capacity and decreased oxidative defences preferentially in ENDO layer may underlie the ROS excess in this layer.

ROS abolish ECC gradient through a PKA-dependent pathway

Raised ROS levels led to oxidation of numerous proteins resulting in myocardial dysfunction [46]. Among ROS potential targets, ECC proteins are particularly sensitive to redox modulation [15]. A key finding of the present study is that acute antioxidant treatment with NAC recovered the contractile defects in cardiomyocyte from ENDO during HF, by recovering both systolic Ca^{2+} release and myofilament Ca^{2+} sensitivity, supporting the notion of ROS-dependent ECC alterations in this layer. The beneficial effects of NAC observed in the present study involved a decreased activity of PKA thus suggesting that ROS production during HF may activate PKA. The ROS-dependent PKA activation leads to PKA-dependent hyperphosphorylation of both TnI and RyR-2. TnI is a key regulatory protein of the myofilaments which phosphorylation by PKA is associated with decreased myofilament Ca^{2+} sensitivity. The differences in myofilament Ca^{2+} sensitivity between Sham, MI and MI-NAC rats disappeared after PKA stimulation, suggesting the involvement of a ROS-dependent activation of PKA activation that modulates the myofilaments. On the other hand, the RyR2 hyperphosphorylation could explain the decreased systolic Ca^{2+} release observed in ENDO layer. Indeed, it has been shown that RyR2 phosphorylation dissociates the channel stabilizing protein FKBP12.6 leading to anarchic Ca^{2+} release during diastole, reduced SR Ca^{2+} load and decreased systolic Ca^{2+} release [47,48]. Thus, we can suppose here that the ROS-induced RyR2 hyperphosphorylation in ENDO layer of MI rats dissociated FKBP12.6 thus decreasing the amount of Ca^{2+} released during systole. Our study established a link between ROS

production, PKA activity and cardiac contractility during HF. However, we can not exclude direct redox modulation on both contractile machinery and Ca^{2+} homeostasis. Indeed, it has been shown that oxidation of myofilament protein sulfhydryl groups [33] as well as the gluthationylation of cysteine residues sites on myosin regulatory light chain lead to decreased myofilament Ca^{2+} sensitivity [49]. On the other hand, nitrosylation of RyR2 has also been reported to be responsible for the dissociation of FKBP12.6 [50]. Thus, ROS are a key target involved in ECC homogenization across LV wall of HF population.

Acute treatment with NAC did not fully recover cell shortening in ENDO failing myocytes despite full recovery of Ca^{2+} homeostasis and myofilament properties (Figure 2B). This result could be due to the expression of different myosin heavy chain (MHC) isoforms. Rodents express mostly the fast α-MHC in normal conditions while the β-MHC is re-expressed during HF [4]. α-MHC has been shown to have markedly higher ATPase activity, faster shortening velocity, and faster rates of force development; whereas β-MHC exhibits a lower tension cost and is thus more efficient [51]. Thus the incomplete recovering of contractile dysfunction following ROS scavenging could be due to the maintained expression of β-MHC in HF animals.

Clinical relevance

It is now established that cardiac function is non-uniform across the wall due to larger and faster contraction of the sub-endocardial layer as compared with the sub-epicardial tissue one, allowing efficient cardiac output [52]. We show in the present study that this spatial heterogeneity of cardiac function results from a spatial heterogeneity of mitochondrial metabolism. Regionalized mitochondrial dysfunction during heart failure induced ROS generation contributing to homogenization of ECC across LV and loss of global contractile gradient. A chronic antioxidant treatment for 4 weeks improved the cardiac function *in vivo* due to recovering of ECC properties in ENDO layer through a PKA pathway. Our results disclose antioxidant supplementation as a possible complementary treatment to current medical therapies for HF patients.

Legends

Figure 1: Regionalized alterations of mitochondrial function results in increased ROS production in ENDO cardiomyocytes of MI rats. A: Left panel: Typical images showing NADH autofluorescence in ENDO cells from Sham (open bar) and MI (dash bar) rats at resting state, and after 5 minutes of 0.5 Hz stimulation. Right panel: Averaged datas of the variation of NADH autofluorescence of Sham and MI cardiomyocytes in both ENDO and EPI layers after a stimulation train at 0.5 Hz, expressed as the variation from the resting state (25-38 cells / 4 hearts). **B**: Activities of citrate syntase (CS), and complex I and IV of the electron chain transporter in both ENDO and EPI layer of Sham and MI hearts (8 hearts for each group). **C**: Left panel: Typical images showing mitochondrial $O_2^{\cdot -}$ production at rest and after 5 minutes stimulation using MitoSOX Red in ENDO cells from Sham and MI rats. Right panel: Averaged datas of mitochondrial $O_2^{\cdot -}$ production after 5-min stimulation in Sham and MI cardiomyocytes (32-40 cells / 4 hearts). **D**: SOD and catalase activities in both ENDO and EPI layers of Sham and MI hearts (8 hearts for each group). * $P<0.05$ within layer, † $P<0.05$ between layer

Figure 2: ROS provoked regionalized contractile dysfunction in MI rats. A: Representative traces of cell shortening at 0.5 Hz in both ENDO (left panel) and EPI (right panel) myocytes isolated from Sham (full line) and MI rats (dark dash line). Some MI myocytes have been treated for 1 hour with NAC (MI-NAC, light dash line). **B:** Averaged datas of SL shortening (left), contraction (middle) and relaxation velocities (right) of Sham (open bar), MI (dash bar) and MI cells treated with NAC (MI-NAC, grey filled bar) in both ENDO and EPI layers (35-50 cells / 4-5 hearts). * $P<0.05$ within layer, † $P<0.05$ between layer

Figure 3: ROS provoked regionalized alterations of Ca^{2+} handling and contractile machinery properties in MI rats. A: Representative traces of indo-1 Ca^{2+} transient in cardiomyocyte isolated from ENDO and EPI layers of Sham (full line) and MI rats (dark dash line). Some MI myocytes have been treated for 1 hour with NAC (MI-NAC, light dash line). **B :** Averaged datas for Ca^{2+} transient amplitude (left), diastolic Ca^{2+} (middle), and kinetic of Ca^{2+} transient reuptake, Tau (right) of Sham (open bar), MI (dash bar) and MI-NAC (grey bar) cardiomyocytes in both ENDO and EPI layers (35-50 cells / 4-5 hearts). **C:** Averaged tension-pCa curves of Sham, MI and MI-NAC permeabilized cardiomyocytes isolated from ENDO and EPI layers. **D:** Averaged datas of maximal active tension and myofilament Ca^{2+} sensitivity (pCa_{50}) of Sham, MI and MI-NAC cardiomyocytes isolated from ENDO and EPI layers (10-15 cells / 4 hearts). * $P<0.05$ within layer, † $P<0.05$ between layer

Figure 4: ROS-induced PKA activation and subsequent substrates phosphorylation in MI rats. A: Myofilament Ca^{2+} sensitivity evaluated before and after PKA treatment (100U/mL, incubation for 60 min) in permeabilized myocytes of Sham and MI rats previously untreated or treated with NAC. (* $P<0.05$ *vs*. condition without PKA). **B:** Averaged data for

PKA activity measured in cardiac strips isolated from ENDO and EPI layers of Sham and MI rats previously treated or not with NAC (n= 8-10 strips/ 4 heart)/ **C:** Effect of acute NAC treatment on the phosphorylation level of cTnI and RyR2 in MI cardiac strips. Phosphorylation levels were determined by Western blotting with antibodies to cTnI phosphorylated at the PKA sites Ser^{22}/Ser^{23} (P-cTnI) and to Ser^{2809} RyR2-phosphorylation, as described in the methods. * $P<0.05$ within layer, † $P<0.05$ between layer

Figure 5: Effects of chronic NAC treatment for 4 weeks on cardiac contractile properties. A: Typical images showing *in vivo* cardiac function evaluated by echocardiography. **B:** Effects of chronic NAC treatment on end systolic strain (left panel), aortic velocity time integral ($VTI_{AO,}$ middle panel) and transmural gradient of velocity of MI (grey bar) animals compared with sham (open bar) and MI (dash bar) animals (7 animals per group) **C:** Effects of chronic NAC treatment on cell shortening (left panel), Ca^{2+} transient amplitude (middle panel) and myofilament Ca^{2+} sensitivity (right panel) of cardiomyocytes from Sham, MI and chronic MI treated rats in both ENDO and EPI layer (35-50 cells / 4-5 hearts). * $P<0.05$ within layer, † $P<0.05$ between layer

Figure 6: Effects of chronic NAC treatment on ECC proteins. A: Averaged data for PKA activity measured in cardiac strips isolated from ENDO and EPI layers of Sham, MI and MI-NAC rats (n= 8-12 strips/ 4 heart)/ **C:** Phosphorylation status of of cTnI and RyR2 in Sham, MI and MI-NAC cardiac strips. Phosphorylation levels were determined by Western blotting with antibodies to cTnI phosphorylated at the PKA sites Ser^{22}/Ser^{23} (P-cTnI) and to Ser^{2809} RyR2-phosphorylation, as described in the methods. * $P<0.05$ within layer, † $P<0.05$ between layer

References

1. **Derumeaux G, Ovize M, Loufoua J, et al. Assessment of nonuniformity of transmural myocardial velocities by color-coded tissue Doppler imaging: characterization of normal, ischemic, and stunned myocardium. *Circulation.* Mar 28 2000;101(12):1390-1395.**
2. **Furukawa T, Myerburg RJ, Furukawa N, et al. Differences in transient outward currents of feline endocardial and epicardial myocytes. *Circ Res.* Nov 1990;67(5):1287-1291.**
3. **Anyukhovsky EP, Sosunov EA, Rosen MR. Regional differences in electrophysiological properties of epicardium, midmyocardium, and endocardium. In vitro and in vivo correlations. *Circulation.* Oct 15 1996;94(8):1981-1988.**
4. **Mou YA, Reboul C, Andre L, et al. Late exercise training improves non-uniformity of transmural myocardial function in rats with ischaemic heart failure. *Cardiovasc Res.* Feb 15 2009;81(3):555-564.**
5. **Cazorla O, Szilagyi S, Le Guennec JY, et al. Transmural stretch-dependent regulation of contractile properties in rat heart and its alteration after myocardial infarction. *Faseb J.* Jan 2005;19(1):88-90.**
6. **Feigl EO. Coronary physiology. *Physiol Rev.* Jan 1983;63(1):1-205.**
7. **Weiss HR, Neubauer JA, Lipp JA, et al. Quantitative determination of regional oxygen consumption in the dog heart. *Circ Res.* Mar 1978;42(3):394-401.**
8. **Kainulainen H, Komulainen J, Leinonen A, et al. Regional differences of substrate oxidation capacity in rat hearts: effects of extra load and endurance training. *Basic Res Cardiol.* Nov-Dec 1990;85(6):630-639.**
9. **Swynghedauw B. Molecular mechanisms of myocardial remodeling. *Physiol Rev.* Jan 1999;79(1):215-262.**
10. **Derumeaux G, Mulder P, Richard V, et al. Tissue Doppler imaging differentiates physiological from pathological pressure-overload left ventricular hypertrophy in rats. *Circulation.* Apr 2 2002;105(13):1602-1608.**
11. **Neubauer S. The failing heart--an engine out of fuel. *N Engl J Med.* Mar 15 2007;356(11):1140-1151.**
12. **Ventura-Clapier R, Garnier A, Veksler V. Energy metabolism in heart failure. *J Physiol.* Feb 15 2004;555(Pt 1):1-13.**
13. **Ide T, Tsutsui H, Kinugawa S, et al. Direct evidence for increased hydroxyl radicals originating from superoxide in the failing myocardium. *Circ Res.* Feb 4 2000;86(2):152-157.**
14. **Heymes C, Bendall JK, Ratajczak P, et al. Increased myocardial NADPH oxidase activity in human heart failure. *J Am Coll Cardiol.* Jun 18 2003;41(12):2164-2171.**
15. **Zima AV, Blatter LA. Redox regulation of cardiac calcium channels and transporters. *Cardiovasc Res.* Jul 15 2006;71(2):310-321.**
16. **de Lamirande E, O'Flaherty C. Sperm activation: role of reactive oxygen species and kinases. *Biochim Biophys Acta.* Jan 2008;1784(1):106-115.**

17. **Bourraindeloup M, Adamy C, Candiani G, et al. N-acetylcysteine treatment normalizes serum tumor necrosis factor-alpha level and hinders the progression of cardiac injury in hypertensive rats. *Circulation.* Oct 5 2004;110(14):2003-2009.**
18. **Andre L, Boissiere J, Reboul C, et al. Carbon Monoxide Pollution Promotes Cardiac Remodeling and Ventricular Arrhythmia in Healthy Rats. *Am J Respir Crit Care Med.* Dec 17 2009.**
19. **Fauconnier J, Andersson DC, Zhang SJ, et al. Effects of palmitate on Ca(2+) handling in adult control and ob/ob cardiomyocytes: impact of mitochondrial reactive oxygen species. *Diabetes.* Apr 2007;56(4):1136-1142.**
20. **Cazorla O, Ait Mou Y, Goret L, et al. Effects of high-altitude exercise training on contractile function of rat skinned cardiomyocyte. *Cardiovasc Res.* Sep 1 2006;71(4):652-660.**
21. **Beers RF, Jr., Sizer IW. A spectrophotometric method for measuring the breakdown of hydrogen peroxide by catalase. *J Biol Chem.* Mar 1952;195(1):133-140.**
22. **Marklund S. Spectrophotometric study of spontaneous disproportionation of superoxide anion radical and sensitive direct assay for superoxide dismutase. *J Biol Chem.* Dec 10 1976;251(23):7504-7507.**
23. **Srere PA. An eclectic view of metabolic regulation: control of citrate synthase activity. *Adv Enzyme Regul.* 1970;9:221-233.**
24. **Janssen AJ, Trijbels FJ, Sengers RC, et al. Spectrophotometric assay for complex I of the respiratory chain in tissue samples and cultured fibroblasts. *Clin Chem.* Apr 2007;53(4):729-734.**
25. **Wharton DC. Purification of electron-transfer components from Pseudomonas. *Methods Enzymol.* 1978;53:646-661.**
26. **Stanley WC, Recchia FA, Lopaschuk GD. Myocardial substrate metabolism in the normal and failing heart. *Physiol Rev.* Jul 2005;85(3):1093-1129.**
27. **Droge W. Free radicals in the physiological control of cell function. *Physiol Rev.* Jan 2002;82(1):47-95.**
28. **Maack C, Cortassa S, Aon MA, et al. Elevated cytosolic Na+ decreases mitochondrial Ca2+ uptake during excitation-contraction coupling and impairs energetic adaptation in cardiac myocytes. *Circ Res.* Jul 21 2006;99(2):172-182.**
29. **Liu T, O'Rourke B. Enhancing mitochondrial Ca2+ uptake in myocytes from failing hearts restores energy supply and demand matching. *Circ Res.* Aug 1 2008;103(3):279-288.**
30. **Pitkanen S, Robinson BH. Mitochondrial complex I deficiency leads to increased production of superoxide radicals and induction of superoxide dismutase. *J Clin Invest.* Jul 15 1996;98(2):345-351.**
31. **Luo X, Pitkanen S, Kassovska-Bratinova S, et al. Excessive formation of hydroxyl radicals and aldehydic lipid peroxidation products in cultured skin fibroblasts from patients with complex I deficiency. *J Clin Invest.* Jun 15 1997;99(12):2877-2882.**
32. **Ide T, Tsutsui H, Kinugawa S, et al. Mitochondrial electron transport complex I is a potential source of oxygen free radicals in the failing myocardium. *Circ Res.* Aug 20 1999;85(4):357-363.**
33. **Hertelendi Z, Toth A, Borbely A, et al. Oxidation of myofilament protein sulfhydryl groups reduces the contractile force and its Ca2+ sensitivity in human cardiomyocytes. *Antioxid Redox Signal.* Jul 2008;10(7):1175-1184.**

34. **Kaumann A, Bartel S, Molenaar P, et al. Activation of beta2-adrenergic receptors hastens relaxation and mediates phosphorylation of phospholamban, troponin I, and C-protein in ventricular myocardium from patients with terminal heart failure. *Circulation.* Jan 5-12 1999;99(1):65-72.**
35. **Brennan JP, Bardswell SC, Burgoyne JR, et al. Oxidant-induced activation of type I protein kinase A is mediated by RI subunit interprotein disulfide bond formation. *J Biol Chem.* Aug 4 2006;281(31):21827-21836.**
36. **Sakamoto T, Webb MR, Forgacs E, et al. Direct observation of the mechanochemical coupling in myosin Va during processive movement. *Nature.* Sep 4 2008;455(7209):128-132.**
37. **Harris DA, Das AM. Control of mitochondrial ATP synthesis in the heart. *Biochem J.* Dec 15 1991;280 (Pt 3):561-573.**
38. **Beyar R, Sideman S. Left ventricular mechanics related to the local distribution of oxygen demand throughout the wall. *Circ Res.* May 1986;58(5):664-677.**
39. **Bin JP, Le E, Pelberg RA, et al. Mechanism of inducible regional dysfunction during dipyridamole stress. *Circulation.* Jul 2 2002;106(1):112-117.**
40. **Gallagher KP. Transmural steal with isoproterenol and exercise in poststenotic myocardium. *Basic Res Cardiol.* 1990;85 Suppl 1:145-155.**
41. **Path G, Robitaille PM, Merkle H, et al. Correlation between transmural high energy phosphate levels and myocardial blood flow in the presence of graded coronary stenosis. *Circ Res.* Sep 1990;67(3):660-673.**
42. **Hittinger L, Shannon RP, Bishop SP, et al. Subendomyocardial exhaustion of blood flow reserve and increased fibrosis in conscious dogs with heart failure. *Circ Res.* Oct 1989;65(4):971-980.**
43. **Hill MF, Singal PK. Right and left myocardial antioxidant responses during heart failure subsequent to myocardial infarction. *Circulation.* Oct 7 1997;96(7):2414-2420.**
44. **Sawyer DB, Colucci WS. Mitochondrial oxidative stress in heart failure: "oxygen wastage" revisited. *Circ Res.* Feb 4 2000;86(2):119-120.**
45. **Giordano FJ. Oxygen, oxidative stress, hypoxia, and heart failure. *J Clin Invest.* Mar 2005;115(3):500-508.**
46. **Takimoto E, Kass DA. Role of oxidative stress in cardiac hypertrophy and remodeling. *Hypertension.* Feb 2007;49(2):241-248.**
47. **Marx SO, Reiken S, Hisamatsu Y, et al. PKA phosphorylation dissociates FKBP12.6 from the calcium release channel (ryanodine receptor): defective regulation in failing hearts. *Cell.* May 12 2000;101(4):365-376.**
48. **Lehnart SE, Mongillo M, Bellinger A, et al. Leaky Ca2+ release channel/ryanodine receptor 2 causes seizures and sudden cardiac death in mice. *J Clin Invest.* Jun 2008;118(6):2230-2245.**
49. **Reece KL, Moss RL. Intramolecular interactions in the N-domain of cardiac troponin C are important determinants of calcium sensitivity of force development. *Biochemistry.* May 6 2008;47(18):5139-5146.**
50. **Zissimopoulos S, Docrat N, Lai FA. Redox sensitivity of the ryanodine receptor interaction with FK506-binding protein. *J Biol Chem.* Mar 9 2007;282(10):6976-6983.**
51. **Locher MR, Razumova MV, Stelzer JE, et al. Determination of rate constants for turnover of myosin isoforms in rat myocardium: implications for in vivo contractile kinetics. *Am J Physiol Heart Circ Physiol.* Jul 2009;297(1):H247-256.**

52. Bogaert J, Rademakers FE. Regional nonuniformity of normal adult human left ventricle. ***Am J Physiol Heart Circ Physiol.*** **Feb 2001;280(2):H610-620.**

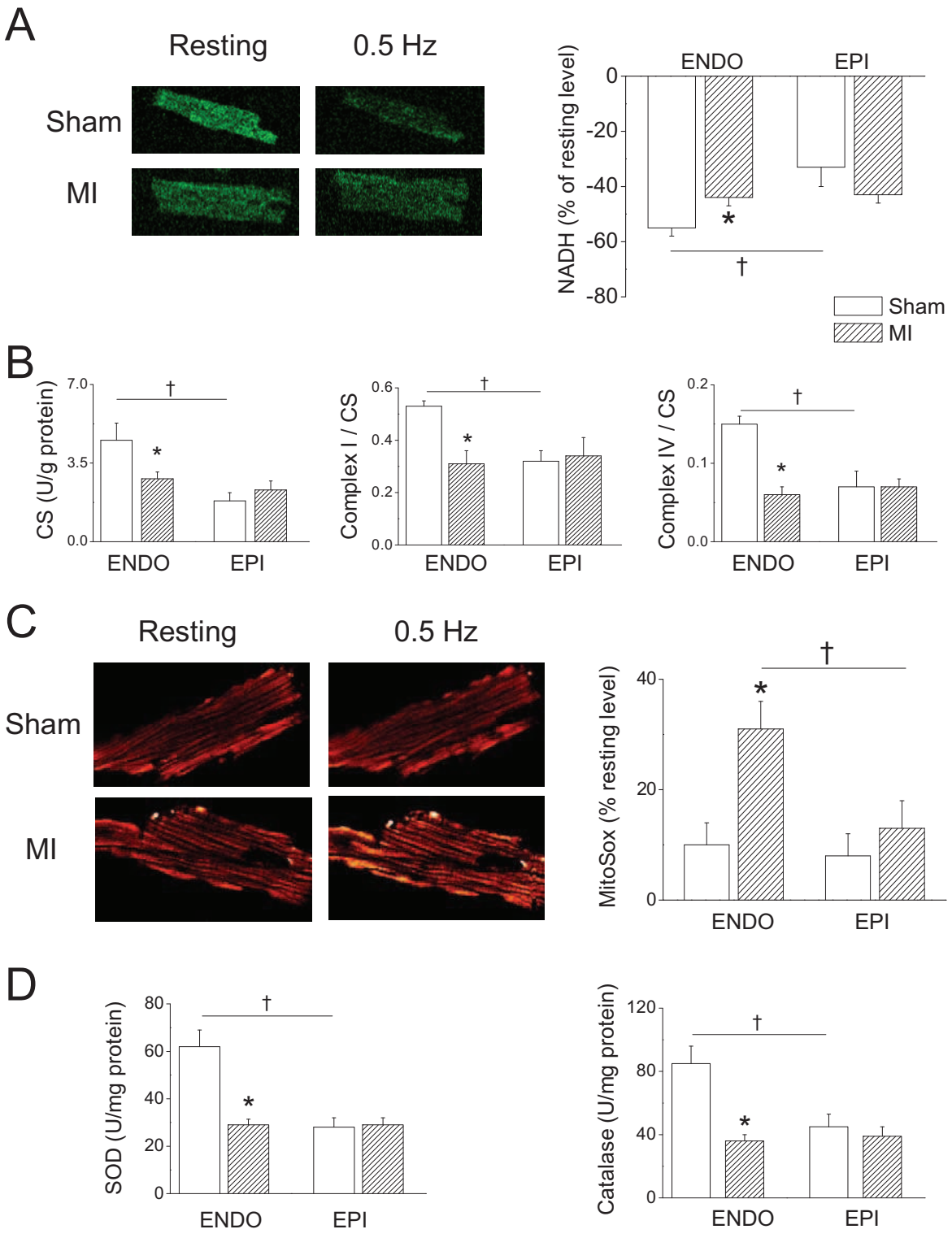

Figure 1, Andre *et al.*

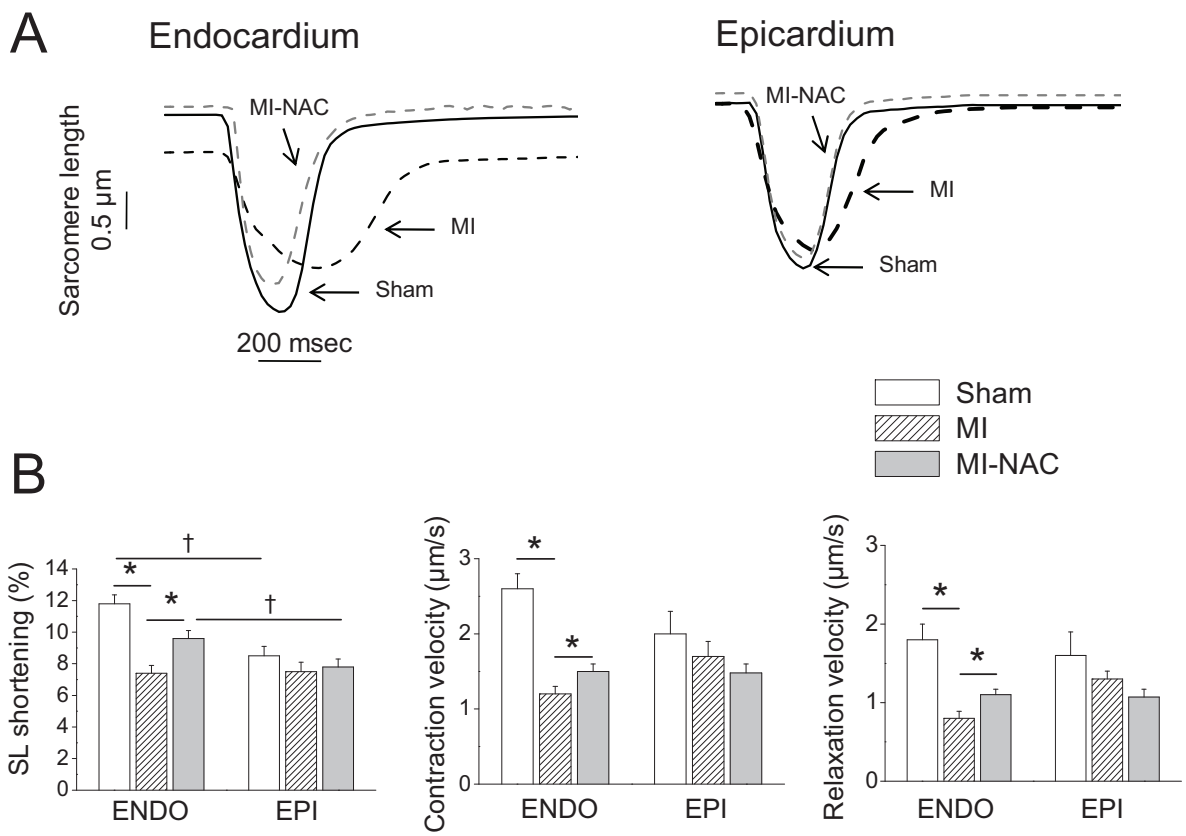

Figure 2, Andre *et al.*

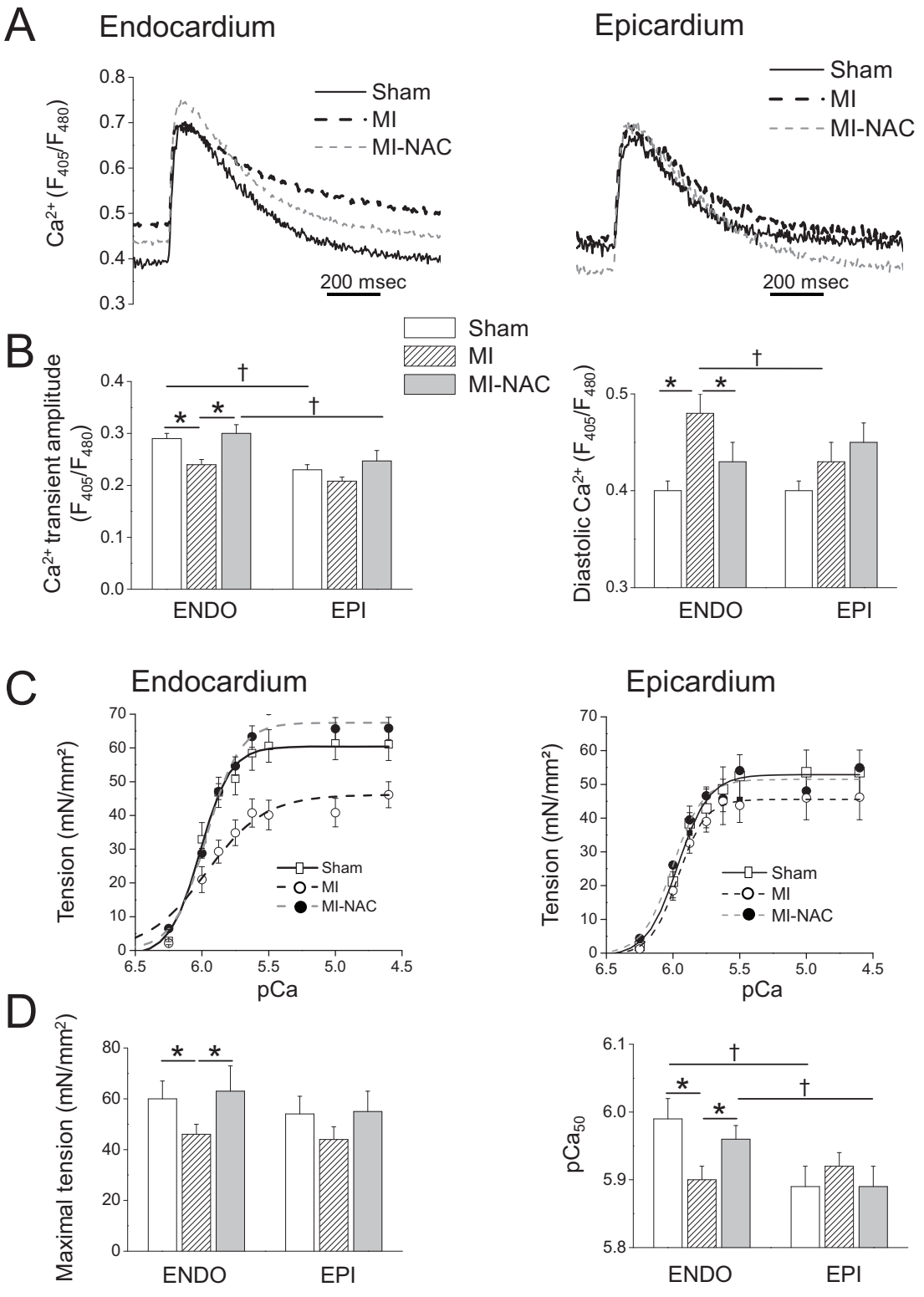

Figure 3, Andre *et al.*

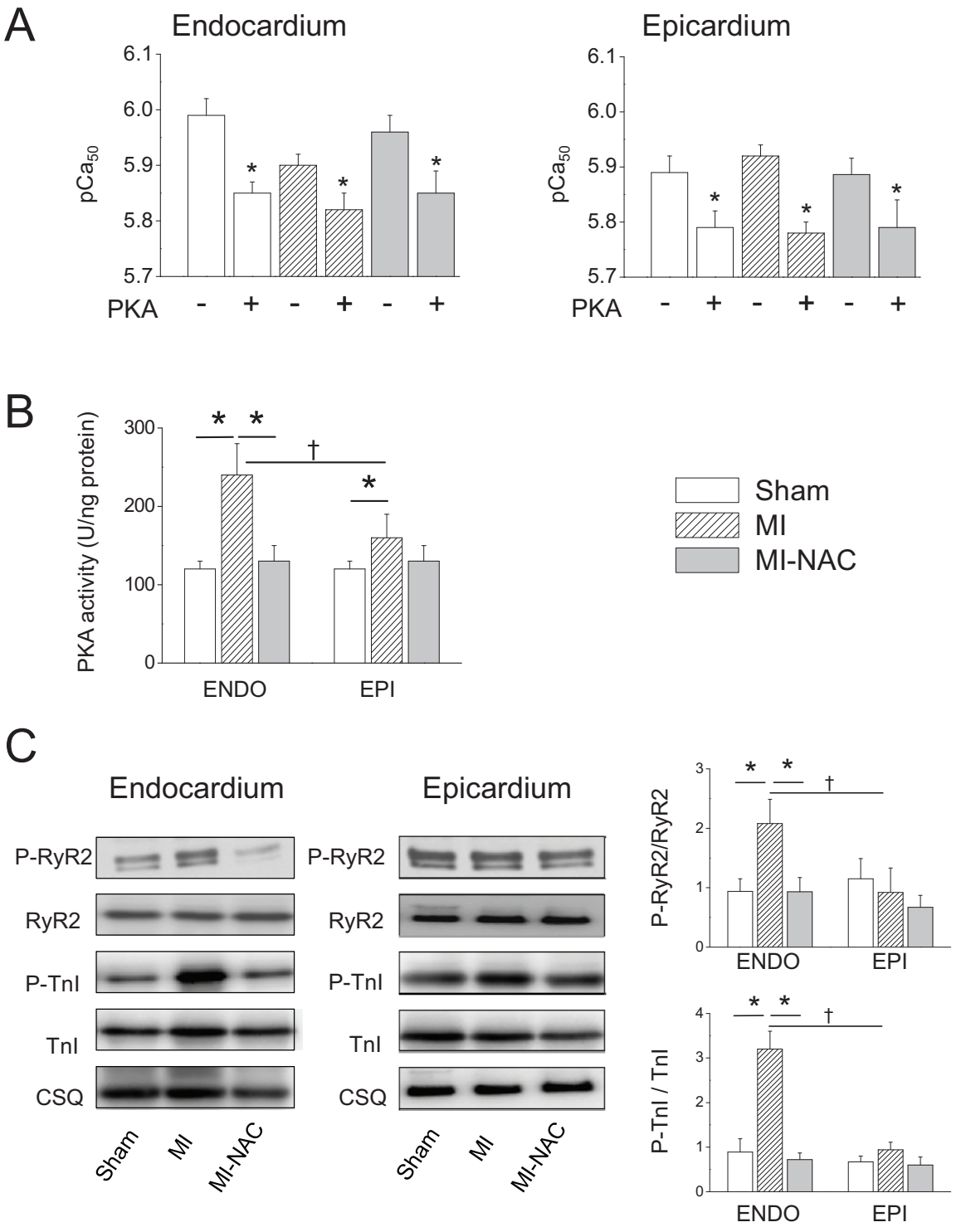

Figure 4, Andre *et al.*

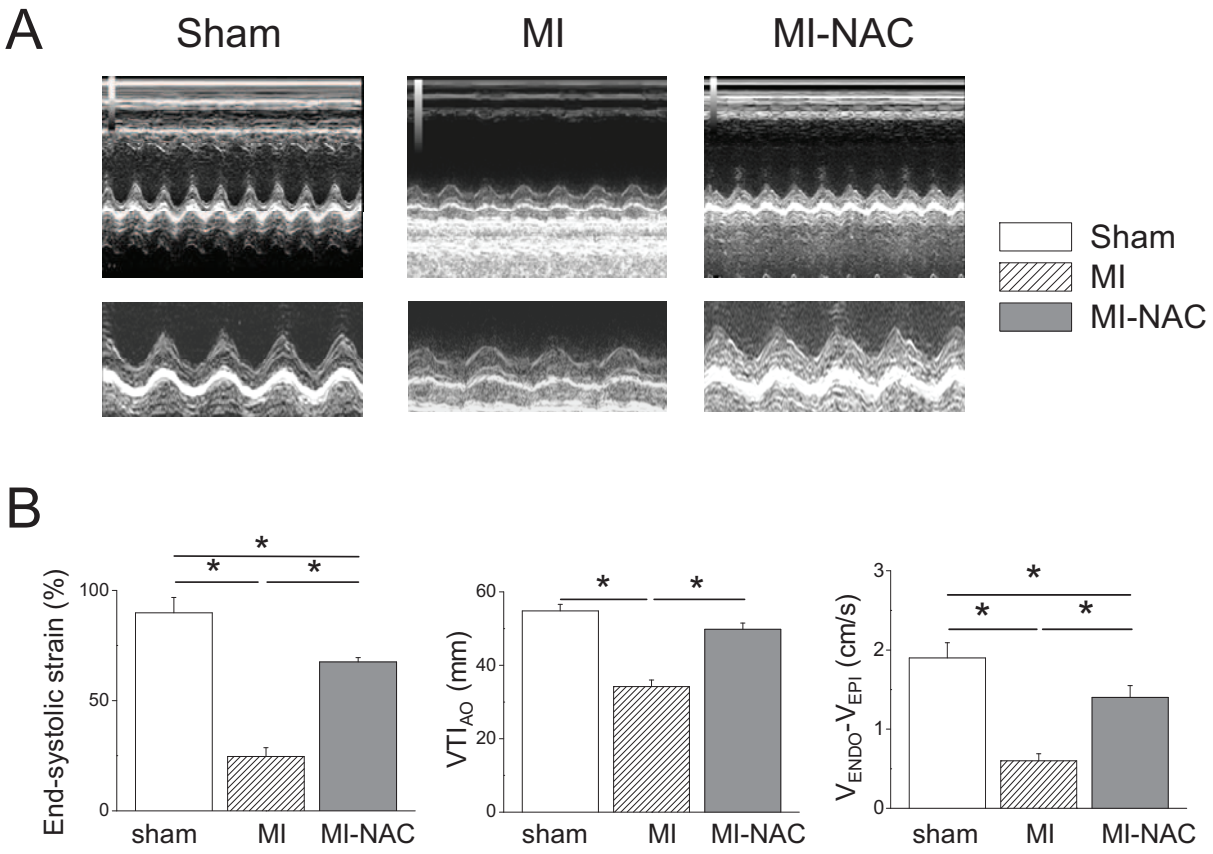

Figure 5, Andre *et al.*

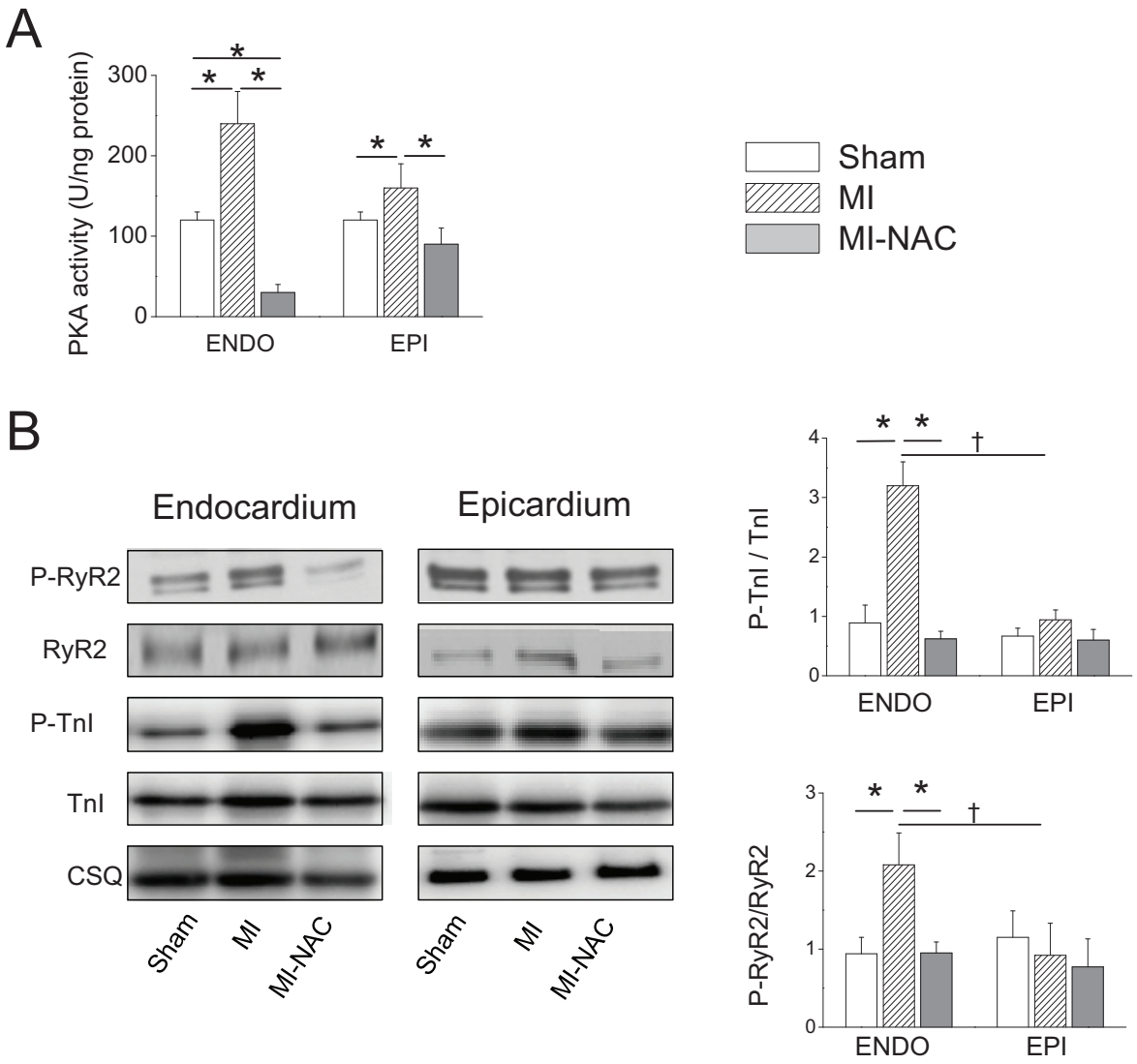
A
PKA activity (U/ng protein)
300
200
100
0
ENDO
EPI
Sham
MI
MI-NAC
B
Endocardium
Epicardium
P-RyR2
RyR2
P-TnI
TnI
CSQ
Sham
MI
MI-NAC
Sham
MI
MI-NAC
P-TnI / TnI
ENDO
EPI
P-RyR2/RyR2
ENDO
EPI

3. Conclusion

Cette étude met en évidence une perte du gradient des propriétés mitochondriales dans l'IC ischémique en raison d'une dysfonction mitochondriale associée à une production excessive de ROS dans l'ENDO. Les ROS entrainent alors une hyper-activation de la PKA, laquelle phosphoryle notamment la troponine I, ce qui a pour conséquence de diminuer la sensibilité au Ca^{2+} des myofilaments dans l'ENDO. Ainsi, les altérations régionalisées des propriétés métaboliques mitochondriales semblent être à l'origine de l'homogénéisation des propriétés contractiles dans l'IC. Ces résultats légitiment alors l'utilisation de stratégies thérapeutiques antioxydantes afin de prévenir ce remodelage cardiaque délétère. En effet, dans cette même étude, un traitement antioxydant avec le NAC pendant 4 semaines prévient les dysfonctions contractiles dans l'ENDO et restaurent le gradient transmural de contraction à travers la paroi ventriculaire gauche. L'absence d'altérations et l'insensibilité de l'EPI aux traitements antioxydants est cohérente avec des données étudiant les modifications morpho-fonctionnelles régionalisées suite à une exposition en altitude [148], ou suite à un protocole d'exercice physique [50]. Il semblerait que la grande stabilité de la région EPI face aux stress physiopathologiques externes résulte d'une répartition des forces hétérogène : l'ENDO étant situé dans la partie intérieure du myocarde, cette région est directement en contact avec les modifications pariétales lors d'un stress. Cette pression mécanique proximale pourrait alors agir comme initiateur du remodelage. A l'inverse, l'EPI est positionné de manière plus distale par rapport aux stress pariétaux et serait alors moins sollicitée. Les études 1 et 2 ont montré l'importance des ROS dans le processus de remodelage cardiaque à l'origine des troubles contractiles et arythmiques au cours de l'IC. La troisième étude s'est alors intéressée aux effets de l'exercice physique, stratégie connue pour réduire la production de ROS et augmenter les défenses antioxydantes, dans la prévention du phénotype arythmique chez des populations IC.

III. L'exercice physique réduit les phénomènes arythmiques dans l'IC ischémique : rôle de la mitochondrie

1. Introduction

Les arythmies ventriculaires sont responsables d'environ 50% des décès dans l'IC. Ces phénomènes arythmiques sont retrouvés majoritairement dans l'ENDO, en raison notamment d'une production anormalement élevée de ROS dans cette région au cours de l'IC (Etude 1). Le RyR-2 est l'élément pivot régulant les flux de Ca^{2+} intracellulaire. Il est particulièrement impliqué dans la genèse de phénomènes arythmiques au cours de l'IC ; notamment, l'oxydation et la phosphorylation de ce récepteur entrainent une fuite de Ca^{2+} du RS laquelle est responsable d'une surcharge calcique diastolique.

Parmi les stratégies thérapeutiques utilisées dans l'IC afin de ralentir la progression de la pathologie, l'exercice physique permet de réduire la production de ROS et diminue l'activation de la voie beta adrénergique, et agit donc sur les 2 sources de dysfonctions du RyR-2. Bien que l'exercice physique prévient le remodelage morpho-fonctionnel et améliore la qualité de vie des patients, ses effets sur la réduction des phénomènes arythmiques associés à l'IC sont mal établis et restent controversés. L'objectif de cette 3ème étude a donc été de tester si l'exercice physique pouvait réduire les arythmies ventriculaires grâce à une prévention des altérations des propriétés électro physiologiques et de l'homéostasie calcique induites par le stress oxydatif au cours de l'IC.

2. Article 3 - Finalisation avant soumission pour publication

Exercise training decreases arrhythmic events in ischemic heart failure: the mitochondrial origin.

Lucas Andre[1], Gregory Meyer[2], Cyril Reboul[2], Julien Boissiere[1,2], Christine Feillet-Coudray[3], Gilles Fouret[3], Philippe Obert[2], Jeremy Fauconnier[1], Sylvain Richard[1], Alain Lacampagne[1], Olivier Cazorla[1]

[1] INSERM U-637, F-34295 Montpellier, France. Université Montpellier1, Université Montpellier2, F-34295 Montpellier, France
[2] EA-4278, Université Avignon et des Pays de Vaucluse, UFR Sciences, F-84000 Avignon, France
[3] INRA UMR 866, Différentiation Cellulaire et Croissance, 34060 Montpellier, France

Correspondence to :
Olivier CAZORLA
Inserm U637 Physiopathologie Cardiovasculaire
CHU Arnaud de Villeneuve
34295 Montpellier, France
Phone : +33 467 41 52 44
Fax : +33 467 41 52 42
olivier.cazorla@inserm.fr

Key words: Oxidative stress, ectopic Ca^{2+} transient, adrenergic system, physical activity

1. Introduction

Heart failure (HF) is the major cause of morbidity and mortality in the developed world. Ventricular arrhythmias leading to sudden cardiac death (SCD) account for ~50% of deaths in patients with heart failure [1]. We have previously shown that arrhythmic events are transmurally distributed across the left ventricular wall during ischemic HF with higher propensity in the inner sub-endocardial (ENDO) layer compared to the outer sub-epicardial (EPI) layer (submitted article). This regionalized arrhythmic phenotype was due to a reactive oxygen species (ROS)-induced ryanodine receptor (RyR-2) dysfunction in ENDO layer of failing hearts. Indeed, we have shown that HF-associated oxidative stress activated the protein kinase A (PKA) in ENDO layer leading to RyR-2 hyperphopshorylation and subsequent diastolic Ca^{2+} overload. RyR-2 hyperphosphorylation, mediated either directly by HF-associated chronic adrenergic activation and/or indirectly by HF-associated oxidative stress, is a key target for fighting arrhythmic events and SCD during HF.
Among various therapeutic strategies aiming to improve outcome and slow the progression of HF, exercise training is a physiological approach known to decrease oxidative stress [2] and reduce adrenergic tone [3 4]. Although exercise training programs have proven to be safe and effective at improving many functional parameters such as exercise capacity and health-related quality of life [5 6] and reduced mortality of HF patients, the effects of exercise training on arrhythmia are not yet well established and remain controversial [7 8]. We aimed to determine whether 4 weeks of exercise training could reduce arrhythmic events through recovering of mitochondrial dysfunction-associated oxidative stress. Results showed that exercise reduced ROS production during HF

2. Materials and Methods

Animal and exercise training
The investigations were carried out in agreement with the *Guide for the Care and Use of Laboratory Animals* published by the US National Institute of Health (NIH Publications No. 85-23, revised 1996) and with the approval of French Agriculture Department. Male Wistar rats (5 weeks old, Charles River) were randomly assigned to left coronary artery ligation in order to induce myocardial infarction (MI rats) or to sham-operated procedure (Sham rats) as previously described (Cazorla et al, FASEB J 2005). Seven weeks after MI, rats were randomly assigned to the sedentary (MI) or 4 weeks moderate treadmill exercised (MI-Ex, 40 min/day, 5 days/week, 15 m/min) groups.

ECG recording, arrhythmias and heart rate variability in vivo
Before the exercise protocol, rats were implanted for ECG telemetry recordings (Dataquest, Data Sciences International, Transoma Medical, Arden Hills, Minnesota, USA). Surface ECG recordings were performed for a 24 h period started one week after anesthesia and surgery. Then, animals were assigned to exercise or sedentary activity for 4 weeks and ECG were recorded again for 24 h. ECG signals were analyzed manually to detect, identify and count spontaneous rhythmic disorders. Subsequently, on the same recordings, heart rate variability (HRV) was analyzed in time domain. The mean RR intervals (RR) and the standard deviation of all normal RR intervals (SDNN) were calculated from 24 h ECG.

Coronary perfusion

Evaluation of myocardial perfusion was performed on a second set of rats under basal condition (n=10 per group) and during a β-adrenergic challenging obtained by isoproterenol infusion (1 mg.kg-1.min-1) (n=10 per group) (Figure 1A). Fluorescent microspheres (15.0±0.2 µm diameter, Dye-Track Fluorescent Yellow part 130–0485, Triton Technology) were used for myocardial perfusion assessment as previously reported [9]. Briefly, we injected 105 microspheres in 0.5 ml of the suspension in the LV. The arterial pressure waveform was monitored continuously to verify proper delivery of microspheres. The microspheres were allowed to flush during 1 min and the heart was immediately removed and placed in cold physiological salt solution for ventricular dissection. The LV (including septum) was placed for 48 hours in 20 ml of 4 N KOH containing 2% Tween 80 for tissue digestion. Microspheres were physically separated from digested tissues by negative pressure filtration. Filters containing microspheres (part 31079, DYE-TRAK, Triton Technology) were placed in 2 ml of solvent (2-ethoxyethyl acetate, Sigma-Aldrich). The peak fluorescent spectrum was read at 485 nm for an excitation wavelength of 450 nm with a spectrofluorometer (Synergy HT, Biotek).

Cell isolation

Single left ventricular myocytes were isolated by enzymatic digestion as previously described (Cazorla et al, British J pharmacol 2003)). Briefly, hearts were quickly removed and mounted on a Langendorff apparatus. The heart was perfused with a Ca^{2+}-free solution followed by perfusion with a collagenase IV (Boeringer) enzymatic solution. Small pieces of ventricular tissues from the inner free wall ENDO layer and from the outer free wall EPI layer were dissected and gently dissociated in Ca^{2+} free solution. Ca^{2+} concentration was gradually increased to 1 mM Ca^{2+}. Solution for isolating intact cells contained (mM): NaCl 117, KCl 5.7, $NaHCO_3$ 4.4, KH_2PO_4 1.5, $MgCl_2$ 1.7, HEPES 21, glucose 11, taurine 20, pH 7.2 adjusted with NaOH. To prevent protein degradation, all solutions contained a calpain inhibitor (E64d: 0.01 mM).

Measurement of mitochondrial NADH

The endogenous autofluorescence of mitochondrial NADH was measured using a two-photon excitation at 720 nm and its emission recorded at λem=450-485 nm in the same cells. Fluorescence images were recorded using a Zeiss LSM 510 inverted two photons confocal microscope with x20 lens. Cells were paced at 0.5 Hz using two platinium electrodes placed in each side of the Petri dish. NADH fluorescence was collected at rest and after 5 min stimulation. For each cell, the resting value was set to 100% and background noise was subtracted by measuring fluorescence close to the cell.

Measurement of mitochondrial Ca^{2+}

Rhod-2 AM was used to measure mitochondrial Ca^{2+} [10]. Isolated cardiomyocytes were loaded with rhod-2 AM (10 µmol/l) for 45 min at 37°C followed by washout. Fluorescence images were recorded using a Zeiss LSM 510 inverted confocal microscope with x40 lens. Confocal images were obtained at 5-min intervals by excitation at 568 nm and measuring the emitted light at 585 nm. Rhod-2 fluorescence was collected at rest and after 5 min stimulation. For each cell, rhod-2 fluorescence value was calculated as the mean of 3 different values collected at 3 different locations. Resting value was set to 100% and background noise was subtracted by measuring fluorescence close to the cell.

Measurement of mitochondrial ROS production

MitoSOX Red was used to measure mitochondrial ROS production [11]. Isolated cardiomyocytes were loaded with MitoSOX Red (5 µmol/l) for 15 min at room temperature, followed by washout. Fluorescence images were recorded using a Zeiss LSM 510 inverted confocal microscope with x25 lens. Confocal images were obtained at 5-min intervals by excitation at 488 nm and measuring the emitted light at 583 nm. MitoSOX Red fluorescence was collected at rest and after 5 min stimulation. For each cell, the resting value was set to 100% and background noise was subtracted by measuring fluorescence close to the cell.

Ca^{2+}transient in intact cardiomyocyte

Cells were loaded for 30 min at room temperature with Indo-1 AM (10 µM Invitrogen inc., France) in order to monitor intracellular Ca^{2+}. Cells were field stimulated at frequency of 0.5 Hz (20V, 1 ms), and simultaneously illuminated at 360 nm using a xenon arc bulb light. Sarcomere length (SL) and Indo-1 fluorescence emitted at 405 nm and 480 nm were simultaneously recorded using IonOptix acquisition software (IonOptix system, Hilton, USA).

Ectopic Ca^{2+} transient were measured after a protocol of stimulation frequencies variation as follow: 0.5 Hz (steady state), then 2 Hz (1 minute) and recover to 0.5 Hz. The spontaneous Ca^{2+} waves, an index of cellular arrhythmia, were analyzed during the recovery phase at 0.5 Hz.

Ca^{2+} sparks

Isolated cardiomyocytes were loaded with fluo-4 AM (5µM) for 20 minutes at room temperature. Fluorescence images were recorded using a Zeiss LSM 510 inverted confocal microscope with x63 lens. Confocal images were obtained by line scanning along the long axis, with focus in the middle of the cell at two different places. Linescan rate was 3.07 ms per line; 512 x 512 pixel, 8 bit xy images of single or dual channel were taken at the speed of 3.0 s per frame. Stored confocal images were analyzed with ImageJ (National Institutes of Health [available at http://rsb.info.nih.gov/ij]) according to the methods described by Picht et al [12]. Ca^{2+} sparks frequency was calculated as the number of sparks obtained on the 10 successive images of one cell divided by 10.

SR Ca^{2+} load

The sarcoplasmic reticulum (SR) Ca^{2+} was measured inn intact cardiomyocytes loaded with fluo-4. After 5 minutes of electrical field stimulation at 0.5 Hz, rapid perfusion of caffeine (20mM) was used to release SR Ca^{2+} store.

Determination of antioxidant activities in cardiomyocytes

After cell lysis in hypotonic buffer (phosphate buffer 8mM, pH 7.4), catalase activity was measured according to the method of Beers and Sizer [13] and total superoxide dismutase (SOD) was measured according to the method of Marklund [14]. Protein levels in cells lysates were measured by the Bradford technique [15].

Determination of mitochondrial enzymatic activities in cardiomyocytes

After cell lysis in hypotonic buffer (phosphate buffer 8mM, pH 7.4), citrate synthase (CS) activity was measured according to Srere [16]: the activity of the enzyme was measured by following the color of 5-thio-2-nitrobenzoic acid, which was generated from 5,5'-dithiobis-2-nitrobenzoic acid present in the reaction of citrate synthesis, and caused by the deacetylation of Acetyl-CoA.

Complex I of the electron transport chain (ETC) was evaluated through the measurement of the reduction of the 2 ,6 – dichlorophenolindophenol by the NADH dehydrogenase at 600 nm (37°C) [17]. Complex IV of the ETC was measured through the measure of the cytochrome-c oxidase (Cyt-c oxidase) activity according to Wharton and Tzagoloff [18]: oxidation of reduced cytochrome c was followed spectrophotometrically.

Protein Analysis

Proteins were separated using 2-20 % SDS-PAGE and blotted onto a nitrocellulose membrane (Protran, Schleichen and Schuele, Dassel, Germany). Membranes were incubated overnight at 4°C with the following primary antibodies: RyR-2 antibody (Covalab, France), Phospho Ser^{2809}-RyR-2 antibody (A010-30, Badrilla, UK). RyR-2 levels were expressed relative to calsequestrin content (Cat # PA1-913, ABR, USA) on the same membrane. Immunodetection was carried out using the ECL Plus system (Amersham Pharmacia, Little Chalfont Buckinghamshire, England).

PKA activity was measured using a non-radioactive PKA activity assay kit (Assay design). Tissue extracts originated from ENDO and EPI layers were mixed with ATP for 90 minutes. Phosphospecific and anti-rabbit antibody were consecutively added before measuring the absorbance at 450 nm.

Statistical analysis

Data were analyzed using one-way or 2-way ANOVA between groups. When significant interactions were found, a Bonferroni post-hoc test was applied with $P< 0.05$ (Statview 5.0). Data are presented as mean±SEM.

3. Results

Effects of exercise on ECG, HRV, intracardiac conduction and arrhythmia after MI

Surface ECGs were recorded and analyzed in conscious rats from the sham, MI and MI-Ex groups (Table 1). The averaged heart rate during 24 hours analysis was increased in MI rats and was restored by exercise. The PR duration was similar in the three groups. In contrast, the QT, QTc and QRS were prolonged in MI rats when compared to sham, indicating intraventricular conduction abnormality. Exercise reversed all these prolongations. The normal-to-normal interval (NN), the standard deviation of the NN (SDNN, an estimate of total autonomic variability), and the root mean square successive difference in heart rate period (RMSSD, reflecting short-terms variation in HR) were all decreased in MI animals (table 1). Exercise reversed partially the HRV parameters. The number of premature ventricular beats (PVB) was increased in MI rats and reversed by exercise. Non-sustained tachycardia, absent in sham, were detected in 67% of MI rats, and only in 20% of MI-Ex rats. The number of atrio-ventricular blocks was increased in MI rats. Exercise tended to decrease the occurrence of atrio-ventricular blocks without reaching significance. These data thus support the anti-arrhythmic effect of exercise training.

Exercise improved oxidative capacity in ENDO layer

Mitochondrial dysfunction plays a central role in arrythmogenesis [19]. We thus evaluated whether exercise training could improve the mitochondrial function during HF. Mitochondria

are the primary ATP provider in cardiomyocyte in order to match energy demand and supply. Both fatty acid and carbohydrate metabolism converge to the Krebs cycle. This results in the generation of reduced redox carriers NADH and $FADH_2$ that are oxidized in the inner membrane of mitochondria by complexes (I-IV) of the ETC. The electron transfer of both NADH and FADH2 generates a proton motive force driving ATP synthesis via the terminal complex (complex V) [20]. We measured NADH autofluorescence after 5 minutes of 0.5 Hz stimulation in both ENDO and EPI layers, as an index of the oxidative metabolism [21 22]. Cell stimulation decreased NADH level in each group reflecting NADH utilization under stress condition. As previously observed, this NADH decrease following stimulation was lower in ENDO layer of MI rats suggesting altered mitochondrial metabolism (Figure 2A). Exercise restored the amplitude of NADH autofluorescence decline induced by stimulation in ENDO layer, thus restoring the transmural metabolic state observed in physiological condition. Epi layer was not affected by pathology and exercise.

NADH autofluorescence reflects both NADH production by the Krebs cycle and NADH oxidation within the electron transport chain. We evaluated whether beneficial effects of exercise on NADH homeostasis could be attributed to improved ETC activity. Complex I and IV (Cyt-c Oxydase) activities were normalized to CS activity, an index of mitochondrial content. In MI rats, CS activity was decreased in ENDO layer, suggesting a lower mitochondrial content in this layer (Figure 2B), and was associated with decreased activity of both complex I and IV of the ETC (Figure 2B). Exercise partially reversed the MI-induced abnormalities for CS and complex I activities in ENDO layer. Complex IV was not modified by exercise. EPI layer was not affected neither by pathology nor by exercise (Figure 2B). In MI rats, the altered cardiac mitochondrial metabolism has been previously attributed to perturbations in the oxygen delivery through the vascular coronary network [23]. We thus evaluated whether the coronary perfusion could account for the improvements of NADH homeostasis consecutive to exercise training in MI rats. The coronary perfusion was decreased in both ENDO and EPI layer of MI rats (Figure 2C). Exercise recovered the perfusion only in ENDO layer (Figure 2B3).

Mitochondrial Ca^{2+} plays a central role in metabolism regulation. Indeed intra-mitochondrial Ca^{2+} oscillation during alternance of systole and diastole stimulates TCA cycle enzyme [24]. We thus evaluated whether mitochondrial Ca^{2+} could account for the beneficial effects of exercise on oxidative capacity in ENDO layer of MI rats. Mitochondrial Ca^{2+} was increased in cardiomyocytes isolated from ENDO layer of MI rats compared to sham rats (Figure 2C). Exercise significantly decreased these MI-induced mitochondrial Ca^{2+} overload in ENDO layer. EPI layer was not affected neither by pathology nor by exercise (Figure 2C). Taken together, these results suggest that exercise restored coronary perfusion and partially reversed the MI-induced mitochondrial dysfunction in ENDO layer.

Exercise reduced oxidative stress in ENDO layer

We had previously shown that altered mitochondrial metabolism in MI rats was associated with increased ROS production in ENDO layer. We evaluated whether exercise could prevent the stimulation-induced ROS overproduction in MI rats. Exercise completely restored the ROS overproduction in MI ENDO layer (Figure 3A). EPI layer was not affected by exercise. Oxidative stress results of an imbalance between pro-oxidant activities and antioxidant defenses buffering ROS. We thus evaluated antioxidant enzyme activities: SOD, which convert O_2^{-*} to H_2O_2, and catalase, which convert H_2O_2 to H_2O. SOD and catalase activities decreased only in ENDO layer of MI rats. Exercise increased both SOD and catalase activities in ENDO

layer, without affecting EPI layer (Figure 3B). Taken together, these results indicate that 4 weeks exercise training reduced oxidative stress of MI rats in ENDO layer by improving at least partially antioxidant defenses.

Effects of exercise on cellular electrophysiological properties

Oxidative stress may affect electrophysiological properties [25] in cardiomyocytes originated from failing ENDO layer.

We analyzed the cellular action potential (AP) and the major ionic currents involved in its repolarizing phase (Figure 4). All the repolarizing phases of the AP were prolonged in MI rats as shown by the significant increases in AP. Exercise shortened AP duration only in ENDO layer. Prolongation of AP duration could due to various currents that were thus explored. The depolarizing inward L-type Ca^{2+} current ($I_{Ca,L}$) and the transient outward K^+ current (I_{to}) both contribute significantly to the repolarizing plateau phase of the AP. The density of I_{CaL} was increased by 25% at its maximal amplitude (at 0 mV) in MI rats in both ENDO and EPI layers. This increase occurred for all depolarizations as shown by the current-to-voltage relationship (Figure 4B). Exercise normalized the density of I_{CaL} in both ENDO and EPI layers. The density of the transient outward K^+ currents was reduced in both ENDO and EPI layer of MI rats. Considering that I_{to} is almost absent in ENDO cells the major effects were observed in EPI cells. Exercise completely reversed this reduction in ENDO layer and slightly increased I_{to} in EPI layer. The inward rectifier K+ current (I_{K1}) is another potassium current that is mostly involved in the late phase of repolarization and in the resting potential. I_{k1} was not modified neither by pathology nor by exercise in both ENDO and EPI layer. Thus the main effect of exercise on electrophysiological properties was to reduced action potential duration in ENDO MI myocytes by normalizing calcium current.

Effects of exercise on cellular Ca^{2+} homeostasis

Ca^{2+} handling proteins are sensitive to redox variations [26]. We next investigated whether exercise could affect the ROS-induced RyR-2 dysfunction in ENDO layer of MI rats. As previously observed, the Ca^{2+} sparks frequency, which reflects the spontaneous SR Ca^{2+} release events from small clusters of SR-Ca^{2+} RyR, was increased in ENDO layer of MI rats (Figure 5A). This SR Ca^{2+} leak was associated with, diastolic Ca^{2+} overload, reduced SR Ca^{2+} release during systole, and SR Ca^{2+} depletion as indicated by the reduced SR load in ENDO layer of MI rats (Figure 5B and C). Exercise reversed partially MI-induced Ca^{2+} signaling in ENDO layer, without affecting EPI (Figure 5A, B and C).

Increased Ca^{2+} sparks activity and subsequent diastolic Ca^{2+} overload was proposed to promote arrhythmic events in failing cardiomyocytes [27]. We thus evaluated whether exercise could reduce the MI-associated ectopic Ca^{2+} transients following changes of stimulation frequency. For this purpose, we induced abrupt changes in stimulation frequency (0.5 Hz / 2 Hz / 0.5 Hz) in order to trigger ectopic Ca^{2+} transients (Figure 5A). MI rats displayed higher number of arrhythmic cells when compared to Sham rats (47 %. *vs* 25, respectively; *$p<0.05$), only in ENDO layer (Figure 5D). Exercise totally recovered this alteration in ENDO layer, and did not affect EPI layer (Figure 5D).

RyR-2 Post-translational modifications of the ryanodine receptor (RyR-2) have been proposed to participate in the alterations of Ca^{2+} homeostasis during heart failure (Ref). RyR-2RyR-2 content determined by Western blot analysis was unchanged among three groups in both ENDO and EPI layer. Beta-adrenergic pathway is highly solicited during HF and we have previously shown that ROS overproduction activates PKA which was responsible for a RyR-2

hyperphosphorylation in ENDO layer of MI rats (article submitted). Here, we observed that exercise training decreased RyR-2 hyperphosphorylation in ENDO layer of MI rats on the PKA site, consistent with a reduced adrenergic activity with exercise. We sought to determine whether this exercise-induced decreased phosphorylation was due to a PKA activity reduction. We thus measured PKA activity on cardiac tissue originated from ENDO and EPI layer. In MI rats, PKA activity was increased in both layers compared to Sham animals in ENDO and EPI layers, respectively (Figure 6B). Exercise normalized PKA activity in both layers suggesting decreased ß-adrenergic tone (Figure 6B).

4. Discussion

This study highlights the antiarrythmic effects of exercise training during ischemic heart failure. In MI rats with HF, we demonstrated that exercise: (i) restores the MI-induced mitochondrial dysfunction and reduces mitochondrial ROS production in ENDO layer; (ii) improves Ca^{2+} handling and RyR-2 function through a decrease of PKA activity (iii) reduces HF arrhythmic phenotype.

Beneficial effects of exercise training on arrhythmia and conduction

HF is associated with high mortality rates related to malignant arrhythmia. Roughly half of all HF patients die of SCD [28]. Despite few studies showing that exercise training improves ventricular repolarization and corrects QT dispersion in patients with HF [29] [7], there is currently to our knowledge no experimental evidence of a direct anti-arrhythmic effect of exercise training on the LV. In this context, one key finding of our study was the beneficial effect of exercise training on electrical properties of the heart and the prevention of arrhythmic events (Table 1, Figure 1). QT interval prolongation and reduced HRV are strongly correlated with an increased risk of ventricular arrhythmia and subsequent SCD, and are predictors of cardiac morbidity and mortality in patients with various form of heart disease. We show here that mechanisms underlying anti-arrhythmic effects of exercise training in HF involve mitochondrial function improvement.

Exercise training improves mitochondrial function in HF rats

There is growing evidence that mitochondrial defects play central role in arrhythmogenesis [19]. Ischemic HF pathogenesis involves mitochondrial alterations characterized by altered oxidative capacity [30]. We had previously shown that NADH homeostasis was disturbed in the inner sub-endocardial layer after MI (submitted article). Here, we provide the first direct evidence that 4 weeks of exercise training restores the NADH homeostasis through a recovering of both TCA cycle and electron transport chain activities. It has been shown that exercise improves coronary blood flow and endothelium-dependent vasodilatation, improving oxygen and substrates supply to the failing heart in coronary artery diseases in humans [31]. Moreover, exercise training induces a coordinated decrease in myocardial O_2 uptake indicating improved cardiac energetic efficiency [2]. We provide evidence here that exercise training-associated metabolic improvements occur only in the layer altered during HF, the sub-endocardial layer, and are correlated to reduced mitochondrial Ca^{2+} overload in this layer. Although enhancing mitochondrial Ca^{2+} uptake restores energy supply and demand matching in failing cardiomyocyte [32], a mitochondrial Ca^{2+} overload can induce the opening of

mitochondria permeability pore, leading to ROS production [33]. We show in our study that the recovering of MI-induced oxidative capacity disorders and mitochondrial Ca^{2+} alterations by exercise were accompanied with a decreased of ROS level in the ENDO layer. We can suppose that exercise decreases ROS production through both recovering of oxidative capacity function and mitochondrial Ca^{2+} homeostasis and increasing of antioxidant defenses buffering ROS. Previous studies have reported that exercise reduced oxidative stress in HF patients through increasing in antioxidant enzyme activity [6 34]. Here we observed increased activity of both SOD and catalase in the ENDO layer supporting the notion of regionalized antioxidant effects of exercise.

Beneficial effects of exercise training on ectopic Ca^{2+} transient

Oxidative stress play a critical role in the pathogenesis of heart failure [35 36 37]. Among ROS potential targets, Ca^{2+} handling [26] and action potential [25] are particularly sensitive to redox modulation. Exercise-associated reduction of oxidative stress in ENDO layer was associated with recovering of the MI-induced electrophysiological abnormalities. In MI rats, we ascertained that AP prolongation is determined by both an increase of the depolarizing inward L-type Ca^{2+} ($I_{Ca,L}$)current and more modestly to a decrease of the transient outward K^+ current (I_{to}), which are all known to trigger ventricular arrhythmia [38]. We show for the first time that MI-associated electrophysiological remodeling was restored by exercise training in ENDO layer. This recovering may be a consequence of the reduced oxidative stress. Indeed it has been shown that oxygen peroxide increases $I_{Ca,L}$ through a CAMKII pathway leading to action potential shortening and increased afterdepolarizations [25].

Another key element underlying arrythmogenesis is the diastolic Ca^{2+} [38]. We show in the present study that exercise reversed the MI-induced cytosolic Ca^{2+} overload through recovering of RyR-2 function. It is now established that oxidative stress may change the RyR-2 open probability [39]. Indeed, normal closing of the RyR-2 in diastole prevents Ca^{2+} leak and subsequent SR Ca^{2+} depletion, thereby preserving appropriate conditions for an optimal Ca^{2+} release during systole. The FK506-binding protein (FKBP) is an important regulator of channel activity, and disruption of the RyR-2-FKBP12.6 association has been implicated in cardiac disease-associated Ca^{2+} leak [40]. In addition, cumulative evidences indicate that RyR-2 redox state modify FKBP binding affinity which leads to SR Ca^{2+} leak [41 42 43]. The reduction of oxidative stress in ENDO layer after 4 weeks of exercise could improve the RyR-2/FKBP12.6 association and prevent subsequent ectopic Ca^{2+} transient in MI rats.

Exercise has other known beneficial effects that could explain the effects observed in the present study. Renin–angiotensin–aldosterone system (RAS) activation, commonly associated with adrenergic enhancement, also contributes to HF progression by inducing vasoconstriction, antinatriuresis, apoptosis, superoxide production, pathological remodeling and arrhythmogenesis [44]. It has been shown that reduced cardiac RAS explains, at least in part, the beneficial effects of exercise training on cardiac function in a genetic model of HF [45]. Additionally, by reducing sympathetic outflow, chronic exercise training suppresses one of the primary HF associated mediators of adverse cardiac remodeling.

In conclusion, exercise recovers the HF-associated mitochondrial disorders leading to diminished ROS production in the ENDO layer. The reduction of oxidative stress protects Ca^{2+} handling and electrophysiological proteins from oxidation and preserves their function allowing to recover a normal Ca^{2+} release. Stabilization of RyR-2 and recovering of electrical function after exercise training reduce arrhythmic events in heart failure.

References

1. Cohn JN, Levine TB, Olivari MT, et al. Plasma norepinephrine as a guide to prognosis in patients with chronic congestive heart failure. *N Engl J Med.* Sep 27 1984;311(13):819-823.

2. Stolen KQ, Kemppainen J, Ukkonen H, et al. Exercise training improves biventricular oxidative metabolism and left ventricular efficiency in patients with dilated cardiomyopathy. *J Am Coll Cardiol.* Feb 5 2003;41(3):460-467.

3. Roveda F, Middlekauff HR, Rondon MU, et al. The effects of exercise training on sympathetic neural activation in advanced heart failure: a randomized controlled trial. *J Am Coll Cardiol.* Sep 3 2003;42(5):854-860.

4. Leosco D, Rengo G, Iaccarino G, et al. Exercise promotes angiogenesis and improves beta-adrenergic receptor signalling in the post-ischaemic failing rat heart. *Cardiovasc Res.* May 1 2008;78(2):385-394.

5. Flynn KE, Pina IL, Whellan DJ, et al. Effects of exercise training on health status in patients with chronic heart failure: HF-ACTION randomized controlled trial. *Jama.* Apr 8 2009;301(14):1451-1459.

6. Belardinelli R. Exercise training in chronic heart failure: how to harmonize oxidative stress, sympathetic outflow, and angiotensin II. *Circulation.* Jun 19 2007;115(24):3042-3044.

7. Nishiyama Y, Maeda H, Tanaka M, et al. Effect of physical training on corrected QT dispersion in patients with nonischemic heart failure. *Circ J.* Oct 2004;68(10):946-949.

8. Deligiannis A. Exercise rehabilitation and skeletal muscle benefits in hemodialysis patients. *Clin Nephrol.* May 2004;61 Suppl 1:S46-50.

9. Kolarova JD, Ayoub IM, Gazmuri RJ. Cariporide enables hemodynamically more effective chest compression by leftward shift of its flow-depth relationship. *Am J Physiol Heart Circ Physiol.* Jun 2005;288(6):H2904-2911.

10. Trollinger DR, Cascio WE, Lemasters JJ. Selective loading of Rhod 2 into mitochondria shows mitochondrial Ca2+ transients during the contractile cycle in adult rabbit cardiac myocytes. *Biochem Biophys Res Commun.* Jul 30 1997;236(3):738-742.

11. Fauconnier J, Andersson DC, Zhang SJ, et al. Effects of palmitate on Ca(2+) handling in adult control and ob/ob cardiomyocytes: impact of mitochondrial reactive oxygen species. *Diabetes.* Apr 2007;56(4):1136-1142.

12. Picht E, Zima AV, Blatter LA, et al. SparkMaster: automated calcium spark analysis with ImageJ. *Am J Physiol Cell Physiol.* Sep 2007;293(3):C1073-1081.

13. Beers RF, Jr., Sizer IW. A spectrophotometric method for measuring the breakdown of hydrogen peroxide by catalase. *J Biol Chem.* Mar 1952;195(1):133-140.

14. Marklund S. Spectrophotometric study of spontaneous disproportionation of superoxide anion radical and sensitive direct assay for superoxide dismutase. *J Biol Chem.* Dec 10 1976;251(23):7504-7507.

15. Bradford MM. A rapid and sensitive method for the quantitation of microgram quantities of protein utilizing the principle of protein-dye binding. *Anal Biochem.* May 7 1976;72:248-254.

16. Srere PA. An eclectic view of metabolic regulation: control of citrate synthase activity. *Adv Enzyme Regul.* 1970;9:221-233.

17. Janssen AJ, Trijbels FJ, Sengers RC, et al. Spectrophotometric assay for complex I of the respiratory chain in tissue samples and cultured fibroblasts. *Clin Chem.* Apr 2007;53(4):729-734.
18. Wharton DC. Purification of electron-transfer components from Pseudomonas. *Methods Enzymol.* 1978;53:646-661.
19. Akar FG, Aon MA, Tomaselli GF, et al. The mitochondrial origin of postischemic arrhythmias. *J Clin Invest.* Dec 2005;115(12):3527-3535.
20. Stanley WC, Lopaschuk GD, Hall JL, et al. Regulation of myocardial carbohydrate metabolism under normal and ischaemic conditions. Potential for pharmacological interventions. *Cardiovasc Res.* Feb 1997;33(2):243-257.
21. Maack C, Cortassa S, Aon MA, et al. Elevated cytosolic Na+ decreases mitochondrial Ca2+ uptake during excitation-contraction coupling and impairs energetic adaptation in cardiac myocytes. *Circ Res.* Jul 21 2006;99(2):172-182.
22. Liu H, Colavitti R, Rovira, II, et al. Redox-dependent transcriptional regulation. *Circ Res.* Nov 11 2005;97(10):967-974.
23. Parodi O, De Maria R, Oltrona L, et al. Myocardial blood flow distribution in patients with ischemic heart disease or dilated cardiomyopathy undergoing heart transplantation. *Circulation.* Aug 1993;88(2):509-522.
24. McCormack JG, Halestrap AP, Denton RM. Role of calcium ions in regulation of mammalian intramitochondrial metabolism. *Physiol Rev.* Apr 1990;70(2):391-425.
25. Xie LH, Chen F, Karagueuzian HS, et al. Oxidative-stress-induced afterdepolarizations and calmodulin kinase II signaling. *Circ Res.* Jan 2 2009;104(1):79-86.
26. Zima AV, Blatter LA. Redox regulation of cardiac calcium channels and transporters. *Cardiovasc Res.* Jul 15 2006;71(2):310-321.
27. Hove-Madsen L, Llach A, Bayes-Genis A, et al. Atrial fibrillation is associated with increased spontaneous calcium release from the sarcoplasmic reticulum in human atrial myocytes. *Circulation.* Sep 14 2004;110(11):1358-1363.
28. Cohn JN, Archibald DG, Ziesche S, et al. Effect of vasodilator therapy on mortality in chronic congestive heart failure. Results of a Veterans Administration Cooperative Study. *N Engl J Med.* Jun 12 1986;314(24):1547-1552.
29. Ali A, Malik FS, Dinshaw H, et al. Reduction in QT dispersion with rheolytic thrombectomy in acute myocardial infarction: evidence of electrial stability with reperfusion therapy. *Catheter Cardiovasc Interv.* Jan 2001;52(1):56-58.
30. Neubauer S. The failing heart--an engine out of fuel. *N Engl J Med.* Mar 15 2007;356(11):1140-1151.
31. Gielen S, Hambrecht R. Effects of exercise training on vascular function and myocardial perfusion. *Cardiol Clin.* Aug 2001;19(3):357-368.
32. O'Rourke B, Blatter LA. Mitochondrial Ca2+ uptake: tortoise or hare? *J Mol Cell Cardiol.* Jun 2009;46(6):767-774.
33. Green DR, Reed JC. Mitochondria and apoptosis. *Science.* Aug 28 1998;281(5381):1309-1312.
34. Ennezat PV, Malendowicz SL, Testa M, et al. Physical training in patients with chronic heart failure enhances the expression of genes encoding antioxidative enzymes. *J Am Coll Cardiol.* Jul 2001;38(1):194-198.
35. Giordano FJ. Oxygen, oxidative stress, hypoxia, and heart failure. *J Clin Invest.* Mar 2005;115(3):500-508.

36. Bolli R, Marban E. Molecular and cellular mechanisms of myocardial stunning. *Physiol Rev.* Apr 1999;79(2):609-634.
37. Takimoto E, Kass DA. Role of oxidative stress in cardiac hypertrophy and remodeling. *Hypertension.* Feb 2007;49(2):241-248.
38. Ter Keurs HE, Boyden PA. Calcium and arrhythmogenesis. *Physiol Rev.* Apr 2007;87(2):457-506.
39. Yan Y, Liu J, Wei C, et al. Bidirectional regulation of Ca2+ sparks by mitochondria-derived reactive oxygen species in cardiac myocytes. *Cardiovasc Res.* Jan 15 2008;77(2):432-441.
40. Marx SO, Reiken S, Hisamatsu Y, et al. PKA phosphorylation dissociates FKBP12.6 from the calcium release channel (ryanodine receptor): defective regulation in failing hearts. *Cell.* May 12 2000;101(4):365-376.
41. Zissimopoulos S, Docrat N, Lai FA. Redox sensitivity of the ryanodine receptor interaction with FK506-binding protein. *J Biol Chem.* Mar 9 2007;282(10):6976-6983.
42. Terentyev D, Gyorke I, Belevych AE, et al. Redox modification of ryanodine receptors contributes to sarcoplasmic reticulum Ca2+ leak in chronic heart failure. *Circ Res.* Dec 5 2008;103(12):1466-1472.
43. Bellinger AM, Reiken S, Carlson C, et al. Hypernitrosylated ryanodine receptor calcium release channels are leaky in dystrophic muscle. *Nat Med.* Mar 2009;15(3):325-330.
44. Paul B, Goyal RK. Angiotensin II type 1 receptor blocking agents in regression of cardiac hypertrophy--how and why? *Indian Heart J.* Jan-Feb 2000;52(1):19-22.
45. Pereira AH, Clemente CF, Cardoso AC, et al. MEF2C silencing attenuates load-induced left ventricular hypertrophy by modulating mTOR/S6K pathway in mice. *PLoS One.* 2009;4(12):e8472.

	Sham	MI	MI-TR
ECG			
HR (bpm)	311 ± 8.78	329 ± 6.7*	308 ± 14.88*†
PR (ms)	45 ± 0.5	47 ± 6	41 ± 4
QRS (ms)	18.49 ± 0.2	53.3 ± 7.5 *	41.8 ± 3.9 *†
QT (ms)	61.67 ± 0.67	88.02 ± 7.48 *	71.04 ± 10.06 *†
QTc (ms)	4.28 ± 0.05	6.12 ± 0.49 *	4.86 ± 0.62 *†
HRV			
NN (ms)	192 ± 5	180 ± 4*	196 ± 10*†
SDNN (ms)	24 ± 1	12 ± 2.8*	17 ± 3.4*†
RMSSD (ms)	3.6 ± 0.17	7.92 ± 0.92*	7.51 ± 0.20*†

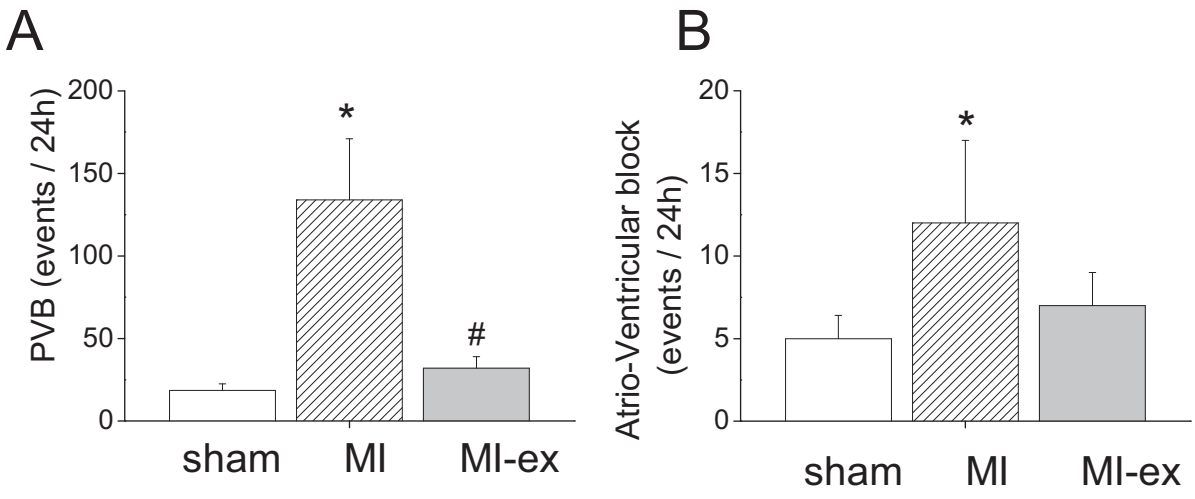

Figure 1, Andre *et al*

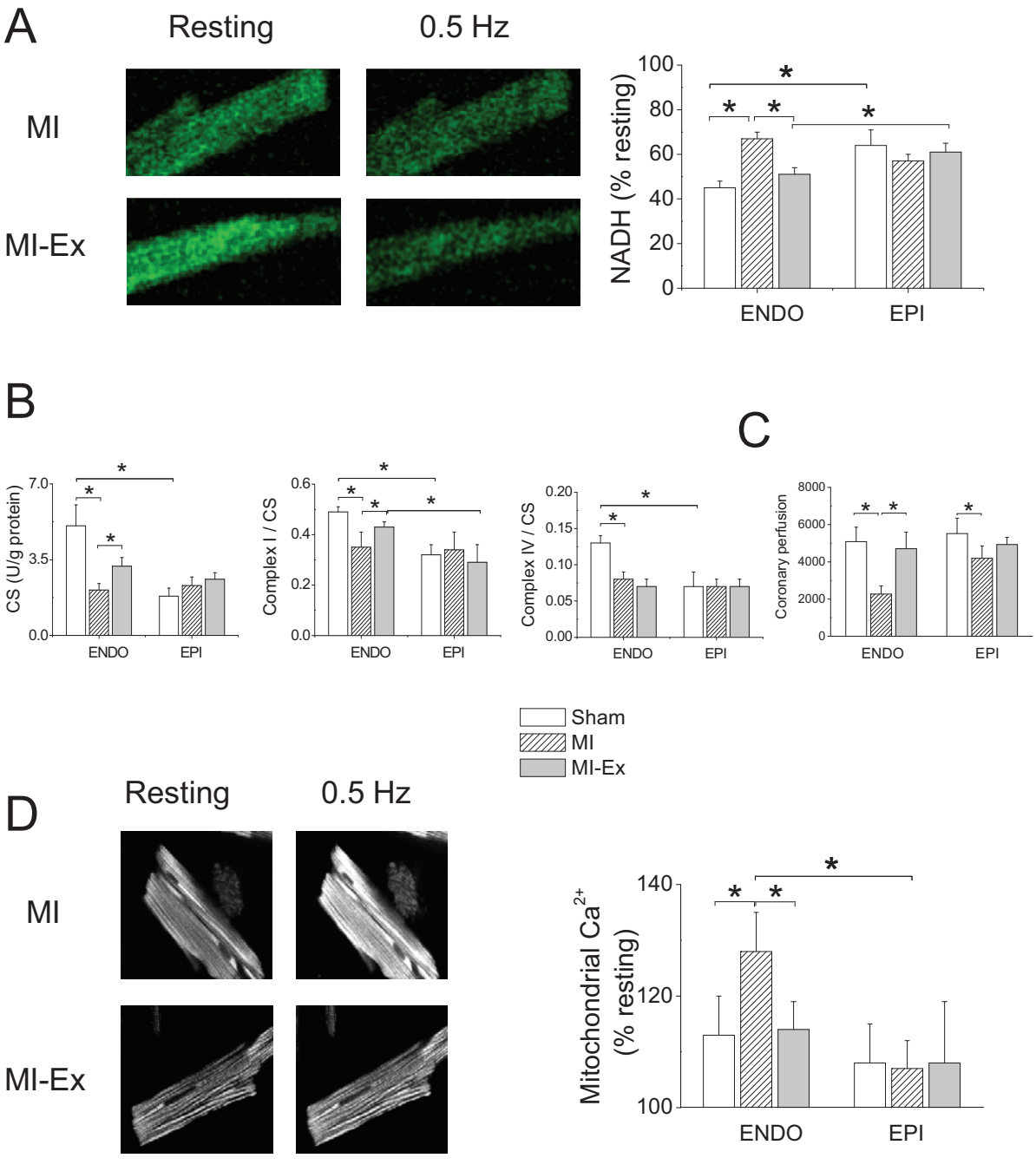

Figure 2, Andre *et al*

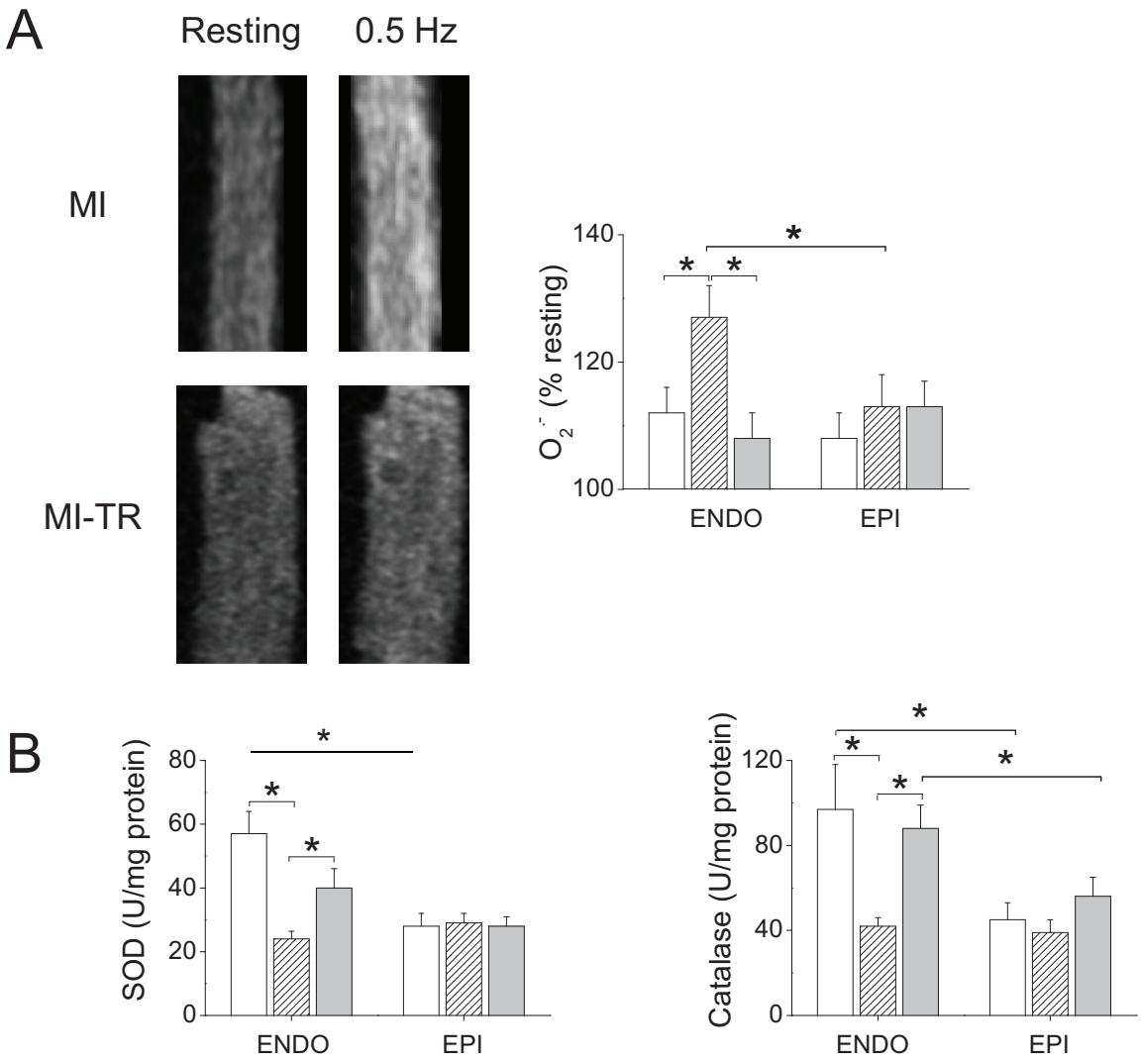

Figure 3, Andre *et al*

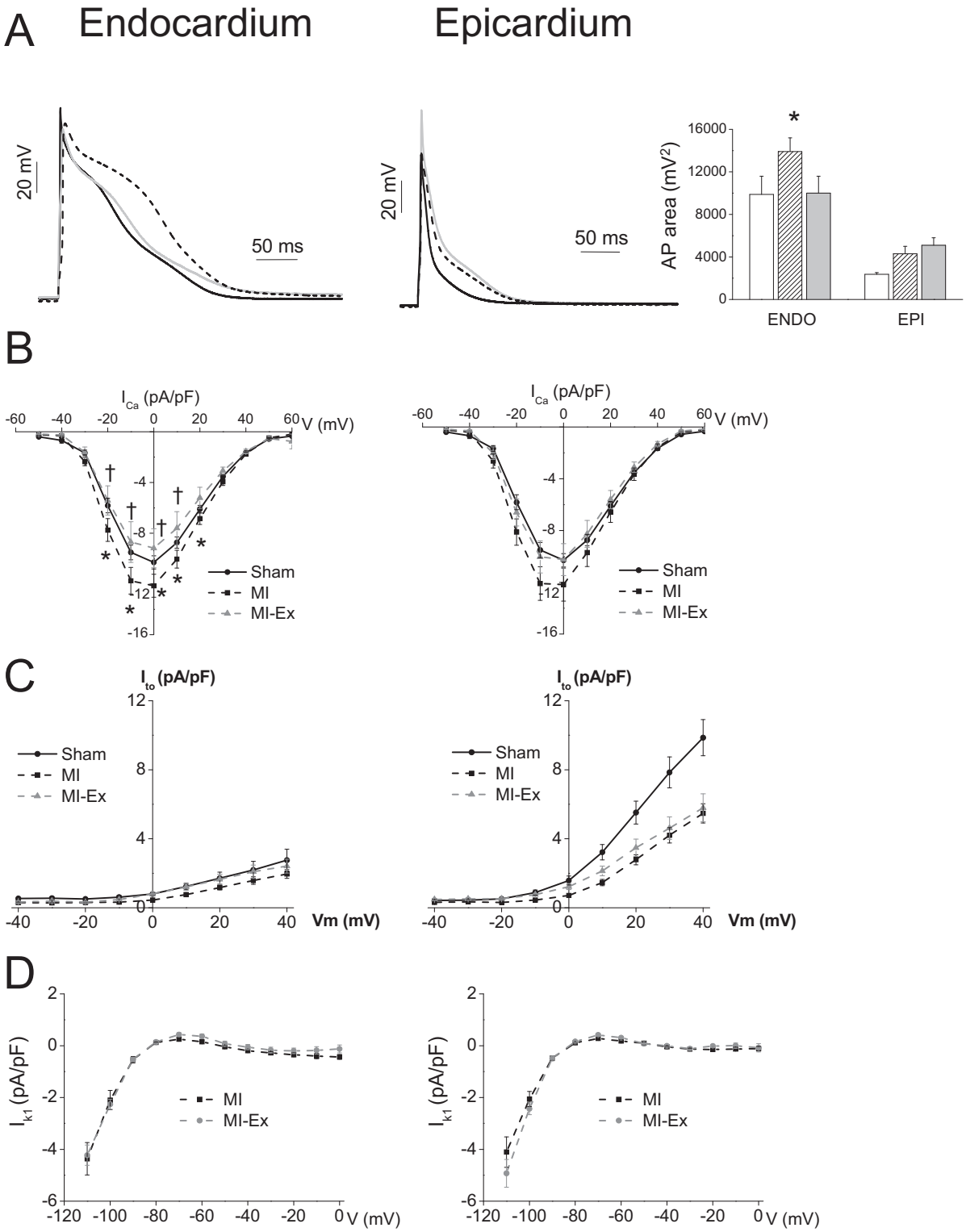

Figure 4, Andre *et al*

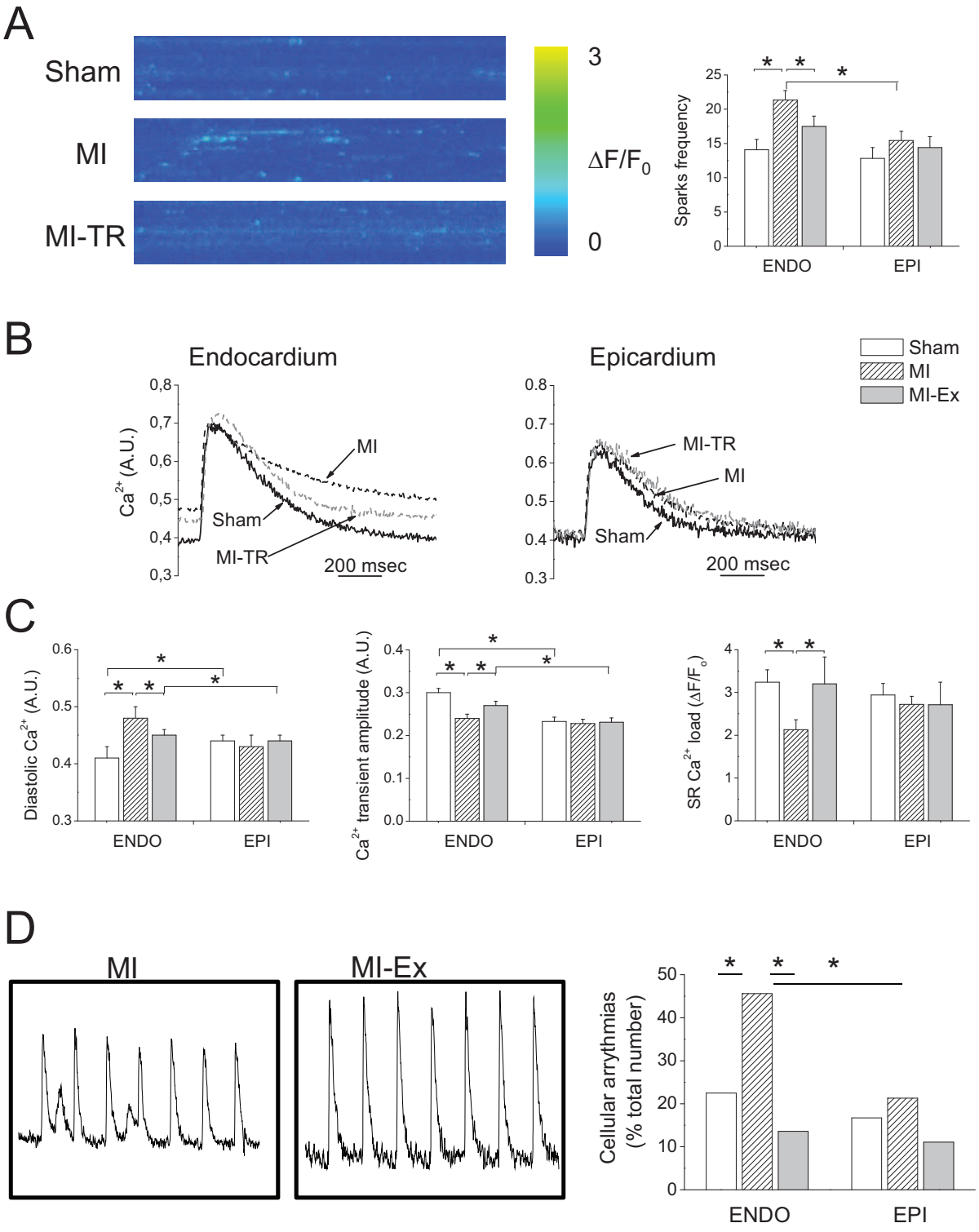

Figure 5, Andre *et al*

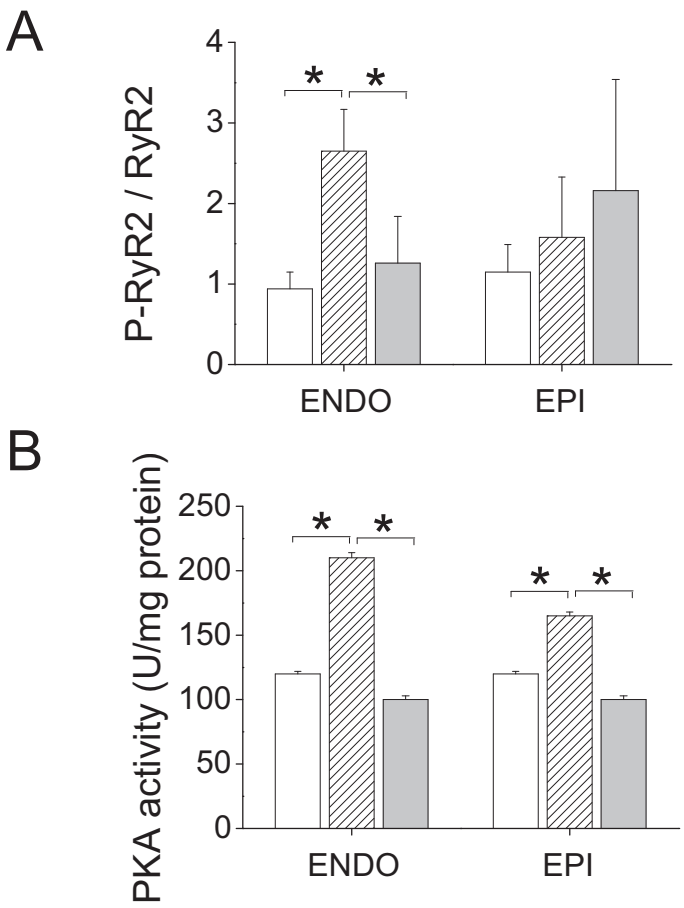

Figure 6, Andre *et al.*

3. Conclusion

Cette étude met en évidence chez le rat les effets anti-arythmiques de l'exercice physique au cours de l'IC, grâce à une amélioration de l'homéostasie calcique et des propriétés électrophysiologiques. L'exercice permet en fait un rétablissement de l'homéostasie redox et prévient l'activation ROS-dépendante de la PKA puis la phosphorylation PKA-dépendante du RyR-2. L'inhibition de cette voie permet de rétablir une fonction du RyR-2 proche de la normale, limitant alors les libérations stochastiques de Ca^{2+}. Cette étude prouve donc que l'exercice physique, outre son action positive sur la prévention du remodelage cardiaque délétère post-infarctus, permet de réduire le déclenchement de phénomènes arythmiques, ce qui pourrait expliqué la réduction du nombre d'événements cardiovasculaires et morts subites chez les patients IC pratiquant une activité physique régulière. Cependant, bien que les résultats de cette étude révèle une amélioration du phénotype arythmique et s'inscrivent ainsi dans la suite des données publiées par différents groupes attribuant à l'exercice physique des effets bénéfiques dans l'insuffisance cardiaque [132], il est important de noter que l'exercice physique ne semblerait toutefois pas jouer de rôle dans la prévention de la mortalité cardiovasculaire [180].

Conclusion 1ère partie

Cette première partie met en évidence que le couplage excitation-métabolisme-contraction, coordonné dans le myocarde sain afin d'assurer un fonctionnement cardiaque optimal est profondément altéré au cours de la pathologie ischémique. En effet, un découplage des activités électriques, énergétiques et mécaniques se met en place au décours d'un infarctus du myocarde et se caractérise par une dysfonction mitochondriale et une production excessive de ROS. Les ROS, outre leur pouvoir oxydant direct, sont impliqués dans de nombreuses voies de signalisation intracellulaire. Ainsi, les ROS peuvent modifier l'activité de différentes kinases. Notamment l'activation de la protéine kinase A entraine la phosphorylation de ses protéines cibles, parmi lesquelles le RyR-2 et la TnI. Or ces deux protéines sont des éléments majeurs très largement impliqués dans les dysfonctions du CEC rapportées chez l'IC. Il apparait donc que les dysfonctions mitochondriales soient à l'origine des troubles de l'homéostasie calcique, lesquels seraient responsables des dysfonctions contractiles observées dans le cœur défaillant. Cependant, cette hiérarchisation des événements nécessitent d'autres études complémentaires, notamment pour vérifier un concept émergent selon lequel ROS, Ca^{2+} et ATP seraient intégrés dans un cercle vicieux. En effet, l'excès de ROS produit suite à une dysfonction mitochondriale provoquerait des troubles de l'homéostasie calcique

caractérisé notamment par une surcharge calcique diastolique. Cette surcharge agirait à son tour comme élément délétère sur l'homéostasie redox en favorisant une production plus importante de ROS. Ainsi, l'initiation de cette cascade d'événements délétères se potentialise au cours du temps et peut aboutir à la nécrose cellulaire. Dans ce contexte, l'intérêt de thérapies permettant d'agir directement sur les dysfonctions mitochondriales prend tout son sens. Les ROS seraient produits en grande partie en raison d'une réduction de l'activité des complexes respiratoires mitochondriaux, notamment des complexes I et IV. Il n'existe à l'heure actuelle, aucune molécule capable de stimuler directement l'activité de ces complexes. Cependant, l'exercice physique régulier est un puissant stimulateur de la respiration mitochondriale et permet de rétablir un métabolisme efficace dans l'IC. Ainsi, on constate logiquement qu'un exercice physique modéré et régulier (4 semaines) permet de restaurer les fonctions contractiles et électriques cardiaques. D'autre part, un traitement antioxydant pur de 4 semaines au NAC, limite la production excessive de ROS accompagnant l'IC et entraine des effets similaires à l'exercice physique. Il semble donc qu'il soit utile de combattre le stress oxydatif associé à l'IC de manière précoce au décours de l'infarctus. Des stratégies plus globales, comme l'exercice physique, permettent cependant des effets plus systémiques améliorant différentes composantes impliquées dans la physiopathologie et son certainement plus efficaces au long cours. D'autre part, l'exercice reste une thérapeutique physiologique dont la tolérance est bien supportée contrairement à certains traitements antioxydant pouvant entrainer une altération des fonctions hépatiques. Les effets des traitements (NAC et exercice physique) ont été étudiés 7 semaines après l'infarctus du myocarde chez l'animal. L'anthropisation de ces résultats expérimentaux doit tenir compte des spécificités organiques de l'homme. D'autre part, bien que des effets importants du traitement chronique en NAC ou par l'exercice physique soient observés sur les paramètres cardiaques mesurés, ces deux approches doivent être considérées comme des solutions complémentaires au traitement médicamenteux (inhibiteur de l'enzyme de conversion de l'angiotensine, β-bloquants, inhibiteurs Ca^{2+}, diurétiques, antagonistes de l'angiotensine, statines). Le choix de la thérapeutique pour la prise en charge d'un patient dépend de la balance bénéfice/risque du traitement. Les fonctions hépatiques et musculaires sont souvent la cible d'altérations des traitements médicamenteux. L'exercice physique permettrait, lui, de préserver ces organes et pourrait alors être envisagé comme thérapie durable. Cependant, le manque d'informations sur l'ensemble des effets de l'exercice physique et sur la compliance au traitement, c'est-à-dire le respect des séances tant en intensité qu'en fréquence ne permet pas d'indiquer l'exercice physique comme traitement de référence pour l'insuffisance cardiaque ischémique.

2ème partie : Effet d'une pollution au monoxyde de carbone sur le couplage excitation-métabolisme-contraction de populations saines et insuffisantes cardiaques

III. Effet d'une pollution au monoxyde de carbone sur la fonction cardiaque globale et cellulaire

1. Introduction

De nombreuses études épidémiologiques associent la pollution atmosphérique aux accidents cardiovasculaires. Il est en effet rapporté une recrudescence du taux de fréquentation des hôpitaux, notamment des services de cardiologie, lors de pic de pollution. Parmi les agents présents dans l'air atmosphérique, le monoxyde de carbone (CO) est majoritairement associé à la survenue d'accidents cardiovasculaires et à une augmentation de la mortalité cardiaque. Cependant, la physiopathologie des effets du CO est très peu documentée. La compréhension des mécanismes sous-jacents aux altérations induites par une pollution au CO permettrait alors une meilleure prévention des risques environnementaux.
L'objectif de cette 4ème étude était d'évaluer les effets d'une pollution chronique au CO, à des doses simulant une pollution citadine, sur la fonction cardiaque globale et cellulaire chez un modèle expérimental sain (rat).

2. Article 4 : Accepté dans Am J Resp crit Care Med, 2010

Carbon Monoxide Pollution Promotes Cardiac Remodeling and Ventricular Arrhythmia in Healthy Rats

Lucas Andre[1]*, Julien Boissière[1,2]*, Cyril Reboul[2], Romain Perrier[1], Santiago Zalvidea[1], Gregory Meyer[2], Jérôme Thireau[1], Stéphane Tanguy[2], Patrice Bideaux[1], Maurice Hayot[3], François Boucher[4], Philippe Obert[2], Olivier Cazorla[1], and Sylvain Richard[1]

[1]INSERM, U-637 and [3]INSERM ERI25, Université Montpellier1, Université Montpellier2, Montpellier; [2]EA-4278, Université Avignon et des Pays de Vaucluse, UFR Sciences, Avignon; and [4]UMR5525, Laboratoire TIMC-PRETA, Université de Grenoble, La Tronche, France

Rationale: **Epidemiologic studies associate atmospheric carbon monoxide (CO) pollution with adverse cardiovascular outcomes and increased cardiac mortality risk. However, there is a lack of data regarding cellular mechanisms in healthy individuals.**

Objectives: **To investigate the chronic effects of environmentally relevant CO levels on cardiac function in a well-standardized healthy animal model.**

Methods: **Wistar rats were exposed for 4 weeks to filtered air (CO < 1 ppm) or air enriched with CO (30 ppm with five peaks of 100 ppm per 24-h period), consistent with urban pollution. Myocardial function was assessed by echocardiography and analysis of surface ECG and *in vitro* by measuring the excitation-contraction coupling of single left ventricular cardiomyocytes.**

Measurements and Main Results: **Chronic CO pollution promoted left ventricular interstitial and perivascular fibrosis, with no change in cardiomyocyte size, and had weak, yet significant, effects on *in vivo* cardiac function. However, both contraction and relaxation of single cardiomyocytes were markedly altered. Several changes occurred, including decreased Ca^{2+} transient amplitude and Ca^{2+} sensitivity of myofilaments and increased diastolic intracellular Ca^{2+} subsequent to decreased SERCA-2a expression and impaired Ca^{2+} reuptake. CO pollution increased the number of arrhythmic events. Hyperphosphorylation of Ca^{2+}-handling and sarcomeric proteins, and reduced responses to β-adrenergic challenge were obtained, suggestive of moderate CO-induced hyperadrenergic state.**

Conclusions: **Chronic CO exposure promotes a pathological phenotype of cardiomyocytes in the absence of underlying cardiomyopathy. The less severe phenotype *in vivo* suggests a role for compensatory mechanisms. Arrhythmia propensity may derive from intracellular Ca^{2+} overload.**

Keywords: heart failure; atmospheric pollution; Ca^{2+} handling; protein kinase A pathway

AT A GLANCE COMMENTARY

Scientific Knowledge on the Subject

Most studies of the effects of atmospheric pollution provide correlations between air quality and cardiovascular outcomes, but do not provide mechanistic information owing to technical limitations in human subjects. Our findings provide a rationale at the cellular and molecular levels in support of epidemiologic studies pointing to the deleterious effects of carbon monoxide pollution on cardiac function.

What This Study Adds to the Field

This study shows that the deleterious effects of chronic carbon monoxide exposure may be barely detectable. However, even in the absence of underlying cardiopathy, cardiomyocytes may develop a pathological phenotype with some features commonly observed at the early stages of heart failure.

The World Health Organization estimates that 3 million people are killed annually worldwide by outdoor air pollution caused by vehicles and industrial emissions (http://www.who.int; http://www.infoforhealth.org). Notably, air pollution increases the risk of mortality from cardiovascular disease by 76% (1) with deaths related to ischemia, ventricular arrhythmia (VA), and heart failure (HF) (2–4). Among the various agents that constitute the mix of atmospheric pollution, carbon monoxide (CO) is a ubiquitous pollutant found in many common sources (secondhand smoke, vehicular exhaust, industrial emissions, etc.). Outdoor CO exposure is closely associated with hospital admissions for cardiovascular disease (5) as well as cardiac mortality (6). In addition, CO pollution increases HF risk factors, such as blood viscosity and arrhythmia (7), and decreases heart rate variability (8, 9). However, studies investigating the effects of urban air pollution in humans are mainly restricted to epidemiological studies that only establish correlations between air quality and cardiovascular outcome. In this context, it is particularly difficult to discriminate the pathophysiological effects of various major atmospheric pollutants, such as CO, particulate matter, or lead. In addition, the mechanisms underlying the effects of chronic CO exposure on the heart have not been well established. In this regard, the use of an animal model has several advantages, including better standardization of experimental approaches and insights into cellular mechanisms.

The aim of our work was to investigate the effects of chronic CO exposure, under conditions mimicking urban air pollution, on rat cardiac function both *in vivo* and at the cardiomyocyte level. Our principal results were that chronic CO pollution initiated a pathological phenotype characterized by serious remodeling of the excitation-contraction coupling (ECC) of cardiomyocytes, with major alterations of Ca^{2+} handling leading to increased risk of VA.

(*Received in original form May 27, 2009; accepted in final form December 16, 2009*)

Supported by a French National Research Agency grant (COMYOCARD).

*These authors contributed equally to this work.

Correspondence and requests for reprints should be addressed to Sylvain Richard, Ph.D., INSERM U-637 Physiopathologie Cardiovasculaire, CHU Arnaud de Villeneuve, F-34295 Montpellier, France. E-mail: sylvain.richard@inserm.fr

This article has an online supplement, which is accessible from this issue's table of contents at www.atsjournals.org

Am J Respir Crit Care Med Vol 181. pp 587–595, 2010
Originally Published in Press as DOI: 10.1164/rccm.200905-0794OC on December 17, 2009
Internet address: www.atsjournals.org

METHODS

For a detailed description, *see* METHODS in the online data supplement. Experiments were performed with approval of the institutional animal care and use committee.

Animal Model and Chronic CO Exposure

In urban areas, ambient CO usually varies between 2 and 40 ppm, but under certain circumstances, such as during heavy traffic, its concentration may reach levels as high as 150–200 ppm (10, 11). In our study, male Wistar rats (13 wk old, n = 35) were exposed to CO in an airtight exposure container over 4 weeks. Rats were exposed to a basal CO concentration of 30 ppm during a 12-hour period completed with five peaks of 100 ppm (1 h each), to reproduce environmentally relevant variations in air quality (schema included in supplemental data). For the remaining 12 hours, the CO-exposed group of rats was exposed to filtered air (<1 ppm CO). The CO content was continuously monitored with an infrared aspirative CO analyzer (CHEMGARD, NEMA 4 Version, MSA, Greer, SC). Rats exposed to CO pollution were compared with rats exposed to filtered ambient air (CO <1 ppm; control, n = 25). Experiments were performed 24 h after the last CO exposure to avoid acute CO effects. Carboxyhemoglobin level measured 24 hours after the last CO exposure (1.2 ± 0.4%) did not differ from that of the control group (1.02 ± 0.22%) and was consistent with levels reached in human population exposed to high atmospheric pollution (12, 13).

In vivo Cardiac Investigation

Doppler echocardiography was performed to evaluate cardiac function and morphology (14). Hemodynamic evaluation (arterial and ventricular pressures) was performed in intact closed-chest anesthetized rats 24 hours after echocardiography (14). Measurements were performed before and after a β-adrenergic challenge by isoproterenol perfusion (1 mg/kg/min). Surface ECG recordings (Dataquest; Data Sciences International, Transoma Medical, Arden Hills, MN) were performed for a 24-hour period after the CO exposure protocol. Spontaneous rhythmic disorders, heart rate variability, mean, and standard deviation of all normal RR intervals were calculated from ECGs (24 h).

Histology

The quantification of interstitial fibrillar collagen content was performed on Sirius red–stained sections using morphometry (Lucia digital image analysis software; Nikon, Melville, NY).

Cardiac ECC Analysis

Ca^{2+} transient and cell fractional shortening. Single ventricular myocytes were isolated by enzymatic digestion as previously described (15). Unloaded cell shortening and Ca^{2+} concentration (Indo-1 dye) were measured using field stimulation (0.5 Hz, 22°C, 1.8 mM external Ca^{2+}). Sarcomere length (SL) and fluorescence (405 and 480 nm) were simultaneously recorded (IonOptix system, Milton, MA) under basal conditions and after β-adrenergic stimulation with isoproterenol (100 nM).

Action potentials, L-type Ca^{2+} current, and K^+ currents. Whole-cell patch-clamp experiments were performed (22 ± 2°C) with an Axopatch 200B (Axon Instruments, Burlingham, CA) (16). Currents were normalized to cell membrane capacitance (Cm) and expressed as densities. Because of the heterogeneity in action potential (AP) duration across the left ventricular (LV) free wall (17), we separated subepicardial and subendocardial cells.

Force measurements in permeabilized cardiomyocytes. Isometric force was measured in single permeabilized cardiomyocytes (18). Force was normalized to the cross-sectional area measured by imaging (IonOptix system). The relationship between Ca^{2+} activated force and internal Ca^{2+} concentration was measured at 2.3 μm SL and was fitted with a modified Hill equation. In some experiments, permeabilized cardiomyocytes were incubated with a recombinant catalytic subunit of protein kinase A (PKA, Sigma, St. Quentin, France) for 50 min at room temperature (19).

Protein Analysis

Ca^{2+} handling. Proteins were separated using 2 to 20% sodium dodecyl sulfate–polyacrylamide gel electrophoresis. Proteins were revealed with specific antibodies and were expressed relative to calsequestrin content.

Myofilament proteins. Myofibrillar proteins were analyzed on skinned muscle strips from the LV (18). Phosphorylated and nonphosphorylated MLC-2 forms were detected with a cardiac MLC-2–specific antibody (Coger SA, Paris, France). TnI was revealed using specific antibodies for total cardiac TnI (Cat#4T21; Hytest, Turku, Finland) or the PKA-phosphorylated form of cardiac TnI (Cat#4T45; Hytest).

Cardiac Oxidative Status

Hearts (n = 6 per group) were freeze-clamped and the frozen ventricular tissue was homogenized in TRIS HCl buffer (TRIS HCl 60 mM, diethyltriaminopentaacetic acid 1 mM, pH 7.4, 10 ml/g wet wt.), using a Teflon Potter homogenizer. Tissue homogenates were then centrifuged (10 min at 20,000 × *g* at 4°C). Activities of total superoxide dismutase, catalase, and glutathione peroxidase, reflecting the antioxidant status, and thioredoxin reductase, reflecting the oxidant status, were measured in supernatants (20).

Statistical Analysis

Statistics were performed using StatView 5.0 (SAS Institute, Cary, NC). Data are presented as mean ± SEM unless otherwise specified. The effects of CO exposure, time, and/or β-adrenergic challenge were analyzed using one-way factorial analysis of variance or analysis of variance with repeated measures depending on the variables studied. Bonferroni *post hoc* tests were realized where appropriate. Statistical significance was defined as P less than 0.05.

RESULTS

Effects of CO Exposure on *In Vivo* Cardiac Morphology and Function

Chronic exposure to CO altered heart morphology and function. Rats from the CO group exhibited hypertrophic features, with increased heart weight/body weight as well as LV/body weight ratios. LV interstitial and perivascular fibrous tissue was

TABLE 1. EFFECTS OF CHRONIC CARBON MONOXIDE EXPOSURE ON CARDIOVASCULAR FUNCTION AND CARDIAC MORPHOLOGY *IN VIVO*

	Control (*n = 12*)	CO (*n = 16*)
Morphological data		
Body wt, g	514 ± 9	511 ± 5
Heart wt/100 g body wt, mg/100 g	259 ± 4	276 ± 6*
LV/100 g body wt, mg/100 g	204 ± 5	219 ± 4*
Fibrosis, % of total area	1.96 ± 0.29	3.72 ± 0.4*
Echocardiographic data		
LVEdD, mm	9.46 ± 0.14	9.61 ± 0.21
LVEsD, mm	5.76 ± 0.17	6.30 ± 0.16*
Anterior wall thickness, mm	1.02 ± 0.04	1.06 ± 0.06
Posterior wall thickness, mm	1.16 ± 0.11	1.29 ± 0.19*
LV shortening fraction, %	39.22 ± 1.18	34.35 ± 1.11*
Posterior wall end-systolic strain, %	98 ± 7	78 ± 9*
E/A-wave velocity ratio	1.89 ± 0.33	1.98 ± 0.34
Hemodynamic data		
Systolic arterial pressure, mm Hg	120 ± 10	121 ± 4
Diastolic arterial pressure, mm Hg	93 ± 9	96 ± 4
Mean arterial pressure, mm Hg	102 ± 10	105 ± 5
LV developed pressure, mm Hg	104 ± 5	106 ± 5
LV dP/dt max, mm Hg/s	5018 ± 326	4781 ± 255
LV dP/dt min, mm Hg/s	−4700 ± 285	−4676 ± 287
LV tau, s	8.22 ± 0.27	8.31 ± 0.16

Definition of abbreviations: CO = carbon monoxide; LV = left ventricular; LVEdD = left ventricular end-diastolic diameter; LVEsD = left ventricular end-systolic diameter; LV dP/dt max = maximal first derivative of left ventricular pressure; LV dP/dt min = minimal first derivative of left ventricular pressure; LV tau = time constant of left ventricular pressure decay; *$P < 0.05$ vs. control.

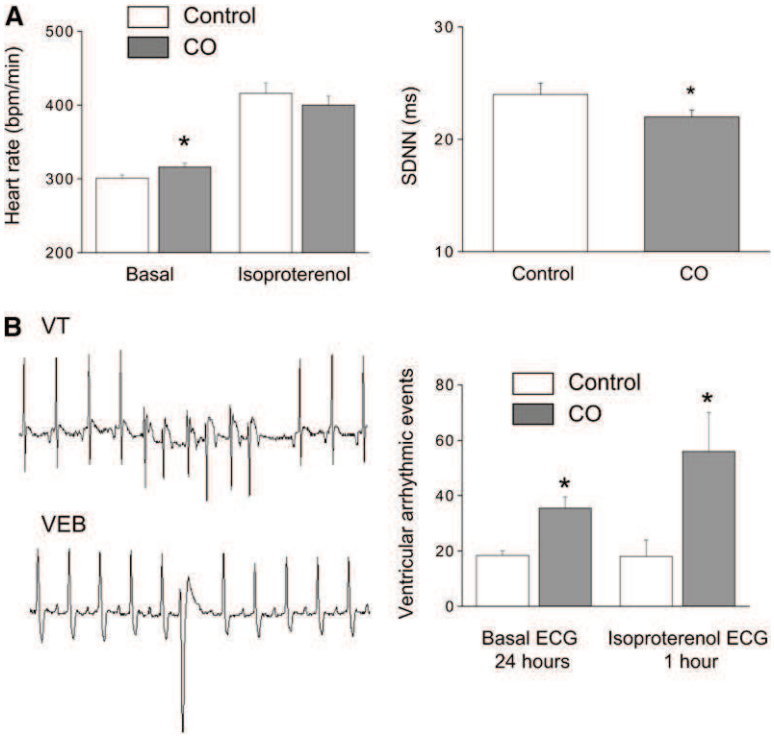

Figure 1. Analysis of *in vivo* arrhythmic events from ECG recordings and heart rate variability analysis in control and carbon monoxide (CO)-exposed rats. (*A*) Heart rate under basal conditions and after injection of isoproterenol (1 mg/kg i.p.) (*right*) and standard deviation of the normal RR intervals (*left*) (n = 9 rats in each group). (*B*) Typical examples of arrhythmic events occurring during 24-hour ECG recordings (*left*); analysis of the occurrence of arrhythmic events during 24-h measurements and after acute challenge with isoproterenol (average number of arrhythmic events over 1 h post-injection) (*right*). *$P < 0.05$. VEB = ventricular ectopic beat; VT = ventricular tachycardia

nearly doubled (Table 1; *see* Figure E2 in the online supplement). An increase in posterior wall thickness was observed, associated with a slight but significant global contractile dysfunction as indicated by a decrease in the LV shortening fraction and posterior wall end-systolic strain (Table 1). However, arterial blood pressure and LV hemodynamic parameters were similar in CO-exposed and control rats (Table 1). Taken together, our data suggested that chronic CO exposure has a weak, yet significant, effect on *in vivo* cardiac function.

Electrical Activity of Heart Measured *In Vivo* and Heart Rate Variability

Surface ECGs were recorded and analyzed in conscious rats from control and CO groups. Chronic CO exposure increased basal heart rate (Figure 1A) from 297 ± 2 bpm in control rats (n = 8) to 320 ± 8 bpm in CO-exposed rats (n = 9; $P < 0.02$), whereas the QTc interval remained unchanged (44.1 ± 0.8 ms vs. 43.1 ± 0.5 ms, respectively). The PR intervals were also unchanged between control and CO-exposed rats (45.0 ± 0.5 and 44.0 ± 0.7 ms, respectively). After the animals were challenged with the β-adrenergic receptor agonist isoproterenol (1 mg/kg i.p.), the difference in heart rate between the two groups was abolished, reflecting a weaker response to β-adrenergic stimulation in CO-exposed rats (Figure 1A). The standard deviation of normal-to-normal intervals, an estimate of overall heart rate variability, was decreased in CO-exposed rats (Figure 1A). The number of premature ventricular beats doubled in this group (Figure 1B). The occurrence of nonsustained tachycardia, which is absent in controls, was detected in CO-exposed rats. The number of atrioventricular blocks was unchanged between control and CO-exposed rats (5.2 ± 1.2 and 6.3 ± 1.5 atrioventricular blocks/24 h, respectively). After the animals were

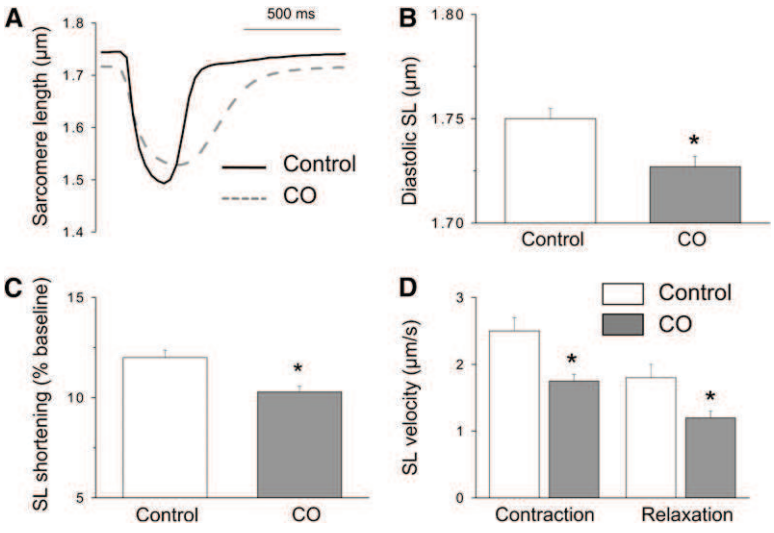

Figure 2. Chronic exposure to carbon monoxide (CO) pollution alters cardiomyocyte contraction. (*A*) Contraction of intact myocytes, measured by sarcomere length (SL) shortening at 0.5 Hz, isolated from rats exposed to CO pollution (CO, *dashed line*) and from control rats (*solid line*). (*B*) Diastolic SL, (*C*) the amplitude of SL shortening, and (*D*) velocities of contraction and relaxation were decreased after chronic CO exposure. Results represent the mean ± SEM of cells from five hearts (n = 112–145). *$P < 0.05$.

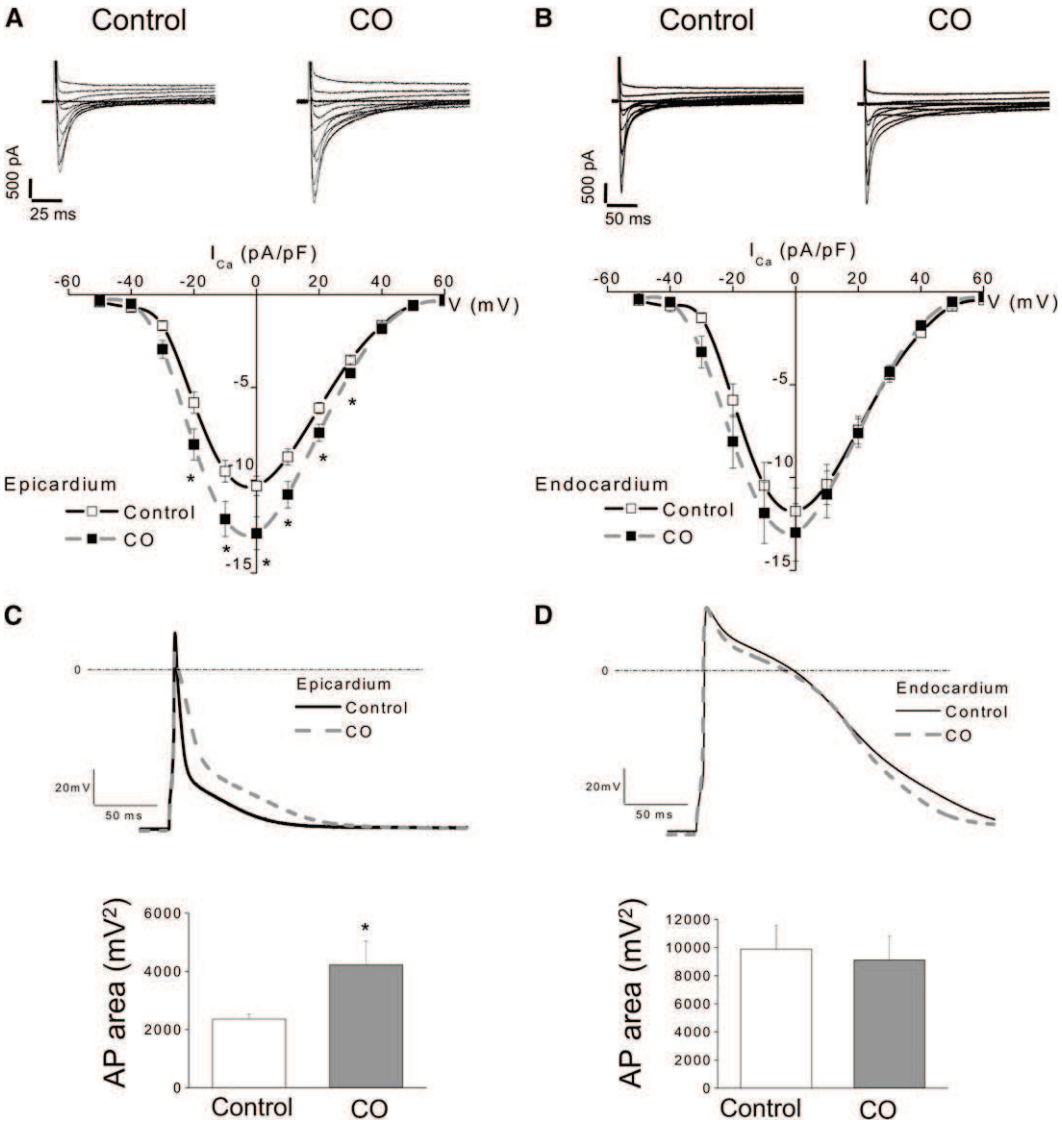

Figure 3. Chronic carbon monoxide (CO) pollution modifies the action potential (AP) in ventricular myocytes. Typical L-type inward calcium current ($I_{Ca,L}$) evoked by depolarizations between −50 mV and + 60 mV at 10-mV increments, from a holding potential of −80 mV, in control and CO cardiomyocytes from (*A*) the epicardial area and (*B*) the endocardial area, with the corresponding average current-to-voltage relationships of $I_{Ca,L}$. (*C*, *D*) Superimposed APs recorded at 0.1 Hz, and corresponding averaged AP area in control and CO cardiomyocytes from (*C*) the epicardial area and (*D*) the endocardial area. For all groups (n = 8–14 cells/5 hearts), $*P < 0.05$.

challenged with isoproterenol, the number of premature ventricular beats (measured during the 2 h after isoproterenol perfusion) increased in the two groups. However, not only did the absolute risk of arrhythmic events remain greater in the CO-exposed group, but the risk was potentiated (Figure 1B) with the promotion of ventricular ectopic beats that are potential triggers, inducing the start of a sustained arrhythmia.

Effects of CO Exposure on Cardiac ECC

At the cellular level, chronic CO exposure decreased cell fractional shortening (reflecting contraction) in intact ventricular myocytes (Figures 2A and 2C). This decrease was associated with a reduction in diastolic SL (Figure 2B) and in the maximal velocity of cell contraction and relaxation, calculated by the first derivative of cell shortening (delta SL/delta time) (Figure 1D). These results indicate that ECC is modified by chronic CO exposure.

Because of the well-known heterogeneity in AP duration across the LV free wall (17), we separated subendocardial and subepicardial cells to measure the AP and major ionic currents involved in the AP repolarizing phase. Chronic CO exposure had no effect on cardiomyocyte size, as estimated from measurements of cell membrane capacitance both in epicardial cells (Cm = 193 ± 10 pF, n = 16 in controls vs. 203 ± 12 pF, n = 24 in the CO-exposed group) and endocardial cells (Cm = 212 ± 11 pF, n = 13 in controls vs. 204 ± 13 pF, n = 20 in the CO-exposed group), indicating the absence of cellular hypertrophy. In epicardial cells, CO increased the density of L-type inward calcium current ($I_{Ca,L}$) by 20% at 0 mV, and prolonged the AP, as determined from a significant increase in AP area (Figures 3A and 3C). CO had no effect on endocardial cells. In addition, CO had no effect on the repolarizing outward K^+ current in both cell types. Thus, the regional differences in the effects of CO on the AP may have a limited impact on the whole-heart electrical activity.

We next investigated the effects of chronic CO exposure on intracellular Ca^{2+} in Indo-1–loaded cardiomyocytes stimulated at 0.5 Hz. Diastolic (or basal) Ca^{2+} was higher and Ca^{2+} transient amplitude smaller in the CO-exposed group when compared with the control group (Figure 4A). The Ca^{2+} load of the sarcoplasmic reticulum (SR), assessed by caffeine application (10 mM), was also reduced (0.27 ± 0.02 vs. 0.34 ± 0.02 in CO-exposed and control rats, respectively), possibly contributing to Ca^{2+} transient diminution. The increase in diastolic Ca^{2+} could be due to a Ca^{2+} leak through the ryanodine receptors (RyR-2) of the SR during the diastolic phase, or to altered Ca^{2+}

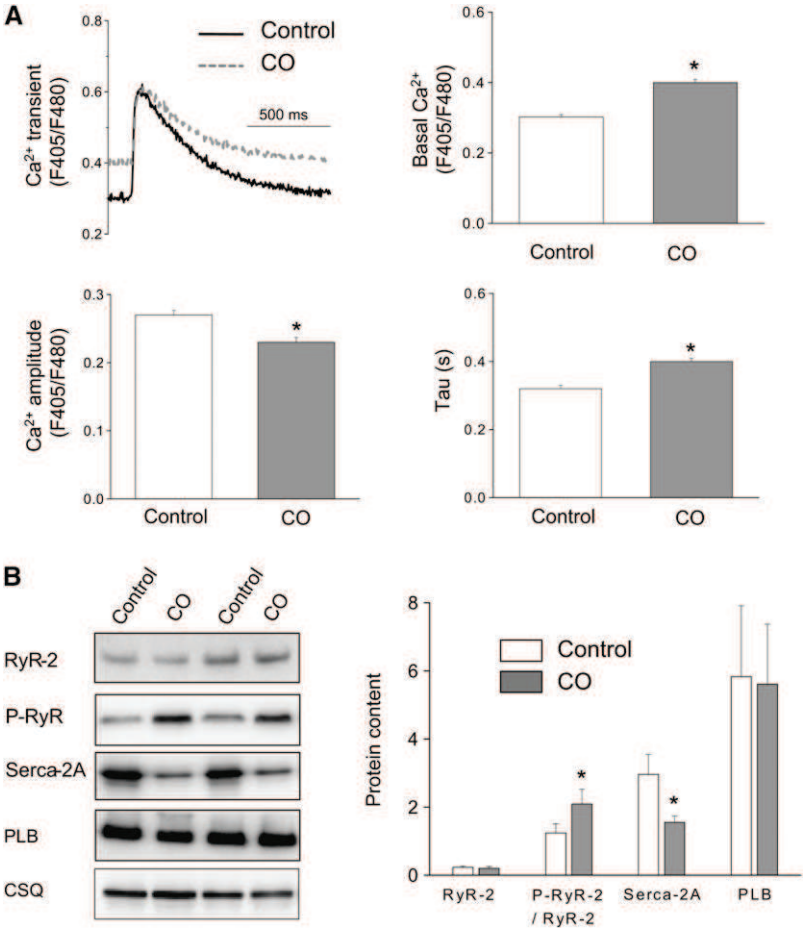

Figure 4. Chronic carbon monoxide (CO) pollution alters the Ca^{2+} dynamics of ventricular myocytes. (*A*) Superimposed Ca^{2+} transients in intact myocytes isolated from control and CO-exposed rats. Average diastolic intracellular Ca^{2+}, Ca^{2+} transient amplitude, and Ca^{2+} reuptake kinetics (tau) (n = 112–145 cells/5 hearts). (*B*) Effect of chronic exposure to CO on the abundance of Ca^{2+} handling proteins (RyR-2, PLB, and SERCA-2a), analyzed by Western blot analysis. Protein content was normalized to calsequestrin content and Ser^{2809} RyR-phosphorylation normalized to total RyR-2 content. Results are mean ± SEM for five hearts. *$P < 0.05$.

reuptake by the SR (21). Chronic CO exposure had no effect on RyR-2 protein abundance (Figure 4B). However, it increased the level of RyR-2 phosphorylation on the PKA-dependent site Ser^{2809}, which has previously been correlated with a Ca^{2+} leak through the RyR-2 (22). The slowing of the Ca^{2+} transient decay (i.e., increase in tau) in CO myocytes (Figure 4A) is consistent with an impairment of Ca^{2+} reuptake due either to diminished SERCA2a expression or to an inhibition of SERCA2a/PLB activity. We found that chronic CO exposure decreased SERCA-2a expression with no effect on PLB expression (Figure 4B).

Force developed by cardiomyocytes depends on both the amount of Ca^{2+} released by the SR and Ca^{2+} sensitivity of the contractile machinery. We measured the relationship between Ca^{2+}-activated force and internal Ca^{2+} concentration in single permeabilized LV myocytes (Figure 5A). The cross-sectional area in permeabilized cells did not differ between the two groups (203 ± 12 mm^2 vs. 200 ± 11 mm^2 in control and CO-exposed rats, respectively), thus confirming the absence of cardiomyocyte hypertrophy revealed by cell capacitance measurements. Maximal isometric tension normalized to cross-sectional area was similar in control and CO-exposed animals. However, a rightward shift in the tension-pCa curve (i.e., decrease in myofilaments Ca^{2+} sensitivity, pCa_{50}) in the CO-exposed group indicated that, for a given amount of Ca^{2+}, less force was generated by the myofilaments (Figure 5A). Myofilaments Ca^{2+} sensitivity is regulated by the phosphorylation status of sarcomeric proteins, such as MLC2 and cTnI (23). Chronic CO exposure did not change the phosphorylation level of MLC2 but increased the phosphorylation of cTnI at PKA sites ($Ser^{23/24}$) (Figure 5B). Taken together, these data demonstrate that chronic CO exposure alters cardiac cell contractility by modifying various stages of ECC.

Cardiac Response to β-Adrenergic Stimulation

We investigated the effects of CO exposure on the β-adrenergic reserve. *In vivo*, an acute β-adrenergic stimulation (using isoproterenol 1 mg/kg) modified both the maximal rate of increase of LV pressure and the relaxation time constant tau in CO-treated and control rats. However, these effects were less pronounced in the CO group (Figure 6A). Isoproterenol increased the maximal and minimal first derivative of LV pressure by 65.4 ± 9.1% in controls, but only by 27.9 ± 9.7% in CO-exposed rats. Similarly, tau decreased by 15.1 ± 3.3% in controls, but only by 3.7 ± 3.9% in CO-exposed rats, highlighting a reduction in the lusitropic effect of isoproterenol after chronic CO exposure.

At the cardiomyocyte level, β-adrenergic stimulation activates PKA, which phosphorylates both Ca^{2+}-handling proteins involved in ECC (RyR, PLB) and myofilament regulatory proteins (cTnI and MyBP-C). In our study, the positive inotropic effect of isoproterenol (100 nM) on cell shortening was smaller in myocytes from CO-exposed animals than from controls. However, the potentiating effect of isoproterenol on Ca^{2+} transient amplitude was similar in control and CO myocytes (Figure 6B), suggesting that an alteration in the myofilament response is responsible for the decrease in contraction. Permeabilized myocytes were therefore incubated with a recombinant catalytic subunit of PKA (Figure 6C). PKA led to classic myofilament Ca^{2+} desensitization (decrease in pCa_{50}). However this effect was

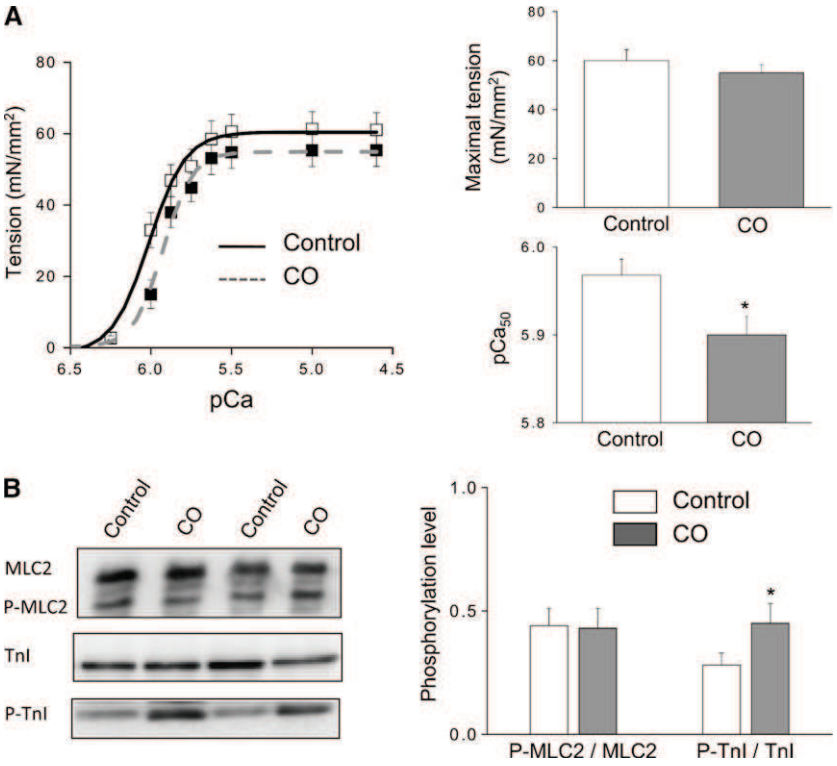

Figure 5. Effects of carbon monoxide (CO) pollution on contractile machinery in permeabilized cardiomyocytes. (*A*) The relationship between Ca^{2+}-activated tension and intracellular Ca^{2+} content was measured at 2.3 μm sarcomere length in permeabilized cardiomyocytes isolated from control and CO-exposed rats. The relationship was fitted with a modified Hill equation. The pCa at which half the maximal tension is developed (pCa_{50}, where $pCa = -\log_{10}[Ca^{2+}]$) was determined as an index of myofilament Ca^{2+} sensitivity (n = 25–28 cells/5 hearts). (*B*) Effect of chronic exposure to CO on the phosphorylation level of MLC-2 and cTnI in permeabilized cardiac strips from control and CO-exposed rats. Phosphorylation levels were determined by Western blotting with antibodies to P-MLC2 and to cTnI phosphorylated at the protein kinase A sites Ser^{22}/Ser^{23} (P-cTnI), as described in METHODS. *$P < 0.05$.

more pronounced in controls than in CO-exposed myocytes, such that the difference in myofilament Ca^{2+} sensitivity disappeared between control and CO myocytes after PKA treatment. Taken together, these data indicate that the β-adrenergic response is altered in animals exposed to chronic CO pollution.

Oxidative Status in CO- exposed Animals

It is well documented that CO binding to cytochrome-c oxidase in the electron transport chain as well as CO interaction with nitric oxide synthase (24) lead to generation of reactive oxygen species (ROS) and nitrogen species (25, 26). We thus evaluated whether the CO-associated cardiac remodeling could involve oxidative stress. Cardiac antioxidant and oxidant statuses are presented in Figure 7. Chronic CO exposure decreased antioxidant enzyme activities of superoxide dismutase, catalase, and glutathione peroxidase. This decrease of antioxidant defenses buffering ROS was associated with increased activity of thioredoxin reductase, confirming a CO-induced oxidative stress (27).

DISCUSSION

It is well established that air pollution is associated with cardiovascular outcome and can cause premature death. However, the mechanisms underlying these effects are poorly understood. We found that exposure of healthy rats to CO for a period limited to 4 weeks, under conditions mimicking urban air pollution, promoted cardiac remodeling and increased arrhythmogenic events. Although only a weak alteration of myocardium function was observed *in vivo*, marked changes in Ca^{2+} handling and Ca^{2+} sensitivity of contractile proteins occurred. To our knowledge, our data provide the first evidence at the cardiomyocyte level that chronic CO exposure promotes a pathological phenotype in the absence of underlying cardiopathy.

A key finding of the present study is that chronic CO exposure depresses the contraction of single rat ventricular myocytes because of reduction of both systolic Ca^{2+} release and myofilament Ca^{2+} sensitivity. In addition, the velocity of both the onset and the relaxation of contraction was markedly reduced, in agreement with a slowing of the Ca^{2+} transient decay. The reduced SERCA-2a expression induced by CO exposure is likely to account for the impairment in Ca^{2+} reuptake by the SR, and, therefore, for the delay in cell relaxation. The increase in PKA-phosphorylation of RyR-2 observed in CO-exposed animals is consistent with a Ca^{2+} leak in the SR, known to contribute to intracellular Ca^{2+} overload and SR Ca^{2+} depletion (22, 28, 29). A decrease in SERCA-2a expression could play a role not only in the reduction of SR Ca^{2+} content but also, as a consequence, in the elevation of diastolic Ca^{2+}.

Another major finding of this study is the proarrhythmogenic effect of chronic CO exposure in a healthy population. This result provides experimental support to previous reports that CO is associated with life- threatening VA in populations with cardiopathies (30, 31). The arrhythmic events may have an electrical origin or a Ca^{2+} origin (32). The lack of effect of CO on QT interval, the regionalized effect on AP duration, and the increase in diastolic Ca^{2+} concentration together support the hypothesis that the VAs observed after CO exposure are mediated by Ca^{2+} overload (33). The pathway proposed involves the Ca^{2+}-dependent activation of I_{ti} (the transient depolarizing inward Na^+ current), triggering delayed afterdepolarizations (34), with a facilitating role for β-adrenergic stimulation. Our demonstration of a PKA-dependent hyperphosphorylation of both RyR-2 and TnI is consistent with chronic β-adrenergic overstimulation during CO exposure, and contributes to its proarrhythmogenic effects.

The causative mechanisms involved in the chronic CO pollution–induced pathological cardiac phenotype could have a vascular origin, with limited blood delivery to the cardiac pump (35). Indeed, we demonstrated that, although coronary density was not modified after 4 weeks of CO exposure, perfusion was reduced during a cardiac stress (data not shown). A decreased oxygen delivery due to functional impairment, associated with probable repeated ischemia/reperfusion cycles induced by alternation of CO and ambient air exposure, is very

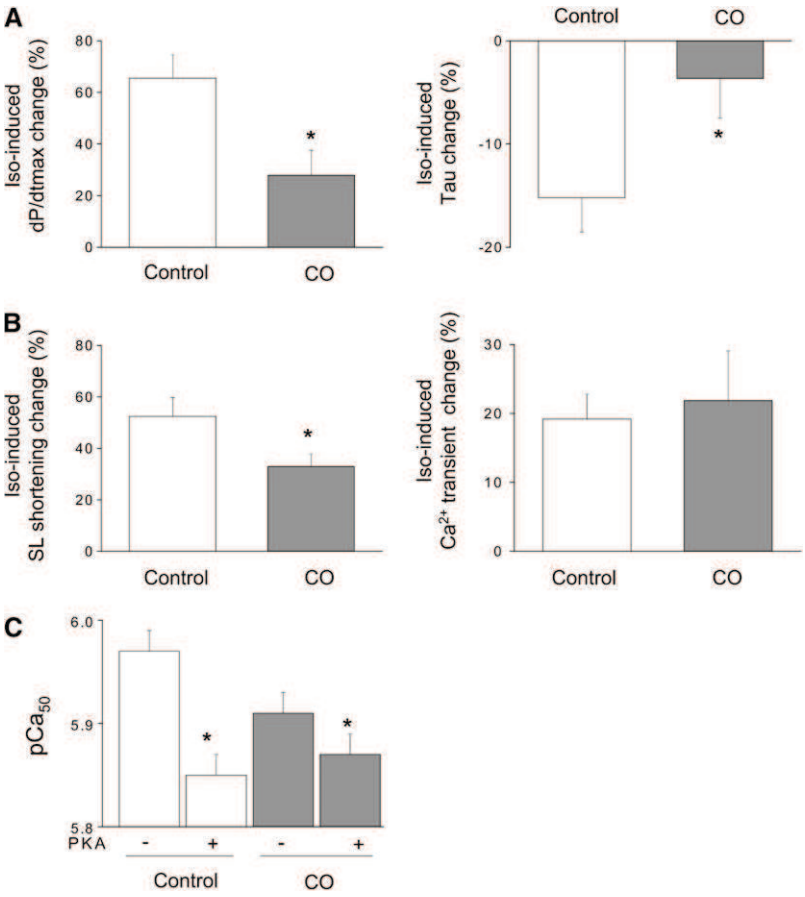

Figure 6. Effect of carbon monoxide (CO) pollution on the β-adrenergic reserve *in vivo* and *in vitro*. (*A*) Variation of the maximal first derivative (dP/dt max) and relaxation time constant (tau) of left ventricular (LV) pressure after isoproterenol injection (1 mg/kg; iso-induced) evaluated *in vivo* in control and CO-exposed animals (n = 9 rats in each group). (*B*) Variation of contraction (sarcomere length [SL] shortening) and Ca^{2+} transients in isolated LV cells in presence of 100 nM isoproterenol (iso-induced) (n = 22 cells for control rats and 37 cells for CO-exposed rats). (*C*) Myofilament Ca^{2+} sensitivity was similar between control and CO-exposed permeabilized cells after protein kinase A (PKA) treatment (100 U/ml, incubation for 60 min) (n = 21–27 cells/4 hearts). *$P < 0.05$.

likely to induce recurrent stresses and initiate the pathological cardiac remodeling demonstrated in the CO group. Moreover, vascular alterations could enhance the well-established CO-associated production of ROS and nitrogen species (25, 26). Indeed, CO binds to cytochrome-c oxidase of the electron transport chain and interacts with nitric oxide synthase, leading to peroxynitrite generation (24). Previous studies have shown that low-level CO exposure, as for urban pollution, causes oxidative stress (24). In accordance with these studies, we observed a marked increase in thioredoxin reductase activity in the CO-exposed rats associated with decreased antioxidant enzyme activities, suggesting increased oxidative stress. As proteins involved in Ca^{2+} handling are potential targets for redox modifications (36, 37), the cellular impairments observed in this study could be attributed partially to CO-induced ROS production. We show that chronic CO exposure increases PKA-dependent phosphorylation of both RyR-2 and TnI. ROS may be responsible for the PKA-dependent phosphorylation of cardiac proteins because it has been shown that ROS can activate the PKA pathway (38, 39).

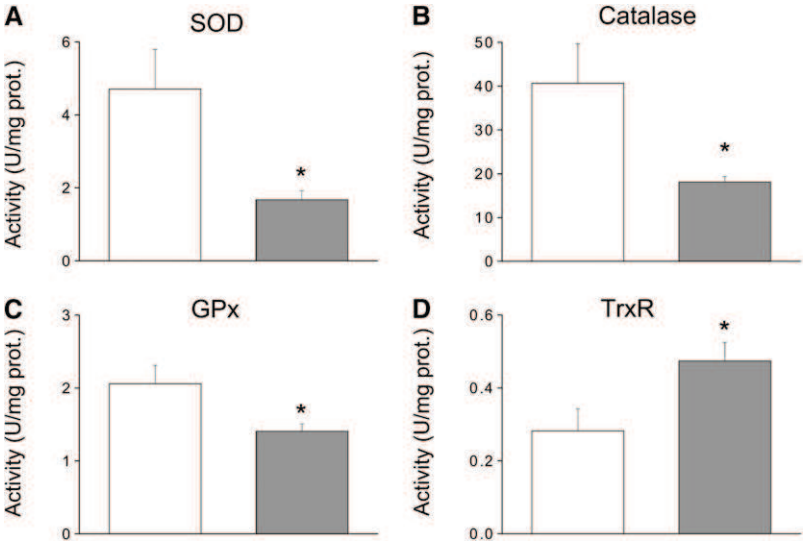

Figure 7. Cardiac oxidative status after chronic carbon monoxide (CO) exposure. Antioxidant activities of (*A*) superoxide dismutase, (*B*) catalase, and (*C*) glutathione peroxidase evaluated in whole heart of control and CO-exposed animals (n = 7 rats in each group). (*D*) Thioredoxin reductase activities, an index of oxidative stress, measured in control and CO-exposed animals (n = 7 rats in each group). *$P < 0.05$.

The toxic effect of high concentrations of CO is recognized. However, there is increasing evidence that a low concentration of CO is beneficial in diverse diseases in rodents, large animals, and humans (40). Low CO-dose gas inhalation but also synthetic CO-releasing molecules (CORM) have been recently used as potential therapeutic agents, particularly for cardiovascular diseases (41). CORM reduces infarct size (42), has a protective effect against myocardial infarction (42), prolongs survival of transplanted hearts, increases resistance to hypoxia-reoxygenation (43, 44), and improves cardiac mitochondrial metabolism (45). However, the beneficial cardiac effects of CORM were seen after acute perfusion, which differs from the chronic animal exposure model in the present study. The cardioprotective effects of low CO may be due to inhibition of L-type Ca^{2+} currents (46) occurring via redox modulation of key cysteine residues by mitochondrial ROS (47). In cardiac myocytes, rapid changes in cellular oxygen and ROS generation can contribute to electrophysiological instability and occurrence of arrhythmias via increased L-type Ca^{2+} current (*see* Reference 48 for review). Although moderate and variable across the LV wall, the increase in L-type Ca^{2+} current reported here might be consistent with an increased oxidative stress. At the moment, CO-based therapeutic strategies use short-term exposure. However, the potential toxicological effect of nontoxic doses of CO (30 ppm/d on average) on cardiac function should be relevant for future investigations of chronic treatment with low-dose CO gas inhalation or CORM.

Study Limitations

The cardiac effects of CO may result from a direct action on the heart and/or from indirect consequences of alterations in the respiratory system function. In fact, the level of carboxyhemoglobin measured 24 hours after the last CO exposure was not different from that of control rats, and was consistent with levels reached in human populations exposed to high atmospheric pollution (12, 13). These levels of carboxyhemoglobin are not reported to be associated, in the literature and in medical practice, with direct hypoxic stress. The pulmonary effects of CO remain controversial and are usually reported after chronic exposure to toxic doses, associated or not with other toxic agents (49, 50). In a set of preliminary experiments, we demonstrated that the mass of the right ventricle was not different between control and CO-exposed rats (0.276 ± 0.015 vs. 0.286 ± 0.015 g, $n = 7$ in each group; $P = 0.64$), whereas that of the LV was significantly increased ($P = 0.007$) after chronic CO exposure (1.02 ± 0.01 vs. 1.11 ± 0.01 g, in control and CO-exposed rats, respectively). Altogether, these data do not support a role for the respiratory system in the cardiac effects of CO reported here.

Clinical Relevance

Chronic CO exposure induced signs of cardiac stress and remodeling with several features commonly observed in pathology, such as HF, wherein impairment of myocardial pump function elicits chronic sympathetic nervous system activity to maintain cardiac output and blood pressure (16). Adrenergic hyperactivation promotes hypertrophy, increases heart rate, favors the development of interstitial fibrosis, and increases the risk of sudden cardiac death (51). Although chronic CO exposure induced only modest alterations in cardiac function *in vivo*, several abnormalities commonly observed in HF were detected. At the integrated level, they included a reduction in fractional shortening and end-systolic strain, parietal hypertrophy of the LV, an increase in fibrosis, an increase in basal heart rate, and a decrease in heart rate variability. At the cellular level, despite the absence of cellular hypertrophy and change in repolarizing I_{to} density, cardiomyocytes in CO-exposed rats exhibited features typical of HF, including elevated diastolic Ca^{2+} (22), reduced SR Ca^{2+} load (52), decreased systolic Ca^{2+} release (53), a lengthening of Ca^{2+} reuptake (54), and diminished Ca^{2+} sensitivity of the myofilaments (15, 18, 55). In addition, the positive inotropic effect of isoproterenol was partially lost *in vivo* and *in vitro*, consistent with a decrease in the phosphorylation reserve, possibly because of an elevation of the adrenergic (hyperadrenergic) state to compensate for the altered contraction of cardiomyocytes. However, even if the pathological cellular function seems to be rescued *in vivo* under basal conditions, CO-exposed rats exhibited an enhanced arrhythmogenic potential on β-adrenergic stimulation, suggesting an increased risk for cardiac events under conditions of exercise and stress. Interestingly, because ROS are involved in the deleterious effects of CO pollution, antioxidant therapy provided by pharmacology, nutrition, or physical exercise could prevent the alterations reported here.

In conclusion, chronic exposure to CO levels consistent with environmental air pollution promotes moderate cardiac dysfunction *in vivo* in healthy rats. However, serious alterations occur at the cardiomyocyte level, potentially reflecting an early stage of cardiac pathology. Our findings provide a rationale at the cellular and molecular levels in support of earlier epidemiologic studies pointing to the deleterious effects of CO pollution on cardiac function. Further studies will aim at investigating whether the pathologic cellular phenotype evidenced in our study could exacerbate the effects of an acute stress, such as ischemia reperfusion or acute oxidative stress.

Conflict of Interest Statement: None of the authors has a financial relationship with a commercial entity that has an interest in the subject of this manuscript.

References

1. Miller KA, Siscovick DS, Sheppard L, Shepherd K, Sullivan JH, Anderson GL, Kaufman JD. Long-term exposure to air pollution and incidence of cardiovascular events in women. *N Engl J Med* 2007; 356:447–458.
2. Brook RD, Franklin B, Cascio W, Hong Y, Howard G, Lipsett M, Luepker R, Mittleman M, Samet J, Smith SC Jr, *et al.* Air pollution and cardiovascular disease: a statement for healthcare professionals from the Expert Panel on Population and Prevention Science of the American Heart Association. *Circulation* 2004;109: 2655–2671.
3. Finkelstein MM. Pollution-related mortality and educational level. *JAMA* 2002;288:830; author reply 830.
4. Pope CA III, Burnett RT, Thun MJ, Calle EE, Krewski D, Ito K, Thurston GD. Lung cancer, cardiopulmonary mortality, and long-term exposure to fine particulate air pollution. *JAMA* 2002;287:1132–1141.
5. Henry CR, Satran D, Lindgren B, Adkinson C, Nicholson CI, Henry TD. Myocardial injury and long-term mortality following moderate to severe carbon monoxide poisoning. *JAMA* 2006;295:398–402.
6. Samoli E, Touloumi G, Schwartz J, Anderson HR, Schindler C, Forsberg B, Vigotti MA, Vonk J, Kosnik M, Skorkovsky J, *et al.* Short-term effects of carbon monoxide on mortality: an analysis within the APHEA project. *Environ Health Perspect* 2007;115:1578–1583.
7. Peters A, Doring A, Wichmann HE, Koenig W. Increased plasma viscosity during an air pollution episode: a link to mortality? *Lancet* 1997;349:1582–1587.
8. Dales R. Ambient carbon monoxide may influence heart rate variability in subjects with coronary artery disease. *J Occup Environ Med* 2004; 46:1217–1221.
9. Simkhovich BZ, Kleinman MT, Kloner RA. Air pollution and cardiovascular injury epidemiology, toxicology, and mechanisms. *J Am Coll Cardiol* 2008;52:719–726.
10. Stern FB, Halperin WE, Hornung RW, Ringenburg VL, McCammon CS. Heart disease mortality among bridge and tunnel officers exposed to carbon monoxide. *Am J Epidemiol* 1988;128:1276–1288.

11. Wright GR, Jewczyk S, Onrot J, Tomlinson P, Shephard RJ. Carbon monoxide in the urban atmosphere: hazards to the pedestrian and the street-worker. *Arch Environ Health* 1975;30:123–129.
12. Joumard R, Chiron M, Vidon R, Maurin M, Rouzioux JM. Mathematical models of the uptake of carbon monoxide on hemoglobin at low carbon monoxide levels. *Environ Health Perspect* 1981;41:277–289.
13. Cole PV. Comparative effects of atmospheric pollution and cigarette smoking on carboxyhaemoglobin levels in man. *Nature* 1975;255:699–701.
14. Reboul C, Tanguy S, Juan JM, Dauzat M, Obert P. Cardiac remodeling and functional adaptations consecutive to altitude training in rats: implications for sea level aerobic performance. *J Appl Physiol* 2005;98:83–92.
15. Mou YA, Reboul C, Andre L, Lacampagne A, Cazorla O. Late exercise training improves non-uniformity of transmural myocardial function in rats with ischaemic heart failure. *Cardiovasc Res* 2009;81:555–564.
16. Fauconnier J, Bedut S, Le Guennec JY, Babuty D, Richard S. Ca2+ current-mediated regulation of action potential by pacing rate in rat ventricular myocytes. *Cardiovasc Res* 2003;57:670–680.
17. Stoll M, Quentin M, Molojavyi A, Thamer V, Decking UK. Spatial heterogeneity of myocardial perfusion predicts local potassium channel expression and action potential duration. *Cardiovasc Res* 2008;77:489–496.
18. Cazorla O, Szilagyi S, Le Guennec JY, Vassort G, Lacampagne A. Transmural stretch-dependent regulation of contractile properties in rat heart and its alteration after myocardial infarction. *FASEB J* 2005;19:88–90.
19. Cazorla O, Szilagyi S, Vignier N, Salazar G, Kramer E, Vassort G, Carrier L, Lacampagne A. Length and protein kinase A modulations of myocytes in cardiac myosin binding protein C-deficient mice. *Cardiovasc Res* 2006;69:370–380.
20. Boucher F, Tanguy S, Besse S, Tresallet N, Favier A, de Leiris J. Age-dependent changes in myocardial susceptibility to zero flow ischemia and reperfusion in isolated perfused rat hearts: relation to antioxidant status. *Mech Ageing Dev* 1998;103:301–316.
21. Cheng H, Lederer WJ. Calcium sparks. *Physiol Rev* 2008;88:1491–1545.
22. Marx SO, Reiken S, Hisamatsu Y, Jayaraman T, Burkhoff D, Rosemblit N, Marks AR. PKA phosphorylation dissociates FKBP12.6 from the calcium release channel (ryanodine receptor): defective regulation in failing hearts. *Cell* 2000;101:365–376.
23. Solaro RJ. Multiplex kinase signaling modifies cardiac function at the level of sarcomeric proteins. *J Biol Chem* 2008;283:26829–26833.
24. Thom SR, Fisher D, Xu YA, Notarfrancesco K, Ischiropoulos H. Adaptive responses and apoptosis in endothelial cells exposed to carbon monoxide. *Proc Natl Acad Sci USA* 2000;97:1305–1310.
25. Piantadosi CA. Carbon monoxide poisoning. *N Engl J Med* 2002;347: 1054–1055.
26. Piantadosi CA. Biological chemistry of carbon monoxide. *Antioxid Redox Signal* 2002;4:259–270.
27. Zhang J, Piantadosi CA. Mitochondrial oxidative stress after carbon monoxide hypoxia in the rat brain. *J Clin Invest* 1992;90:1193–1199.
28. Yano M, Ikeda Y, Matsuzaki M. Altered intracellular Ca2+ handling in heart failure. *J Clin Invest* 2005;115:556–564.
29. Bers DM, Eisner DA, Valdivia HH. Sarcoplasmic reticulum Ca2+ and heart failure: roles of diastolic leak and Ca2+ transport. *Circ Res* 2003;93:487–490.
30. Wellenius GA, Coull BA, Batalha JR, Diaz EA, Lawrence J, Godleski JJ. Effects of ambient particles and carbon monoxide on supraventricular arrhythmias in a rat model of myocardial infarction. *Inhal Toxicol* 2006;18:1077–1082.
31. Peters A, Liu E, Verrier RL, Schwartz J, Gold DR, Mittleman M, Baliff J, Oh JA, Allen G, Monahan K, *et al.* Air pollution and incidence of cardiac arrhythmia. *Epidemiology* 2000;11:11–17.
32. Pasquie JL, Richard S. Prolongation in QT interval is not predictive of Ca2+-dependent arrhythmias: implications for drug safety. *Expert Opin Drug Saf* 2009;8:57–72.
33. Ter Keurs HE, Boyden PA. Calcium and arrhythmogenesis. *Physiol Rev* 2007;87:457–506.
34. Janse MJ. Electrophysiological changes in heart failure and their relationship to arrhythmogenesis. *Cardiovasc Res* 2004;61:208–217.
35. Favory R, Lancel S, Tissier S, Mathieu D, Decoster B, Neviere R. Myocardial dysfunction and potential cardiac hypoxia in rats induced by carbon monoxide inhalation. *Am J Respir Crit Care Med* 2006;174: 320–325.
36. Zima AV, Blatter LA. Redox regulation of cardiac calcium channels and transporters. *Cardiovasc Res* 2006;71:310–321.
37. Zissimopoulos S, Docrat N, Lai FA. Redox sensitivity of the ryanodine receptor interaction with FK506-binding protein. *J Biol Chem* 2007; 282:6976–6983.
38. Brennan JP, Bardswell SC, Burgoyne JR, Fuller W, Schroder E, Wait R, Begum S, Kentish JC, Eaton P. Oxidant-induced activation of type I protein kinase A is mediated by RI subunit interprotein disulfide bond formation. *J Biol Chem* 2006;281:21827–21836.
39. de Lamirande E, O'Flaherty C. Sperm activation: role of reactive oxygen species and kinases. *Biochim Biophys Acta* 2008;1784:106–115.
40. Otterbein LE. The evolution of carbon monoxide into medicine. *Respir Care* 2009;54:925–932.
41. Foresti R, Bani-Hani MG, Motterlini R. Use of carbon monoxide as a therapeutic agent: promises and challenges. *Intensive Care Med* 2008;34:649–658.
42. Guo Y, Stein AB, Wu WJ, Tan W, Zhu X, Li QH, Dawn B, Motterlini R, Bolli R. Administration of a CO-releasing molecule at the time of reperfusion reduces infarct size in vivo. *Am J Physiol Heart Circ Physiol* 2004;286:H1649–H1653.
43. Clark JE, Naughton P, Shurey S, Green CJ, Johnson TR, Mann BE, Foresti R, Motterlini R. Cardioprotective actions by a water-soluble carbon monoxide-releasing molecule. *Circ Res* 2003;93:e2–e8.
44. Varadi J, Lekli I, Juhasz B, Bacskay I, Szabo G, Gesztelyi R, Szendrei L, Varga E, Bak I, Foresti R, *et al.* Beneficial effects of carbon monoxide-releasing molecules on post-ischemic myocardial recovery. *Life Sci* 2007;80:1619–1626.
45. Lancel S, Hassoun SM, Favory R, Decoster B, Motterlini R, Neviere R. Carbon monoxide rescues mice from lethal sepsis by supporting mitochondrial energetic metabolism and activating mitochondrial biogenesis. *J Pharmacol Exp Ther* 2009;329:641–648.
46. Uemura K, Adachi-Akahane S, Shintani-Ishida K, Yoshida K. Carbon monoxide protects cardiomyogenic cells against ischemic death through L-type Ca2+ channel inhibition. *Biochem Biophys Res Commun* 2005;334:661–668.
47. Scragg JL, Dallas ML, Wilkinson JA, Varadi G, Peers C. Carbon monoxide inhibits L-type Ca2+ channels via redox modulation of key cysteine residues by mitochondrial reactive oxygen species. *J Biol Chem* 2008;283:24412–24419.
48. Hool LC. Acute hypoxia differentially regulates K(+) channels. Implications with respect to cardiac arrhythmia. *Eur Biophys J* 2005;34:369–376.
49. Zheng H, Liu Y, Huang T, Fang Z, Li G, He S. Development and characterization of a rat model of chronic obstructive pulmonary disease (COPD) induced by sidestream cigarette smoke. *Toxicol Lett* 2009;189:225–234.
50. Ghosh S, Wilson MR, Choudhury S, Yamamoto H, Goddard ME, Falusi B, Marczin N, Takata M. Effects of inhaled carbon monoxide on acute lung injury in mice. *Am J Physiol Lung Cell Mol Physiol* 2005; 288:L1003–L1009.
51. Maass AH, Ikeda K, Oberdorf-Maass S, Maier SK, Leinwand LA. Hypertrophy, fibrosis, and sudden cardiac death in response to pathological stimuli in mice with mutations in cardiac troponin T. *Circulation* 2004;110:2102–2109.
52. Hobai IA, O'Rourke B. Decreased sarcoplasmic reticulum calcium content is responsible for defective excitation-contraction coupling in canine heart failure. *Circulation* 2001;103:1577–1584.
53. Gomez AM, Valdivia HH, Cheng H, Lederer MR, Santana LF, Cannell MB, McCune SA, Altschuld RA, Lederer WJ. Defective excitation-contraction coupling in experimental cardiac hypertrophy and heart failure. *Science* 1997;276:800–806.
54. Piacentino V III, Weber CR, Chen X, Weisser-Thomas J, Margulies KB, Bers DM, Houser SR. Cellular basis of abnormal calcium transients of failing human ventricular myocytes. *Circ Res* 2003;92:651–658.
55. Perez NG, Hashimoto K, McCune S, Altschuld RA, Marban E. Origin of contractile dysfunction in heart failure: calcium cycling versus myofilaments. *Circulation* 1999;99:1077–1083.

3. Conclusion

L'exposition chronique à des concentrations de CO simulant une pollution atmosphérique urbaine entraine une dysfonction cardiaque modérée *in vivo* chez des rats sains. Cependant, de graves altérations cellulaires se produisent, reflétant potentiellement un stade précoce de la pathologie cardiaque. Nos résultats apportent alors un rationnel cellulaire et moléculaire aux études épidémiologiques montrant les effets néfastes de la pollution au CO sur la fonction cardiaque. D'autre part, cette étude suggère qu'un stress environnemental comme la pollution atmosphérique peut provoquer des effets à priori invisibles lors d'un examen clinique routinier par échocardiographie. Après 4 semaines d'exposition à la pollution au CO, les altérations cellulaires sont « masquées » certainement en raison de mécanismes compensateurs, telle la voie β-adrénergique, permettant le maintien d'une cohérence cardiaque globale. Il eut été alors intéressant de réaliser les investigations à divers stades d'exposition afin de déterminer si ces mécanismes compensateurs s'essoufflent dans le temps et laissent place à la survenue d'une pathologie cardiaque. Ce type de protocole étant très chronophage, il n'a pu être envisagé dans le cadre de cette thèse.

III. Effet d'une pollution au monoxyde de carbone sur la susceptibilité cardiaque à l'ischémie-reperfusion

1. Introduction

Dans la précédente étude, nous avons apporté des éléments de réponse face aux corrélations épidémiologiques entre pollution atmosphérique et accidents cardiovasculaires. En effet, nous avons montré qu'une pollution au CO générait des troubles cellulaires cardiaques similaires à ceux associés à des pathologies cardiaques telles que l'IC, à l'origine d'évènements arythmiques. Ces effets délétères corrélaient notamment avec un stress oxydatif chez les populations exposées au CO. Ce phénotype arythmique, sous-tendu par un remodelage de l'homéostasie Ca^{2+}, pourrait rendre le cœur plus vulnérable lors d'un stress ischémique perturbant de manière importante l'homéostasie redox. Nous avons donc cherché à déterminer dans cette étude si l'exposition à une pollution au CO augmentait la sensibilité myocardique de rats à un évènement coronarien aigu : l'ischémie-reperfusion.

2. Article 5 – Accepté dans AJP Heart Circ Phys, 2010

G. Meyer, L. André, S. Tanguy, J. Boissiere, C. Farah, F. Lopez-Lauri, S. Gayrard, S. Richard, F. Boucher, O. Cazorla, P. Obert and C. Reboul
Am J Physiol Heart Circ Physiol 298:1445-1453, 2010. First published Mar 5, 2010;
doi:10.1152/ajpheart.01194.2009

You might find this additional information useful...

This article cites 39 articles, 22 of which you can access free at:
http://ajpheart.physiology.org/cgi/content/full/298/5/H1445#BIBL

Updated information and services including high-resolution figures, can be found at:
http://ajpheart.physiology.org/cgi/content/full/298/5/H1445

Additional material and information about ***AJP - Heart and Circulatory Physiology*** can be found at:
http://www.the-aps.org/publications/ajpheart

This information is current as of July 8, 2010 .

AJP - Heart and Circulatory Physiology publishes original investigations on the physiology of the heart, blood vessels, and lymphatics, including experimental and theoretical studies of cardiovascular function at all levels of organization ranging from the intact animal to the cellular, subcellular, and molecular levels. It is published 12 times a year (monthly) by the American Physiological Society, 9650 Rockville Pike, Bethesda MD 20814-3991. Copyright © 2005 by the American Physiological Society. ISSN: 0363-6135, ESSN: 1522-1539. Visit our website at http://www.the-aps.org/.

Downloaded from ajpheart.physiology.org on July 8, 2010

Am J Physiol Heart Circ Physiol 298: H1445–H1453, 2010.
First published March 5, 2010; doi:10.1152/ajpheart.01194.2009.

Simulated urban carbon monoxide air pollution exacerbates rat heart ischemia-reperfusion injury

G. Meyer,[1] L. André,[2] S. Tanguy,[1] J. Boissiere,[2] C. Farah,[1] F. Lopez-Lauri,[4] S. Gayrard,[1] S. Richard,[2] F. Boucher,[3] O. Cazorla,[2] P. Obert,[1] and C. Reboul[1]

[1]*Research Laboratory: Equipe d'Accueil 4278, Physiology and Physiopathology of Cardiovascular Adaptations to Exercise, and* [4]*Research Laboratory: Equipe d'Accueil 4279, Faculty of Sciences, Avignon University, Avignon;* [2]*Research Laboratory: Institut National de la Santé et de la Recherche Médicale Unité 637, Cardiovascular Physiopathology, Montpellier University, Faculty of Medicine, Montpellier; and* [3]*Research Laboratory: Unite Mixte de Recherche 5525 Physiologie cardio-Respiratoire Expérimentale Théorique et Appliquée-Techniques de l'Ingénierie Médicale et de la Complexité, Grenoble University Joseph Fourier, Grenoble, France*

Submitted 15 December 2009; accepted in final form 28 February 2010

Meyer G, André L, Tanguy S, Boissiere J, Farah C, Lopez-Lauri F, Gayrard S, Richard S, Boucher F, Cazorla O, Obert P, Reboul C. Simulated urban carbon monoxide air pollution exacerbates rat heart ischemia-reperfusion injury. *Am J Physiol Heart Circ Physiol* 298: H1445–H1453, 2010. First published March 5, 2010; doi:10.1152/ajpheart.01194.2009.—Myocardial damages due to ischemia-reperfusion (I/R) are recognized to be the result of a complex interplay between genetic and environmental factors. Epidemiological studies suggested that, among environmental factors, carbon monoxide (CO) urban pollution can be linked to cardiac diseases and mortality. The aim of this work was to evaluate the impact of exposure to CO pollution on cardiac sensitivity to I/R. Regional myocardial I/R was performed on isolated perfused hearts from rats exposed for 4 wk to air enriched with CO (30–100 ppm). Functional variables, reperfusion ventricular arrhythmias (VA) and cellular damages (infarct size, lactate dehydrogenase release) were assessed. Sarcomere length shortening and Ca^{2+} handling were evaluated in intact isolated cardiomyocytes during a cellular anoxia-reoxygenation protocol. The major results show that prolonged CO exposure worsens myocardial I/R injuries, resulting in increased severity of postischemic VA, impaired recovery of myocardial function, and increased infarct size (60 ± 5 vs. 33 ± 2% of ischemic zone). The aggravating effects of CO exposure on I/R could be explained by a reduced myocardial enzymatic antioxidant status (superoxide dismutase −45%; glutathione peroxidase −49%) associated with impaired intracellular Ca^{2+} handling. In conclusion, our results are consistent with the idea that chronic CO pollution dramatically increases the severity of myocardial I/R injuries.

environmental pollution; myocardial infarction; antioxidant status

MYOCARDIAL DAMAGES RESULTING from ischemia-reperfusion (I/R) are a major cause of morbidity and mortality in western nations. Those myocardial I/R injuries result in cardiac dysfunction, arrhythmias, as well as irreversible myocyte damages (25, 28). The sensitivity of the myocardium to I/R-induced cellular injuries is recognized today to be the result of a complex interplay between genetic, pathological, and environmental factors. Moreover, it appears to be aggravated in several diseases, including hypertension, metabolic disorders, and complications from cigarette smoking and environmental pollution.

Address for reprint requests and other correspondence: C. Reboul, Research Laboratory: EA 4278, Physiology and Physiopathology of Cardiovascular Adaptations to Exercise, Faculty of Sciences, Avignon Univ., F-84000 Avignon, France (e-mail: Cyril.reboul@univ-avignon.fr).

Among the environmental factors that could influence the development of cardiovascular diseases, several epidemiological studies have recently suggested that urban atmospheric pollution may exert adverse effects on cardiovascular health (7, 11, 12, 15). Among the numerous pollutants, carbon monoxide (CO) has been described as one of the main pollutants responsible for the development of cardiovascular diseases (9, 35). In urban environments, CO concentration usually varies from 2 to 40 ppm, but during heavy traffic it may be as high as 170 ppm (10, 34, 40). At this level, CO exposure has been correlated with hospital admissions, mortality, and morbidity related to cardiovascular diseases (9, 13, 29). Today, although the pathophysiological mechanisms regarding acute CO poisoning are well known, mechanisms associated with chronic exposure to lower concentrations of CO, consistent with urban environmental pollution, remain unclear. We (2) and Bye et al. (14) have recently reported that prolonged CO exposure induces a pathological myocardial cellular phenotype characterized by a major remodeling of the excitation-contraction coupling. Such deleterious consequences may worsen the effect of cardiovascular diseases.

The aim of this experimental work was to challenge the impact of a chronic exposure to simulated CO urban pollution on the sensitivity of the myocardium to I/R in a rat model. The major result shows that prolonged exposure to CO at a level found in the urban environment has a dramatic deleterious impact on the sensitivity of the myocardium to I/R.

METHODS

Experiments complied with the *Guide for the Care and Use of Laboratory Animals* published by the United States National Institutes of Health (National Institutes of Health Publications no. 85-23, revised 1996) and was approved by the French Ministry of Agriculture.

Animals and CO Exposure

Adult, male Wistar rats ($n = 64$; 345 ± 7 g; Charles River Laboratories) were randomly assigned to the following two groups: CO rats (exposed for 4 wk to simulated CO urban pollution, $n = 32$) and control animals (Ctrl rats, exposed to standard filtered air, $n = 32$). CO rats were housed in an airtight exposure container for 4 wk. Exposure was performed according to a 12:12-h CO in the air-ambient air cycle. To simulate CO urban pollution, exposure was performed as follows: during CO exposure, a CO concentration of 30 ppm was maintained in the airtight container and monitored with an aspirative CO analyzer (CHEMGARD Infrared Gas Monitor NEMA 4 Version;

 0363-6135/10 $8.00 Copyright © 2010 the American Physiological Society

Downloaded from ajpheart.physiology.org on July 8, 2010

MSA). This initial concentration was supplemented with five 1-h peaks at 100 ppm CO. During ambient air exposure, animals were placed in the laboratory animal house with a CO concentration of 0 ppm. Ctrl rats were confined in the laboratory animal house for 4 wk and were manipulated daily. At the end of the 4-wk CO exposure, rats were housed 24 h in standard filtered air to avoid the acute effects of CO on the myocardium.

Regional Myocardial Ischemia and Reperfusion on Isolated Perfused Rat Heart

Rats were anaesthetized with pentobarbital sodium (50 mg/kg ip). A thoracotomy was performed, and the heart was rapidly removed, by cutting the great vessels, and immersed in ice-cold Krebs solution. The heart was transferred to the perfusion apparatus, and the aorta was cannulated for perfusion with oxygenated (95% O_2-5% CO_2) Krebs solution (37°C) composed of (in mM) 118.3 NaCl, 25 $NaHCO_3$, 4.7 KCl, 1.2 $MgSO_4$, 1.2 KH_2PO_4, 11.1 glucose, and 2.5 CaCl (pH = 7.4). The hearts were perfused at a constant pressure (80 mmHg).

Evaluation of postischemic reperfusion injury. On a first set of rats (n = 8/group), the atrioventricular node was crushed using fine forceps, the right atrium was excised, and the hearts were paced at a rate of 300 beats/min with an electrical stimulator (low voltage stimulator, BSL MP35 SS58L, 3V). An ultrathin, water-filled balloon was inserted in the left ventricle via the mitral valve, and the balloon volume was adjusted to achieve a left ventricular (LV) end diastolic pressure of 5 mmHg. Coronary blood flow was measured by collection of the infiltration effluents. A suture on a round-bodied needle was placed around the left anterior descending coronary artery (LAD), and the suture ends were placed around a small length of tubing to form a snare. The heart was allowed to stabilize for 30 min. Following the stabilization period, the LAD was occluded for 30 min. Subsequently, the snare occluder was released to allow reperfusion of the previously ischemic vascular bed for 120 min. The LAD was then reoccluded, and Evans blue dye solution (5 ml, 2%) was injected in the left ventricle to allow perfused (stained blue) and nonperfused (unstained) areas of the heart to be distinguished. After removal of the hearts, it was divided into five slices perpendicular to the apex-base axis. Triphenyltetrazolium chloride staining (0.5 mg/ml for 20 min at 37°C) was used to assess myocardial tissue viability and to determine myocardial infarct size. Tissue slices were photographed, and area at risk and infarcted area were then determined using a computer-based system (ImageJ; NIH).

Evaluation of postischemic reperfusion-induced ventricular arrhythmias. On a second set of rats (n = 14/group), arrhythmic events were evaluated on isolated nonpaced hearts. The heart was mounted, and the LAD occlusion was performed as previously described. A computerized electrocardiogram was obtained continuously during the protocol. The various types of arrhythmias were defined as described in the Lambeth conventions (39). The analysis of the electrocardiogram enabled assessment of the incidence (percent no. of hearts exhibiting a given type of arrhythmia) of different types of ventricular arrhythmias (Fig. 1*A*) as follows: sinus rhythm, ventricular premature beats (VPB), ventricular tachycardia (VT), and ventricular fibrillation (VF). To allow the comparison of the severity of rhythm disturbances occurring upon reperfusion, each individual heart was characterized according to a five-point arrhythmic score previously described by Tanguy et al. (37) and designed so that the more severe the arrhythmia, the larger the number (Fig. 1*B*). Such a simplified scoring system allows the assignment of a single number to each heart, and the comparison of the distribution of the hearts by various scores.

Cardiomyocyte Excitation-Contraction Analysis After Cellular Anoxia-Reoxygenation

On a third set of rats (n = 4/group), single ventricular cardiomyocytes were isolated by enzymatic digestion as previously described (24). Cardiomyocytes were transferred to a glass petri dish and placed in an anoxic chamber (O_2 level ~2%) for 60 min, followed by a 60-min reoxygenation in ambient air (O_2 ~19.4%). Unloaded cell shortening and Ca^{2+} concentration (indo 1 dye) were measured using field stimulation (0.5 Hz, 22°C, 1.8 mM external Ca^{2+}) before and after anoxia-reoxygenation (A/R). Sarcomere length (SL) and fluorescence (405 and 480 nm) were recorded simultaneously (IonOptix system; Hilton). The A/R experiment was then carried out in the presence or absence of a nonspecific antioxidant [*N*-acetylcystein (NAC), 20 μM].

Biochemical Assays

Heart antioxidant enzyme activity. A fourth set of rats (n = 6/group) was used to evaluate the enzymatic antioxidant status of the myocardium consecutive to chronic CO exposure and before I/R. After the end of CO exposure (24 h), the hearts were freeze-clamped, and the frozen ventricular tissue was homogenized in Tris·HCl buffer (60 mM Tris·HCl and 1 mM diethyltriaminopentaacetic acid, pH 7.4, 10 ml/g wet wt) using a Teflon potter homogenizer. Tissue homogenates were then centrifuged for 10 min at 200 *g* at 4°C to remove all nuclear debris. Cardiac superoxide dismutase (SOD) activity was assessed in the supernatant according to the method described by Marklund (22). Cardiac glutathione peroxidase (GPx) activity was assessed spectrophotometrically on the cytosolic fraction according to the method described by Flohe and Günzler (18). Catalase activity was determined according to the method described by Beers and Sizer (8). All enzyme activities were expressed in units per milligram protein (U/mg protein). The modified method of Lowry et al. (21) was used to determine protein content of tissue homogenates, using BSA as standard.

Lactate dehydrogenase in coronary effluents. Lactate dehydrogenase (LDH) activity was measured in coronary effluents by spectrophotometry using an LDH kit (LDH-P; BIOLABO). Measurements were made at the end of stabilization and at 10, 30, and 60 min of reperfusion. LDH activity was normalized to coronary blood flow.

Thiobarbituric acid-reactive substances in LV tissues. Thiobarbituric acid-reactive substances (TBARS) were assessed in LV tissues after 30 min of reperfusion using the thiobarbituric acid (TBA) test. Frozen heart tissue (120 mg) was homogenized in 1 ml 0.1% TCA solution. The homogenate was centrifuged at 12,000 *g* for 15 min, and 0.5 ml of the supernatant was added to 1 ml of 0.5% TBA in 20% TCA. The mixture was incubated in boiling water for 30 min, and the reaction was stopped by placing the reaction tubes in an ice bath. Tubes were briefly vortexed, triplicate 200-μl aliquots were taken from each tube and placed in 96-well plates, and the supernatant absorbance was read at 532 nm in a microplate reader. The value for nonspecific absorption at 600 nm was subtracted. The amount of TBARS (red pigment) was calculated using an extinction coefficient of 155 $mM^{-1} \cdot cm^{-1}$.

Statistics

Data were analyzed using one-way ANOVA between groups and repeated-measures ANOVA when necessary. When significant interactions were found, a Tukey-Kramer test was applied. The distribution of the hearts based on the various arrhythmic scores was analyzed by a nonparametric Mann-Whitney *U*-test. Binomially distributed variables (such as incidence of VF) were analyzed using nonparametric Yates' chi square test (Statview; Adept Scientific, Letchworth, UK). A level of $P < 0.05$ was considered statistically significant. Data are expressed as group means or group mean fractions of baseline ± SE.

RESULTS

Effects of CO Exposure on Myocardial Reperfusion Ventricular Arrhythmias

The time course of reperfusion-induced VPB, VT, and VF in individual hearts is shown in Fig. 1*C*. Figure 1*D* shows a

Downloaded from ajpheart.physiology.org on July 8, 2010

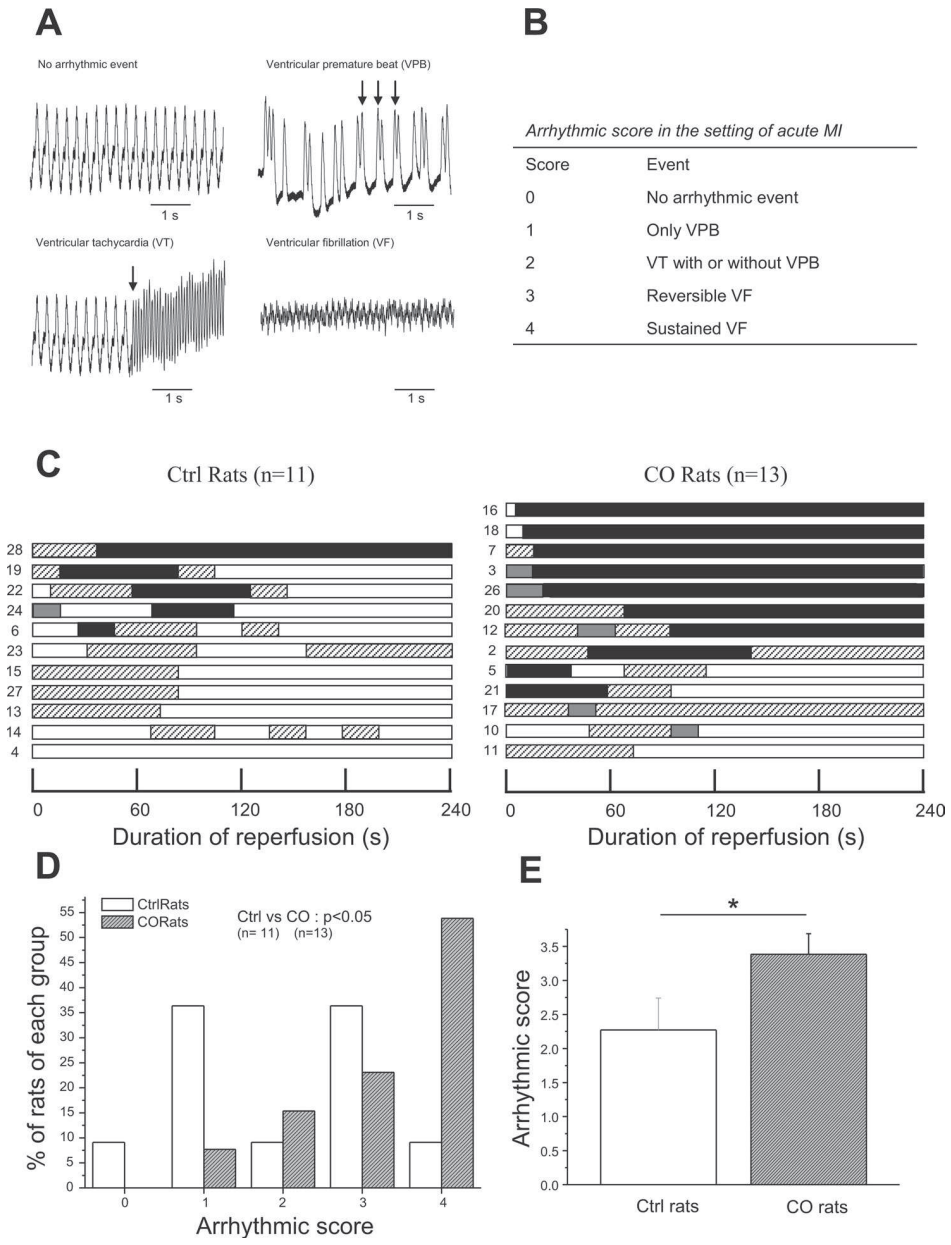

Fig. 1. Effects of carbon monoxide (CO) exposure on the severity of postischemic reperfusion-induced arrhythmic events. Electrocardiographic recordings (*A*) of normal sinus rhythm and of arrhythmias identified during postischemic reperfusion as described in the Lambeth Convention [sinus rhythm, ventricular premature beat (VPB), ventricular tachycardia (VT), and ventricular fibrillation (VF)] and related arrhythmic scores (*B*). *C*: time course of reperfusion-induced VPB (crossed out bars), VT (gray bars), and VF (black bars) of each heart of the control (Ctrl) group (*left*) and CO (*right*) group (nos. on *left* refer to the order of the experiments). *D*: categorization of arrhythmia classes (score) according to *B*. Values are expressed as a percentage of the total no. of hearts for each group (Ctrl rats $n = 11$, CO rats $n = 13$, distribution was tested using nonparametric Mann-Whitney's test, Ctrl vs. CO rats: $P < 0.05$). MI, myocardial infarction. *E*: effects of CO exposure on mean arrhythmic score (data are presented as means ± SE, Ctrl rats $n = 11$, CO rats $n = 13$, one-way ANOVA, $^*P < 0.05$, Ctrl vs. CO rats).

significant difference in the distribution of the arrhythmic scores observed in both experimental groups. According to the increased mean arrhythmic score observed in CO rats during reperfusion, the arrhythmia severity was higher in CO rats compared with Ctrl rats (Fig. 1*E*). Moreover, sustained VF were triggered more frequently in the CO rats compared with Ctrl rats (54 vs. 9%, $P < 0.05$ nonparametric Yates' chi square test).

Effects of CO Exposure on Postischemic Recovery of Myocardial Function

Any difference regarding cardiac function was reported between CO and Ctrl rats before ischemia (Table 1). Postischemic recovery of LV developed pressure and contractility, assessed during reperfusion, was significantly lower in CO rats compared with Ctrl (Fig. 2). Indeed, the postischemic recovery of LV developed pressure, $+dP/dt_{max}$, and $-dP/dt_{max}$ were significantly altered in the CO rats compared with Ctrl rats (Fig. 2, *A–C*).

These functional results were paired with some deleterious effects of CO exposure on postischemic myocardial coronary blood flow recovery (Fig. 2*D*). Indeed, although no difference in coronary blood flow was reported between CO and Ctrl rats before ischemia (Ctrl rats: 11.5 ± 0.9 ml/min vs. CO rats: 11.8 ± 1.4 ml/min), coronary blood flow was significantly lower in CO rats compared with Ctrl rats during reperfusion.

Effects of CO Exposure on Myocardial Postischemic Reperfusion-Induced Cellular Death

The deleterious effects of CO exposure on I/R-induced injury were characterized by an increase in myocardial infarct

Downloaded from ajpheart.physiology.org on July 8, 2010

Table 1. *Myocardial function during regional ischemia-reperfusion protocol in Ctrl and CO rats*

	LVDP, mmHg	$+dP/dt_{max}$, mmHg/s	$-dP/dt_{max}$, mmHg/s
Baseline			
Ctrl rats	91.79 ± 7.47	3,365 ± 304	−1,944 ± 123
CO rats	93.85 ± 12.11	2,932 ± 369	−1,994 ± 219
30 min of Ischemia			
Ctrl rats	65.50 ± 4.82	2,304 ± 487	−1,447 ± 199
CO rats	53.29 ± 5.66	1,757 ± 240	−1,111 ± 162
5 min of Reperfusion			
Ctrl rats	61.28 ± 3.05	2,169 ± 318	−1,255 ± 103
CO rats	41.86 ± 3.61*	1,372 ± 276*	−902 ± 131*
30 min of Reperfusion			
Ctrl rats	63.31 ± 5.15	2,376 ± 331	−1,344 ± 114
CO rats	43.71 ± 5.66*	1,541 ± 364*	−887 ± 216*
60 min of Reperfusion			
Ctrl rats	50.99 ± 1.85	1,996 ± 320	−1,063 ± 81
CO rats	36.10 ± 6.62*	1,332 ± 365	−761 ± 115*
90 min of Reperfusion			
Ctrl rats	43.54 ± 1.33	1,747 ± 376	−920 ± 120
CO rats	31.78 ± 9.76	1,203 ± 331	−703 ± 121
120 min of Reperfusion			
Ctrl rats	39.85 ± 2.52	1,609 ± 258	−832 ± 110
CO rats	24.52 ± 5.91*	1,028 ± 237*	−570 ± 169*

Values are means ± SE; LVDP, left ventricular developed pressure; $+dP/dt_{max}$, maximal derivative of left ventricular pressure; $-dP/dt_{min}$, minimal derivative of left ventricular pressure; Ctrl rats, rats exposed to filtered standard air; CO rats, rats exposed to carbon monoxide. *$P < 0.05$ vs. Ctrl rats.

size in CO rats compared with Ctrl rats (Fig. 3, *A* and *B*). Indeed, no difference regarding the risk zone (ischemic zone) was observed between CO and Ctrl rats after 120 min of reperfusion. However, the infarct size was markedly increased in CO rats (60 ± 5 vs. 33 ± 2% of the risk zone; $P < 0.05$). LDH released in coronary effluents, used as an index of cell death, was significantly augmented at the onset of reperfusion in both Ctrl and CO rats (1.91 ± 0.30 to 5.84 ± 1.45 U/min for Ctrl rats; 2.69 ± 0.54 to 14.26 ± 3.20 U/min for CO rats; $P < 0.05$). Moreover, the peak of LDH release at the onset of reperfusion was significantly higher in CO rats than in Ctrl rats. Finally, LDH release remained significantly higher in CO rats after 30 and 60 min of reperfusion. No difference regarding LDH release was observed during the stabilization period (Fig. 3*C*). LV TBARS concentration was significantly increased in CO compared with Ctrl rats after 30 min of reperfusion (6.43 ± 0.76 vs. 4.40 ± 0.35 nmol/g; Fig. 3*D*).

Effects of CO Exposure on Cardiomyocyte Excitation-Contraction Coupling Before and After A/R

At the cellular level, prolonged CO exposure induced impairments of ventricular myocyte function (Fig. 4). Indeed, before A/R, SL shortening (Fig. 4, *A* and *B*) as well as Ca^{2+} transient (Fig. 4, *C* and *D*) were significantly impaired in CO rats compared with Ctrl rats. In addition, diastolic cytosolic Ca^{2+} was markedly higher in CO compared with Ctrl rats (Fig. 4*E*). Consecutively to A/R, SL shortening was decreased in both groups (Fig. 4, *A* and *B*) and remained significantly lower in CO compared with Ctrl rats. This decreased SL shortening was associated with a decreased Ca^{2+} transient in both groups consecutive to A/R. It is of note that Ca^{2+} transient from CO rats remained lower than Ca^{2+} transient from Ctrl rats (Fig. 4, *C* and *D*). Following A/R, diastolic Ca^{2+} increased in the two experimental groups; however, for this parameter, statistical significance was reported only in Ctrl rats. Consequently,

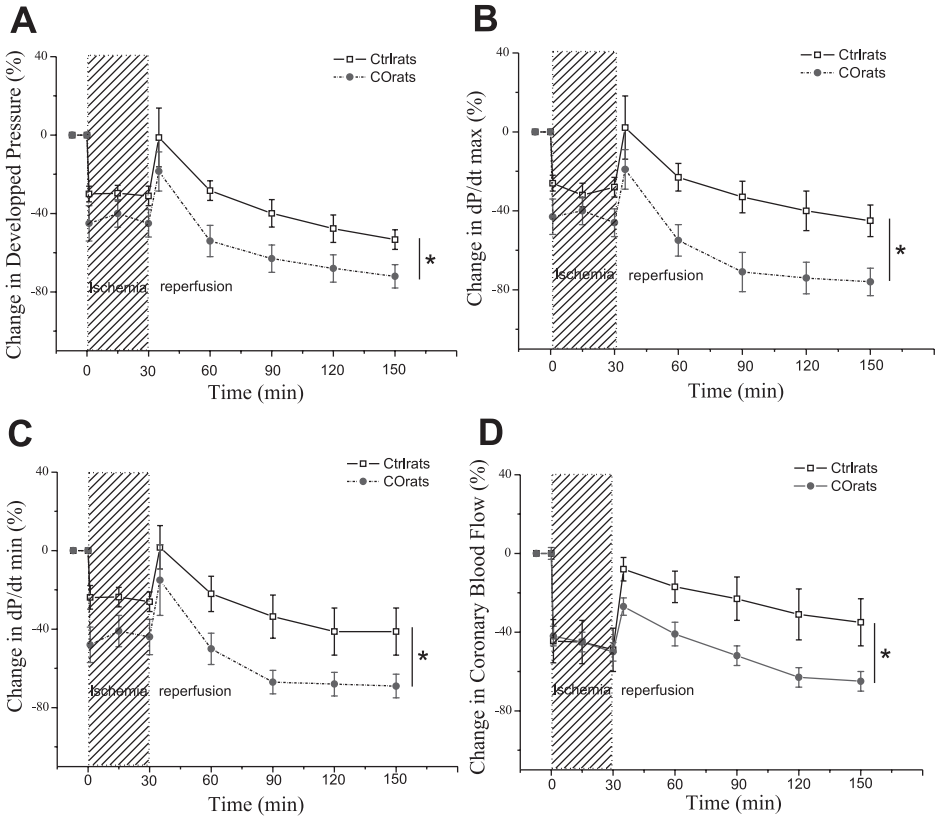

Fig. 2. Effects of CO exposure on the time course of changes in left ventricular function parameters during a 30-min ischemia and 120 min of reperfusion. Change in left ventricle developed pressure (*A*), maximal ($+dP/dt_{max}$, *B*), and minimal ($-dP/dt_{max}$, *C*) derivative of left ventricular pressure over time, and coronary blood flow (*D*). Data are presented as mean fraction of baseline ± SE ($n = 6$ rats/group, repeated-measures ANOVA, *$P < 0.05$, Ctrl vs. CO rats).

Downloaded from ajpheart.physiology.org on July 8, 2010

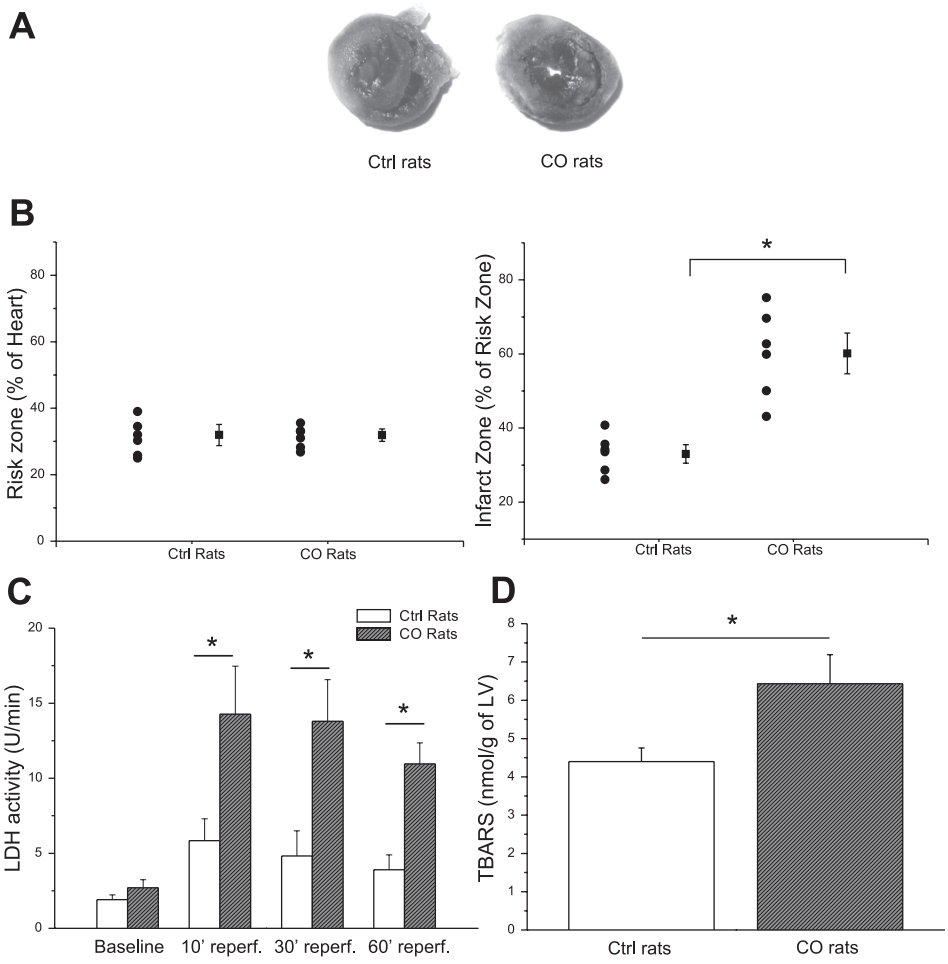

Fig. 3. Effects of CO exposure on I/R-induced cellular death. *A*: representative sections of rat hearts stained with triphenyltetrazolium chloride (TTC) after a regional ischemia of 30 and 120 min reperfusion from the isolated heart experiments in Ctrl and CO rats. *B*: risk zone expressed as a percentage of heart area (*left*) and infarct zone expressed as a percentage of risk zone (*right*). Data are presented as means ± SE ($n = 6$/group, one-way ANOVA, $^*P < 0.05$, Ctrl vs. CO rats). *C*: lactate dehydrogenase (LDH) release in coronary effluents during stabilization and reperfusion, and used as a marker of cell death. *D*: thiobarbituric acid-reactive substances (TBARS) concentration in left ventricular (LV) tissues after 30 min of postischemic reperfusion, and used as a marker of lipid peroxidation. Data are presented as means ± SE ($n = 6$ rats/group, repeated-measures ANOVA, $^*P < 0.05$, Ctrl vs. CO rats).

following A/R, no difference was observed concerning intracellular diastolic Ca^{2+} between Ctrl and CO rats (Fig. 4*E*).

Following A/R, the incubation of NAC (a nonspecific antioxidant) reduced the impairment of cardiac cell contraction in both Ctrl and CO rats. In addition, NAC infusion partly blunted the higher sensitivity of CO rat cardiomyocytes to A/R, since in this condition no difference was reported between Ctrl and CO groups regarding SL shortening (Fig. 5*A*). As far as the alterations of Ca^{2+} handling are concerned, the incubation of NAC improved Ca^{2+} transient in both Ctrl and CO rats. However, the difference between the two experimental populations was still reported (Fig. 5*B*). Finally, diastolic cytosolic Ca^{2+} was significantly reduced in CO rat cardiomyocytes in the presence of NAC compared with the corresponding controls (Fig. 5*C*). In the presence of NAC, no difference was reported regarding this variable between Ctrl and CO rats.

Effects of CO Exposure on Myocardial Antioxidant Enzyme Activity

In CO rats, following 4 wk of exposure to simulated urban CO pollution, cardiac SOD and GPx activities were significantly lower compared with Ctrl rats (Fig. 6, *A* and *B*). No significant change in catalase activity was observed in this model of CO exposure (Fig. 6*C*).

DISCUSSION

To the best of our knowledge, our study is the first to investigate the effects of prolonged exposure to simulated urban environmental CO pollution on myocardial sensitivity to I/R. The major result is that prolonged exposure to simulated urban CO pollution worsens myocardial I/R injuries, promoting a major increase in the severity of arrhythmic events, an impairment of myocardial function observed at both global and cellular levels, and an increase in the infarct size. These phenomena could be mainly related to hidden effects of CO exposure on myocardial phenotype, including *1*) an impairment of cellular Ca^{2+} handling and *2*) an altered antioxidant status of the myocardium.

CO Exposure and Myocardial I/R

Eventhough CO urban pollution has been associated with increased cardiovascular disease and cardiac mortality (9, 13, 29), we demonstrate here that chronic CO exposure renders the heart more vulnerable to I/R. Previous experimental studies have only documented the effect of acute CO exposure or to CO-releasing molecules used as preconditioning strategies to protect the myocardium against I/R injury (3, 6, 19). It was also reported that endogenous CO production could protect the heart from I/R injuries. These beneficial effects of endogenous

Downloaded from ajpheart.physiology.org on July 8, 2010

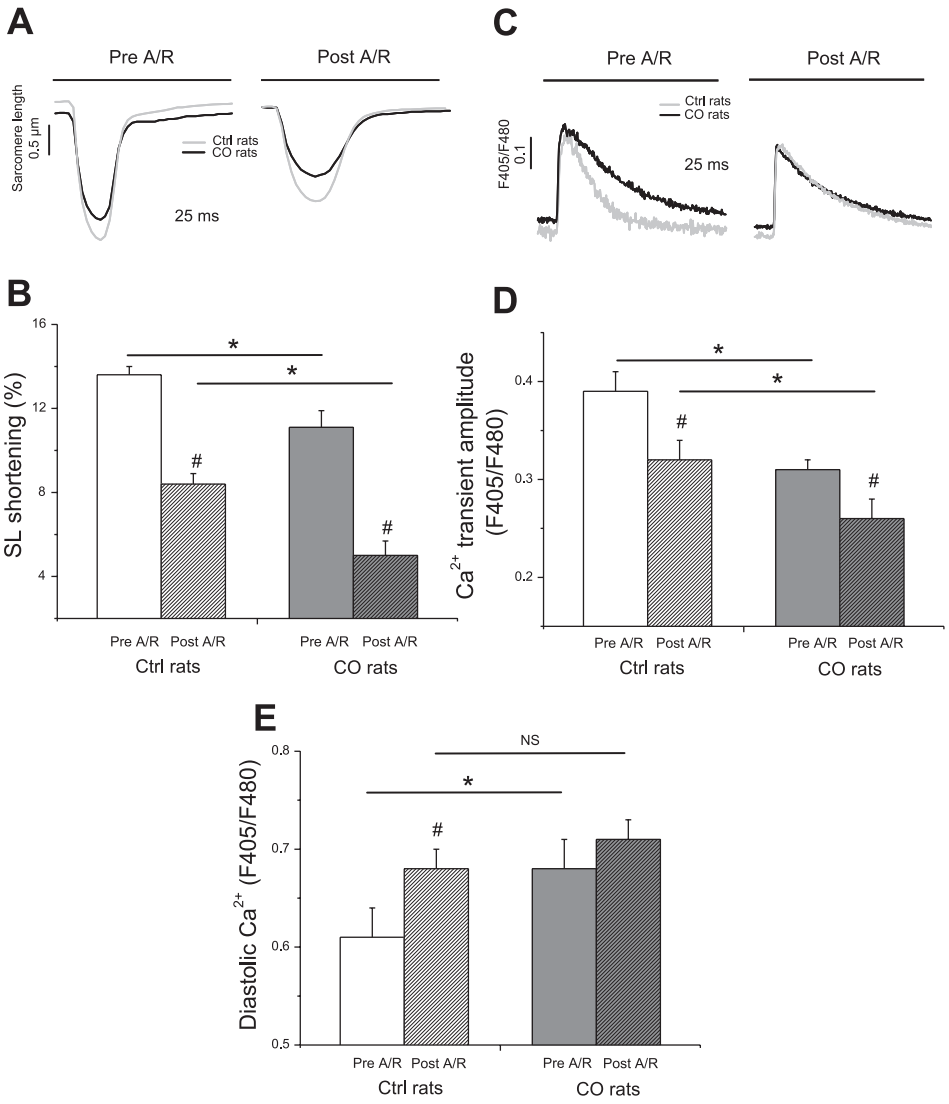

Fig. 4. Effects of CO exposure on cardiomyocyte excitation-contraction before and after cellular anoxia-reoxygenation (A/R). *A*: representative contraction of intact myocytes. *B*: contraction of intact myocytes, measured by sarcomere length (SL) shortening. SL shortening is presented as a mean of the percentage of shortening ± SE [$n = 4$ rats/group, 2-way ANOVA; $P < 0.05$, pre-A/R vs. post-A/R (#) and Ctrl vs. CO rats (*)]. *C*: representative superimposed Ca^{2+} transients in intact myocytes. Ca^{2+} transients (*D*) and diastolic Ca^{2+} (*E*) in intact myocytes. Ca^{2+} transients and diastolic Ca^{2+} are presented as means ± SE [$n = 4$ rats/group, 2-way ANOVA; $P < 0.05$, pre-A/R vs. post-A/R (#) and Ctrl vs. CO rats (*)]. NS, not significant.

CO production during I/R could be because of a decrease in oxidative stress (26), an enhanced Ca^{2+} handling (36), and CO anti-inflammatory and anti-apoptotic properties (20), which may ultimately lead to a decrease in I/R-induced VF (4, 5). In our model, no difference regarding cardiac function and coronary blood flow was evidenced between Ctrl and CO rats before I/R. Remarkably, only postischemic reperfusion allowed us to distinguish the hearts of CO-exposed rats from those of Ctrl rats, thereby pointing out the deleterious effect of CO. These results are in line with our previous study (2), which exhibited no difference of cardiac function in the basal condition but highlighted functional impairments in CO rats in stressful conditions (i.e., β-adrenergic stimulation). Therefore, discrepancies between our results and studies reporting the protective role of CO exposure could be explained by differences in the duration and severity of CO exposure (3, 6, 19). In our model, CO rats experimented a chronic (4 wk with 12 h daily exposure) CO exposure mimicking urban concentrations (30–100 ppm). In addition, it has to be noted that, in our model, to avoid the acute effects of CO on the myocardium, rats were housed for 24 h in standard filtered air before I/R study. Therefore, under our experimental conditions, no difference of carboxyhemoglobin was made obvious between Ctrl and CO rats at the time of the I/R procedure (carboxyhemoglobin 24 h after exposure, CO rats: 1.2 ± 0.4% vs. Ctrl rats 1.0 ± 0.5%; not significant).

Effects of CO Exposure on Postischemic Myocardial Injuries

The higher susceptibility of the myocardium to I/R in CO-exposed rats was notably characterized by higher propensity to arrhythmic events at the onset of reperfusion. Higher arrhythmic score and higher occurrence of sustained VF (54 vs. 9%) were evidenced. Arrhythmias, and more particularly sustained VF, are the most dangerous consequences of myocardial I/R, since they induce an impairment of blood circulation and ultimately lead to sudden cardiac death. Sheps et al. (31, 32) have already highlighted the proarrhythmic effect of CO exposure (1 day at 100 or 200 ppm) in patients with documented coronary artery diseases. However, as mentioned above, in our model, no difference of carboxyhemoglobin was reported between Ctrl and CO rats

Downloaded from ajpheart.physiology.org on July 8, 2010

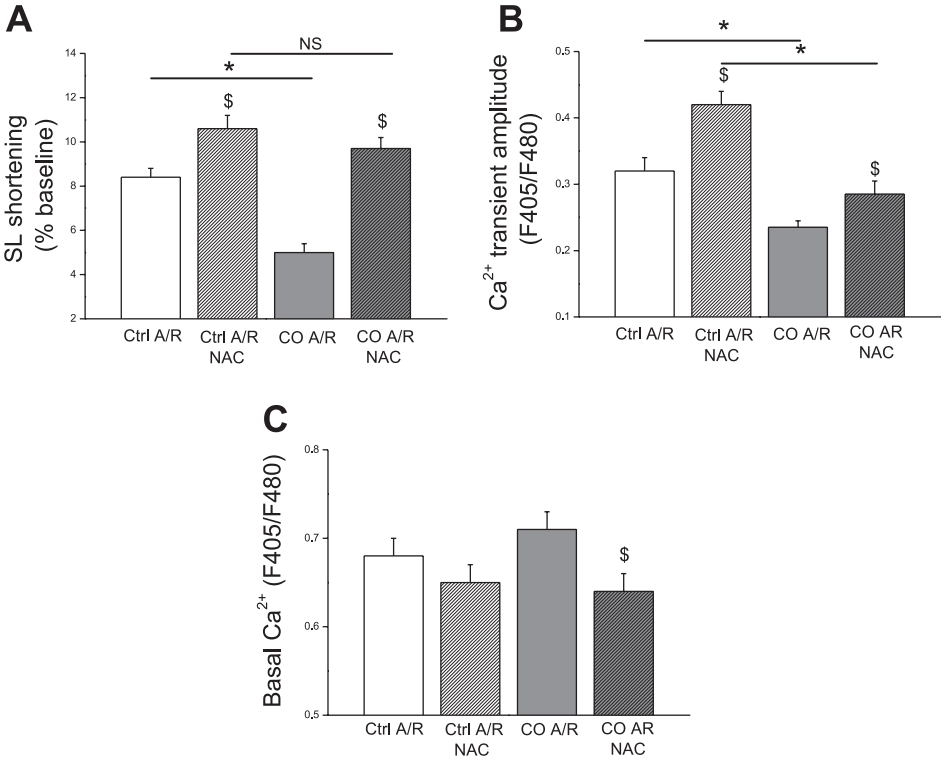

Fig. 5. Effects of *N*-acetylcystein (NAC) incubation on the sensitivity to A/R of cardiomyocytes from Ctrl and CO rats. *A*: contraction of intact myocytes, measured by SL shortening. SL shortening is presented as a mean of the percentage of shortening ± SE. *B* and *C*: Ca^{2+} transients (*B*) and (C) diastolic Ca^{2+} (*C*) in intact myocytes. Ca^{2+} transients and diastolic Ca^{2+} are presented as means ± SE [$n = 4$ rats/group, 2-way ANOVA; $P < 0.05$, with NAC vs. without NAC ($) and Ctrl vs. CO rats (*)].

at the time of the I/R procedure, avoiding then the acute effects of CO on the myocardium. In CO rats, the higher sensitivity of the myocardium was also characterized by an impairment of postischemic recovery of myocardial function. This could be related to the significantly impaired cellular contractile function observed, consecutive to A/R, on isolated cardiomyocytes of CO rats compared with Ctrl rats. This result suggests that cardiomyocyte damages lead to a reduced postischemic recovery of cardiac function. It seems, however, that the main factor involved in the explanation of this result was that CO pollution is associated, in our model, with a marked increase of I/R-induced cardiac cell death. I/R injuries, including cardiomyocyte impairments as well as arrhythmic events, were mainly explained, in past literature, by increased oxidative stress and Ca^{2+}-handling alteration (25, 41).

Implication of Ca^{2+} and Oxidative Stress

The increased sensitivity to I/R of the myocardium after CO exposure was characterized by the increase of arrhythmic events, increased functional disturbances, and cell death. The cellular mechanisms underlying theses aspects of the reperfusion syndrome may involve impairments of Ca^{2+} handling or overproduction of oxygen-derived free radicals. In a recent study, we have shown that CO pollution by itself initiates a pathological phenotype of the cardiomyocytes involving a profound remodeling of the excitation-contraction coupling through Ca^{2+}-handling alteration (2), which was confirmed in the present work. This remodeling was characterized by an impairment of cardiomyocyte shortening that was not observed at the whole heart level. This phenomenon, which has already been reported by our team, may involve compensatory mechanisms (2) that remain to be investigated. The cardiomyocytes also exhibit an increase in diastolic Ca^{2+} resulting from an altered Ca^{2+} reuptake in the sarcoplasmic reticulum (SR) due to a decreased sarco-(endo)plasmic reticulum Ca^{2+}-ATPase (SERCA) 2a expression and also potentially from a Ca^{2+} leak from the SR through the ryanodine receptors (2). Alterations of Ca^{2+} handling may be involved in cardiomyocyte dysfunction and ultimately in cell death during I/R (1, 33, 38). It is therefore very likely that these alterations, associated with CO exposure, increase the severity of cardiomyocytes and whole heart injuries related to I/R. Indeed, in our study, at the whole heart level, CO exposure increases cardiomyocyte death after I/R. Considering only viable myocytes, we report here that SL shortening and Ca^{2+} handling are altered by A/R to the same extent in both Ctrl and CO rats, resulting therefore in more pronounced dysfunctions in CO rats compared with Ctrl rats. Therefore, it seems that Ca^{2+} handling in viable cardiomyocytes was not more impaired by A/R in CO rats, but that the lower amplitude of Ca^{2+} transient reported in this population following A/R was the result of prolonged CO exposure-induced phenotypical changes. Consequently, a major finding of the present study was that the impaired Ca^{2+} handling observed before to A/R is a key factor in the development of functional impairments and arrhythmic events observed at the onset of reperfusion in CO rats and is therefore a candidate to explain higher sensitivity of CO rat myocardium to I/R.

The essential role of oxidative stress in the pathogenesis of myocardial I/R injury has been largely reported (16, 30, 41). Indeed, exacerbated oxidative stress during I/R is a key factor in the worsening of postischemic arrhythmias, cardiac dysfunction, and irreversible cardiomyocyte damages (16, 17, 25, 41). Oxidative stress is defined as an imbalance between the pro-

Downloaded from ajpheart.physiology.org on July 8, 2010

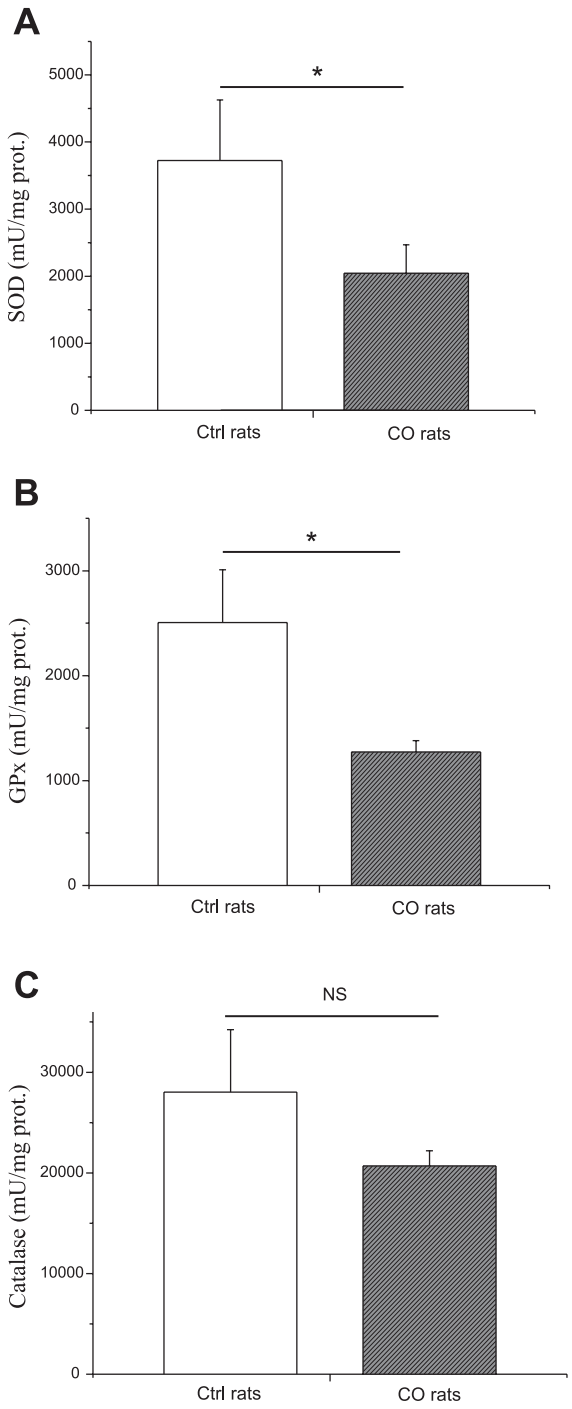

Fig. 6. Effects of CO exposure on superoxide dismutase (SOD, *A*), glutathione peroxidase (GPx, *B*), and catalase (*C*) activities expressed in mU/mg protein. Data are presented as means ± SE ($n = 6$ rats/group, 1-way ANOVA, $*P < 0.05$, Ctrl vs. CO rats).

duction of reactive oxygen species and biological antioxidant systems that are involved in the detoxification of reactive intermediates. An important result of our study is the impaired enzymatic antioxidant status of the myocardium, including a major decreased activity of SOD (−45%), GPx (−49%), and catalase (−26%, not statistically significant). We previously discussed the potential role of altered redox status of the myocardium to explain the effects of prolonged exposure to CO on excitation-contraction coupling (2). Indeed, since proteins involved in Ca^{2+} handling are potential targets for redox alterations, decrease of antioxidant defenses associated with the increased activity of thioredoxin reductase observed in our previous study (2) confirmed a CO-induced oxidative stress. Therefore, those alterations of enzymatic antioxidant defense could play a major role in phenotypical changes of CO-exposed rat myocardium, mainly affecting Ca^{2+} homeostasy. Besides, SOD prevents changes in myocardial function, and Ca^{2+} homeostasis in isolated hearts subjected to I/R (27), catalase, and GPx plays a major role in protecting the myocardium from I/R injury (16). We have observed an increase in TBARS production, used as a marker of lipid peroxidation, and therefore oxidative stress, in CO-exposed rats following I/R. Therefore, we can postulate that the lower enzymatic antioxidant defense that was observed consecutively to CO exposure could contribute to the increased sensitivity of the myocardium to I/R damages. To prevent oxidative stress-induced alterations, an acute antioxidant strategy, using a nonspecific antioxidant (NAC), was performed during cellular A/R. This acute antioxidant strategy was found able to prevent the deleterious effects of CO exposure on SL shortening during A/R. This result highlights the implication of an increased cardiac oxidative stress in our model of CO-exposed rats. However, the deleterious effects of CO exposure on Ca^{2+} transient were not prevented by this acute antioxidant strategy. This observation is not surprising, since prolonged exposure to CO pollution results in phenotypical remodeling of Ca^{2+}-handling proteins, such as decreased SERCA2a expression (2). This profound remodeling of the Ca^{2+}-handling phenotype, which was reported in CO rat myocardium, could not be reversed by such an acute antioxidant strategy. Therefore, chronic antioxidant therapy, notably by preventing myocardial phenotypical changes, could be a promising strategy for protecting the heart against the deleterious effects of chronic CO exposure on myocardial sensitivity to I/R.

In conclusion, this study shows that chronic exposure to CO consistent with air pollution from the urban type significantly increases the effects of a myocardial infarction in rats and could be considered as a major health risk. Indeed, the World Health Organization estimates that air pollution is responsible for 800,000 premature deaths worldwide each year, and, particularly, exposure to air pollution increases the risk of mortality from cardiovascular disease by 76% (23). Among the numerous pollutants, CO has been described as one of the main pollutants responsible for the development of cardiovascular diseases (9, 35). Prolonged CO exposure worsens I/R-linked cardiac injuries and therefore provides an experimental rationale to explain the increased risk of cardiac mortality observed in exposed populations. In summary, prolonged CO exposure-induced cardiac phenotypical changes, such as an imbalance in the cardiomyocyte oxidant status and an impairment of Ca^{2+} handling, are likely to predispose the heart to I/R injuries.

GRANTS

This work was funded by a French National Research Agency grant (COMYOCARD).

DISCLOSURES

No competing financial interests exist.

Downloaded from ajpheart.physiology.org on July 8, 2010

REFERENCES

1. **Abdallah Y, Gkatzoflia A, Gligorievski D, Kasseckert S, Euler G, Schluter KD, Schafer M, Piper HM, Schafer C.** Insulin protects cardiomyocytes against reoxygenation-induced hypercontracture by a survival pathway targeting SR Ca2+ storage. *Cardiovasc Res* 70: 346–353, 2006.
2. **Andre L, Boissiere J, Reboul C, Perrier P, Zalvidea S, Thireau J, Meyer G, Bideaux P, Obert P, Cazorla O, Richard S.** Carbon monoxide pollution promotes cardiac remodeling and ventricular arrythmia in healthy rats. *Am J Respir Crit Care Med* In press.
3. **Bagul A, Hosgood SA, Kaushik M, Nicholson ML.** Carbon monoxide protects against ischemia-reperfusion injury in an experimental model of controlled nonheartbeating donor kidney. *Transplantation* 85: 576–581, 2008.
4. **Bak I, Papp G, Turoczi T, Varga E, Szendrei L, Vecsernyes M, Joo F, Tosaki A.** The role of heme oxygenase-related carbon monoxide and ventricular fibrillation in ischemic/reperfused hearts. *Free Radic Biol Med* 33: 639–648, 2002.
5. **Bak I, Szendrei L, Turoczi T, Papp G, Joo F, Das DK, de Leiris J, Der P, Juhasz B, Varga E, Bacskay I, Balla J, Kovacs P, Tosaki A.** Heme oxygenase-1-related carbon monoxide production and ventricular fibrillation in isolated ischemic/reperfused mouse myocardium. *FASEB J* 17: 2133–2135, 2003.
6. **Bak I, Varadi J, Nagy N, Vecsernyes M, Tosaki A.** The role of exogenous carbon monoxide in the recovery of post-ischemic cardiac function in buffer perfused isolated rat hearts. *Cell Mol Biol (Noisy-le-grand)* 51: 453–459, 2005.
7. **Barnett AG, Williams GM, Schwartz J, Best TL, Neller AH, Petroeschevsky AL, Simpson RW.** The effects of air pollution on hospitalizations for cardiovascular disease in elderly people in Australian and New Zealand cities. *Environ Health Perspect* 114: 1018–1023, 2006.
8. **Beers RF Jr, Sizer IW.** A spectrophotometric method for measuring the breakdown of hydrogen peroxide by catalase. *J Biol Chem* 195: 133–140, 1952.
9. **Bell ML, Peng RD, Dominici F, Samet JM.** Emergency Hospital Admissions for Cardiovascular Diseases and Ambient Levels of Carbon Monoxide. Results for 126 United States Urban Counties, 1999–2005. *Circulation* 120: 949–955, 2009.
10. **Bevan MA, Proctor CJ, Baker-Rogers J, Warren ND.** Exposure to carbon monoxide, respirable syspended particulates, and volatile organic compounds while commuting by bicycle. *Environ Sci Technol* 25: 788–779, 1991.
11. **Bhatnagar A.** Environmental cardiology: studying mechanistic links between pollution and heart disease. *Circ Res* 99: 692–705, 2006.
12. **Brook RD, Franklin B, Cascio W, Hong Y, Howard G, Lipsett M, Luepker R, Mittleman M, Samet J, Smith SC Jr, Tager I.** Air pollution and cardiovascular disease: a statement for healthcare professionals from the Expert Panel on Population and Prevention Science of the American Heart Association. *Circulation* 109: 2655–2671, 2004.
13. **Burnett RT, Cakmak S, Brook JR, Krewski D.** The role of particulate size and chemistry in the association between summertime ambient air pollution and hospitalization for cardiorespiratory diseases. *Environ Health Perspect* 105: 614–620, 1997.
14. **Bye A, Sorhaug S, Ceci M, Hoydal MA, Stolen T, Heinrich G, Tjonna AE, Najjar SM, Nilsen OG, Catalucci D, Grimaldi S, Contu R, Steinshamn S, Condorelli G, Smith GL, Ellingsen O, Waldum H, Wisloff U.** Carbon monoxide levels experienced by heavy smokers impair aerobic capacity and cardiac contractility and induce pathological hypertrophy. *Inhal Toxicol* 20: 635–646, 2008.
15. **Chen TM, Shofer S, Gokhale J, Kuschner WG.** Outdoor air pollution: overview and historical perspective. *Am J Med Sci* 333: 230–234, 2007.
16. **Dhalla NS, Temsah RM, Netticadan T.** Role of oxidative stress in cardiovascular diseases. *J Hypertens* 18: 655–673, 2000.
17. **Dumitrescu C, Biondi R, Xia Y, Cardounel AJ, Druhan LJ, Ambrosio G, Zweier JL.** Myocardial ischemia results in tetrahydrobiopterin (BH4) oxidation with impaired endothelial function ameliorated by BH4. *Proc Natl Acad Sci USA* 104: 15081–15086, 2007.
18. **Flohe L, Gunzler WA.** Assays of glutathione peroxidase. *Methods Enzymol* 105: 114–121, 1984.
19. **Fujimoto H, Ohno M, Ayabe S, Kobayashi H, Ishizaka N, Kimura H, Yoshida K, Nagai R.** Carbon monoxide protects against cardiac ischemia–reperfusion injury in vivo via MAPK and Akt–eNOS pathways. *Arterioscler Thromb Vasc Biol* 24: 1848–1853, 2004.
20. **Li Volti G, Rodella LF, Di Giacomo C, Rezzani R, Bianchi R, Borsani E, Gazzolo D, Motterlini R.** Role of carbon monoxide and biliverdin in renal ischemia/reperfusion injury. *Nephron Exp Nephrol* 104: e135–e139, 2006.
21. **Lowry OH, Rosebrough NJ, Farr AL, Randall RJ.** Protein measurement with the Folin phenol reagent. *J Biol Chem* 193: 265–275, 1951.
22. **Marklund S.** Spectrophotometric study of spontaneous disproportionation of superoxide anion radical and sensitive direct assay for superoxide dismutase. *J Biol Chem* 251: 7504–7507, 1976.
23. **Miller KA, Siscovick DS, Sheppard L, Shepherd K, Sullivan JH, Anderson GL, Kaufman JD.** Long-term exposure to air pollution and incidence of cardiovascular events in women. *N Engl J Med* 356: 447–458, 2007.
24. **Mou YA, Reboul C, Andre L, Lacampagne A, Cazorla O.** Late exercise training improves non-uniformity of transmural myocardial function in rats with ischaemic heart failure. *Cardiovasc Res* 81: 555–564, 2009.
25. **Murphy E, Steenbergen C.** Mechanisms underlying acute protection from cardiac ischemia-reperfusion injury. *Physiol Rev* 88: 581–609, 2008.
26. **Nakao A, Neto JS, Kanno S, Stolz DB, Kimizuka K, Liu F, Bach FH, Billiar TR, Choi AM, Otterbein LE, Murase N.** Protection against ischemia/reperfusion injury in cardiac and renal transplantation with carbon monoxide, biliverdin and both. *Am J Transplant* 5: 282–291, 2005.
27. **Netticadan T, Temsah R, Osada M, Dhalla NS.** Status of Ca^{2+}/calmodulin protein kinase phosphorylation of cardiac SR proteins in ischemia-reperfusion. *Am J Physiol Cell Physiol* 277: C384–C391, 1999.
28. **Ruiz-Meana M, Garcia-Dorado D.** Translational cardiovascular medicine (II) Pathophysiology of ischemia-reperfusion injury: new therapeutic options for acute myocardial infarction. *Rev Esp Cardiol* 62: 199–209, 2009.
29. **Samoli E, Touloumi G, Schwartz J, Anderson HR, Schindler C, Forsberg B, Vigotti MA, Vonk J, Kosnik M, Skorkovsky J, Katsouyanni K.** Short-term effects of carbon monoxide on mortality: an analysis within the APHEA project. *Environ Health Perspect* 115: 1578–1583, 2007.
30. **Schulz R, Kelm M, Heusch G.** Nitric oxide in myocardial ischemia/reperfusion injury. *Cardiovasc Res* 61: 402–413, 2004.
31. **Sheps DS, Herbst MC, Hinderliter AL, Adams KF, Ekelund LG, O'Neil JJ, Goldstein GM, Bromberg PA, Ballenger M, Davis SM.** Effects of 4 percent and 6 percent carboxyhemoglobin on arrhythmia production in patients with coronary artery disease. *Res Rep Health Eff Inst* 1–58, 1991.
32. **Sheps DS, Herbst MC, Hinderliter AL, Adams KF, Ekelund LG, O'Neil JJ, Goldstein GM, Bromberg PA, Dalton JL, Ballenger MN.** Production of arrhythmias by elevated carboxyhemoglobin in patients with coronary artery disease. *Ann Intern Med* 113: 343–351, 1990.
33. **Siegmund B, Schlack W, Ladilov YV, Balser C, Piper HM.** Halothane protects cardiomyocytes against reoxygenation-induced hypercontracture. *Circulation* 96: 4372–4379, 1997.
34. **Stern FB, Halperin WE, Hornung RW, Ringenburg VL, McCammon CS.** Heart disease mortality among bridge and tunnel officers exposed to carbon monoxide. *Am J Epidemiol* 128: 1276–1288, 1988.
35. **Stieb DM, Szyszkowicz M, Rowe BH, Leech JA.** Air pollution and emergency department visits for cardiac and respiratory conditions: a multi-city time-series analysis (Abstract). *Environ Health* 8: 25, 2009.
36. **Szabo ME, Gallyas E, Bak I, Rakotovao A, Boucher F, de Leiris J, Nagy N, Varga E, Tosaki A.** Heme oxygenase-1-related carbon monoxide and flavonoids in ischemic/reperfused rat retina. *Invest Ophthalmol Vis Sci* 45: 3727–3732, 2004.
37. **Tanguy S, Boucher F, Besse S, Ducros V, Favier A, de Leiris J.** Trace elements and cardioprotection: increasing endogenous glutathione peroxidase activity by oral selenium supplementation in rats limits reperfusion-induced arrhythmias. *J Trace Elem Med Biol* 12: 28–38, 1998.
38. **Venetucci LA, Trafford AW, O'Neill SC, Eisner DA.** The sarcoplasmic reticulum and arrhythmogenic calcium release. *Cardiovasc Res* 77: 285–292, 2008.
39. **Walker MJ, Curtis MJ, Hearse DJ, Campbell RW, Janse MJ, Yellon DM, Cobbe SM, Coker SJ, Harness JB, Harron DW.** The Lambeth Conventions: guidelines for the study of arrhythmias in ischaemia infarction, and reperfusion. *Cardiovasc Res* 22: 447–455, 1988.
40. **Wright GR, Jewczyk S, Onrot J, Tomlinson P, Shephard RJ.** Carbon monoxide in the urban atmosphere: hazards to the pedestrian and the street-worker. *Arch Environ Health* 30: 123–129, 1975.
41. **Zhao X, Chen YR, He G, Zhang A, Druhan LJ, Strauch AR, Zweier JL.** Endothelial nitric oxide synthase (NOS3) knockout decreases NOS2 induction, limiting hyperoxygenation and conferring protection in the postischemic heart. *Am J Physiol Heart Circ Physiol* 292: H1541–H1550, 2007.

Downloaded from ajpheart.physiology.org on July 8, 2010

3. Conclusion

Cette étude montre qu'une exposition chronique au CO aggrave les effets d'un infarctus du myocarde en augmentant les phénomènes arythmiques, altérant la fonction myocardique globale et cellulaire et en augmentant la taille de l'infarctus. L'altération du statut antioxydant du myocarde est responsable de l'exacerbation des troubles post infarctus chez la population exposée au CO. En effet, les perturbations de l'homéostasie redox observées suite à une exposition chronique de 4 semaines au CO sont potentialisées lors d'un accident cardiaque ischémique. Cette surcharge de ROS soudaine active alors de nombreuses voies de signalisation responsables d'altérations morpho-fonctionnelles cardiaques, notamment la stimulation des processi d'apoptose entrainant une plus grande nécrose myocardique. Cette étude apporte donc un rationnel expérimental pour expliquer le risque accru de mortalité cardiaque observé chez des populations exposées en environnement pollué.

III. Pollution au monoxyde de carbone et phénomènes arythmiques post-exercice : implication des ROS

1. Introduction

La légitimité clinique des évènements arythmiques en période post-exercice est maintenant bien établie. En effet les extrasystoles ventriculaires observées dans la phase de récupération d'un exercice physique prédisent fortement le risque de mort cardiovasculaire. La pollution atmosphérique peut déclencher la survenue d'évènements arythmiques et augmente le risque de mort subite. Parmi, les agents polluants, le CO est particulièrement corrélé à ces évènements cardiaques. Nous avons notamment montré dans l'étude 1 qu'une exposition chronique en milieu pollué au CO augmente les événements arythmiques chez une population saine ; ce phénomène arythmique étant notamment exacerbé lors d'un stress (stimulation beta adrénergique à la dobutamine). La pollution au CO est également à l'origine d'un stress oxydatif systémique. Or, les ROS, comme précédemment décrit dans l'étude 1, sont pro-arythmogènes.

L'objectif de cette étude a alors été de déterminer si une pollution au CO simulant une pollution urbaine pouvait générer un stress oxydatif qui influencerait les événements arythmiques post-exercice chez des populations saines. Cette étude a été conduite chez une population de patients sains pour lesquels l'exposition au CO était évaluée à travers la mesure

de l'HbCO. Une corrélation positive entre arythmies post-exercice, stress oxydatif et exposition au CO a alors été retrouvée. Afin de déterminer les mécanismes sous-jacents aux effets délétères d'une pollution au CO, un modèle animal bien standardisé et précédemment décrit dans l'étude 4 a été utilisé.

2. Article 6 – Soumis pour publication

Post-exercise arrhythmic events are enhanced by carbon monoxide exposure: involvement of reactive oxygen species

Lucas Andre[1], PhD ; Fares Gouzi[2], MD, PhD ; Jérome Thireau[1], PhD ; Jeremy Fauconnier[1], PhD; Gregory Meyer[3], PhD; Julien Boissiere[1,3], PhD; Martine Delage[4]; Aldja Abdellaoui[2], MS; Christine Feillet-Coudray[5], PhD; Gilles Fouret[5]; Jean-Paul Cristol[4], MD, PhD; Alain Lacampagne[1], PhD; Philippe Obert[3], PhD; Cyril Reboul[3], PhD; Maurice Hayot[2], MD, PhD; Sylvain Richard[1], PhD; Olivier Cazorla[1], PhD.

[1] INSERM U-637, F-34295 Montpellier, France. Université Montpellier1, Université Montpellier2, F-34295 Montpellier, France
[2] INSERM ERI25, F-34295 Montpellier, France. Université Montpellier1, F-34295 Montpellier, France
[3] EA-4278, Université Avignon et des Pays de Vaucluse, UFR Sciences, F-84000 Avignon, France
[4] Department of Biochemistry, Lapeyronie Hospital, F-34295 Montpellier, France
[5] INRA UMR 866, Différentiation Cellulaire et Croissance, 34060 Montpellier, France

Correspondence to :
Olivier CAZORLA
Inserm U637 Physiopathologie Cardiovasculaire
CHU Arnaud de Villeneuve
34295 Montpellier, France
Phone : +33 467 41 52 44
Fax : +33 467 41 52 42
olivier.cazorla@inserm.fr

Key words: Oxidative stress, ectopic Ca^{2+} transient, antioxidant, atmospheric pollution

Abstract

Rationale: Post-exercise ventricular ectopic beats are a key factor for predicting risk of death in human population. Atmospheric pollution, notably sustained carbon monoxide (CO) exposure, promotes oxidative stress, modifies arrhythmic phenotype and increases risk of sudden cardiac death. The present study aimed to determine whether and how the ambient CO exposure could influence the occurrence of ventricular arrhythmic events following exercise in healthy populations. **Methodology/results:** The number of arrhythmic events during the recovery phase of a maximal cycle ergometer exercise test was evaluated in healthy subjects using a standard 12-lead ECG. We found positive correlations between levels of carboxyhaemoglobin used as an index of ambient CO exposure, as well as isoprostane, an index of oxidative stress, and the number of post-exercise ventricular arrhythmic events. In order to determine the pathway involved in CO-mediated post exercise arrhythmias, we used an experimental model of rats exposed chronically (4 weeks) to sustained urban CO pollution. We measured reactive oxygen species production (MitoSox dye) and intracellular Ca^{2+} concentration (indo-1) after a high pacing sequence of field stimulated cardiomyocytes, as well as Ca^{2+} handling proteins by western blot. We found that chronic CO pollution was responsible for an increased ROS production, which activated PKA leading to ryanodine receptor phosphorylation and enhanced the occurrence of ectopic Ca^{2+} transients in cardiomyocytes. Acute treatment with a ROS scavenger (N-acetylcystein, 20 mmol/L, 1 hour) prevented this sequence of alterations and the number of arrhythmic cells. **Conclusion:** Chronic CO pollution promotes oxidative stress, which alters Ca^{2+} homeostasis and thereby mediates the triggering of ventricular arrhythmias.

1. Introduction

The clinical importance of arrhythmic phenotype following exercise stress is well recognized since ventricular ectopic beats during recovery have been reported to represent an important factor for predicting risk of death in healthy population [1]. Air pollution has been involved in the development of arrhythmic events, triggering of heart attacks and risk of cardiovascular death [2]. Indeed, epidemiological studies have associated air pollution with decreased heart rate variability, increased propensity toward arrhythmic events [3] and sudden cardiac death [4-6]. Among the various agents that constitute the mix of atmospheric pollution, carbon monoxide (CO) is an ubiquitous pollutant found in many common sources (secondhand smoke, vehicular exhaust, industrial emissions…), which is closely associated with hospital admissions for cardiovascular disease [7] and cardiac mortality [8]. We have recently shown that healthy animals exposed chronically to CO levels mimicking pollution in urban areas had increased premature ventricular beats due to a heart failure-like Ca^{2+} homeostasis remodeling in the ventricular myocytes [9]. However, whether atmospheric pollution, notably CO exposure, could influence occurring of post-exercise arrhythmic events has never been questioned yet.
We thus aimed to determine in the present study whether CO exposure could influence the post-exercise arrhythmic phenotype in healthy population. We observed a positive relationship between the level of CO exposure assessed by carboxyhaemoglobin (HbCO) measurement and the number of arrhythmic events evaluated after an incremental exercise test in healthy human subjects. We then investigated the signaling pathway associating CO exposure and post-exercise arrhythmic phenotype in a cellular rat model. Results showed that rats submitted to adrenergic stress had increased arrhythmias and risk of sudden death. On the other hand, chronic CO exposure induced a reactive oxygen species (ROS) production that activates PKA which in turn altered Ca^{2+} homeostasis resulting in an arrhythmic phenotype.

2. Materials and Methods

Analysis of electrocardiogram from patients during effort test
Healthy subjects were recruited on the basis of the following criteria: aged from 50 to 75 years old (average age = 62.4±1.3, 15 males, 7 females), non-smokers, no medical disease and spending less than 150 minutes of moderate-to-vigorous physical activity per week. These exclusion criteria allowed us to evaluate a homogeneous population, independently of factors modifying cardiac function and occurrence of arrhythmic events. All subjects had a complete clinical examination. Subjects with cardiologic treatment or suspicion of cardiac disease were excluded from the study. All participants performed a physician-supervised incremental exercise test until exhaustion on an electrically-braked cycle ergometer (Ergoselect 200P, Ergolyne, Bitz, Germany) [10]. During the exercise test, electrocardiogram (ECG) was recorded using standard 12-lead derivations, at rest, during exercise, and 5 minutes during recovery. Ectopic ventricular beats including

isolated, sequential or repetitive extra-systole, and ventricular tachycardia during recovery were then reviewed by two physicians blindly.

Human carboxyhaemoglobin and isoprostane blood levels

To estimate the degree of CO exposure in human subjects, we measured the concentration of carboxyhemoglobin (HbCO). HbCO is considered as a specific and sensitive biomarker of CO exposure and has been correlated with air pollution [11]. HbCO levels were measured in healthy subjects prior to exercise testing (COoxymeter IL682, Instrumentation Laboratory) in the Pharmacology and toxicology laboratory (Lapeyronie Hospital, Montpellier, France).

Arterial and venous blood was sampled in standard, sterile, heparinized, ethylenediaminetetraacetic acid-containing, and clot-activator tubes. Immediately after sampling, serum and plasma were removed by centrifugation (2500 rpm for 10 minutes at 4°C), put into 500 µl aliquots, and stored at -80°C until analysis. Plasma free and esterified isoprostanes (F_2-IsoP) were evaluated as markers of lipid peroxidation as previously described [12]. Lipids were first extracted from samples (1 ml of plasma containing [$^2H_4$]-15-F_{2t}-IsoP as internal standard) with Folch solution (chloroform/methanol 2:1; v/v) and then subjected to alkaline hydrolysis. The pH of the extract was adjusted to 2.2 with HCl and diluted in water to 10 ml. Samples were then treated with two extraction procedures using successively an inverse-phase and an aminopropyl-phase cartridge (Sep-Pak Vac RC C_{18} and Vac RC NH_2, Waters S.A., Guyancourt, France). After the last step of purification, samples were derivatized as pentafluorobenzylester and trimethylsilyl ethers. The derivatized samples were analyzed by gas chromatography-negative ion chemical ionization mass spectrometry. Quantification was achieved by relating the peak area of the F_2-IsoP to the internal standard.

Animal model for chronic CO exposure

In urban areas, ambient CO usually varies between 2 and 40 ppm, but under certain circumstances, such as during heavy traffic, its concentration may reach levels as high as 150-200 ppm [13 14]. In our study, male Wistar rats (13 week old, n=35) were exposed to CO in an airtight exposure container over 4 weeks as previously described [9]. Rats were exposed to a basal CO concentration of 30 ppm during a 12 hour period completed with 5 peaks of 100 ppm (1 hour each), to reproduce air quality variations environmentally relevant. For the remaining 12 hours, the CO group of rats was exposed to filtered air (< 1 ppm CO). The CO content was continuously monitored with an infrared aspirative CO analyzer (CHEMGARD, NEMA 4 Version, MSA). Rats exposed to CO pollution were compared with rats exposed to filtered ambient air (CO <1 ppm; control, n=25). Experiments were performed 24 hours after the last CO exposure to avoid acute effects of CO.

Surface ECG recordings (Dataquest, Data Sciences International, Transoma Medical, Arden Hills, Minnesota, USA) were performed after the CO-exposure protocol as previously [9]. Spontaneous rhythmic disorders were calculated from ECGs during the recovery of a β-adrenergic challenge with isoprenaline injection (1 $mg.kg^{-1}$).Ectopic ventricular beats including isolated, sequential or repetitive extra-systole, and ventricular tachycardia were counted over a period of 20 min starting at a heart rate 15% below the maximal iso-induced heart rate to avoid the rhythmic storm. The average heart rate was similar during the sequence of analysis between sham and CO rats (367±1 bpm and 365 ±1 bpm, respectively).

Cell isolation

Single ventricular myocytes were isolated by enzymatic digestion [15]. Briefly, hearts were quickly removed, mounted on a Langendorff apparatus, and perfused with an enzymatic solution (1.25 $mg.mL^{-1}$ collagenase type IV, Worthington Freehold, NJ, U.S.A) for 10-20 min, at 37°C. The left ventricle (LV) was dissected and cardiomyocytes were dissociated from the inner sub-endocardial layer (ENDO) and the outer sub-epicardial layer (EPI) in a free Ca^{2+} solution. Ca^{2+} concentration was gradually increased to 1 mM Ca^{2+}. Solutions for isolating intact cardiomyocytes contained (mM): NaCl 117, KCl 5.7, $NaHCO_3$ 4.4, KH_2PO_4 1.5, $MgCl_2$ 1.7, HEPES 21, glucose 11, taurine 20, pH 7.2 adjusted with NaOH.

Measurement of mitochondrial ROS production

Mitochondrial ROS production was measured using MitoSOX Red as described previously [16]. Single cardiomyocytes were loaded with MitoSOX Red (5 µmol/l) for 15 min at room temperature. MitoSOX Red fluorescence was obtained by illuminating the cells at 488 nm and measuring the emitted light at 583 nm using a Zeiss LSM 510 inverted confocal microscope with x40 lens. In order to reproduce an exercise test protocol, cardiomyocytes were subjected to changes of workload. Cardiomyocytes were paced at 0.5 Hz for 5 min, followed by 5 minutes at high pacing (4Hz, HP), and then back to 0.5 Hz stimulation for 5 min. MitoSOX Red fluorescence was collected at the end of each phase. For each cell, the resting value was set to 100% and background noise was subtracted.

Determination of antioxidant activities in cardiomyocytes

Catalase and total superoxide dismutase (SOD) activities were measured in cardiomyocytes as described elsewhere [17] [18].

Determination of mitochondrial respiratory complex activities in cardiomyocytes

Complex I activity was measured as described [19]. Complex IV (cytochrome-c oxidase) activity was measured as described [20]. Oxidation of cytochrome-c was followed by spectrophotometry. Citrate synthase (CS) activity was measured as described [21]: the activity of the enzyme was measured by following the color of 5-thio-2-nitrobenzoic acid, which was generated from 5,5'-dithiobis-2-nitrobenzoic acid present in the reaction of citrate synthesis, and caused by the deacetylation of acetyl-CoA.

Measurement of Ca^{2+} transient

Cardiomyocytes were loaded for 30 min at room temperature with Indo-1 AM (10 µM Invitrogen inc., France) in order to monitor intracellular Ca^{2+}. Cells were illuminated at 305 nm using a xenon arc bulb light. Sarcomere length (SL) and Indo-1 fluorescence emitted at 405 nm and 480 nm were simultaneously recorded using IonOptix acquisition software (IonOptix system, Hilton, USA). Diastolic Ca^{2+} fluorescence was collected during the HP phase, and during recovery at 0.5 Hz. Ectopic Ca^{2+} transients were counted over the 5 min period at 0.5 Hz after the HP phase. In some experiments, myocytes were pre-treated with a ROS scavenger N-acetylcystein (20 mmol/L for 1 hour).

Ca^{2+} handling proteins analysis

Proteins were separated using 2-20 % SDS-PAGE and blotted onto a PVDF membrane (Protran, Schleichen and Schuele, Dassel, Germany). Membranes were incubated overnight at 4°C with the following primary antibodies: RyR-2 antibody (Covalab, France), Phospho Ser^{2809}-RyR-2 antibody (A010-30, Badrilla, UK), SERCA-2a antibody (A010-20, Badrilla, UK) and PLB antibody (A010-14, Badrilla, UK). RyR-2, SERCA-2A and PLB levels were expressed relative to calsequestrin content (Cat # PA1-913, ABR, USA) on the same membrane. Immunodetection was carried out using the ECL Plus system (Amersham Pharmacia, Little Chalfont Buckinghamshire, England).

PKA activity was measured using a non-radioactive PKA activity assay kit according to manufacturer recommendations (Assay designs, France).

Statistical analysis

Data were analyzed using one-way or 2-way ANOVA between groups. When significant interactions were found, a Bonferroni post-hoc test was applied with $P< 0.05$ (Statview 5.0). For comparing the number of arrhythmic cells between control and CO-exposed rats a chi-square has been used. Data are presented as mean±SEM.

3. Results

Post-exercise arrhythmic events in human subjects

We measured the number of arrhythmic events recorded from ECGs (Figure 1A) during the recovering phase (5 minutes) of an incremental maximal cycle ergometer test in non-smoker healthy volunteers. The number of arrhythmic events was correlated with marker of CO exposure. One way to estimate in human population the level of chronic CO exposure is to evaluate the level of HbCO [11]. We thus studied the relationship between the number of arrhythmic events recorded from ECGs and HbCO levels in non-smoker healthy human subjects during the recovery phase (5 minutes) after an incremental maximal test on ergocycle. Figure 1B shows a positive correlation between the HbCO level and the number of arrhythmic events during exercise test recovery (R^2=0.76). This result supports the idea that human subjects exposed to high CO levels are more prone to trigger arrhythmic events during the recovering phase of an exercise test. CO exposure has been shown to be associated with oxidative stress [22]. We thus evaluated whether HbCO was correlated with Isoprostane, an index of oxidative stress. A linear correlation was found between the levels of HbCO and Isoprostane (R^2=0.82) consistent with a pro-oxidative action of CO exposure (Figure 1C). Given that CO exposure was correlated with Isoprostane, and that oxidative stress plays a critical role in the arrythmogenesis, we evaluated the possible link between the number of arrhythmic

events after exercise and the concentration of Isoprostane. The results showed a trend for a positive linear correlation between Isoprostane production and arrhythmic events, which was at the limit of significance (p=0.07) most probably due to the small number of subjects recruited. No interaction has been found between the various parameters measured and the age or gender of the subjects. Altogether these results suggest a link between (CO-induced) oxidative stress and the occurrence of arrhythmic events in healthy human subjects.

Impact of CO on arrhythmic events after beta adrenergic challenge in a rat model

In order to explore the cardiac response to beta adrenergic stimulation in standardized conditions, we performed an injection of isoproterenol to rats exposed to CO pollution for 4 weeks as previously characterized [9]. We measured the number of arrhythmic events occurring during the resting phase, i.e. when the heart rate starts to decrease (Figure 2A). CO-exposed rats displayed about twice more arrhythmias compared to Sham animals in this period, suggesting a higher sensitivity toward adrenergic stress in this population (Figure 2B and C).

Impact of CO on arrhythmic events after high pacing in a rat model

In order to explore the cellular mechanisms underlying this CO-associated ventricular arrhythmia, we investigated LV cardiomyocytes isolated from rat exposed to CO pollution for 4 weeks as previously characterized [9]. Myocytes were submitted to abrupt changes in stimulation frequency from 0.5 Hz to 4 Hz (high pacing –HP) followed by a recovering phase to 0.5 Hz (post HP) (Figure 3A). Occurrence of arrhythmic events was quantified by measuring the number of ectopic Ca^{2+} transients. During the pre-HP and HP phase, no ectopic Ca^{2+} transient was observed in both sham and CO cardiomyocytes. During the recovery phase when returning to low pacing (Figure 3A) the occurrence of ectopic Ca^{2+} transient was higher in cardiomyocytes from CO-exposed rats. In control conditions, ectopic Ca^{2+} transients were observed in about 10% of the post HP sequences (Figure 3B) and in 30% of cardiomyocytes from CO exposed rats.

Diastolic intracellular Ca^{2+} overload can trigger spontaneous Ca^{2+} waves and ectopic Ca^{2+} transients [24]. During the pre-HP, diastolic Ca2+ levels were higher in cardiomyocytes isolated from CO-exposed rats compared with sham animal (Figure 3C). Surprisingly, the differences between the groups disappeared at HP. After HP sequences, the diastolic Ca^{2+} level was significantly higher in myocytes from the of CO rats when compared with control cells (Figure 3C). The alterations in diastolic Ca^{2+} levels, observed in cells from CO rats, were associated with a reduced Serca-2a expression and a higher phosphorylation level of RyR-2 on the PKA-dependent Ser^{2809} site (Supplemental data 1), which confirmed previous results from our group [9].

Effects of CO exposure on oxidative stress after high pacing

There are growing evidences to suggest an involvement of mitochondrial dysfunction and subsequent ROS production in the development of arrhythmias [25]. Since CO is known to disturb mitochondrial function and promote oxidative stress [26] [27], we measured the ROS production using MitoSOX Red [16] in cardiomyocytes. Chronic

exposure to CO increased ROS production at pre-HP, HP and during post HP phases in myocytes when compared with control rats (Figure 4A and B).
ROS production results from an imbalance between pro-oxidant activity and antioxidant defense buffering ROS. We thus evaluated antioxidant enzyme activities such as superoxide dismutase (SOD), which converts $O_2^{\cdot -}$ to H_2O_2, and catalase, which converts H_2O_2 to H_2O. We observed a decrease of both SOD and catalase activities in cells from CO-exposed rats (Figure 4C). In addition, sustained CO exposure decreased activities of both complex I and IV of the electron transport chain in ENDO layer (Figure 4D), which is known to further increase ROS production [28 29 30].
Taken together, the results suggest that chronic CO exposure led to reduced antioxidant defenses and altered electron transport chain activities, resulting in ROS overproduction notably after high pacing.

ROS dependency of CO-associated Ca^{2+} handling alterations
Our results showed that chronic CO exposure induced an oxidative stress that was associated with alterations of diastolic Ca^{2+} homeostasis, due to modifications in Ca^{2+} handling proteins activity, and subsequent arrhythmic events. In order to determine whether ROS were responsible for these defects, we incubated the cardiomyocytes for 1 hour with a ROS scavenger, the N-acetyl cysteine (NAC, 20 mmol/l) prior to testing the effect of HP sequence. NAC treatment reduced the number of arrhythmic cells after HP to a level similar to that of control rats (Figure 5A). NAC treatment also normalized the diastolic Ca^{2+} levels (Figure 5B) and PKA-dependent phosphorylation of RyR-2 (Figure 5C) in CO cardiomyocytes. Consistently, PKA activity, which was increased in myocytes exposed to CO, was normalized by NAC treatment (Figure 5D).

4. **Discussion**

The prevalence of ventricular ectopic events during recovery from exercise is a valuable predictor of mortality. The main results of the present study demonstrate a correlation between CO exposure level, oxidative stress and occurrence of post-exercise ventricular ectopic beats (VEB) in healthy human subjects. In an experimental model of chronic exposure to atmospheric CO pollution, we highlighted the mechanisms underlying the CO-induced cardiac alterations at the cardiomyocyte level : ROS-dependent defects in diastolic Ca^{2+} handling were revealed after high pacing of single cells, which were mediated at least in part by PKA activation. These cellular alterations provided a substrate favouring occurrence of subsequent ectopic Ca^{2+} transients.

CO pollution increases ROS production
Chronic CO exposure decreased antioxidant activities and altered mitochondrial electron transport chain complexes, which could be accounted for by the biochemical properties of CO. Indeed, CO competes with oxygen for haemoglobin binding and has a 200 times higher affinity [31] thereby resulting in decreased oxygen carrying

capacity and cardiomyocytes oxygenation. Moreover, CO binding on cardiac myoglobin reinforces tissue hypoxia [27] leading to disturbed cardiac mitochondrial oxidation [32]. Alternatively, CO is known to bind to the cytochrome p-450 and directly inhibits complex IV of the electron transport chain, leading to ROS production [26]. One key finding here is that changes in workload due to HP rate potentiates mitochondrial alterations and ROS overproduction, which occurred in CO-exposed rats. Similar trend has been observed in healthy human individuals as suggested by the close relationships between arrhythmic events, the level of HbCO, and the concentration of plasma isoprostane.

CO-mediated ROS production triggers ectopic Ca^{2+} transients

Excessive ROS production plays a pivotal role in the triggering of arrhythmic events through changes in RyR-2 activity [33, 34]. Here, we show that acute treatment with NAC, a ROS scavenger, reversed the Ca^{2+} homeostasis defects and reduced the associated-ectopic Ca^{2+} transients, thus supporting the concept that disturbed ROS homeostasis promotes the alterations observed in the CO rats. The pathway underlying the ROS-mediated RyR-2 defects involves PKA activation. Indeed, ROS can affect the phosphorylation status of proteins by inhibiting protein phosphatase activity [35] and activating PKA [36 37]. In our study, we show a PKA-dependent hyperphosphorylation of RyR-2 in the subendocardium after chronic CO exposure, which results from a ROS-dependent activation of PKA (Figure 4C). It has been reported that PKA-dependent RyR-2 hyperphosphorylation leads to sarcoplasmic reticulum (SR) Ca^{2+} leak contributing to increased diastolic Ca^{2+} levels through disruption of the channel-stabilizing FK506 Binding Protein 12.6 (FKBP12.6) [38 39 40]. Although diastolic Ca^{2+} overload results, at least in part, from ROS-induced PKA activation, we cannot exclude a direct redox modification of RyR-2 reported to occur *via* direct FKBP12.6 dissociation [41]. In addition, it has been proposed that Ca^{2+} leak through RyR-2 drives the generation of reactive nitrogen species, which further aggravates Ca^{2+} leak [42]. The concept of cross talk between Ca^{2+} and ROS leading to a vicious circle in which these two components potentiate themselves could be a central element in the CO-mediated Ca^{2+} handling troubles.

A second major protein involved in cardiac Ca^{2+} homeostasis is SERCA-2a, responsible for Ca^{2+} reuptake in the SR during diastole. The reduced expression of SERCA-2a in ENDO cells after CO exposure, resulting in diminished SR Ca^{2+} reuptake, may also contribute to the rise in diastolic Ca^{2+}. However, acute NAC treatment normalized diastolic Ca^{2+} level, which may suggest that this is a secondary mechanism for the increased Ca^{2+} level. The impact of ROS overproduction on SERCA-2a function after CO exposure needs however further investigation since previous reports have shown that ROS inhibit SERCA activity and expression [43].

Diastolic Ca^{2+} overload is a major substrate for oscillations of the cellular membrane potential and triggering of delayed after depolarizations (DAD) [24]. We provide direct evidence that sustained CO exposure favours the triggering of ectopic Ca^{2+} transients following increased workload. A central mechanism involves a ROS-induced PKA activation pathway. Consequently, scavenging of excessive ROS production reduced the occurrence of ectopic Ca^{2+} transients, presumably through normalisation of RyR-2 activity. The propensity of CO-exposed subjects to trigger arrhythmia is also expected to be enhanced by beta-adrenergic activation during

exercise or heart failure, as shown previously *in vivo* after a bolus of isoproterenol in CO-exposed rats compared with control animals [9].

Conclusions

The present study provides evidences that environmental stress such as urban CO pollution, directly impacts the occurrence of arrhythmic events following an increased workload. Indeed, we show here a positive correlation between the level of HbCO and the number of arrhythmic events in post-exercise test, suggesting a role of CO exposure in the occurrence of arrhythmic phenotype. Since post-exercise ectopic beats are a key factor predicting sudden death [1], our findings suggest that CO exposure represent a potential risk factor for triggering cardiac events and could be considered with importance for the prevention of cardiovascular risk in clinical examination. Since ROS play a pivotal role in the CO-associated arrhythmic events, antioxidant supplementation might be a potential preventive strategy for protection of individuals with cardiovascular risk against atmospheric pollution. The present results may also be of interest for therapeutic strategies using low CO-dose gas inhalation and synthetic CO-releasing molecules (CORM), particularly for cardiovascular diseases [44]. At the moment, CO-based therapeutic strategies use short-term exposure. However, the potential toxicological effect of low doses of CO (30 ppm/d on average) on cardiac function should stimulate future investigations of the effect of chronic treatment with low-dose CO gas inhalation or CORM. Our results may offer interesting perspectives for populations exposed to chronic CO sources (urban pollution, second-hand smoke).

Limitations

For the experiments performed in humans, there has been no control of the amount and source of CO exposure that could affect the parameters measured. In particular, the amount of carbon monoxide in the room air has not been controlled and was not correlated with potential peak pollution of CO. Volunteers performed the test at the same period (early morning) but not the same day. Possible secondhand smoke exposure cannot be excluded and has been standardized by the presence of the volunteer in the hospital several hours before the test for clinical investigation. The present study has been performed in a relative small number of individuals (n=17) that affected the number of correlations that could be tested. A bigger cohort is required to investigate the effect of gender and/age, which have been correlated with the level of exhaled CO [45].

Sources of funding

This work was supported by a French National Research Agency grant (COMYOCARD). SR, JF, AL, and OC are scientists from the CNRS.

Legends

Figure 1: Relationship between chronic CO exposure, arrhythmic events and oxidative stress in healthy human subjects. A: Typical example of VEBs recorded in patients during the recovery phase of a maximal exercise test realized on ergocyle. **B:** Correlation between the number of VEBs measured during the recovery phase of a maximal exercise test and the level of carboxyhaemoglobin (HbCO) measured in blood sample (n=22 healthy human subjects). Data have been fitted with a exponential decay function (Y=5.1exp(-x/(-1.9))+5.5exp(-x/(-1.9))+8.9exp(-x/(-0.1))-17.1, Chi-squared = 75.8, $p<0.05$). **C:** Correlation between plasmatic concentration of isoprostane and the level of carboxyhaemoglobin (HbCO) (n=17 subjects). Data have been fitted with a linear function (Y= 553x-601, Chi-squared =0.82, $p<0.001$). **D:** Correlation between isoprostane and the number of ectopic ventricular beats measured during the recovering phase of a maximal exercise test (n=17 subjects). Data have been fitted with a linear function (Y= 7.1x+230, Chi-squared =0.28, p=0.07).

Figure 2: Arrhythmic phenotype following beta-adrenergic challenge in CO-exposed rats. A: Isoprenaline (1 $mg.kg^{-1}$) was injected in awakened rats equipped for surface ECG recordings. Heart beat frequency increased rapidly, stabilized for about 90 min and recovered its basal value. Spontaneous rhythmic disorders were investigated over a period of 20 min starting at a heart rate 15% below the maximal iso-induced heart rate. **B:** Ventricular ectopic beats were counted. An example of isolated extrasystole is shown. **C:** In CO-exposed rats we observed more complex arrhythmic events such as extrasystoles in salve, and ventricular tachycardia or fibrillation that lead to death in 2 rats out of 9. * $P<0.05$ *vs* sham rats.

Figure 3: CO-associated alterations of Ca^{2+} homeostasis. A: Typical example of ectopic Ca^{2+} transients in myocytes from CO-exposed rats after high pacing (HP). **B:** Number of arrhythmic cells in Sham and CO rats measured during pre-HP, HP and post-HP phases (15-25 cells / 4-5 hearts). **C:** Diastolic Ca^{2+} levels in control and CO cardiomyocytes measured during pre-HP, HP and post-HP phases (15-25 cells / 4-5 hearts).* $P<0.05$ *vs* sham rats

Figure 4: Effects of CO pollution on ROS production. A: Typical images showing MitosoxRed fluorescence (reflect of superoxide anion, $O_2^{\cdot -}$) in ENDO cells from control and CO-exposed rats at rest and after HP. **B:** Production of $O_2^{\cdot -}$ in control and CO-exposed cardiomyocytes measured during pre-HP, HP and post-HP phases relative to the value at resting state (n=22-30 cells / 4 hearts). **C:** Myocardial anti-oxidant defences were evaluated with the measurement of SOD and catalase activities of control and CO rats (4 hearts per group). **D:** Myocardial Citrate synthase (CS), complex I and complex IV activities of control and CO rats (4 hearts per group). * $P<0.05$ *vs* sham rats

Figure 5: Effect of acute NAC treatment on CO-associated Ca^{2+} handling alterations. A: Number of arrhythmic cells of Sham, CO and CO-NAC cardiomyocytes from ENDO cardiomyocytes measured during the recovering phase after HP (15-25 cells / 4-5 hearts). **B:** Diastolic Ca^{2+} levels in ENDO control, CO and CO-NAC cardiomyocytes (35-50 cells / 4-5 hearts). **C:** Level of PKA-dependent Ser^{2809} RyR-2 phosphorylation normalized to the total RyR-2 content. (n= 5 hearts).

D: PKA activity was measured in cardiac tissue originated from ENDO layer of control and CO hearts treated or not with NAC. (n=5 hearts). * P<0.05 *vs vs* sham rats

Supplemental data 1: CO-associated alterations in Ca^{2+} homeostasis proteins. A: Contents of RyR-2, Ser^{2809} RyR-2 phosphorylation, Serca-2a, PLB and calsequestrin in ENDO and EPI layers of control and CO rats were analyzed by Westernblot. RyR-2, Serca-2a and PLB contents were normalized to calsequestrin. The level of PKA-dependent Ser^{2809} RyR-2 phosphorylation was normalized to the total RyR-2 content. (n= 5 hearts). **B:** PKA activity was measured in cardiac tissue from ENDO and EPI layers of control and CO-exposed hearts. Results are mean±S.E.M. (n=5 hearts). * P<0.05 between control and CO rats; $^{\#}$P<0.05 between ENDO and EPI layers.

References

1. Frolkis JP, Pothier CE, Blackstone EH, et al. Frequent ventricular ectopy after exercise as a predictor of death. *N Engl J Med.* 2003;348(9):781-790.
2. Kaiser J. Epidemiology. How dirty air hurts the heart. *Science.* 2005;307(5717):1858-1859.
3. Simkhovich BZ, Kleinman MT, Kloner RA. Air pollution and cardiovascular injury epidemiology, toxicology, and mechanisms. *J Am Coll Cardiol.* 2008;52(9):719-726.
4. Miller KA, Siscovick DS, Sheppard L, et al. Long-term exposure to air pollution and incidence of cardiovascular events in women. *N Engl J Med.* 2007;356(5):447-458.
5. Finkelstein MM. Pollution-related mortality and educational level. *Jama.* 2002;288(7):830; author reply 830.
6. Robinson CR. Jogging in Tasmania. *N Engl J Med.* 1971;285(22):1267.
7. Henry CR, Satran D, Lindgren B, et al. Myocardial injury and long-term mortality following moderate to severe carbon monoxide poisoning. *Jama.* 2006;295(4):398-402.
8. Samoli E, Touloumi G, Schwartz J, et al. Short-term effects of carbon monoxide on mortality: an analysis within the APHEA project. *Environ Health Perspect.* 2007;115(11):1578-1583.
9. Andre L, Boissiere J, Reboul C, et al. Carbon Monoxide Pollution Promotes Cardiac Remodeling and Ventricular Arrhythmia in Healthy Rats. *Am J Respir Crit Care Med.* 2009.
10. Serres I, Varray A, Vallet G, et al. Improved skeletal muscle performance after individualized exercise training in patients with chronic obstructive pulmonary disease. *J Cardiopulm Rehabil.* 1997;17(4):232-238.
11. Rudra CB, Williams MA, Sheppard L, et al. Relation of whole blood carboxyhemoglobin concentration to ambient carbon monoxide exposure estimated using regression. *Am J Epidemiol.*171(8):942-951.
12. Delample D, Durand F, Severac A, et al. Implication of xanthine oxidase in muscle oxidative stress in COPD patients. *Free Radic Res.* 2008;42(9):807-814.
13. Stern FB, Halperin WE, Hornung RW, et al. Heart disease mortality among bridge and tunnel officers exposed to carbon monoxide. *Am J Epidemiol.* 1988;128(6):1276-1288.
14. Wright GR, Jewczyk S, Onrot J, et al. Carbon monoxide in the urban atmosphere: hazards to the pedestrian and the street-worker. *Arch Environ Health.* 1975;30(3):123-129.
15. Mou YA, Reboul C, Andre L, et al. Late exercise training improves non-uniformity of transmural myocardial function in rats with ischaemic heart failure. *Cardiovasc Res.* 2009;81(3):555-564.
16. Fauconnier J, Andersson DC, Zhang SJ, et al. Effects of palmitate on Ca(2+) handling in adult control and ob/ob cardiomyocytes: impact of mitochondrial reactive oxygen species. *Diabetes.* 2007;56(4):1136-1142.
17. Beers RF, Jr., Sizer IW. A spectrophotometric method for measuring the breakdown of hydrogen peroxide by catalase. *J Biol Chem.* 1952;195(1):133-140.

18. **Marklund S. Spectrophotometric study of spontaneous disproportionation of superoxide anion radical and sensitive direct assay for superoxide dismutase. *J Biol Chem.* 1976;251(23):7504-7507.**
19. **Janssen AJ, Trijbels FJ, Sengers RC, et al. Spectrophotometric assay for complex I of the respiratory chain in tissue samples and cultured fibroblasts. *Clin Chem.* 2007;53(4):729-734.**
20. **Wharton DC. Purification of electron-transfer components from Pseudomonas. *Methods Enzymol.* 1978;53:646-661.**
21. **Srere PA. An eclectic view of metabolic regulation: control of citrate synthase activity. *Adv Enzyme Regul.* 1970;9:221-233.**
22. **Delfino RJ, Staimer N, Tjoa T, et al. Air pollution exposures and circulating biomarkers of effect in a susceptible population: clues to potential causal component mixtures and mechanisms. *Environ Health Perspect.* 2009;117(8):1232-1238.**
23. **Cazorla O, Ait Mou Y, Goret L, et al. Effects of high-altitude exercise training on contractile function of rat skinned cardiomyocyte. *Cardiovasc Res.* 2006;71(4):652-660.**
24. **Ter Keurs HE, Boyden PA. Calcium and arrhythmogenesis. *Physiol Rev.* 2007;87(2):457-506.**
25. **Akar FG, Aon MA, Tomaselli GF, et al. The mitochondrial origin of postischemic arrhythmias. *J Clin Invest.* 2005;115(12):3527-3535.**
26. **Piantadosi CA. Carbon monoxide poisoning. *N Engl J Med.* 2002;347(14):1054-1055.**
27. **Piantadosi CA. Biological chemistry of carbon monoxide. *Antioxid Redox Signal.* 2002;4(2):259-270.**
28. **Green DR, Reed JC. Mitochondria and apoptosis. *Science.* 1998;281(5381):1309-1312.**
29. **Pitkanen S, Robinson BH. Mitochondrial complex I deficiency leads to increased production of superoxide radicals and induction of superoxide dismutase. *J Clin Invest.* 1996;98(2):345-351.**
30. **Ide T, Tsutsui H, Kinugawa S, et al. Mitochondrial electron transport complex I is a potential source of oxygen free radicals in the failing myocardium. *Circ Res.* 1999;85(4):357-363.**
31. **Chu K, Vojtchovsky J, McMahon BH, et al. Structure of a ligand-binding intermediate in wild-type carbonmonoxy myoglobin. *Nature.* 2000;403(6772):921-923.**
32. **Giordano FJ. Oxygen, oxidative stress, hypoxia, and heart failure. *J Clin Invest.* 2005;115(3):500-508.**
33. **Fauconnier J, Thireau J, Reiken S, et al. Leaky RyR2 trigger ventricular arrhythmias in Duchenne muscular dystrophy. *Proc Natl Acad Sci U S A.*107(4):1559-1564.**
34. **Terentyev D, Gyorke I, Belevych AE, et al. Redox modification of ryanodine receptors contributes to sarcoplasmic reticulum Ca2+ leak in chronic heart failure. *Circ Res.* 2008;103(12):1466-1472.**
35. **Rhee SG, Bae YS, Lee SR, et al. Hydrogen peroxide: a key messenger that modulates protein phosphorylation through cysteine oxidation. *Sci STKE.* 2000;2000(53):PE1.**

36. O'Flaherty C, de Lamirande E, Gagnon C. Reactive oxygen species modulate independent protein phosphorylation pathways during human sperm capacitation. *Free Radic Biol Med.* 2006;40(6):1045-1055.
37. de Lamirande E, O'Flaherty C. Sperm activation: role of reactive oxygen species and kinases. *Biochim Biophys Acta.* 2008;1784(1):106-115.
38. Wehrens XH, Lehnart SE, Reiken SR, et al. Protection from cardiac arrhythmia through ryanodine receptor-stabilizing protein calstabin2. *Science.* 2004;304(5668):292-296.
39. Marx SO, Reiken S, Hisamatsu Y, et al. PKA phosphorylation dissociates FKBP12.6 from the calcium release channel (ryanodine receptor): defective regulation in failing hearts. *Cell.* 2000;101(4):365-376.
40. Lehnart SE, Mongillo M, Bellinger A, et al. Leaky Ca2+ release channel/ryanodine receptor 2 causes seizures and sudden cardiac death in mice. *J Clin Invest.* 2008;118(6):2230-2245.
41. Yan Y, Liu J, Wei C, et al. Bidirectional regulation of Ca2+ sparks by mitochondria-derived reactive oxygen species in cardiac myocytes. *Cardiovasc Res.* 2008;77(2):432-441.
42. Durham WJ, Aracena-Parks P, Long C, et al. RyR1 S-nitrosylation underlies environmental heat stroke and sudden death in Y522S RyR1 knockin mice. *Cell.* 2008;133(1):53-65.
43. Adachi T, Matsui R, Xu S, et al. Antioxidant improves smooth muscle sarco/endoplasmic reticulum Ca(2+)-ATPase function and lowers tyrosine nitration in hypercholesterolemia and improves nitric oxide-induced relaxation. *Circ Res.* 2002;90(10):1114-1121.
44. Foresti R, Bani-Hani MG, Motterlini R. Use of carbon monoxide as a therapeutic agent: promises and challenges. *Intensive Care Med.* 2008;34(4):649-658.
45. Cheng S, Lyass A, Massaro JM, et al. Exhaled Carbon Monoxide and Risk of Metabolic Syndrome and Cardiovascular Disease in the Community. *Circulation.*

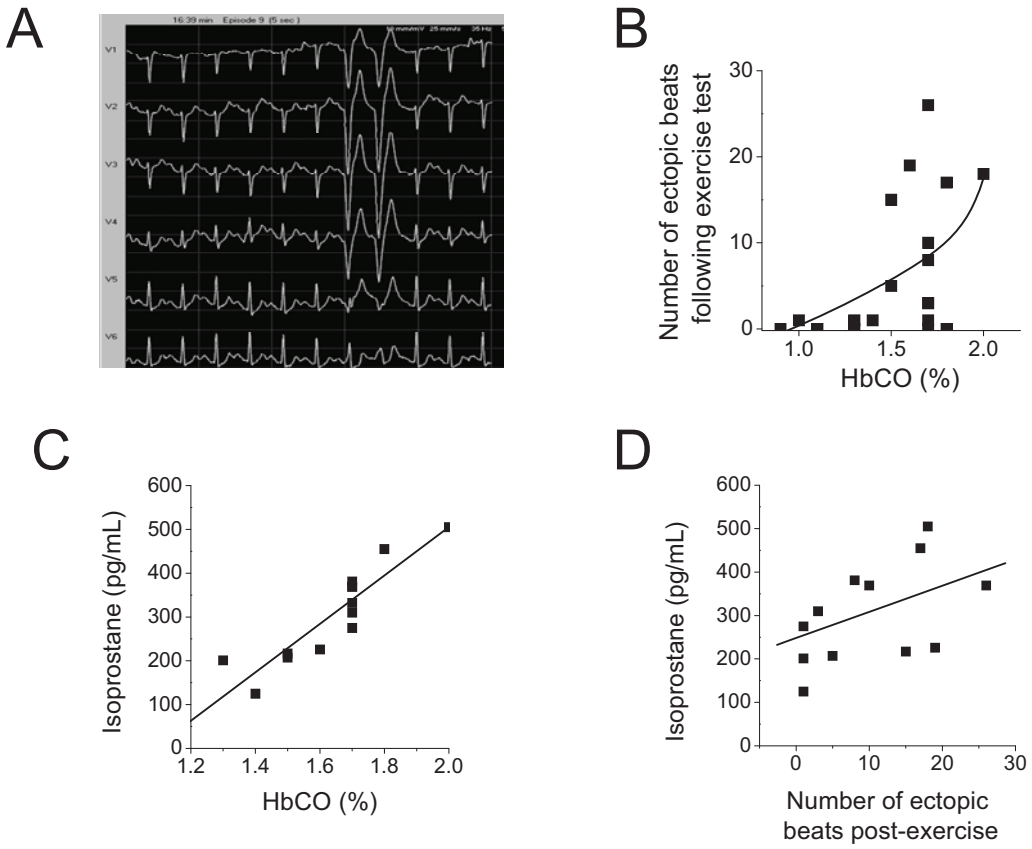
A
B
Number of ectopic beats following exercise test
HbCO (%)
C
Isoprostane (pg/mL)
HbCO (%)
D
Isoprostane (pg/mL)
Number of ectopic beats post-exercise

Figure 1

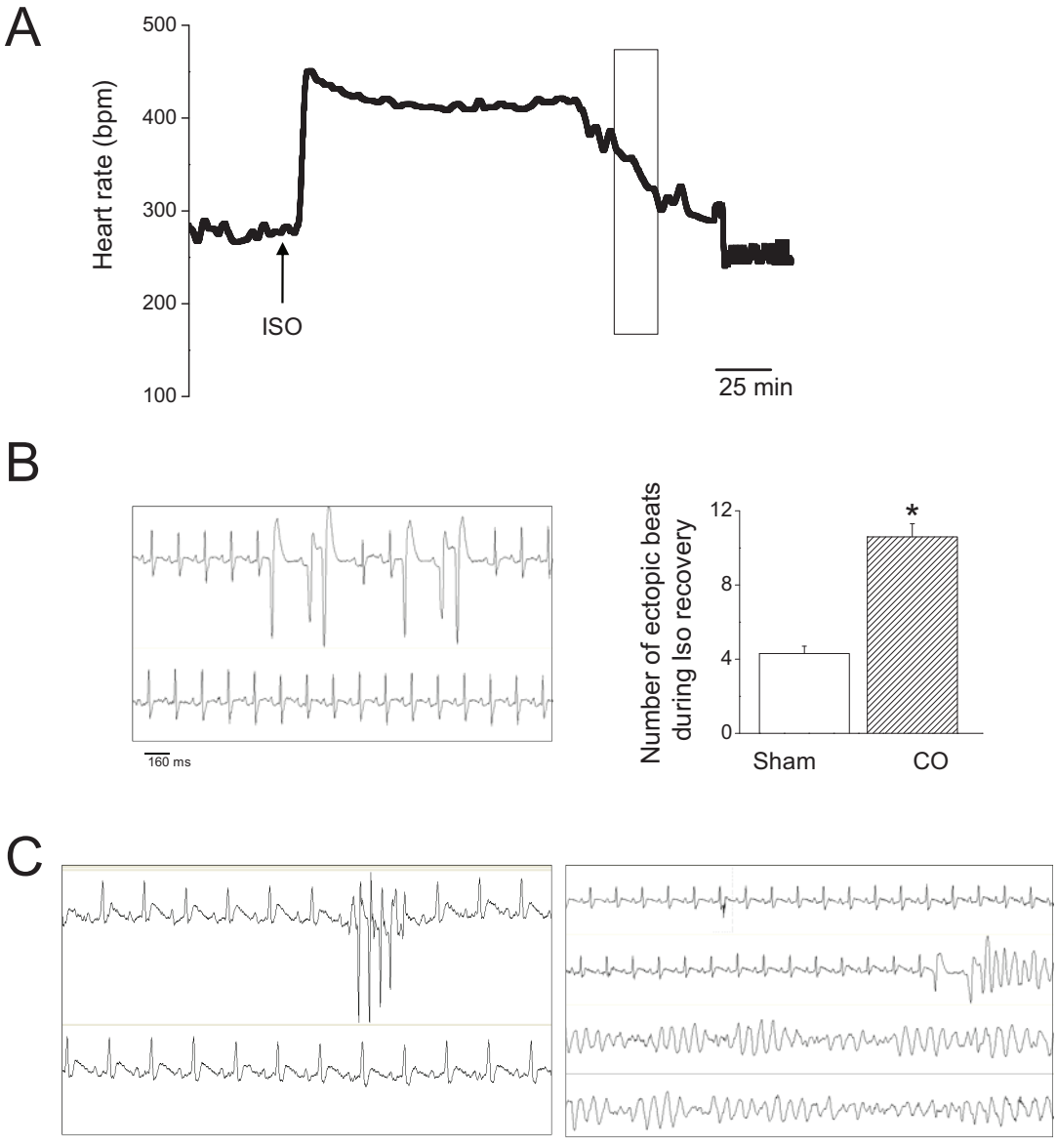
A
500
400
300
200
100
Heart rate (bpm)
ISO
25 min
B
160 ms
Number of ectopic beats during Iso recovery
12
8
4
0
*
Sham
CO
C

Figure 2

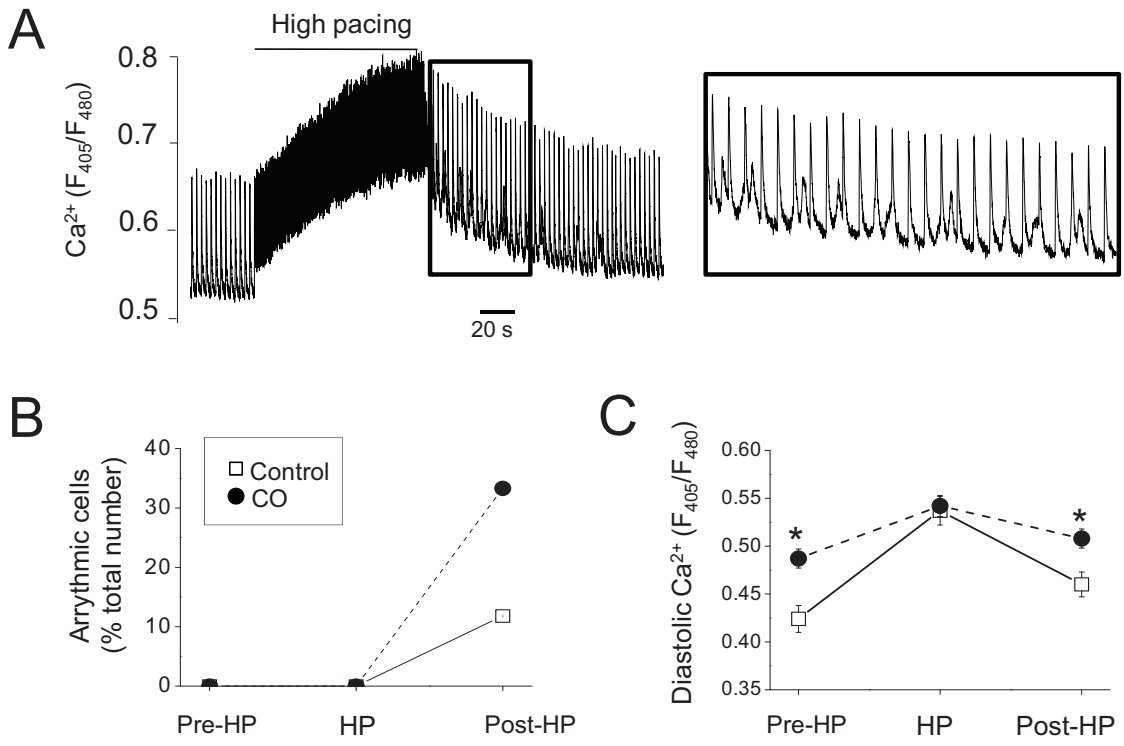
A
High pacing
0.8
0.7
0.6
0.5
Ca2+ (F405/F480)
20 s
B
Arrythmic cells
(% total number)
Control
CO
40
30
20
10
0
Pre-HP
HP
Post-HP
C
Diastolic Ca2+ (F405/F480)
0.60
0.55
0.50
0.45
0.40
0.35
*
*
Pre-HP
HP
Post-HP

Figure 3

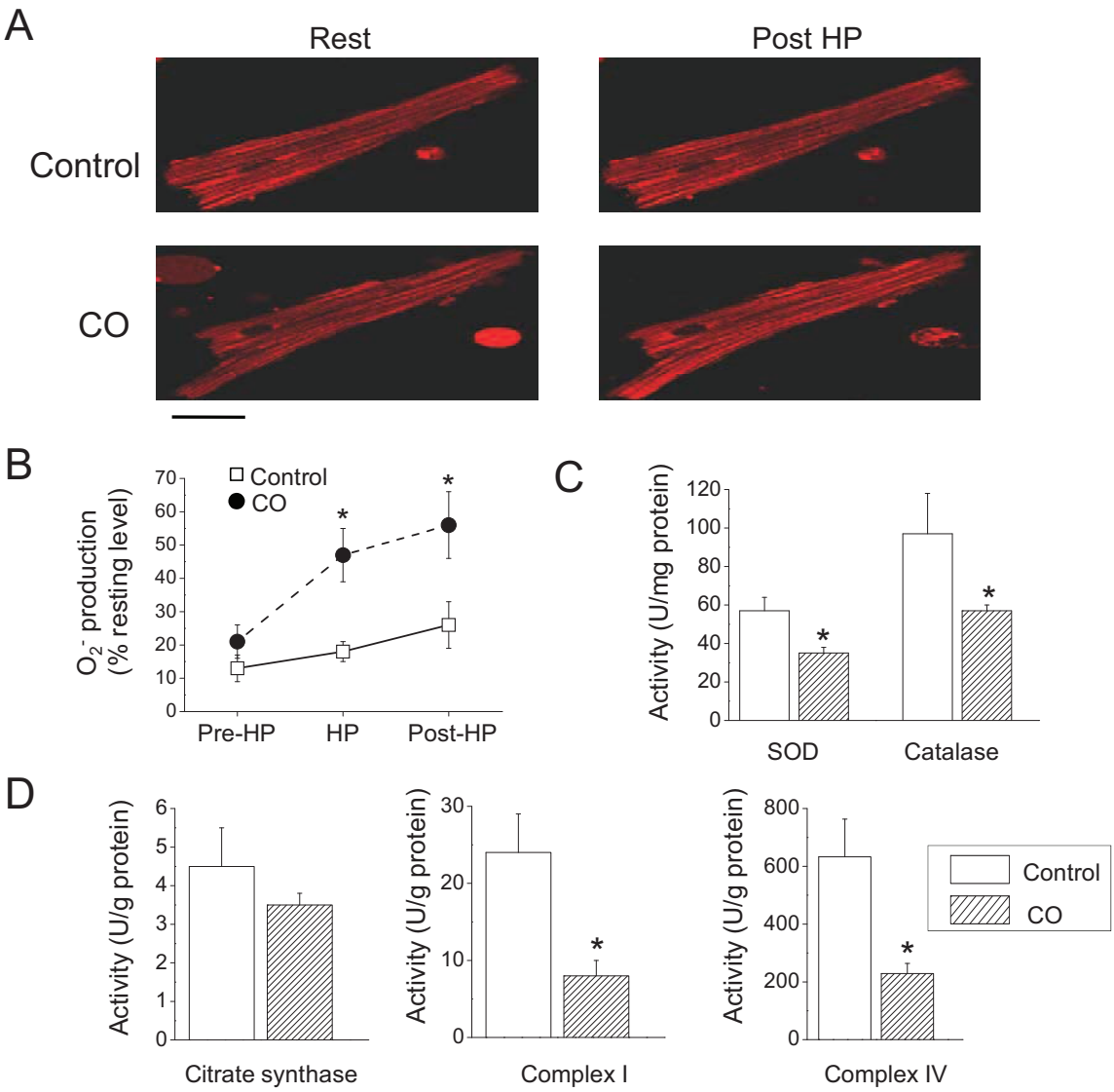
A
Rest
Post HP
Control
CO
B
Control
CO
O_2^- production (% resting level)
Pre-HP
HP
Post-HP
C
Activity (U/mg protein)
SOD
Catalase
D
Activity (U/g protein)
Citrate synthase
Complex I
Complex IV
Control
CO

Figure 4

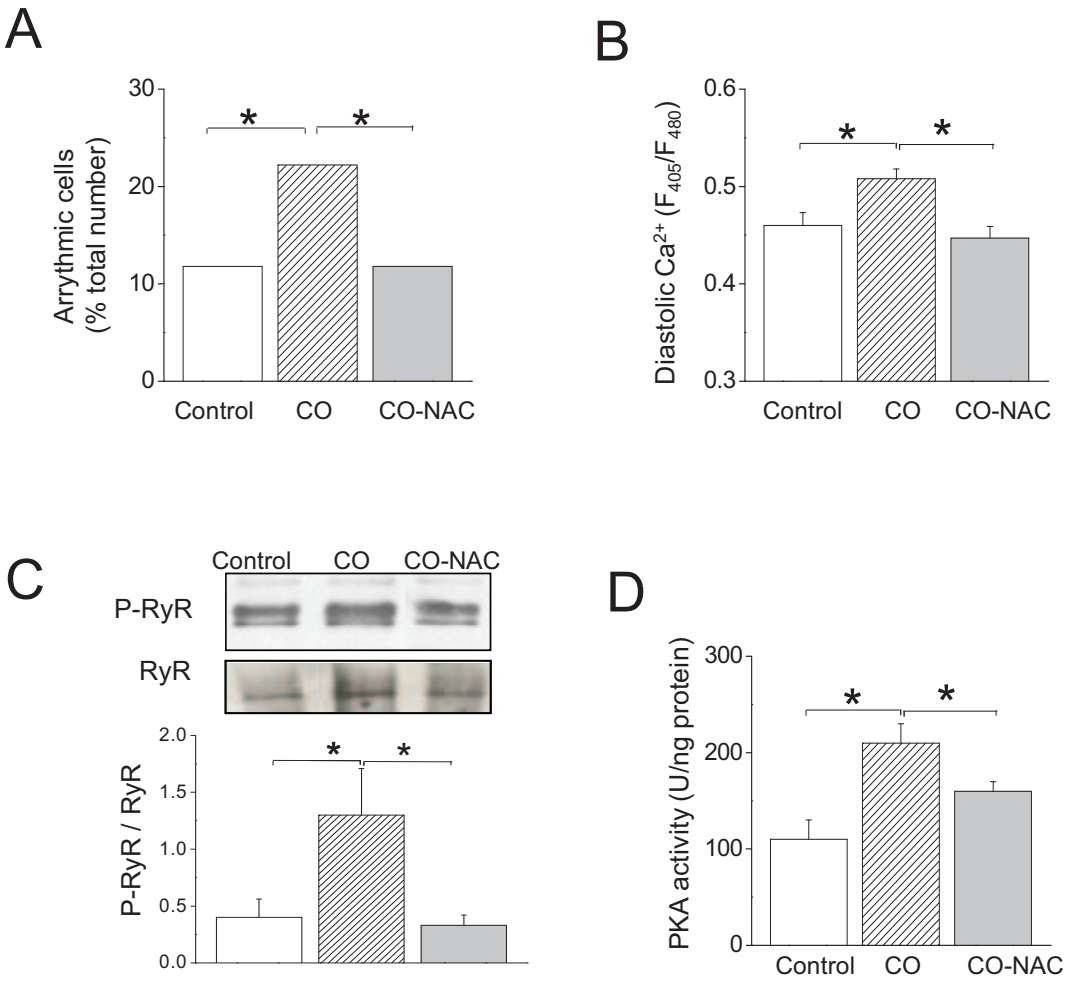
A
Arrythmic cells
(% total number)
30
20
10
0
*
*
Control
CO
CO-NAC
B
Diastolic Ca2+ (F405/F480)
0.6
0.5
0.4
0.3
*
*
Control
CO
CO-NAC
C
Control
CO
CO-NAC
P-RyR
RyR
P-RyR / RyR
2.0
1.5
1.0
0.5
0.0
*
*
D
PKA activity (U/ng protein)
300
200
100
0
*
*
Control
CO
CO-NAC

Figure 5

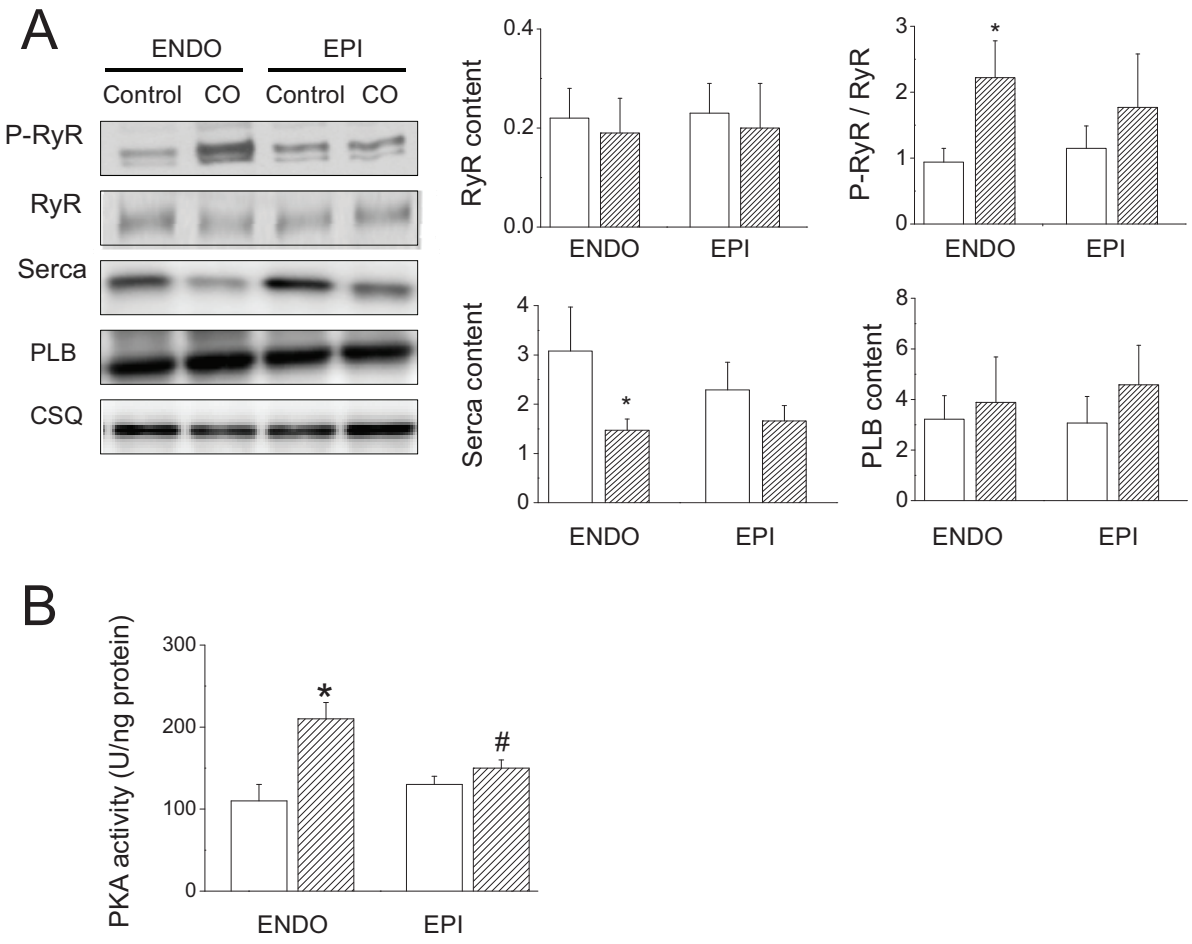

Supplemantary data 1

EPI seulement

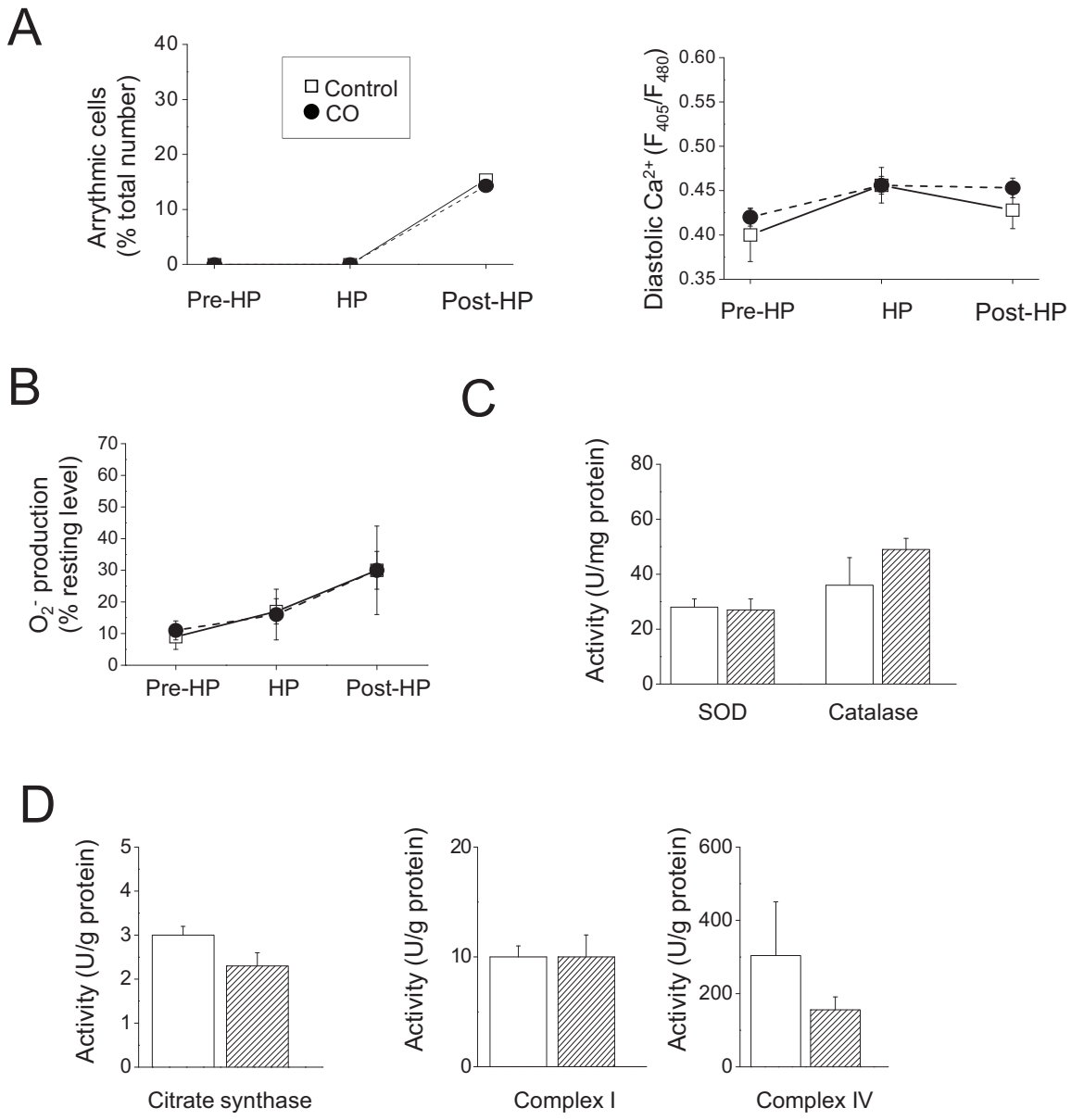

Supplementary data 2

3. Conclusion

Les événements arythmiques post-exercice sont de puissants prédicteurs de risque de survenue d'un évènement cardiovasculaire. Cette 6ème étude rapporte qu'une pollution au monoxyde de carbone génère un stress oxydatif lui-même corrélé à une augmentation des évènements arythmiques post-exercice chez des populations humaines saines. Les ROS associés à la pollution au CO activent en fait la protéine kinase A, laquelle est responsable de la phosphorylation notamment du RyR-2 et de perturbation de l'homéostasie calcique, à l'origine de libération stochastique de Ca^{2+} par le RS. L'exposition en milieu pollué expose ainsi à un risque supérieur d'accidents cardiovasculaires. La mesure de l'HbCO, comme index de l'exposition au CO, pourrait alors être intégrée dans les examens cliniques de routine afin de prévenir de manière plus fiable, en complément des facteurs de risque cardiovasculaire habituels, le risque de survenue d'un événement cardiovasculaire. Compte tenu de l'implication du stress oxydatif dans les troubles arythmiques associés à la pollution, le recours à des stratégies antioxydantes telles que des supplémentations en antioxydants ou l'exercice physique pourrait limiter les altérations cardiaques chez les personnes fortement exposées en environnement pollué. Cependant, l'exercice physique doit être réalisé en environnement sain pour bénéficier des effets protecteurs. En effet, la pratique d'activités en environnement pollué est à l'origine d'une altération des performances et d'une dégradation des fonctions cardiaques [183].

Les études 4, 5 et 6 rapportent une dégradation de la fonction cardiaque chez des populations saines exposées en environnement polluées au CO. Ces altérations sensibilisent le myocarde aux attaques ischémiques et aggravent les dommages organiques et cellulaires suite à un épisode simulé d'infarctus (ischémie-reperfusion). Ces études légitiment alors l'exploration des conséquences d'une pollution au CO sur un myocarde déjà défaillant, afin de comprendre expérimentalement les données des études épidémiologiques rapportant une augmentation des accidents cardiovasculaires chez des populations en insuffisance cardiaque.

III. Effet d'une pollution au monoxyde de carbone dans l'IC ischémique et prévention des effets délétères par l'exercice physique

1. Introduction

De nombreuses études épidémiologiques considèrent la pollution atmosphérique comme un facteur de risque majeur de développer des pathologies cardio-pulmonaires. Notamment, les populations fragilisées par une IC sembleraient particulièrement sensibles aux stress environnementaux. En effet, une recrudescence du taux de fréquentation des hôpitaux, en particulier des services de cardiologie, ainsi qu'une augmentation de la mortalité a été rapportée chez ces populations lors de pics de pollution. Parmi les agents polluants, le CO jouent un rôle majeur dans ces événements cardiovasculaires. En effet, le CO augmente la viscosité sanguine, réduit la variabilité du rythme sinusal et augmentent les phénomènes arythmiques. Cependant, les mécanismes sous-jacents à la sensibilité exacerbée de populations d'insuffisants cardiaques à un milieu pollué au CO sont inconnus. L'objectif de cette étude a alors été de déterminer si une pollution au CO pouvait aggraver le remodelage cardiaque délétère de populations IC, à l'aide d'un modèle de rats PMI exposés chroniquement au CO.

2. Article 7 - Finalisation avant soumission pour publication

Carbon monoxide pollution potentiates ischemic heart failure through a reactive oxygen-species pathway: protective effects of exercise training

Julien Boissiere[1,2,*], Lucas Andre[1,*], Cyril Reboul[2,*], Gregory Meyer[2], Jérome Thireau[1], Ludovit Paulis[1], Christine Feillet-Coudray[3], Gilles Fouret[3], Philippe Obert[3], Olivier Cazorla[1], Sylvain Richard[1]

[1]INSERM, U-637, F-34295 Montpellier, France. Université MONTPELLIER1, UFR de Médecine, F-34295 Montpellier, France

[2] EA-4278, Université Avignon et des Pays de Vaucluse, UFR Sciences, F-84000 Avignon, France.

[3]INRA UMR 866, Unité Différentiation Cellulaire et Croissance, 34060 Montpellier, France

[*] Authors equally contributed to this work

Correspondence to :
Sylvain RICHARD
Inserm U637 Physiopathologie Cardiovasculaire
CHU Arnaud de Villeneuve
34295 Montpellier, France
Phone : +33 467 41 52 44
Fax : +33 467 41 52 42
olivier.cazorla@inserm.fr

Key words: cardiomyopathy, mitochondria, oxidative stress, PKA, cardiac heterogeneity

1. Introduction

Studies conducted over the past 15 years have provided substantial evidence that long-term exposure to air pollution is a major risk factor for cardiopulmonary disease and death [1] [2] [3]. People with heart failure (HF) are particularly sensitive to outdoor air quality as assessed by the increased risk of hospital cardiac readmissions and mortality during peak pollution [4] [5] [2].
Among various environmental air pollutants, carbon monoxide (CO) is an ubiquitous pollutant found in many common sources (second-hand smoke, vehicular exhaust, industrial emissions…) which plays a critical role in pollution-induced cardiac events [6] [7] [8] [9]. It has been described that CO pollution increases HF risk factors such as blood viscosity [10], arrhythmia and decreased heart rate variability [11] [12]. However, the mechanisms underlying the increased cardiac sensitivity of HF patients to CO pollution remain unknown.
We had previously shown from an experimental design that chronic exposure to CO levels mimicking an urban pollution promoted a Ca^{2+} handling remodelling, associated with an arrhythmic phenotype in healthy population [13]. We had also shown that CO pollution renders the heart vulnerable to ischemia-reperfusion stress and aggravates the necrosis and occurrence of arrhythmias in the early phase post-infarcts [14]. In the present study, we aimed to determine whether chronic CO pollution could worsen cardiac remodelling of myocardial infracted (MI) rats.

The main results show that chronic CO exposure exacerbates cardiac remodelling in MI rats and dramatically increases the propensity to trigger ventricular tachycardia. This worsened phenotype reflected aggravation of impaired excitation-contraction coupling (ECC) in the cardiomyocytes, resulting from alterations of mitochondrial function. Exercise training, performed in standard filtered air, attenuated cardiac remodelling and prevented the additional effect of CO.

2. Materials and Methods

Animals and chronic CO exposure model

The investigations were carried out in agreement with the Guide for the Care and Use of Laboratory Animals published by the US National Institute of Health (NIH Publications No. 85-23, revised 1996) and approved by the French Agriculture Department. In urban areas, ambient CO usually varies between 2 and 40 ppm, but in certain circumstances, such as during heavy traffic, its concentration may reach values as high as 150-200 ppm [15] [16]. In the present study, male Wistar rats (6 weeks old, n=35) were submitted to permanent ligation of the left coronary artery or were sham operated as previously described [17]. Seven weeks after artery ligation, rats were exposed to CO in an airtight exposure container for 4 weeks as previously described (André et al., 2009). Briefly, rats were exposed to a basal CO concentration of 30 ppm during a 12 hours period completed with 5 peaks of 100 ppm (1 hour each), to reproduce air quality variations environmentally relevant. For the remaining 12 hours, the CO group of rats was exposed to filtered air (< 1 ppm CO). The CO content was monitored with an aspirative CO analyzer (CHEMGARD Infrared Gas Monitor NEMA 4 Version, MSA). The rats exposed to CO pollution were compared with MI animals exposed to filtered ambient air. Sham-operated animals served as controls. All rats were fed ad libitum with standard rodent chow and free tap water in room with a 12:12-h light-dark cycle and a temperature of 21°C.

Cardiac morphology and function *in vivo*

Doppler-echocardiography was performed using a MyLab 25 echograph (ESAOTE, Italy) as described [17]. Left ventricular end-diastolic (LVEDd) and end-systolic (LVESd) diameters as well as wall thicknesses (anterior and posterior) were measured on a parasternal short axis view at the level of papillary muscles. LV shortening fraction and end-systolic strain of the posterior wall, measured as deformation from end diastole to end systole [17], were calculated. Peak velocities of early diastolic rapid inflow (E), of atrial contraction filling (A) were recorded for E/A wave peak velocity ratio calculation from pulsed-wave Doppler spectra of mitral inflow on apical view. Ascending aortic blood flow was recorded, as previously described via pulsed-wave Doppler permitting measurements of the aortic velocity time integral [18].

Twenty four hours after echocardiography, the right carotid artery was canulated with a micromanometer-tipped catheter (SPR 407, Millar Instruments) in anesthetized rats (pentobarbital sodium, 60 $mg.kg^{-1}$, i.p) to enable the recording of peak systolic, diastolic, and mean arterial pressures, as previously described [19]. The catheter was then advanced into the LV to record the intraventricular pressure and its maximal rate of rise ($LVdP/dt_{max}$) and decrease ($LVdP/dt_{min}$) as well as the relaxation time constant decay (tau). Measurements were made before and after β-adrenergic challenge with isoproterenol perfusion (1 $mg.kg^{-1}.min^{-1}$). The analog outputs of the arterial pressure, LV pressure and heart rate were collected on a MP35 module (Biopac system, Gotela, Santa-Barbara, USA).

Coronary perfusion

Evaluation of myocardial perfusion was performed on a second set of rats under basal condition (n=10 per group) and during a β-adrenergic challenging obtained by isoproterenol infusion (1 mg.kg-1.min-1) (n=10 per group). Fluorescent microspheres (15.0±0.2 μm diameter, Dye-Track Fluorescent Yellow part 130–0485, Triton Technology) were used for myocardial perfusion assessment as previously reported [20]. Briefly, we injected 105 microspheres in 0.5 ml of the suspension in the LV. The arterial pressure waveform was monitored continuously to verify proper delivery of microspheres. The microspheres were allowed to flush during 1 min and the heart was immediately removed and placed in cold physiological salt solution for ventricular dissection. The LV (including septum) was placed for 48 hours in 20 ml of 4 N KOH containing 2% Tween 80 for tissue digestion. Microspheres were physically separated from digested tissues by negative pressure filtration. Filters containing microspheres (part 31079, DYE-TRAK, Triton Technology) were placed in 2 ml of solvent (2-ethoxyethyl acetate, Sigma-Aldrich). The peak fluorescent spectrum was read at 485 nm for an excitation wavelength of 450 nm with a spectrofluorometer (Synergy HT, Biotek).

ECG recording, arrhythmias and heart rate variability in vivo

Eighteen rats were implanted for ECG telemetry recordings (Dataquest, Data Sciences International, Transoma Medical, Arden Hills, Minnesota, USA). Surface ECG recordings were performed for a 24 h period started one week after anesthesia and surgery. Then, animals were exposed to filtered air or CO for 4 weeks and ECG were recorded again for 24 h, with an additional 2 h period during which the rats were challenged with isoproterenol injection (1 $mg.kg^{-1}$, i.p). ECG signals were scanned by hand to detect, identify and count spontaneous rhythmic disorders. Subsequently, on the same recordings, heart rate variability was analyzed

in time domain. The mean RR intervals (RR) and the standard deviation of all normal RR intervals (SDNN) were calculated from 24 h ECG.

Cardiac excitation-contraction coupling investigation

Cardiomyocyte isolation: Single ventricular myocytes were isolated by enzymatic digestion [17]. Briefly, hearts were quickly removed and mounted on a Langendorff apparatus. Each heart was perfused 10 min with a Ca^{2+}-free Hanks-HEPES solution followed by perfusion with an enzymatic solution (1.25 $mg.mL^{-1}$ collagenase type IV, Worthington Freehold, NJ, U.S.A) for 10-20 min at 37°C. Small pieces of tissues from the LV were dissected and gently dissociated with a pipette in Ca^{2+} free solution. Ca^{2+} concentration was gradually increased to 1 mM Ca^{2+}. Hanks-HEPES solution for isolating intact cells contained (mM): NaCl 117, KCl 5.7, $NaHCO_3$ 4.4, KH_2PO_4 1.5, $MgCl_2$ 1.7, HEPES 21, glucose 11, taurine 20, pH 7.2 adjusted with NaOH.

Ca^{2+} transient and cell fractional shortening: To measure Ca^{2+} transient and cell shortening, cells were loaded for 30 min at room temperature (22±2°C) with Indo-1 AM (10 µM Invitrogen inc., France). Experiments were performed in 1.8 mM Ca^{2+} containing solution. Cells were electrically stimulated at a frequency of 0.5 Hz (20 V, 1 ms), and simultaneously illuminated at 360 nm using a xenon arc bulb light. Sarcomere length (SL) and fluorescences, emitted at 405 nm and 480 nm, were simultaneously recorded using IonOptix acquisition software (IonOptix system, Hilton, USA). Measurements were done in basal conditions and after a β-adrenergic stimulation with isoproterenol (100 nM).

Force measurements in permeabilized cardiomyocytes: Cardiomyocytes were permeabilized with 3% Triton X100 in relaxing solution. The active force was measured as described [21]. Myocytes were attached to a piezoresistive strain gauge (AE801 sensor, Memscap, Crolle, France) and to a stepper motor driven micromanipulator (MP-285, Sutter Instrument Company, Novato CA, USA) with thin needles and optical glue (NOA 63, Norland products Inc, North Brunswick, NJ) polymerized after 2 min UV illumination. SL was determined online throughout the experiment at 50 Hz (IonOptix system). Force was normalized by the cross-sectional area measured from the imaged cross-section. The relationship between Ca^{2+} activated force and the internal Ca^{2+} concentration was measured at 2.3 µm SL and was fitted with a modified Hill equation. In some experiments permeabilized cardiomyocytes were incubated with a recombinant catalytic subunit of protein kinase A (PKA, Sigma) for 50 min at room temperature as described previously [22].

Ca^{2+}-activating solutions were prepared daily by mixing relaxing (pCa 9.0) and maximal activating (pCa 4.5) solutions. The relaxing and activating solutions contained (in mM): phosphocreatine 12, imidazole 30, free Mg2+ 1, EGTA 10, Na2ATP 3.3, and dithiotreitol 0.3 with pCa 9.0 (relaxing solution) and pCa 4.5 (maximal activating solution), protease inhibitors (PMSF 0.5, leupeptin 0.04, and E64 [trans-epoxysuccinyl-1-leucine-guanidobutylamide] 0.01), pH 7.1 adjusted with acetic acid. Sufficient potassium acetate was added to adjust ionic strength to 180 mM.

Protein analysis

Ca^{2+} handling: Proteins were extracted from intact myocytes 30 min at 4°C in a lysis buffer containing in mM : Tris-HCl 50, NaCl 200, β-glycerophosphate 20; NaF 50, EDTA 2,

benzamidin 10, Na_3VO_4 0.2, DTT 5, Triton 1% and proteases inhibitors. Protein concentration was determined with RCDC kit (Bio-Rad). Proteins were denatured 15 min at 37°C in a Laemmli modified buffer containing in mM : Tris-HCl 50, SDS 3%, urea 8, thio-urea 2, β-glycerophosphate 20; NaF 50, EGTA 1, EDTA 2, benzamidin 10, Na_3VO_4 0.2, DTT 75, SDS 3% and proteases inhibitors. Proteins were separated on a 2-20 % SDS-PAGE and blotted onto PVDF membrane (Protran, Schleichen and Schuele, Dassel, Germany). Membranes were blocked 30 min in 3% BSA TBS-Tween. Primary antibodies were incubated overnight at 4°C: RyR-2 antibody (Covalab, France), Phospho ser^{2809}-RyR-2 antibody (A010-30, badrilla, UK), SERCA-2a antibody (A010-20, Badrilla, UK), PLB antibody (A010-14, Badrilla, UK). RyR-2, SERCA-2A and PLB were expressed relative to Calsequestrin content (Cat # PA1-913, ABR, USA) on the same membrane. Immunodetection was revealed with ECL Plus system (Amersham Pharmacia, Little Chalfont Buckinghamshire, England).

Myofilament proteins: Myofibrilar proteins were analyzed on LV skinned muscle strips as described previously [21]. The heart was pre-skinned by perfusing relaxing solution containing 1% Triton X-100 and protease inhibitors (for composition see above) for 10 min. Skinned LV strips (8-mm long, 2-mm width, 1-mm thick) were dissected in the skinning solution under a microscope following the orientation of the fibers, and frozen in liquid nitrogen. Samples were treated with ice cold trichloroacetate (TCA 10%) to maintain contractile protein phosphorylation status, washed 3 times in acetone/10mM DTT, and then pellets were dried and mixed 1 h at room temperature with urea buffer (containing in M : urea 8, Tris 0.2, glycine 0.25, dithiotreitol (DTT) 0.5, sucrose saturated, ethylenediaminetetraacetic acid (EDTA) 0.4, proteases inhibitors). Phosphorylated and non-phosphorylated MLC-2 forms were separated on 10% urea gel and specifically detected with a cardiac MLC-2 antibody (Coger SA, Paris, France). TnI was separated on 15 % SDS-PAGE and revealed with a total cardiac TnI antibody (Cat#4T21, Hytest, Turku, Finland) and the PKA phosphorylated form of cardiac TnI antibody (Cat#4T45, Hytest). PKA activity was measured using a non-radioactive PKA activity assay kit (Assay design). Tissue extracts originated from ENDO and EPI layer were mixed with ATP for 90 minutes. Phosphospecific and anti-rabbit antibody were consecutively added before measuring the absorbance at 450 nM.

Measurement of mitochondrial NADH

The endogenous autofluorescence of mitochondrial NADH was measured using a two-photons excitation at 720 nm and its emission recorded at λem=450-485 nm in the same cells. Fluorescence images were recorded using a Zeiss LSM 510 inverted two photons confocal microscope with x20 lens. Cells were paced at 0.5 Hz using two platinum electrodes placed in each side of the Petri dish. NADH fluorescence was collected at rest and after 5 min stimulation. For each cell, resting value was set to 100% and background noise was subtracted by measuring fluorescence close to the cell.

Measurement of mitochondrial Ca^{2+}

Rhod-2 AM was used to measure mitochondrial Ca^{2+} (Trollinger, 1997 #69). Isolated cardiomyocytes were loaded with rhod-2 AM (10 μmol/l) for 45 min at 37°C followed by washout. Fluorescence images were recorded using a Zeiss LSM 510 inverted confocal microscope with x40 lens. Confocal images were obtained at 5-min intervals by excitation at 568 nm and measuring the emitted light at 585 nm. Rhod-2 fluorescence was collected at rest and after 5 min stimulation. For each cell, rhod-2 fluorescence value was calculated as the

mean of 3 different values collected at 3 different locations. Resting value was set to 100% and background noise was subtracted by measuring fluorescence close to the cell.

Measurement of mitochondrial ROS production

MitoSOX Red was used to measure mitochondrial $O_2^{\cdot -}$ production as previously described (Fauconnier, 2007 #18). Isolated cardiomyocytes were loaded with MitoSOX Red (5 µmol/L Invitrogen inc., France) for 15 min at room temperature, followed by washout. Fluorescence images were recorded using a Zeiss LSM 510 inverted confocal microscope with x25 lens. Confocal images were obtained at 5-min intervals by excitation at 488 nm and measuring the emitted light at 583 nm. MitoSOX Red fluorescence was collected at rest and after 5 min stimulation. For each cell, resting value was set to 100% and background noise was subtracted by measuring fluorescence close to the cell.

Determination of antioxidant and mitochondrial enzymatic activities in cardiomyocytes

After cell lysis in hypotonic buffer (phosphate buffer 8mM, pH 7.4), catalase activity was measured according to the method of Beers and Sizer (Beers, 1952 #20) and total superoxide dismutase (SOD) was measured according to the method of Marklund (Marklund, 1976 #21). Protein levels in cells lysates were measured by the Bradford technique (Bradford, 1976 #15). Citrate synthase (CS #0) activity was measured according to Srere (Srere, 1970 #23): the activity of the enzyme was measured by following the color of 5-thio-2-nitrobenzoic acid, which was generated from 5,5'-dithiobis-2-nitrobenzoic acid present in the reaction of citrate synthesis, and caused by the deacetylation of Acetyl-CoA.
Complex I of the electron transport chain (ETC) was evaluated through measure of the reduction of the 2 ,6 – dichlorophenolindophenol by the NADH dehydrogenase at 600 nm (37°C) (Janssen, 2007 #71). Complex IV of the ETC was measured through the measure of the cytochrome-c oxidase (Cyt-c oxidase) activity according to Wharton and Tzagoloff (Wharton, 1978 #22): oxidation of reduced cytochrome c was followed spectrophotometrically.

Statistical analysis

The statistical analysis was performed using Statview 5.0 (SAS Institute, Cary, NC, USA). Data are presented as mean ±SEM, otherwise specified. Effects of CO exposure, time and/or β-adrenergic challenge were analyzed using one-way factorial ANOVA or ANOVA with repeated measures depending on variables. These were followed by Bonferroni's *post-hoc* tests where appropriated. Statistical significance was defined as $p<0.05$.

3. Results

MI-associated cardiac dysfunction was aggravated by CO

Coronary ligation induced cardiac morphological and functional remodelling in MI rats when compared to sham aniamls (Table 1). Eleven weeks after coronary ligation, echocardiographic data (Table 1) showed LV remodelling characterized by chamber dilatation, akinetic anterior wall motion and posterior wall hypertrophy. LV hypertrophy was confirmed by *post mortem* dissection demonstrating a significant increase of heart/body weight and LV/body weight ratio (Table 1). MI rats also exhibited systolic function impairment characterized by a decrease of LV shortening fraction and posterior wall end-systolic strain. Global diastolic function was also impaired with a significant increase of peak early/peak late diastolic velocity ratio. With regard to haemodynamic data, coronary ligation induced a decrease of SBP as well as contractile (dP/dtmax) and relaxation (dP/dtmin) indexes of the LV. Nevertheless, resting mean arterial pressure and abdominal aortic flow were unchanged vs.sham rats.
Chronic CO exposure of MI rats altered heart morphology and posterior wall function when compared to their filtered-air exposed counterparts. MI-CO rats exhibited hypertrophic features, with increased heart/body weight as well as LV/body weight ratio when compared to MI (Table 1). Echocardiographic measurements revealed that increased posterior wall thickness was associated with significant contractile dysfunction of the posterior wall characterized by an altered posterior wall end-systolic strain (Table 1). Taken together, our data suggest that chronic CO exposure in MI rats has significant effect on *in vivo* LV regional function with no major consequences on global resting haemodynamic features already impaired by HF.

Effects of CO exposure on arrhythmia *in vivo*

Surface ECGs were recorded and analyzed in conscious animals. The number of single ventricular extrasystole (VES) was increased in MI rats, but unmodified with CO exposure. However, the number of three consecutive VES increased in MI rats and was potentiated in MI-CO rats. On the other hand, the occurrence of sustained tachycardia, absent in controls, was detected in MI rats and was also enhanced in MI-CO rats. We thus provide direct evidence that chronic CO pollution aggravated the arrhythmic phenotype of MI rats (Figure 1).

CO pollution exacerbated cardiac ECC remodeling of MI rats

The cell fractional shortening (reflecting contraction) was decreased in intact ventricular myocytes of MI rats (Figure 2A). This decrease was associated to a reduction of the maximal speeds of cell contraction (2.6±0.2 $\mu m.s^{-1}$ in Sham *vs.* 1.2±0.1 $\mu m.s^{-1}$ in MI rats) and relaxation (2.4±0.2 $\mu m.s^{-1}$ in sham *vs.* 1.7±0.2 $\mu m.s^{-1}$ in MI rats), as indexed by the first derivative of cell shortening and lengthening (delta SL/delta time). CO pollution worsened the decrease of cell shortening in MI rats without modifying the kinetics of both contraction and relaxation (Figure 2A).

Contractile machinery properties
To determine the reasons underlying the CO pollution-induced contractile defects, we investigated the contractile machinery properties. We measured the relationship between the Ca^{2+} activated force and the internal Ca^{2+} concentration in single permeabilized LV myocytes

(Figure 2B). Maximal isometric tension was decreased in MI rats compared to shams. CO exposure exacerbated this contractile alteration. Moreover, the rightward shift in the tension-pCa curve (an index of myofilament Ca^{2+} sensitivity, pCa_{50}) previously observed in MI rats [21] was amplificated with CO pollution. Myofilaments Ca^{2+} sensitivity is regulated by the phosphorylation status of some sarcomeric proteins such as MLC2 and cTnI [23]. In MI rats, the phosphorylation level of MLC2 did not change but was increased for cTnI at PKA sites ($Ser^{23/24}$) (Figure 2C). CO exposed rats displayed reduced MLC-2 phosphorylation when compared to MI-rats, without modifications for TnI-phosphorylation.
Force development of cardiomyocytes depends on both the Ca^{2+} sensitivity of the contractile machinery and the amount of Ca^{2+} released. We thus evaluated whether Ca2+ signaling could be altered by CO.

Ca^{2+} handling
We next investigated the effects of chronic CO exposure on the intracellular Ca^{2+} in indo-1 loaded cardiomyocytes stimulated at 0.5 Hz. As previously described, MI rats cardiomyocytes were characterized by Ca^{2+} handling remodeling including increased diastolic Ca^{2+} (Figure 3A) [24], decreased Ca^{2+} transient amplitude [25] and lengthening of Ca^{2+} reuptake time (tau) compared to the sham group (Figure 3B). The SR-Ca^{2+} load, assessed by caffeine application (10 mM) was also reduced in MI rats (Figure 3C), consistent with others [26]. Thus, CO pollution exacerbated the cellular diastolic Ca^{2+} overload, the reduction of systolic Ca^{2+} release and the SR Ca^{2+} load observed in MI rats. However, no modification for Ca^{2+} reuptake was observed.
Mitochondria is an other organelle which plays a crucial role in Ca^{2+} homeostasis regulation though uptake and release of Ca^{2+} during each cardiac cycle in order to match contractile demand and energetic supply within the cell [27]. We thus evaluated whether the Ca^{2+} handling defects in MI-CO rats could be attributed to an alteration in mitochondrial Ca^{2+} homeostasis. Mitochondrial Ca^{2+} during diastole was unchanged in MI rats after cell stimulation, but chronic CO exposure increased this mitochondrial Ca^{2+} overload by 12% in MI-CO rats (Figure 3D).

To investigate the molecular basis of Ca^{2+} signaling alterations, we performed western blot analysis on some Ca^{2+} handling proteins. The observed diastolic Ca^{2+} increase in MI rats could be due to a Ca^{2+} leak through the ryanodine receptors (RyR-2) of the SR during the diastolic phase or an altered Ca^{2+} reuptake through the sarcoplasmic (SERCA-2a[28]. RyR-2 protein abundance was not affected in MI rats (Figure 3E, right panel). However, it increased the level of phosphorylation of the RyR-2 on the PKA-dependent site Ser^{2809} which has been shown previously to promote Ca^{2+} leak [26]. The slowed (e.g. increase in tau) of the Ca^{2+} transient decay in MI myocytes (Figure 3B) was consistent with an impairment of Ca^{2+} reuptake due to a diminished SERCA-2a expression or an inhibition of the SERCA-2a/PLB activity. We found that SERCA-2a expression was decrease in MI rats with no effect on PLB expression (Figure 3E, right panel). Although CO pollution promoted exacerbation of MI-induced Ca^{2+} homeostasis remodeling, no modifications were observed regarding the RyR-2, SERCA-2a, and PLB content and their phosphorylation status in MI-CO rats.
Altogether, these data demonstrated that chronic CO exposure exacerbates the pathological cellular phenotype in MI rats by modifying various steps of the excitation-contraction coupling.

CO pollution altered mitochondrial function and increased oxidative stress
CO is known to alter mitochondrial metabolic properties, notably through binding to cytochrome p-450 [29]. We then evaluated the mitochondrial function after 4 weeks of CO

exposure in MI rats. Cardiac metabolism requires important oxygen delivery to allow oxidative phosphorylation. We showed here that CO pollution aggravate the HF-associated reduction in coronary perfusion, an index of oxygen delivery to heart pump (Figure Supplemental data 1A). Within the cardiomyocyte, mitochondria use oxygen to oxidize the reduced redox carriers NADH and $FADH_2$ through complexes (I-IV) of the electron transport chain (ETC) in order to provide ATP (Stanley, 2005 #72). We measured NADH autofluorescence after 5 minutes of 0.5 Hz stimulation, as an index of the oxidative metabolism (Droge, 2002 #24),(Maack, 2006 #74),(Liu, 2008 #73) because NADH autofluorescence reflects the balance between NADH production by tricarboxylic acid cycle and NADH oxidation within the ETC. In MI rats, NADH autofluorescence decline was smaller compared to sham rats (55% +/- 3% *vs.* 34% +/- 3%, respectively; † $p<0.05$) Figure Supplemental data 1B). NADH oxidation was weaker in failing cardiomyocytes after 4 weeks of CO exposure in MI rats (27% +/- 2% *vs.* 34% +/- 3%, respectively; * $p<0.05$).
We next evaluated whether this NADH accumulation could be attributed to reduced ETC activity by evaluation of complex I and IV content and Cyt-c Oxydase activity normalized to citrate synthase (CS), an index of cellular mitochondria content. Cyt-c Oxydase activity was decreased in MI rats. Nevertheless, Cyt-c Oxydase activity was not affected by CO exposure (Figure Supplemental data 1C). In addition, both complex I and IV content were reduced in MI rats compared to sham. CO exposure did not modify complex I activity but exacerbated the reduced content of complex IV in MI rats (Figure Supplemental data 1C). All together, these results indicate that the altered mitochondrial metabolism in MI rats was more pronounced after 4 weeks of CO exposure.

Under conditions of inefficient oxidative metabolism mainly due to reduced complex I activity [30 31 32], as well as during mitochondrial Ca^{2+} overload [33], ROS production may be increased. We next measured mitochondrial $O_2^{\cdot-}$ production after 5 minutes stimulation using MitoSOX Red, which is targeted to the mitochondria and increases its fluorescence when oxidized [34]. MI rats exhibited a higher mitochondrial ROS production after 5 minutes stimulation when compared to sham rats (27% +/- 5% *vs* 13% +/- 4%, respectively; *$p<0.05$) (Figure 4A). After 4 weeks of CO exposure, the ROS production was exacerbated in MI rats (35% +/- 4% *vs.* 27% +/- 5%, respectively; *$p<0.05$) (Figure 7A). Oxidative stress results from an imbalance between pro-oxidant activities and antioxidant defense buffering ROS. We thus evaluated antioxidant enzyme activities: SOD which converts $O_2^{\cdot-}$ to H_2O_2, and catalase which converts H_2O_2 to H_2O. Both SOD and catalase activities were reduced in failing cardiomyocytes compared to sham. CO exposure did not modify SOD activity but catalase activity was decreased (Figure 4A). Taken together, these results indicate that the pre-existent oxidative stress in MI rats is exacerbated after 4 weeks of CO pollution.

Oxidative stress may affect Ca^{2+} handling [35] and myofilament properties (Hertelendi, 2008 #16) in cardiomyocytes originated from failing hearts. In order to determine whether ROS affect contractility, we measured cell shortening after incubating cardiomyocytes with the non specific antioxidant N-acetylcystein (NAC, 20 mmol/l) for 1 hour. After NAC treatment, cell shortening was normalized between MI and MI-CO rats. This positive antioxidant effect was due to normalization of both Ca^{2+} handling (diastolic Ca^{2+} and systolic Ca^{2+} release), and contractile machinery properties (myofilament Ca^{2+} sensitivity) (Figure 4B). All together, these results suggest that the deleterious effect of 4 weeks of low level CO exposure on cardiac function was ROS-dependent.

CO pollution did not modify the cardiac β-adrenergic responses

The mechanisms underlying ECC remodeling in MI-CO rats could involve a beta adrenergic defects since we had previously shown that 4 weeks of CO pollution increased β-adrenergic tone and decrease the cardiac reserve in CO-exposed healthy rats [13]. We thus investigated the cardiac response to a β-adrenergic stimulation both *in vivo* and *in vitro*.
In vivo, isoproterenol perfusion induced β-adrenergic stimulation characterized by an increase of LV dP/dtmax and dP/dtmin which was blunted in MI rats when compared to sham (Figure 5A). Nevertheless, CO exposure did not alter these responses in MI-CO rats.

At the cardiomyocyte level, β-adrenergic stimulation activates PKA, which in turn phosphorylates both Ca^{2+}-handling proteins involved in excitation-contraction coupling (RyR, PLB) and myofilament regulatory proteins (cTnI and MyBP-C). In our study, the positive inotropic effect of isoproterenol (100 nM) on cell shortening was smaller in myocytes from MI animals than from controls (Figure 5B, left panel). However, the potentiating effect of isoproterenol on Ca^{2+} transient amplitude was similar in control and MI myocytes (Figure 5B, right panel) and CO exposure did not change the β-adrenergic state of cardiomyocyte originated from MI-CO rats. Incubation of permeabilized myocytes with a recombinant catalytic subunit of PKA (Figure 5C) led to classic myofilament Ca^{2+} desensitization (decrease in pCa_{50}). In addition, PKA activity was altered by MI but not by CO exposure (Figure 5D) Taken together, these data indicate that the altered β-adrenergic response observed in MI animals was not worsen by a chronic exposure to CO pollution.

Cardiac protective effects of exercise training

Exercise training is now admitted and recommended in patients with HF to improve their quality of life, &s well as morbidity and mortality [36]. Improves of cardiac function occurs notably through reduction of oxidative stress. We thus evaluated whether this potential antioxidant therapy could prevent the CO-associated cardiac damages evidenced in our MI rats. Exercise training performed 4 weeks before and during the CO-exposure protocol in ambient air completely prevented the CO-associated morpho-fonctional remodeling in vivo through restoration of alterations of cell shortening, diastolic Ca^{2+}, systolic Ca^{2+} release and myofilament Ca^{2+} sensitivity (Figure 6B) in MI rats.

4. Discussion

It is well established that air pollution is associated with cardiovascular complications and can cause premature death in HF patients. However, the mechanisms underlying these effects are poorly understood. In an animal model, we found that exposure of myocardial infarcted rats to CO for a period limited to 4 weeks under conditions mimicking urban air pollution exacerbated the MI-associated cardiac remodelling resulting in increased occurrence of ventricular tachycardia. The cellular origin for the aggravation of HF phenotype involved a remodeling of both Ca^{2+} handling and contractile machinery properties secondary to mitochondrial dysfunction. To our knowledge, our data provide the first evidence at the cardiomyocytes level that chronic CO exposure exacerbates the cardiac dysfunction which occurs during HF. The CO-associated cardiac defects were completely prevented by regular physical activity, thus promoting exercise as a preventive therapeutics for people exposed to urban pollution.

A key finding of the present study is that chronic CO exposure exacerbated the post myocardial infarction remodelling and subsequent contractile dysfunction and could therefore contribute to accelerate the course towards decompensated heart failure. This global cardiac aggravation results from remodelling of contractile machinery properties and Ca^{2+} handling in cardiomyocyte. Indeed, we show in the present study a recompartimentalization of Ca^{2+} within the cardiomyocyte characterized by increased Ca^{2+} concentration in both cytosol and mitochondria. Although I_{CaL} was increased by CO exposure, the subsequent systolic Ca^{2+} release, an element conditioning the contractile force, was decreased and associated with a reduced SR Ca^{2+} load and increased diastolic Ca^{2+}. Mechanisms underlying cytosolic Ca^{2+} overload and reduced SR Ca^{2+} load involve either reduced Ca^{2+} reuptake *via* SERCA-2a and/ or Ca^{2+} leak through RyR-2. As the SERCA-2a content was not modified after CO exposure during HF, it suggested a direct RyR-2 dysfunction. The HF-associated hyperadrenergic tone and subsequent PKA activation is directly involved in RyR-2 dysfunction during HF through an hyperphosphorylation sate of the channel [26 37]. However, we show here that the cardiac response to adrenergic stimulation did not differ in CO-exposed animals both *in vivo* and *in vitro.* In addition, PKA activity was unchanged after CO exposure, suggesting an absence of PKA-mediated CO troubles during HF. Accordingly, the exacerbation of the myofilament Ca^{2+} sensitivity defects consecutive to CO exposure involve a reduction in the phosphorylation of MLC-2, independently of a PKA pathway. Although we had previously reported that CO exposure increased β-adrenergic activation in healthy population, it seems here, that the adrenergic tone already reached a maximal level in failing hearts, thus making them insensible to CO.

The second mechanism involved in HF-associated RyR-2 dysfunction is the redox modulation of the channel. Indeed, it has been shown that oxidative stress promotes disruption of the channel-stabilizing FK506 Binding Protein12.6 [38 39] resulting in Ca^{2+} leak [40]. We show here that the deleterious effects of CO pollution in failing cardiomyocyte involve a higher oxidative stress. Indeed we provide evidence that 4 weeks exposure to CO pollution increases the mitochondrial $O2^{\cdot-}$ production. Acute treatment with antioxidant NAC completely recovered the Ca^{2+} handling defects, thus supporting a major role of ROS in the CO-induced contractile dysfunction during HF. Moreover, NAC recovered the myofilament Ca^{2+} sensitivity.

Origin of this CO-aggravated oxidative stress during HF could involve the CO biochemical properties. Indeed, it is well documented that CO binds to cytochrome-c oxidase (complex IV) inhibiting the ETC [29] and interacts with nitric oxide-synthase, leading to peroxynitrite generation [41]. We show here that CO reduced complex IV activity thus preventing a correct mitochondrial metabolism. A reduced oxidative capacity is frequently associated with ROS production. On the other hand, we show that catalase activity was still more affected in CO-exposed rats. Thus the both increase of ROS production and reduce antioxidant defenses activity underlie the CO-associated oxidative stress.

Clinical relevance:
In the present study we show that 4 weeks exposure to low CO levels mimicking urban atmospheric pollution potentiates HF-associated cardiac remodelling. Chronic CO pollution worsens pre-existent cardiac dysfunction in pathological population thus providing an explanation for epidemiological reports. These results suggest that pollution, identified as a cardiovascular risk factor, should be considered in clinical follow-up of patients with cardiomyopathy.

Since ROS are centrally involved in the deleterious effects of CO pollution, antioxidant therapy could provide cellular protection against pollution effects. Consistently, exercise training, which stimulates antioxidant protection, conducted before and during CO exposure protocol in ambient air prevented cardiac dysfunction both *in vivo* and at the cellular level.

Legends

Table 1: Effects of chronic CO exposure on cardiovascular function and cardiac morphology *in vivo*.
Body wt: body weight; LVEdD: left ventricular end-diastolic diameter; LVEsD: left ventricular end-systolic
diameter; LV dP/dt max and LV dP/dt min: maximal and minimal first derivative of left ventricular pressure; E/A: early (E) to atrial (A) peak velocity waves ratio recorded from mitral inflow performed in pulsed doppler mode; LV tau: time constant of left ventricular pressure decay. † $p<0.05$ *vs.* Sham, * $p<0.05$ *vs.* MI

Figure 1: CO pollution aggravated arrhythmic phenotype in MI rats *in vivo*. A: Representative examples of ventricular ectopic beat and tachycardia occurring during ECG recordings in MI-CO rats **B:** Analysis of the occurrence of isolated and triple premature ventricular beats (PVB), and tacchycardia in Sham, MI and MI-CO rats (6-8 rats)* $P<0.05$.

Figure 2: CO provoked contractile dysfunction in MI rats. A: Left panel: Representative traces of cell shortening at 0.5 Hz myocytes isolated from Sham (full line) and MI rats (dark dash line). Right panel: Averaged datas of SL shortening, contraction and relaxation velocities of Sham, MI and MI-CO cells (35-50 cells / 4-5 hearts). **B:** Left panel: Averaged tension-pCa curves of Sham, MI and MI-CO permeabilized cardiomyocytes. Right panel: Averaged datas of maximal active tension and myofilament Ca^{2+} sensitivity (pCa_{50}) of Sham, MI and MI-CO cardiomyocytes isolated (11-18 cells / 4 hearts). D: Effect of CO on the phosphorylation level of MLC-2 in permeabilized cardiac strips from Sham, MI and MI-CO rats. Phosphorylation levels were determined by Western blotting with antibodies to P-MLC2 * $P<0.05$.

Figure 3: Chronic CO pollution alters the Ca^{2+} dynamics of ventricular myocytes. A: Left panel: Superimposed Ca^{2+} transients in intact myocytes isolated from Sham, MI and MI-CO cells. Right panel: Average diastolic intracellular Ca^{2+}. **B:** Left panel: Ca^{2+} transient amplitude and Ca^{2+} reuptake kinetics (tau) (n=58-84 cells/5 hearts). **C:** Average caffeine-pulsed SR Ca^{2+} load. **D:** Averaged datas of the variation of Rhod-2 fluorescence of Sham, MI and MI-CO cardiomyocytes after a stimulation train at 0.5 Hz, expressed as the variation from the resting state (9-16 cells / 4 hearts). **E:** Effect of chronic exposure to CO on the abundance of Ca^{2+} handling proteins (RyR-2, PLB, and SERCA-2a), analyzed by Western blot analysis. Protein content was normalized to calsequestrin content and Ser^{2809} RyR-phosphorylation normalized to total RyR-2 content. Results are mean±S.E.M. for 5 hearts. * $P<0.05$.

Figure 4: Oxidative stress is responsible for CO-associated ECC defects in MI rats. A: Right panel: Averaged data of MitosoxRed fluorescence of Sham, MI and MI-CO cardiomyocytes recorded at 0.5 Hz (32-40 cells / 4 hearts). Left panel: SOD and catalase activities in cardiomyocytes from Sham, MI and MI-CO rats (9-14 cells / 5 hearts). * $P<0.05$ *vs.* Sham. **B**: Averaged data of SL shortening, diastolic Ca^{2+}, Ca^{2+} transient amplitude and pCa50 in Mi and MI-CO cells incubated with NAC (20mM) (10-48 cells / 4 hearts).

Figure 5: Effect of CO pollution on the β-adrenergic reserve. A: Variation of the maximal first derivative (dP/dt max) and relaxation time constant (Tau) of LV pressure after isoproterenol injection ($1mg.kg^{-1}$; Iso-induced) evaluated *in vivo* in control and CO-exposed animals. (N= 9 rats in each group). **B:** Variation of contraction (SL shortening) and Ca^{2+} transients in isolated LV cells in presence of 100 nM isoproterenol (Iso-induced) (n=22-34 cells / 4-5 hearts). **C:** Myofilament Ca^{2+} sensitivity of Sham, MI and MI-CO cells after PKA treatment (100U/mL, incubation for 60 min) (n= 14-22 cells/4 hearts). **D:** Averaged data for PKA activity measured on cardiac tissue of Sham, MI and MI-CO cardiomyocytes. * $p<0.05$.

Figure 6: Exercise training prevents cardiac alterations *in vivo* and *in vitro*. B: Averaged data of SL shortening, diastolic Ca^{2+}, Ca^{2+} transient amplitude and pCa50 in Sham, MI, MI-CO, MI-Ex and MI-CO-Ex cells (10-44 cells / 4 hearts).

Supplemental data 1:

A: Averaged datas for coronary perfusion in Sham, MI and MI-CO rats (4-5 hearts) **B**: Averaged datas of the variation of NADH autofluorescence of Sham, MI and MI-CO cardiomyocytes after a stimulation train at 0.5 Hz, expressed as the variation from the resting state (25-38 cells / 4 hearts). **C**: Activities of citrate syntase (CS), and complex I and IV of the electron chain transporter of Sham, MI and MI-CO hearts (8 hearts for each group). * $P<0.05$

References

1. **Dockery DW, Pope CA, 3rd, Xu X, et al. An association between air pollution and mortality in six U.S. cities. *N Engl J Med.* Dec 9 1993;329(24):1753-1759.**
2. **Pope CA, 3rd, Burnett RT, Thun MJ, et al. Lung cancer, cardiopulmonary mortality, and long-term exposure to fine particulate air pollution. *Jama.* Mar 6 2002;287(9):1132-1141.**
3. **Jerrett M, Burnett RT, Pope CA, 3rd, et al. Long-term ozone exposure and mortality. *N Engl J Med.* Mar 12 2009;360(11):1085-1095.**
4. **Miller KA, Siscovick DS, Sheppard L, et al. Long-term exposure to air pollution and incidence of cardiovascular events in women. *N Engl J Med.* Feb 1 2007;356(5):447-458.**
5. **Brook RD, Franklin B, Cascio W, et al. Air pollution and cardiovascular disease: a statement for healthcare professionals from the Expert Panel on Population and Prevention Science of the American Heart Association. *Circulation.* Jun 1 2004;109(21):2655-2671.**
6. **von Klot S, Peters A, Aalto P, et al. Ambient air pollution is associated with increased risk of hospital cardiac readmissions of myocardial infarction survivors in five European cities. *Circulation.* Nov 15 2005;112(20):3073-3079.**
7. **Burnett RT, Dales RE, Raizenne ME, et al. Effects of low ambient levels of ozone and sulfates on the frequency of respiratory admissions to Ontario hospitals. *Environ Res.* May 1994;65(2):172-194.**
8. **Samoli E, Touloumi G, Schwartz J, et al. Short-term effects of carbon monoxide on mortality: an analysis within the APHEA project. *Environ Health Perspect.* Nov 2007;115(11):1578-1583.**
9. **Hickey RJ, Harner EB, Clelland RC. Smoking, pollution, and health. *Lancet.* Dec 23 1972;2(7791):1362-1363.**
10. **Peters A, Doring A, Wichmann HE, et al. Increased plasma viscosity during an air pollution episode: a link to mortality? *Lancet.* May 31 1997;349(9065):1582-1587.**
11. **Dales R. Ambient carbon monoxide may influence heart rate variability in subjects with coronary artery disease. *J Occup Environ Med.* Dec 2004;46(12):1217-1221.**
12. **Simkhovich BZ, Kleinman MT, Kloner RA. Air pollution and cardiovascular injury epidemiology, toxicology, and mechanisms. *J Am Coll Cardiol.* Aug 26 2008;52(9):719-726.**
13. **Andre L, Boissiere J, Reboul C, et al. Carbon Monoxide Pollution Promotes Cardiac Remodeling and Ventricular Arrhythmia in Healthy Rats. *Am J Respir Crit Care Med.* Dec 17 2009.**
14. **Meyer G, Andre L, Tanguy S, et al. Simulated urban carbon monoxide air pollution exacerbates rat heart ischemia-reperfusion injury. *Am J Physiol Heart Circ Physiol.* May;298(5):H1445-1453.**
15. **Stern FB, Halperin WE, Hornung RW, et al. Heart disease mortality among bridge and tunnel officers exposed to carbon monoxide. *Am J Epidemiol.* Dec 1988;128(6):1276-1288.**
16. **Wright GR, Jewczyk S, Onrot J, et al. Carbon monoxide in the urban atmosphere: hazards to the pedestrian and the street-worker. *Arch Environ Health.* Mar 1975;30(3):123-129.**

17. **Mou YA, Reboul C, Andre L, et al. Late exercise training improves non-uniformity of transmural myocardial function in rats with ischaemic heart failure. *Cardiovasc Res.* Feb 15 2009;81(3):555-564.**
18. **Reboul C, Tanguy S, Juan JM, et al. Cardiac remodeling and functional adaptations consecutive to altitude training in rats: implications for sea level aerobic performance. *J Appl Physiol.* Jan 2005;98(1):83-92.**
19. **Tanguy S, Morel S, Berthonneche C, et al. Preischemic selenium status as a major determinant of myocardial infarct size in vivo in rats. *Antioxid Redox Signal.* Aug 2004;6(4):792-796.**
20. **Kolarova J, Yi Z, Ayoub IM, et al. Cariporide potentiates the effects of epinephrine and vasopressin by nonvascular mechanisms during closed-chest resuscitation. *Chest.* Apr 2005;127(4):1327-1334.**
21. **Cazorla O, Szilagyi S, Le Guennec JY, et al. Transmural stretch-dependent regulation of contractile properties in rat heart and its alteration after myocardial infarction. *Faseb J.* Jan 2005;19(1):88-90.**
22. **Cazorla O, Szilagyi S, Vignier N, et al. Length and protein kinase A modulations of myocytes in cardiac myosin binding protein C-deficient mice. *Cardiovasc Res.* Feb 1 2006;69(2):370-380.**
23. **Solaro RJ. Multiplex kinase signaling modifies cardiac function at the level of sarcomeric proteins. *J Biol Chem.* Oct 3 2008;283(40):26829-26833.**
24. **Lehnart SE, Mongillo M, Bellinger A, et al. Leaky Ca2+ release channel/ryanodine receptor 2 causes seizures and sudden cardiac death in mice. *J Clin Invest.* Jun 2008;118(6):2230-2245.**
25. **Gomez AM, Valdivia HH, Cheng H, et al. Defective excitation-contraction coupling in experimental cardiac hypertrophy and heart failure. *Science.* May 2 1997;276(5313):800-806.**
26. **Marx SO, Reiken S, Hisamatsu Y, et al. PKA phosphorylation dissociates FKBP12.6 from the calcium release channel (ryanodine receptor): defective regulation in failing hearts. *Cell.* May 12 2000;101(4):365-376.**
27. **Shannon TR, Bers DM. Integrated Ca2+ management in cardiac myocytes. *Ann N Y Acad Sci.* May 2004;1015:28-38.**
28. **Cheng H, Lederer WJ. Calcium sparks. *Physiol Rev.* Oct 2008;88(4):1491-1545.**
29. **Piantadosi CA. Carbon monoxide poisoning. *N Engl J Med.* Oct 3 2002;347(14):1054-1055.**
30. **Pitkanen S, Robinson BH. Mitochondrial complex I deficiency leads to increased production of superoxide radicals and induction of superoxide dismutase. *J Clin Invest.* Jul 15 1996;98(2):345-351.**
31. **Luo X, Pitkanen S, Kassovska-Bratinova S, et al. Excessive formation of hydroxyl radicals and aldehydic lipid peroxidation products in cultured skin fibroblasts from patients with complex I deficiency. *J Clin Invest.* Jun 15 1997;99(12):2877-2882.**
32. **Ide T, Tsutsui H, Kinugawa S, et al. Mitochondrial electron transport complex I is a potential source of oxygen free radicals in the failing myocardium. *Circ Res.* Aug 20 1999;85(4):357-363.**
33. **Weiss JN, Korge P, Honda HM, et al. Role of the mitochondrial permeability transition in myocardial disease. *Circ Res.* Aug 22 2003;93(4):292-301.**
34. **Fauconnier J, Andersson DC, Zhang SJ, et al. Effects of palmitate on Ca(2+) handling in adult control and ob/ob cardiomyocytes: impact of mitochondrial reactive oxygen species. *Diabetes.* Apr 2007;56(4):1136-1142.**

35. Zima AV, Blatter LA. Redox regulation of cardiac calcium channels and transporters. *Cardiovasc Res.* Jul 15 2006;71(2):310-321.
36. Flynn KE, Pina IL, Whellan DJ, et al. Effects of exercise training on health status in patients with chronic heart failure: HF-ACTION randomized controlled trial. *Jama.* Apr 8 2009;301(14):1451-1459.
37. Wehrens XH, Lehnart SE, Huang F, et al. FKBP12.6 deficiency and defective calcium release channel (ryanodine receptor) function linked to exercise-induced sudden cardiac death. *Cell.* Jun 27 2003;113(7):829-840.
38. Yano M, Ikeda Y, Matsuzaki M. Altered intracellular Ca2+ handling in heart failure. *J Clin Invest.* Mar 2005;115(3):556-564.
39. Zissimopoulos S, Docrat N, Lai FA. Redox sensitivity of the ryanodine receptor interaction with FK506-binding protein. *J Biol Chem.* Mar 9 2007;282(10):6976-6983.
40. Terentyev D, Gyorke I, Belevych AE, et al. Redox modification of ryanodine receptors contributes to sarcoplasmic reticulum Ca2+ leak in chronic heart failure. *Circ Res.* Dec 5 2008;103(12):1466-1472.
41. Thom SR, Fisher D, Xu YA, et al. Adaptive responses and apoptosis in endothelial cells exposed to carbon monoxide. *Proc Natl Acad Sci U S A.* Feb 1 2000;97(3):1305-1310.

	Control (n=12)	MI (n=11)	MI CO (n=11)
Morphological data			
Body wt (g)	521 ± 7	532 ± 14	539 ± 12
Heart wt/100g body wt (mg/100g)	0.36 ± 0.01 †	0.47 ± 0.03 †	0.62 ± 0.04 †,*
Echocardiographic data			
LVEdD (mm)	9.46 ± 0.14	12.20 ± 0.21 †	12.50 ± 0.28 †
LVEsD (mm)	5.76 ± 0.17	10.68 ± 0.26 †	11.15 ± 0.34 †
Anterior wall thickness (mm)	1.02 ± 0.04	0.40 ± 0.06 †	0.34 ± 0.05 †
Posterior wall thickness (mm)	1.16 ± 0.03	1.37 ± 0.03 †	1.46 ± 0.04 †,*
LV shortening fraction (%)	39.2 ± 1.2	12.6 ± 0.8 †	10.9 ± 1.0 †
Posterior Wall End-systolic Strain (%)	98 ± 7	48 ± 5 †	31 ± 4 †,*
E/A-wave velocity ratio	1.9 ± 0.1	3.8 ± 0.5 †	4.7 ± 0.7 †
Haemodynamic data			
Systolic Arterial Pressure (mmHg)	126 ± 3	118 ± 3 †	116 ± 3 †
Diastolic Arterial Pressure (mmHg)	97 ± 3	96 ± 2	94 ± 2
Mean Arterial Pressure (mmHg)	106 ± 3	104 ± 2	101 ± 2
LV Developed Pressure (mmHg)	105 ± 4	102 ± 2	102 ± 3
LV dP/dt max ($mmHg.s^{-1}$)	5113 ± 161	4629 ± 150 †	4418 ± 181 †
LV dP/dt min ($mmHg.s^{-1}$)	-4494 ± 245	-3777 ± 105 †	-3911 ± 219 †
LV Tau (s)	8.19 ± 0.17	11.23 ± 0.68 †	11.77 ± 0.72 †

Table 1: Effects of chronic CO exposure on cardiovascular function and cardiac morphology *in vivo*. Body wt: body weight; LVEdD: left ventricular end-diastolic diameter; LVEsD: left ventricular end-systolic diameter; LV dP/dt max and LV dP/dt min: maximal and minimal first derivative of left ventricular pressure; E/A: early (E) to atrial (A) peak velocity waves ratio recorded from mitral inflow performed in pulsed doppler mode; LV tau: time constant of left ventricular pressure decay. † $p<0.05$ *vs.* Sham, * $p<0.05$ *vs.* MI

Figure 1

A

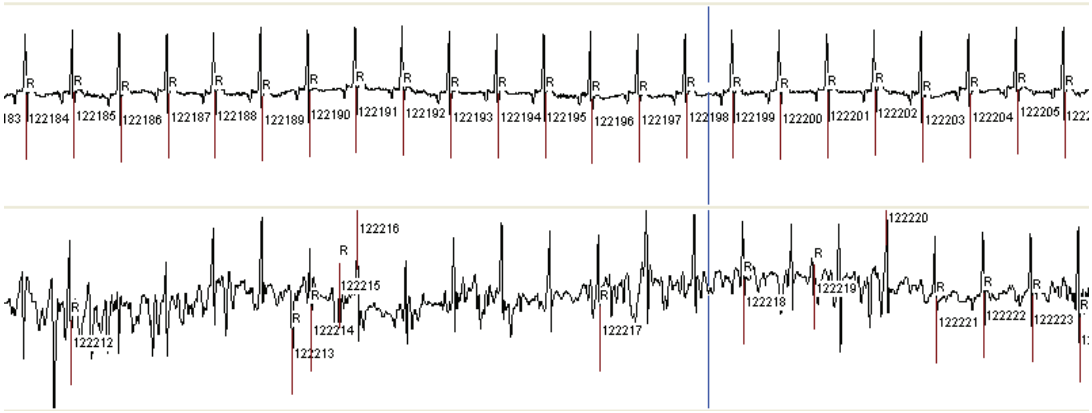
183 122184 122185 122186 122187 122188 122189 122190 122191 122192 122193 122194 122195 122196 122197 122198 122199 122200 122201 122202 122203 122204 122205
122212
122213
122214
122215
122216
122217
122218
122219
122220
122221
122222
122223

B

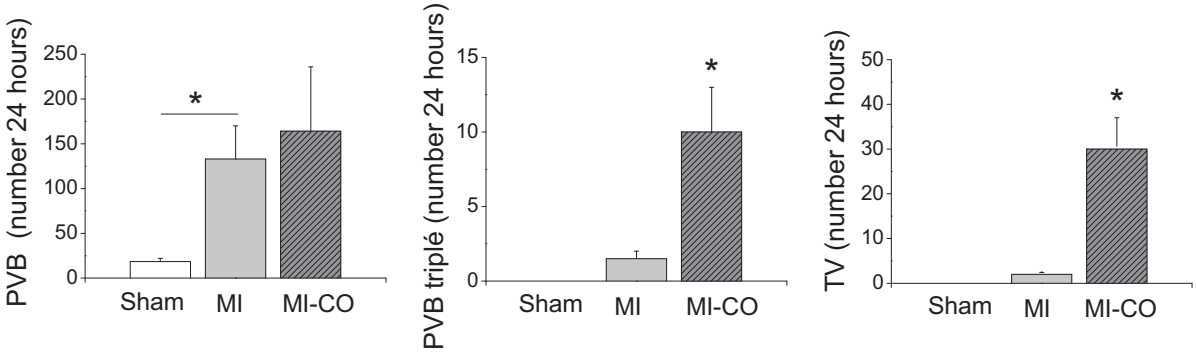
PVB (number 24 hours)
250
200
150
100
50
0
*
Sham
MI
MI-CO
PVB triplé (number 24 hours)
15
10
5
0
*
Sham
MI
MI-CO
TV (number 24 hours)
50
40
30
20
10
0
*
Sham
MI
MI-CO

Figure 2

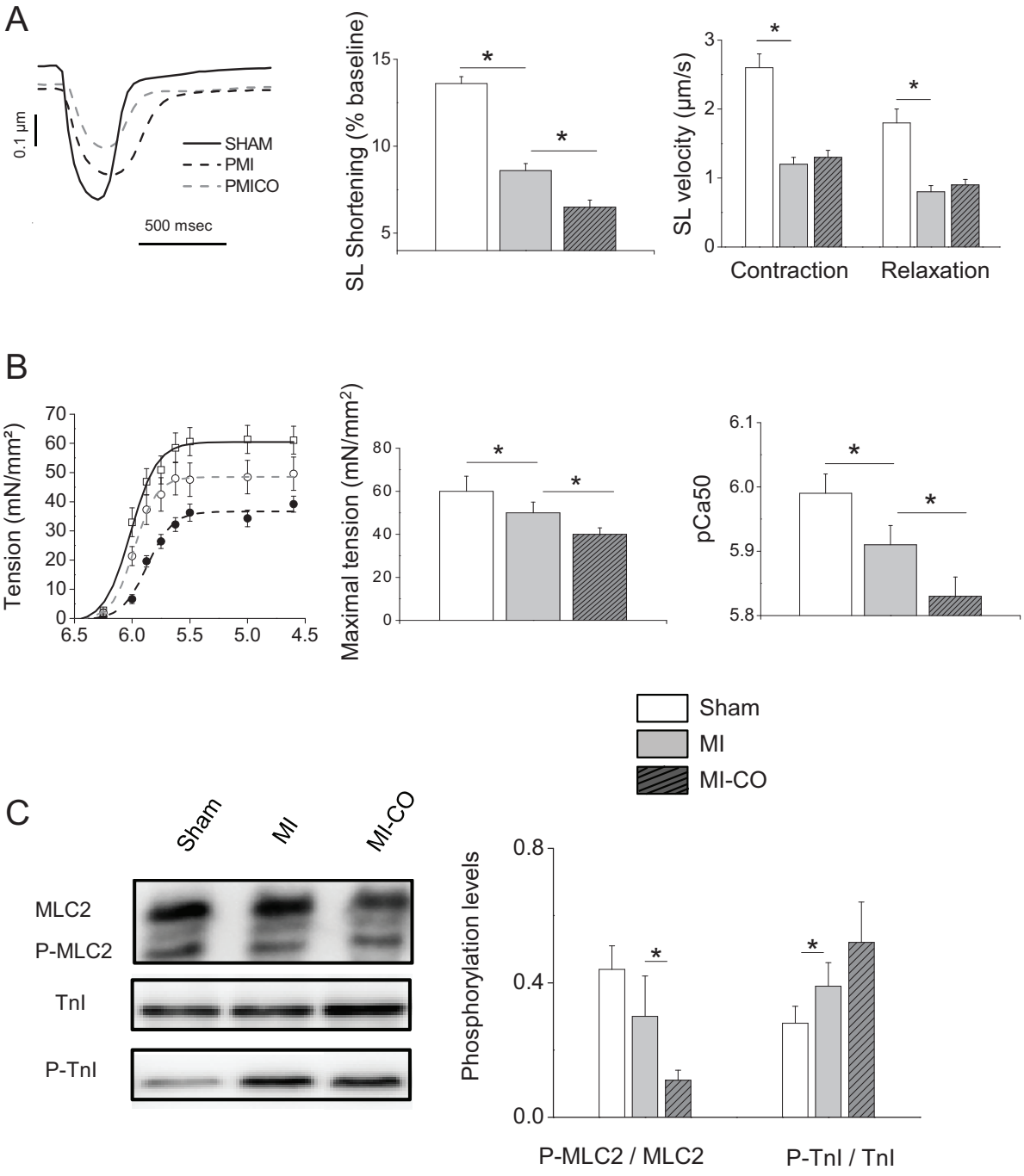
A
0.1 µm
SHAM
PMI
PMICO
500 msec
SL Shortening (% baseline)
SL velocity (µm/s)
Contraction
Relaxation
B
Tension (mN/mm²)
Maximal tension (mN/mm²)
pCa50
Sham
MI
MI-CO
C
Sham
MI
MI-CO
MLC2
P-MLC2
TnI
P-TnI
Phosphorylation levels
P-MLC2 / MLC2
P-TnI / TnI

Figure 3

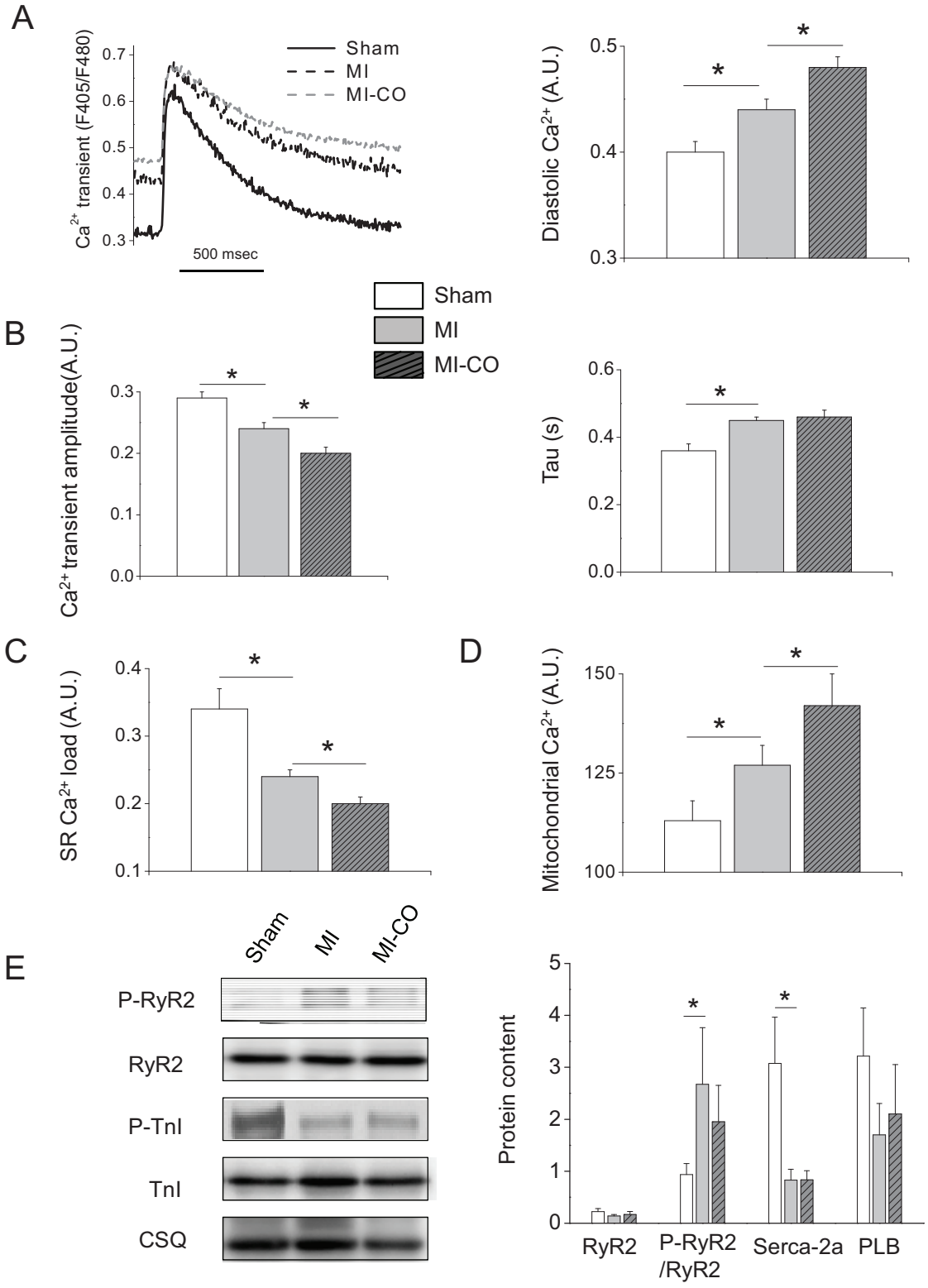
A
Ca2+ transient (F405/F480)
0.7
0.6
0.5
0.4
0.3
500 msec
Sham
MI
MI-CO
Diastolic Ca2+ (A.U.)
0.5
0.4
0.3
*
*
B
Ca2+ transient amplitude(A.U.)
0.3
0.2
0.1
0.0
*
*
Sham
MI
MI-CO
Tau (s)
0.6
0.4
0.2
0.0
*
C
SR Ca2+ load (A.U.)
0.4
0.3
0.2
0.1
*
*
D
Mitochondrial Ca2+ (A.U.)
150
125
100
*
*
E
Sham
MI
MI-CO
P-RyR2
RyR2
P-TnI
TnI
CSQ
Protein content
5
4
3
2
1
0
*
*
RyR2
P-RyR2 /RyR2
Serca-2a
PLB

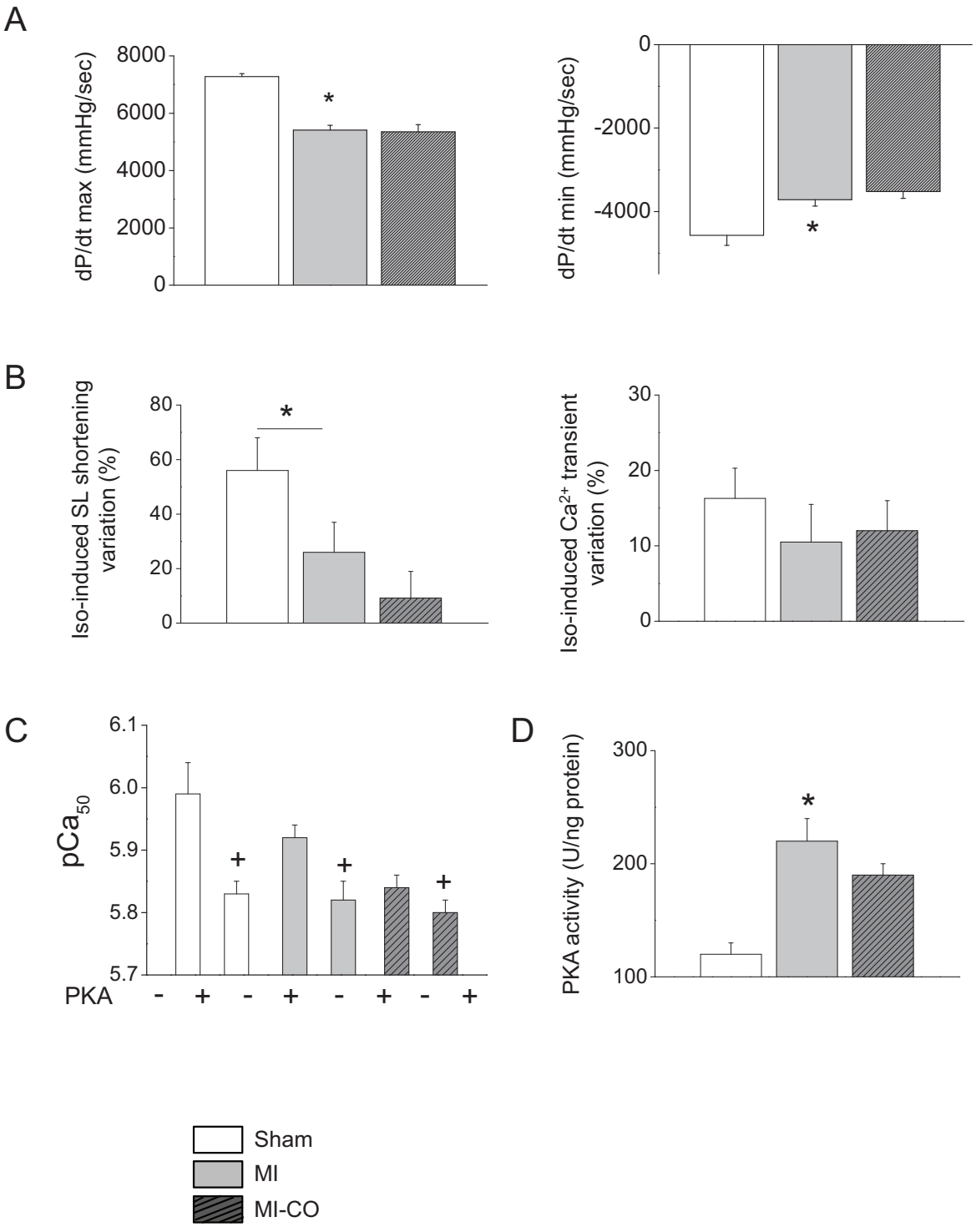
A
dP/dt max (mmHg/sec)
8000
6000
4000
2000
0
*
dP/dt min (mmHg/sec)
0
-2000
-4000
*
B
Iso-induced SL shortening variation (%)
80
60
40
20
0
*
Iso-induced Ca2+ transient variation (%)
30
20
10
0
C
pCa50
6.1
6.0
5.9
5.8
5.7
+
+
+
PKA
- + - + - + - +
D
PKA activity (U/ng protein)
300
200
100
*
Sham
MI
MI-CO

Figure 4

Figure 5

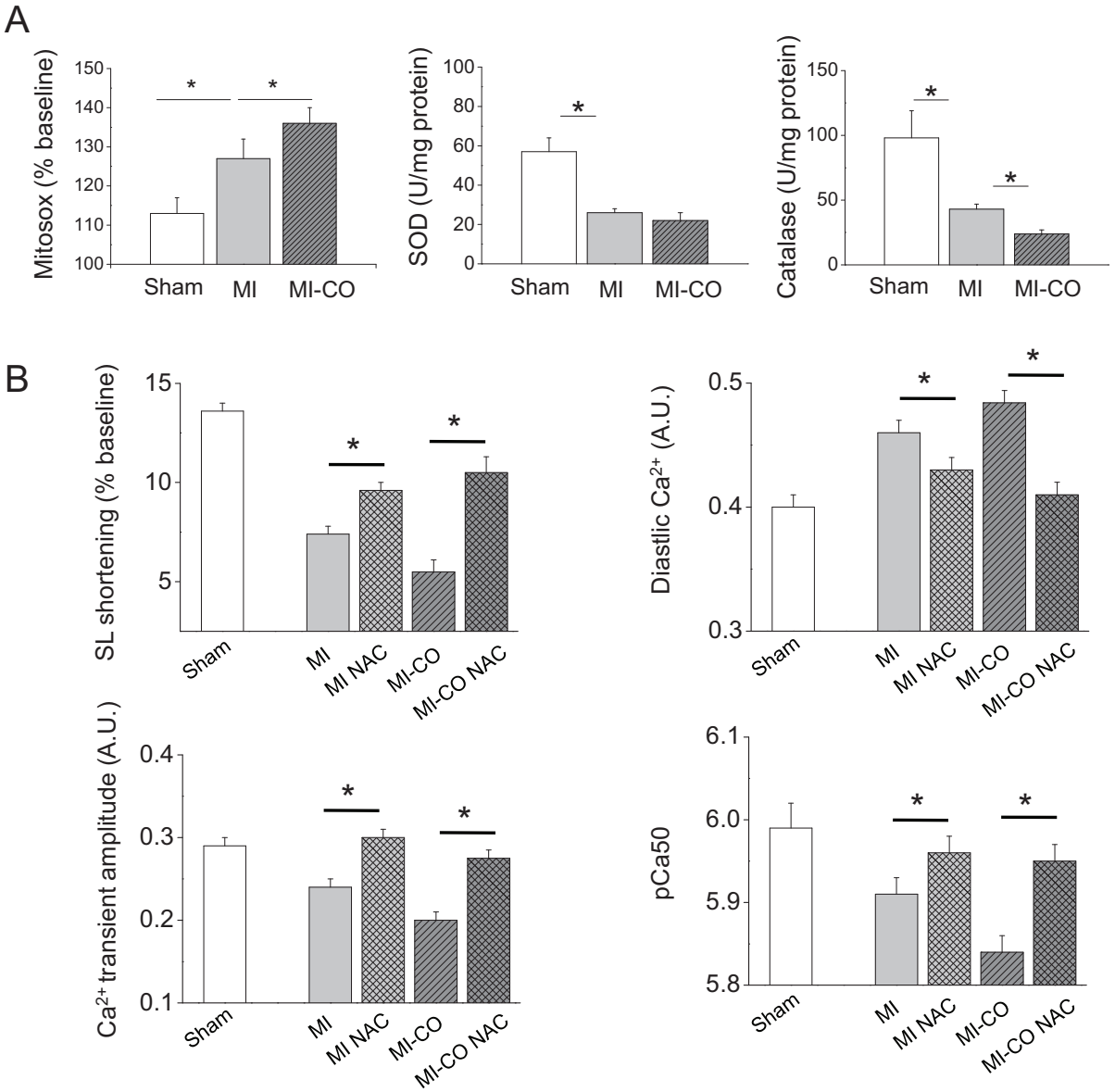
A
Mitosox (% baseline)
150
140
130
120
110
100
*
*
Sham
MI
MI-CO
SOD (U/mg protein)
100
80
60
40
20
0
*
Sham
MI
MI-CO
Catalase (U/mg protein)
150
100
50
0
*
*
Sham
MI
MI-CO
B
SL shortening (% baseline)
15
10
5
*
*
Sham
MI
MI NAC
MI-CO
MI-CO NAC
Diastlic Ca2+ (A.U.)
0.5
0.4
0.3
*
*
Sham
MI
MI NAC
MI-CO
MI-CO NAC
Ca2+ transient amplitude (A.U.)
0.4
0.3
0.2
0.1
*
*
Sham
MI
MI NAC
MI-CO
MI-CO NAC
pCa50
6.1
6.0
5.9
5.8
*
*
Sham
MI
MI NAC
MI-CO
MI-CO NAC

Figure 6

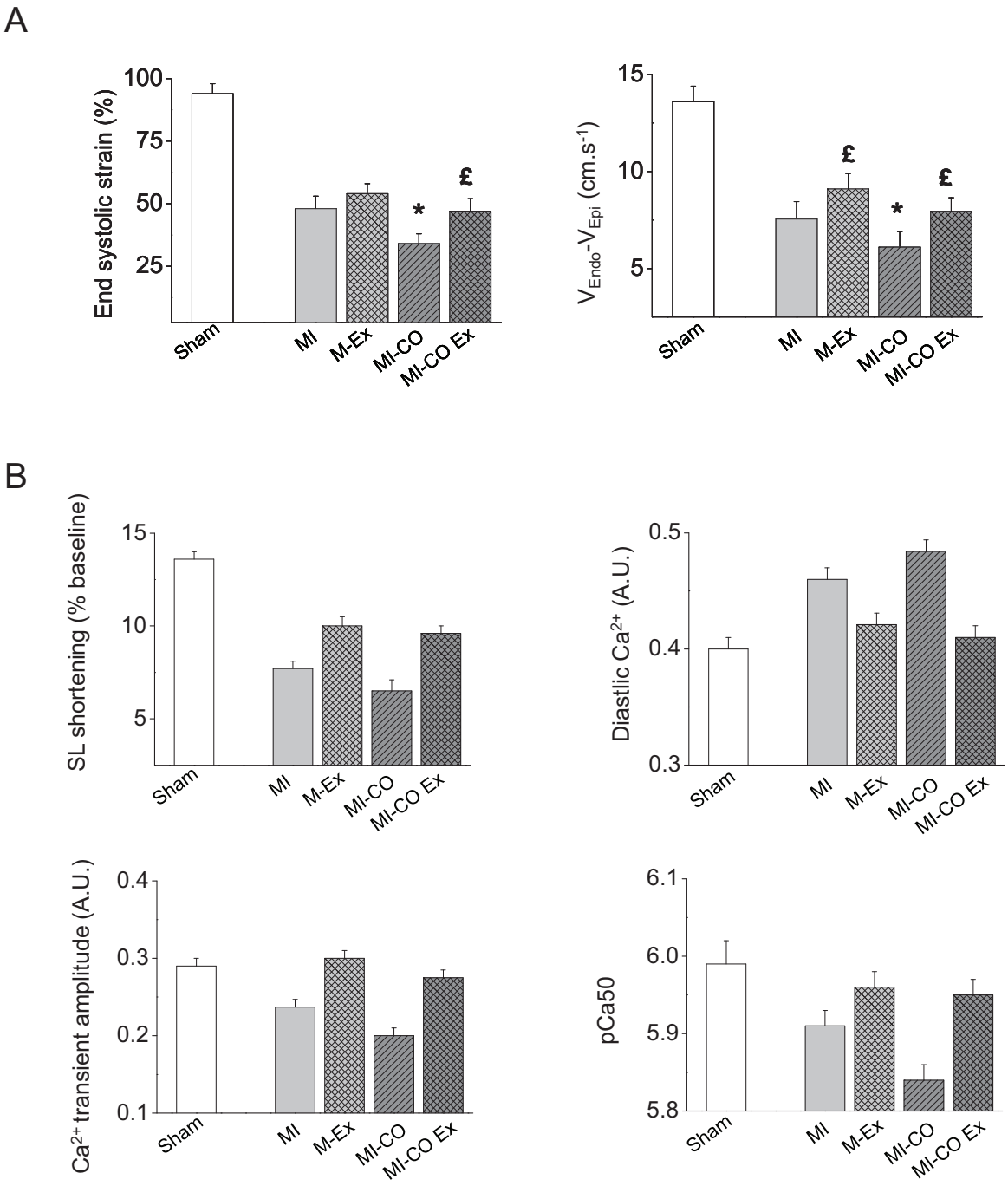
A
End systolic strain (%)
100
75
50
25
*
£
Sham
MI
M-Ex
MI-CO
MI-CO Ex
V_{Endo}-V_{Epi} (cm.s^{-1})
15
10
5
£
£
*
Sham
MI
M-Ex
MI-CO
MI-CO Ex
B
SL shortening (% baseline)
15
10
5
Sham
MI
M-Ex
MI-CO
MI-CO Ex
Diastlic Ca^{2+} (A.U.)
0.5
0.4
0.3
Sham
MI
M-Ex
MI-CO
MI-CO Ex
Ca^{2+} transient amplitude (A.U.)
0.4
0.3
0.2
0.1
Sham
MI
M-Ex
MI-CO
MI-CO Ex
pCa50
6.1
6.0
5.9
5.8
Sham
MI
M-Ex
MI-CO
MI-CO Ex

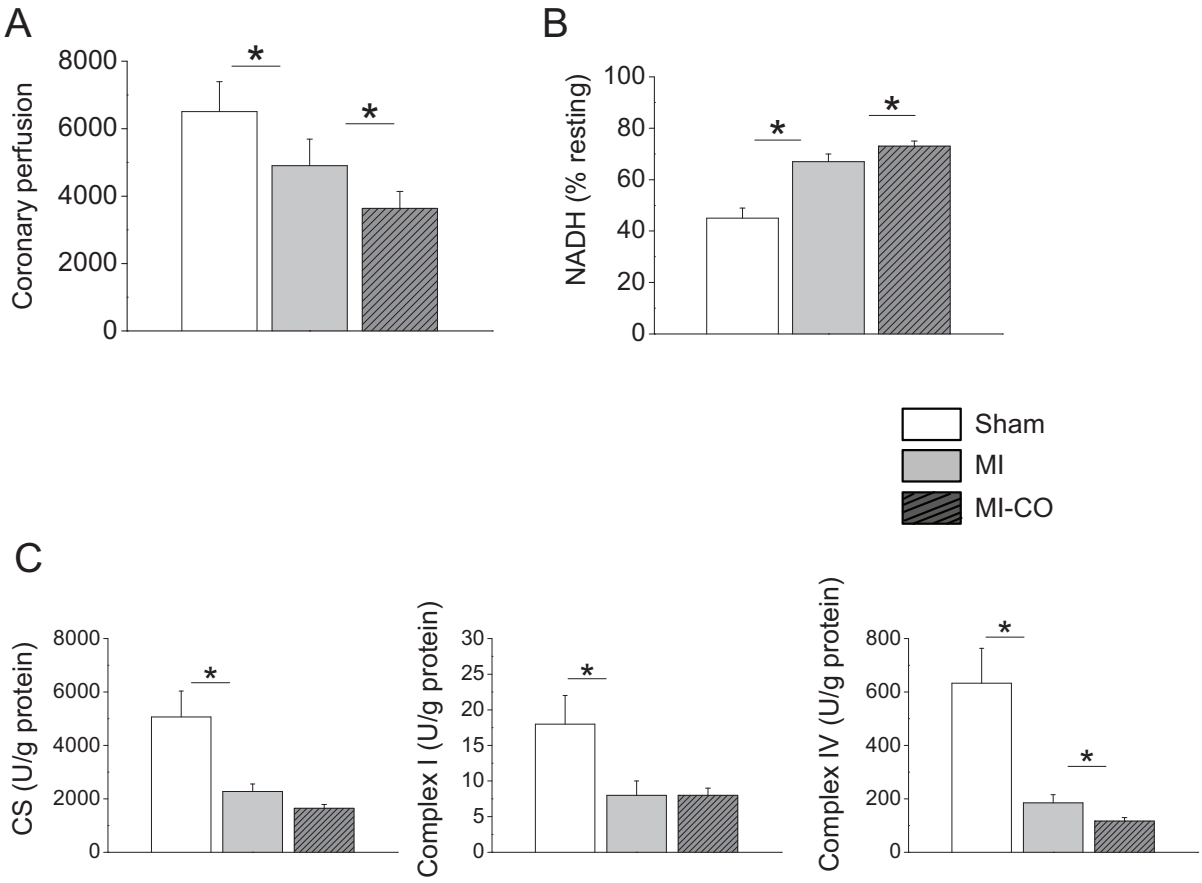

Supplemental data 1

3. Conclusion

Il est admis que la pollution atmosphérique augmente le risque d'accidents cardiovasculaires, notamment chez des populations fragilisées par une IC. Cependant, les mécanismes sous-jacents ne sont pas élucidés. Cette 7ème étude rapporte qu'une exposition chronique au CO exacerbe le remodelage cardiaque délétère de populations IC et amplifie les phénomènes arythmiques, et apporte donc un rationnel cellulaire et moléculaire aux données épidémiologiques associant pollution urbaine et accidents cardiovasculaires chez des populations sensibles. L'exercice physique, permettant de limiter la production de ROS, prévient les altérations liées à la pollution au CO à la fois sur les propriétés de la machinerie contractile et de l'homéostasie calcique, et pourrait donc être considérer comme thérapie préventive chez des populations à risque exposées à de fortes pollutions urbaines.

Conclusion 2ème partie :

L'exposition de populations saines en environnement pollué au CO, à des taux simulant une pollution urbaine, reproduit un phénotype pathologique similaire à celui retrouvé précocement à l'échelon cellulaire dans l'IC. Les altérations observées impliquent un remodelage métabolique induit par le CO (inhibition du complexe IV de la chaine de transport d'électrons) à l'origine de perturbations du récepteur à la ryanodine et de phénomènes arythmiques, observés notamment au décours d'une augmentation de l'activité. Ces résultats sont retrouvés chez des populations de patients sains chez lesquels une corrélation existe entre pollution atmosphérique, phénomènes oxydatifs et arythmies ventriculaires post-exercice. L'exposition au CO accroit également la sensibilité myocardique à un évènement ischémique et aggrave le remodelage délétère au sein de populations insuffisantes cardiaques ischémiques. Ainsi, l'exposition à des facteurs environnementaux, tels que la pollution atmosphérique, expose le système cardiovasculaire à un remodelage délétère. Le couplage excitation-métabolisme-contraction est en effet le siège de profondes altérations. Le découplage entre les activités mitochondriales et contractiles, aboutissant à un déséquilibre des homéostasies ioniques et redox cellulaires, joue un rôle fondamental dans la dysfonction cardiaque et illustre la forte plasticité du myocarde qui s'adapte aux contraintes s'exerçant sur lui. Outre la mise en évidence d'un remodelage cellulaire drastique, proche d'un phénotype pathologique, cette seconde partie de thèse questionne également la prise en considération des facteurs environnementaux comme facteur de risque cardiovasculaire. En effet, la plupart des échelles de mesure de risque cardiovasculaire (Score et Framingham) intègre généralement

l'âge, le sexe, le tabagisme, les dyslipidémies, l'hypertension artérielle et l'obésité comme facteurs de risque pour prédire le risque d'accidents cardiovasculaires. La mesure du degré d'exposition d'un individu à des molécules urbaines toxiques, telles que le CO, pourrait alors être considérée dans ces échelles pour estimer de manière plus fine le risque cardiovasculaire.

Conclusion Générale

Les maladies cardio-vasculaires représentent la première cause de mortalité dans le monde, avec en chef de file les cardiopathies ischémiques. Ce travail de thèse illustre le remodelage cardiaque survenant au cours de stress pathologiques et environnementaux, notamment les adaptations du couplage excitation-métabolisme-contraction. Au cours de l'IC ischémique, une dysfonction mitochondriale chronique est associée à une perturbation de l'homéostasie redox, favorisant des phénomènes oxydatifs liés à une production excessive d'espèces oxygénées réactives (Etude 1). Ces espèces oxygénées réactives activent la protéine kinase A, aboutissant à la phosphorylation puis au dysfonctionnement de différentes protéines impliquées dans le couplage excitation-contraction. Notamment, des ouvertures incontrôlées du récepteur à la ryanodine en diastole génèrent une fuite de Ca^{2+} du réticulum sarcoplasmique ; la surcharge calcique intracellulaire qui en résulte est à l'origine de phénomènes arythmiques (Etude 1). Par ailleurs une modification de l'état de phosphorylation de la troponine I est responsable de la genèse de troubles contractiles (Etude 2). Un traitement antioxydant (traitement chronique au N-acétylcystéine pendant 4 semaines, réduisant les espèces oxygénées réactives) et la pratique d'une activité physique modérée (course sur tapis roulant pendant 4 semaines, permettant de réduire le statut oxydatif et de diminuer l'activation de la voie β-adrénergique et donc de limiter les phosphorylations protéiques), préviennent les troubles contractiles et l'arythmogénicité dans l'ICi (Etude 3).

Une seconde partie de ce travail de thèse s'est intéressée aux effets d'une pollution atmosphérique au monoxyde de carbone (CO) sur la fonction cardiaque de populations saine et fragilisée par une maladie cardiaque ischémique. L'exposition de populations saines en environnement pollué au CO, à des taux simulant une pollution urbaine, reproduit un phénotype pathologique similaire à celui retrouvé précocement à l'échelon cellulaire dans l'ICi (Etude 4). Les altérations cellulaires observées impliquent une production anormale d'espèces oxygénées réactives résultant de modifications métaboliques mitochondriales induites par le CO (inhibition du complexe IV de la chaine de transport d'électrons) à l'origine de perturbations du récepteur à la ryanodine et de phénomènes arythmiques (Etude 5). Ces résultats sont retrouvés dans des populations de patients sains chez lesquels une corrélation existe entre pollution atmosphérique, phénomènes oxydatifs et arythmies ventriculaires (Etude 5).

L'exposition au CO a également pour conséquence d'accroitre la sensibilité myocardique à un évènement ischémique (Etude 6). Des populations exposées chroniquement au CO ont une atteinte cardiaque suite à un épisode d'ischémie–reperfusion (nécrose et altérations des fonctions cardiaques) plus étendue que des populations exposées en air ambiant, notamment en raison d'une production accrue d'espèces oxygénées réactives (Etude 6).

Enfin, l'exposition à une pollution urbaine au CO aggrave le remodelage délétère au sein de populations insuffisantes cardiaques ischémiques (Etude 7). Le remodelage du couplage E-M-C observé dans l'ICi est exacerbé en raison d'une production excessive d'espèces oxygénées réactives venant altérer les protéines de l'homéostasie calcique et myofilamentaires (Etude 7). Les études 4, 5, 6 et 7 suggèrent donc que la pollution atmosphérique pourrait être considérée comme un facteur de risque cardiovasculaire à part entière. L'intégration de ce facteur environnemental dans les échelles de calcul de score de risque cardiovasculaire pourrait alors permettre une estimation plus juste du risque de survenue d'un accident cardiovasculaire chez des populations accumulant les facteurs de risque (âge, tabac, obésité, diabète, hypertension).

Ce travail de thèse met en évidence des modifications du couplage E-M-C cardiaque en condition de stress chronique. Le découplage entre les activités mitochondriales et contractiles, aboutissant à un déséquilibre des homéostasies ioniques et redox cellulaires, semble jouer un rôle fondamental dans la dysfonction cardiaque étudiée dans des contextes d'ICi et d'exposition en milieu pollué au CO. Ainsi, une approche thérapeutique, visant à restaurer les fonctions mitochondriales et à rétablir le couplage E-M-C cardiaque, pourrait être considérée afin de préserver au mieux la fonction myocardique.

Annexe 1

Late exercise training improves non-uniformity of transmural myocardial function in rats with ischaemic heart failure

Younss Ait Mou, Cyril Reboul, Lucas Andre, Alain Lacampagne, and Olivier Cazorla

Cardiovascular Research (2009) 81, 555–564

Cardiovascular Research (2009) **81**, 555–564
doi:10.1093/cvr/cvn229

Late exercise training improves non-uniformity of transmural myocardial function in rats with ischaemic heart failure

Younss Aït Mou[1,2], Cyril Reboul[3], Lucas Andre[1,2], Alain Lacampagne[1,2], and Olivier Cazorla[1,2]*

[1]*INSERM U637, Physiopathologie Cardiovasculaire, CHU Arnaud de Villeneuve, 34295 Montpellier Cedex 5, Montpellier, France;* [2]*Université Montpellier1, UFR de Médecine, F-34295 Montpellier, France; and* [3]*EA-4278, Université Avignon et des Pays de Vaucluse, UFR Sciences F-84000, Avignon, France*

Received 23 June 2008; revised 31 July 2008; accepted 8 August 2008; online publish-ahead-of-print 14 August 2008

Time for primary review: 27 days

KEYWORDS
End-stage heart failure;
Myocardial contractility;
Contraction;
Exercise;
Myocardial infarction

Aims The exercise-induced beneficial mechanisms after long-term myocardial infarction (MI) are incompletely understood. The present study evaluated the effect of treadmill exercise training (5 weeks), started at a late stage of heart failure (HF) (13 weeks post-MI), on rat left ventricle remodelling and dysfunction of the regional global and cellular contractile functions.
Methods and results *In vivo* echocardiography confirmed that sub-endocardial (ENDO) layers contract more (+86%) and faster (+50%) than the sub-epicardial (EPI) layers. This gradient was lost in MI rats due to a predominant reduction in the ENDO layer contractility. Exercise partially restored the amplitude and velocity of ENDO contraction, resulting in a partial recovery of the pump function indexed by the aortic blood-flow velocity time integral. At the cellular level, MI impaired ENDO contractile properties by reducing cell shortening (10–7%), calcium transient, and myofilament Ca^{2+} sensitivity. These alterations were normalized by exercise. Sarcoplasmic reticulum Ca^{2+}-ATPase (SERCA)2a expression and myosin light chain (MLC)-2 phosphorylation in ENDO cells were significantly reduced after MI and were restored by exercise. The EPI layer was only slightly reduced *in vivo* without cellular alterations.
Conclusion This study shows that exercise performed at a late stage after MI restored a transmural non-uniformity of myocardium lost during HF. Recoveries of Ca^{2+} homeostasis and myofilament function of cardiomyocytes contribute to this beneficial effect.

1. Introduction

After myocardial infarction (MI), the heart is characterized by reduced contractility and impaired filling resulting from changes in cardiac structure (hypertrophy, dilatation), cell death, maladaptative remodelling of the extracellular matrix, abnormal energy metabolism, and cellular dysfunction. The underlying cellular mechanisms that have been suggested include altered calcium homeostasis,[1] impaired myofilament calcium responsiveness,[2–4] and reduced cross-bridge cycling rate.[5] A hierarchy of cellular events during the development of heart failure (HF) has been proposed, starting with electrical remodelling and altered Ca^{2+} homeostasis during the early phase followed by myofilament dysfunction.[6] Moreover, transmural myocardial contractile performance is non-uniform across the different layers of the left ventricular (LV) wall.[7,8] This non-uniformity of cardiac function plays a fundamental role in cardiac mechanical work. Its loss has been previously reported to be a sensitive index to discriminate physiological from pathological LV remodelling.[8] We previously reported that HF affects preferentially the contractile machinery of the sub-endocardial (ENDO) cells, leading to the loss of transmural heterogeneity.[3]

In clinic, pharmacological treatments are used to maintain the pump function of the failing heart as much as possible. However, non-pharmacological approaches may be attempted. For example, many clinical studies have shown that exercise training performed by the patients with HF is beneficial for heart performance and quality-of-life.[9,10] In the normal heart of small[11] and large[12] animals, exercise training increases cellular contractile function such as cardiomyocyte shortening, Ca^{2+} dynamics and myocyte power-generating capacity, and myocardial perfusion capacity.[13] There are also clinical evidences that exercise after MI has a beneficial effect on disease progression and survival.[9,10] A recent study has shown that early exercise in MI mice had no effect on LV remodelling but attenuates global LV dysfunction, which can be essentially explained by the

* Corresponding author. Tel: +33 467 41 52 42; fax: +33 467 41 52 42.
E-mail address: olivier.cazorla@inserm.fr

Published on behalf of the European Society of Cardiology. All rights reserved. © The Author 2008.
For permissions please email: journals.permissions@oxfordjournals.org.

Downloaded from cardiovascres.oxfordjournals.org at AstraZeneca R&D Lund on October 25, 2010

exercise-induced improvement of myofilament function.[14] However, after a small MI, exercise has either no effect or improved LV function independently of the starting point of exercise (early or late after MI).[14] For large infarct, exercise can have detrimental effects when performed at an early stage while beneficial effects on LV remodelling and function appear when exercise is started late after MI.[15,16] In animal models, most of the studies tested the effect of exercise on LV global and/or cellular functions, 4 weeks after MI, when LV remodelling is still ongoing.[17,18] Moreover, it has been shown in rat models that 3–5 weeks after MI exercise capacity is still high and close to Sham-operated animals while it decreased significantly from 10 weeks after MI.[19] Thus, the cellular adaptations between early and late exercise after MI may be different. Moreover, part of the discrepancy on the effect of exercise on MI in the literature may be due to the use of swimming training,[15] which is known to have different responses from those to treadmill running, complicated by factors such as the diving reflex, mental stress, and episodes of hypoxia associated with diving.

The present study evaluated, in a rat model, the effect of exercise training, started at a late stage of HF (13 weeks post-MI), on LV remodelling and function of the global and cellular contractile properties in various regions of the LV free wall. The results indicated that *in vivo* systolic function [fractional shortening (FS) and aortic velocity time integral (VTI_{Ao})] was reduced in MI rats in association with a reduction of the amplitude and speed of contraction of the ENDO layer and to a lesser extent of the sub-epicardial (EPI) layer. These alterations led to a uniformity of the transmural myocardial function, which were partially reversed by exercise. Exercise improved part of the systolic parameters and slightly reduced LV dilatation. The *in vivo* beneficial effect of exercise was associated with a restoration of the ENDO cellular properties, by reversing the MI-induced abnormalities in Ca^{2+}-handling function and proteins, phosphorylation status of contractile proteins, and myofilament function.

2. Methods

For a detailed description, see expanded Materials and Methods in Supplementary material online. Experiments complied with the *Guide for the Care and Use of Laboratory Animals* published by the US National Institutes of Health (NIH Publications No. 85–23, revised 1996) and with the approval of the French Ministry of Agriculture.

2.1 Animals and exercise training

MI was produced by permanent ligation of the left coronary artery in male Wistar rats as previously described.[3] Thirteen weeks post-MI, rats were randomly assigned to the sedentary (MI) or 5 weeks treadmill exercised (MI-Ex, 40 min/day, 5 days/week, 16 m/min) groups. At the end of the training protocol, morphological and functional parameters were determined by echocardiography and compared with Sham-operated animals. Animals were then sacrificed for cellular investigations.

2.2 Echocardiography and non-invasive haemodynamics

Doppler-echocardiography was performed with a MyLab 30 (ESAOTE, Italy). Wall Thicknesses and Left Ventricular End Diameters (LVED) were obtained at the level of the papillary muscles. LV shortening fraction and end-systolic strain of the posterior wall measured as deformation from end-diastole to end systole [(PWTs − PWTd)/PWTd] * 100 were calculated. PWTs and PWTd are end-systolic and end-diastolic Posterior Wall Thickness, respectively.[20]

Ascending aortic blood flow was recorded, as previously described,[21] via pulsed-wave Doppler permitting measurements of the VTI_{Ao}. LV ENDO and EPI posterior wall displacements were measured offline at the level of the papillary muscles. Tissue Doppler imaging was performed after each conventional echocardiography as previously described.[22]

2.3 Contractile properties in intact cardiomyocytes

Single LV cardiomyocytes were isolated by enzymatic dissociation from the remaining inner free wall (ENDO) and from the outer free wall (EPI) as previously described ($n = 5$ rats per group).[23] Unloaded cell shortening and calcium concentration [Ca^{2+}] (indo 1 dye) were studied using field stimulation (0.5 Hz, 22°C, 1.8 mM external Ca^{2+}). Sarcomere length (SL) and fluorescence (405 and 480 nm) were simultaneously recorded (IonOptix system, Hilton, USA).

2.4 Force measurements in permeabilized cardiomyocytes

Isometric force was measured in single permeabilized cardiomyocytes at different [Ca^{2+}], at 1.9 then 2.3 μm SL as described previously ($n = 5$ rats per group).[3,23] Force was normalized by the cross-sectional area measured from the imaged cross-section. Force–pCa relationships were fitted to a Hill equation. To prevent degradation, all solutions contained protease inhibitors (PMSF, 0.5 mmol/L; leupeptin, 0.04 mmol/L; and E64, 0.01 mmol/L).

2.5 Myosin-heavy chain composition

Myosin-heavy chain (MyHC) isoforms were separated on a 6% SDS–PAGE and silver stained as previously described.[24] β-MyHC content was expressed relative to the total amount of MyHC protein.

2.6 Western immunoblotting

Sarcoplasmic reticulum Ca^{2+}-ATPase (SERCA)2a and phospholamban (PLB) were separated on a gradient SDS–PAGE (2–20%) and then blotted onto nitrocellulose membrane. Proteins were revealed with specific antibodies and were expressed relative to Calsequestrin content.

Troponin I (TnI) was separated by 15% SDS–PAGE and the protein kinase A phosphorylated form of cardiac TnI was normalized by the total TnI form as previously described.[3] Myosin light chain 2 (MLC-2) phosphorylated and non-phosphorylated forms were separated by a 10% urea gel and were specifically detected with a cardiac MLC-2 antibody.[3]

Immunodetection was revealed with ECL Plus system.

2.7 Statistical analysis

Data were analysed using one-way or two-way ANOVA among groups. When significant interactions were found, a Bonferroni *t*-test was applied with adjusted $P < 0.05$ (SigmaStat 3.5). Data are presented as means ± SEM.

3. Results

3.1 *In vivo* cardiac morphological and functional parameters

MI animals had large antero-lateral infarcts detected by visual inspection. In a preliminary longitudinal study (data not shown), we observed that in our model, most of the

Downloaded from cardiovascres.oxfordjournals.org at AstraZeneca R&D Lund on October 25, 2010

morphological and functional alterations occurred over 11–13 weeks. Minimal changes will occur after this period. Thirteen weeks after MI, LV diameters were increased in MI at the end-diastolic and -systolic phases without hypertrophy of the posterior wall thickness (*Figure 1A*). The posterior wall end-systolic strain during a cardiac cycle was largely reduced (−80%) in MI animals (*Figure 1B*). In Sham animals, the LV ENDO layer contracted faster (+50% of the section motion) than the EPI layers (*Figure 1C*). HF significantly decreased contraction velocities of both EPI and ENDO layers by 15 and 32%, respectively, homogenizing the transmural velocities of contraction towards the slowest values. The global cardiac systolic function was also altered as shown by the reduction in FS (*Figure 1D*). Since the calculation of FS, measured at the level of papillary muscle, is highly affected by the akinetic infarct zone, we measured the VTI_{Ao} as another index of systolic function. VTI_{Ao} was also decreased after MI (*Figure 1D*). Additional weeks after MI corresponding to the training duration had little impact on these parameters (see below).

3.2 Effect of exercise on *in vivo* cardiac function

We then investigated the effect of exercise training while most of the remodelling and dysfunction of the heart had already occurred. Eighteen weeks post-MI, hearts were hypertrophied as shown by the increase in the heart weight/body weight ratio between Sham and MI animals and further increased after exercise training (*Table 1*). Part of this exercise-induced hypertrophy may be explained by an increase of the posterior wall thickness although the difference did not reach significance ($P = 0.069$) (*Table 1*). The main effect of exercise on LV morphologies was a decrease of both end-systolic and -diastolic left ventricular diameters (*Table 1*). Eighteen weeks after MI, we observed a large decrease in the end-systolic strain (from 83 ± 4 to $24 \pm 11\%$ in Sham and MI, respectively) and in the absolute ENDO posterior wall displacement between diastole and systole (from 2.7 ± 0.2 to 1.3 ± 0.2 mm in Sham and MI, respectively). The values obtained were similar to the one measured 13 weeks post-MI confirming the stability of these indexes during this phase of the disease (*Figure 2B*). Exercise had a significant beneficial effect on the end-systolic strain ($63 \pm 7\%$) and on the ENDO posterior wall displacement (1.8 ± 0.4 mm). The section motion (Sm) was similarly decreased between 13 and 18 weeks after MI in both regions. Exercise restored Sm completely in EPI and only partially in the ENDO layers (*Figure 2C*). The gradient of velocity across the LV defined as the difference of velocity between ENDO and EPI, observed in normal conditions

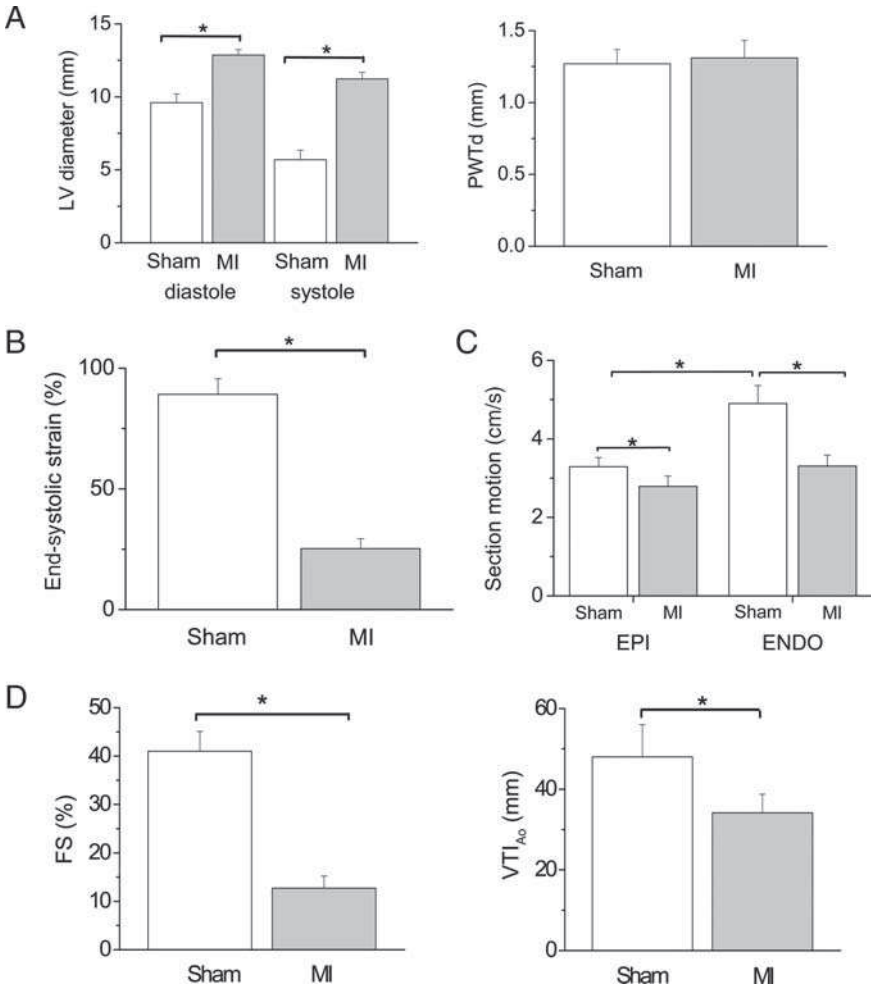

Figure 1 Left ventricular morphological and functional characteristics 13 weeks post-myocardial infarction. End-diastolic and -systolic diameters and diastolic posterior wall thickness (*A*), end-systolic strain (*B*), systolic velocity of the left ventricular epicardial and endocardial layers (*C*), global systolic function (*D*) as indexed by fractional shortening (left), and aortic velocity time integral (right). *Adjusted $P < 0.05$ vs. corresponding Sham ($n = 11$ hearts/group).

Downloaded from cardiovascres.oxfordjournals.org at AstraZeneca R&D Lund on October 25, 2010

Table 1 Cardiac morphological and functional parameters

	Sham ($n = 12$)	MI ($n = 17$)	MI-Ex ($n = 14$)
Body weight (g)	582.9 ± 22.3	605.6 ± 19.2	559.3 ± 16.0
Heart mass (g)	2.11 ± 0.08	2.56 ± 0.11^{a}	2.73 ± 0.11^{a}
Heart mass/body weight (mg/g)	3.65 ± 0.12	4.28 ± 0.22^{a}	$4.92 \pm 0.24^{a,b}$
LVEDs (mm)	5.4 ± 0.1	11.6 ± 0.3^{a}	$10.6 \pm 0.3^{a,b}$
LVEDd (mm)	9.5 ± 0.1	13.3 ± 0.3^{a}	$12.3 \pm 0.2^{a,b}$
AWTd (mm)	1.2 ± 0.1	0.4 ± 0.1^{a}	0.4 ± 0.1^{a}
PWTd (mm)	1.2 ± 0.1	1.2 ± 0.1	1.4 ± 0.1
FS (%)	43.1 ± 0.6	12.2 ± 0.9^{a}	13.8 ± 0.9^{a}
VTI_{Ao} (mm)	51 ± 1	32 ± 1^{a}	$44 \pm 2^{a,b}$
HR (bpm)	280 ± 6	282 ± 5	283 ± 12

LVEDs, left ventricular end-systolic diameter; LVEDd, left ventricular end-diastolic diameter; AWTd, end-diastolic anterior wall thickness; PWTd, end-diastolic posterior wall thickness; FS, Fractional shortening. VTI_{Ao}, aortic velocity time integral; HR, heart rate. Values are means $\pm$ SEM (n, number of cells). [a] vs. Sham [b]MI vs. MI-Ex; $P < 0.05$.

(1.66 ± 0.11 cm/s), disappeared almost completely in MI animals (0.28 ± 0.05 cm/s) and was partially restored in MI-Ex (0.76 ± 0.05 cm/s) (*Figure 2C*). Finally, VTI_{Ao}, used as an accurate index of LV stroke volume, decreased by 37% in MI animals and was partially restored by exercise in MI-EX remaining 14% lower than Sham (*Figure 2D*). Exercise had no impact on the mortality of the animals (*Figure 2E*).

3.3 Effect of exercise on myocyte shortening and Ca^{2+} transient

The effect of exercise on the excitation–contraction coupling of long-term MI was tested in intact LV unloaded cardiomyocytes. For this purpose, SL shortening and intracellular calcium content were simultaneously measured on field stimulated cardiomyocytes. Unloaded contraction decreased significantly with HF only in ENDO cells and was restored by exercise (*Figure 3*). The duration of unloaded shortening (data not shown) and relaxation (*Figure 3B*) was not different between the various groups. However, the speed of contraction and relaxation was significantly reduced in ENDO MI cells and was restored by exercise (*Figure 3C*). The amplitude of Ca^{2+} transient decreased significantly only in ENDO MI cells and was restored by exercise (*Figure 4B*). In addition, the calcium transient decay in both EPI and ENDO MI myocytes was significantly slowed (increase in tau), reflecting an altered calcium reuptake. All parameters were normal in MI-Ex. The calcium transient decay in MI is known to be altered due to changes in SERCA2a expression or in the inhibition of SERCA2a/PLB activity. We found that SERCA2a expression was significantly decreased in MI animals, both in ENDO and EPI layers. PLB expression was unchanged. Levels of protein expression in MI-Ex were similar to Sham samples (*Figure 4C*).

3.4 Force development in single permeabilized myocytes

Force development of intact myocytes depends on the amount of calcium released by the sarcoplasmic reticulum and the myofilament Ca^{2+} sensitivity. Thus, we measured the myofilament Ca^{2+} sensitivity (pCa_{50}) at short length (1.9 μm SL) and at long length (2.3 μm SL). Passive force and maximal isometric tension measured at both SL were similar between Sham, MI, and MI-Ex (*Table 2*). Neither pathology nor exercise had any effect on myofilament Ca^{2+} sensitivity at short SL (*Figure 5* and *Table 2*). Stretching the cells to 2.3 μm SL induced a leftward shift of tension in all conditions reflecting an increase in myofilament Ca^{2+} sensitivity. However, pCa_{50} was significantly lower in the ENDO cells isolated from MI rats. Exercise restored Ca^{2+} sensitivity at 2.3 μm SL (*Figure 5A*). The difference between pCa_{50} at the long and short SL (ΔpCa_{50}), used as an index of the length-dependent activation of contractile machinery, was significantly smaller in ENDO MI cells compared with the Sham and MI-Ex cells. EPI myocytes were affected neither by the pathology nor by the exercise at both lengths (*Figure 5B*).

We have previously shown that ΔpCa_{50} is closely related to passive tension rather than to SL.[3] The differences in passive and active properties across the left free wall described a positive relationship in which ENDO cells develop more passive tension after a stretch to 2.3 μm SL associated with higher stretch-induced myofilament Ca^{2+} sensitivity than did EPI cells (*Figure 5C*). This correlation disappeared in MI rats, mostly due to a decrease in ΔpCa_{50} of ENDO cells. Interestingly, values obtained in MI-Ex myocytes were similar to those found in Sham rats.

3.5 Contractile protein isoforms and phosphorylation

Rat heart expresses two isoforms of MyHC (α- or β-MyHC). Variation in α/β-MyHC expression influences cardiac function. In our conditions, β-MyHC content increased after MI in both ENDO and EPI cells. Exercise had no effect on β-MyHC content in either ENDO or EPI cells of MI rats (*Figure 6A*).

TnI and MLC-2 phosphorylations are known to shift the tension-pCa curves in cardiac muscle. Western blot analysis was performed on non-stretched and stretched skinned muscle strips dissected from the ENDO layer or the EPI layer. Phosphorylation of TnI on the PKA sites was similar between regions, before and after stretch, in Sham, MI and MI-Ex animals (*Figure 6B*). We have previously shown that the linear relationship between pCa_{50} and passive tension was associated with changes in the phosphorylation level of MLC-2.[3] As previously reported, stretch increased by $\approx$10%, the amount of phosphorylated MLC-2 in the ENDO myocardium of Sham animals and not in MI animals

Downloaded from cardiovascres.oxfordjournals.org at AstraZeneca R&D Lund on October 25, 2010

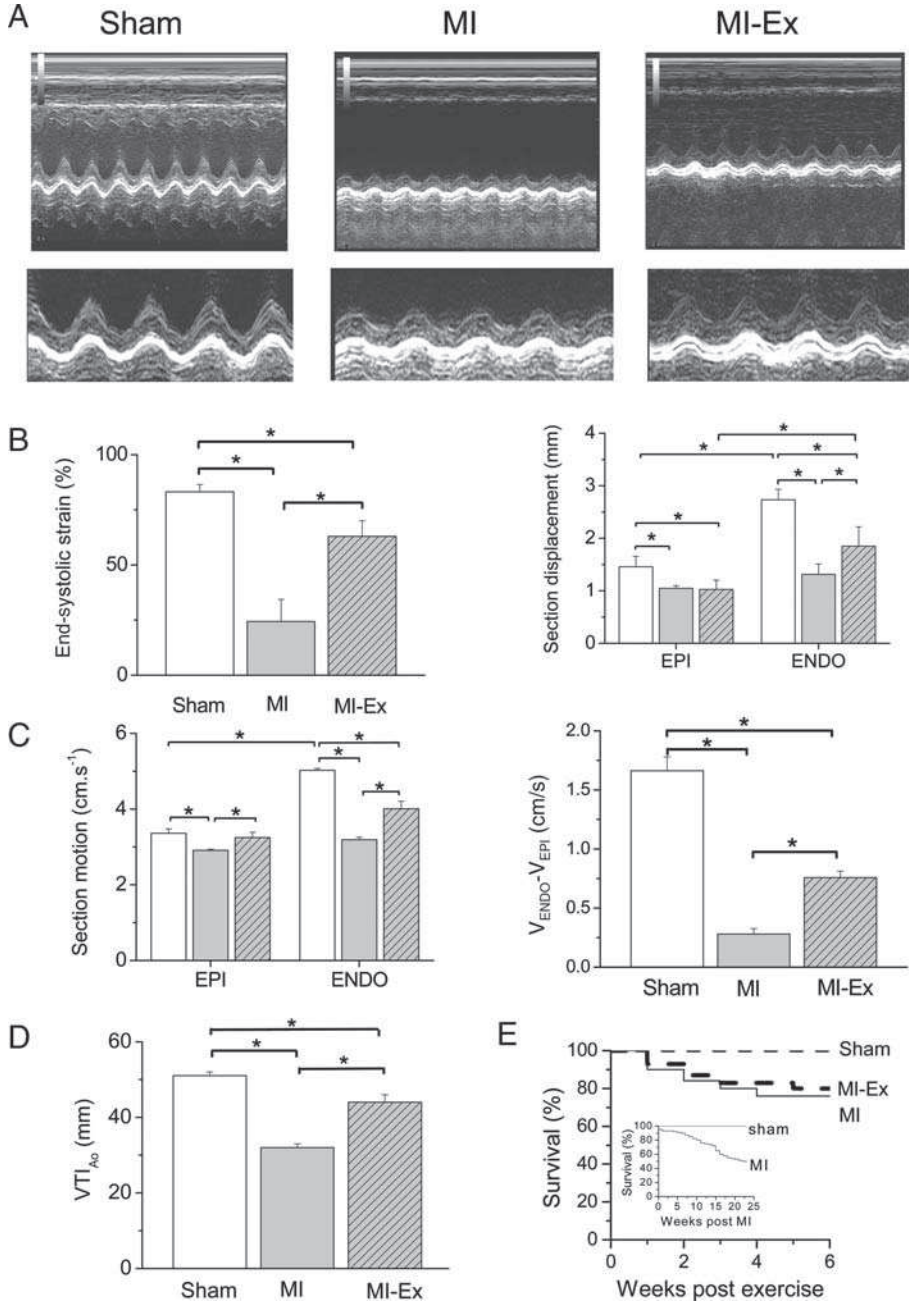

Figure 2 Left ventricular morphological and functional characteristics in myocardial infarction (MI) and MI-exercise rats. (*A*) Echocardiography images with an enlargement of the posterior wall. (*B*) End-systolic strain (left) and displacement of epicardial and endocardial layers during a cardiac cycle (right). (*C*) Systolic velocity (left) and gradient of velocity ENDO–EPI (right). (*D*) Aortic velocity time integral. (*E*) Survival curve following the beginning of exercise program. *Adjusted $P < 0.05$ ($n = 12$–17 hearts/group).

(*Figure 6C*). Exercise restored the stretch-induced increase in MLC-2 phosphorylation in MI animals. MLC-2 phosphorylation was not affected by pathology, stretch, and exercise in EPI myocardium.

4. Discussion

The present study tested whether a remodelled end-stage failing heart following MI could benefit from 5 weeks of endurance exercise training. To this end, we evaluated the effects of exercise on LV remodelling, regional *in vivo* function, cardiomyocyte contractility, Ca^{2+} handling, and myofilament Ca^{2+} sensitivity. The main findings were that[1] normal myocardial function is non-uniform due to heterogeneous cellular properties across the wall[2] transmural non-uniformity of myocardial function was lost in MI rats due to ENDO cellular dysfunction[3] exercise recovered a transmural heterogeneity by improving LV function mostly in ENDO layer, in relation with a normalization of MI-induced dysfunctions of both Ca^{2+} handling and myofilaments Ca^{2+} sensitivity in ENDO cardiomyocytes.

4.1 Regional pathophysiology of myocardial infarction-induced left ventricular dysfunction

It is now established that cardiac function is non-uniform across the wall due to larger and faster contraction of the

Downloaded from cardiovascres.oxfordjournals.org at AstraZeneca R&D Lund on October 25, 2010

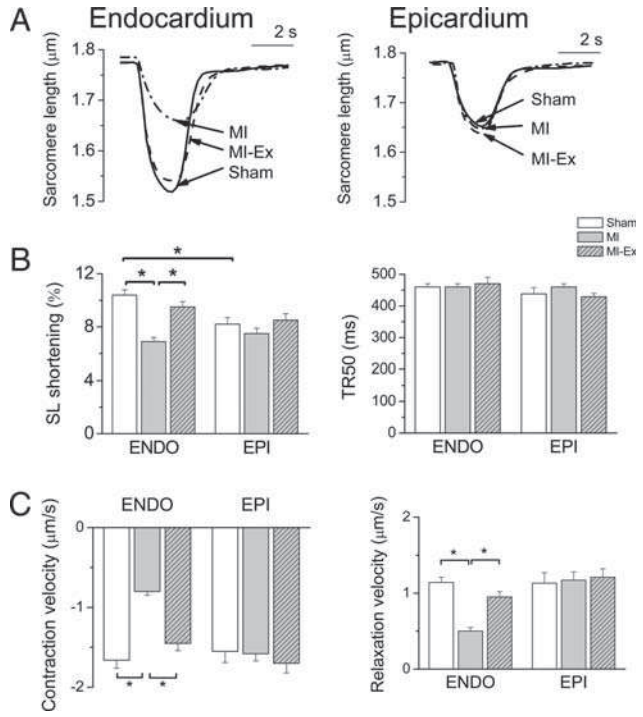

Figure 3 Sarcomere length (SL) shortening in isolated myocardial infarction (MI) and MI-exercise (MI-Ex) cardiomyocytes. (*A*) SL shortening examples of endocardial (left trace) and epicardial (right trace) Sham, MI, and MI-Ex myocytes. (*B*) Averaged data of SL shortening (in percentage on baseline) and time to 50% of relaxation (TR50). (*C*) Speeds of contraction (left) and relaxation (right) ($n = 55$–106 cells/5 hearts). *Adjusted $P < 0.05$.

ENDO layer as compared with the EPI tissue one.[7] A recent study using transmural bead markers under biplane cineradiography showed that the onset of myofibre shortening occurred earlier in endocardium than epicardium, whereas the onset of myofibre relaxation occurred earlier in epicardium than endocardium.[25] These differences in fibre strains may be explained by telediastolic and telesystolic transmural differences in wall stress, increasing towards the endocardium.[26] Our data showed that the higher ENDO fibre shortening during systole was likely due to higher basal cardiomyocyte contractility and a higher stretch-induced increase in myofilament Ca^{2+} sensitivity.

As previously reported,[27,28] the remodelling of MI heart was characterized by LV dilatation, hypertrophy, and dysfunction. The cardiac pump dysfunction was characterized here by a reduction in LV FS and other indexes, such as the VTI_{Ao}, and the amplitudes and velocities of contraction of the myocardial layers. We also observed that the pathology did not affect the heart uniformly. Following MI, wall contractility decreased mostly in the ENDO layer with a higher decrease in the amplitude of displacement (−52 vs. −28%, ENDO vs. EPI) and in the velocity of contraction (−36 vs. −13%, ENDO vs. EPI). These changes resulted in a homogenization in regional myocardial function and the complete loss of transmural non-uniformity.

4.2 Beneficial effects of exercise training on MI cardiac function

In our MI model, most parameters of the LV remodelling and *in vivo* dysfunctions were achieved 13 weeks after MI and were stable 18 weeks after MI (*Figures 1* and *2*). We thus assessed whether exercise could improve myocardial function and restore the transmural heterogeneity in a remodelled MI heart. Studies in humans with large MI reported that exercise had either no[29] or a beneficial[30] effect on ejection fraction and LV volumes. Previous studies in animal models reported that exercise had no effect on LV function parameters such as LV dP/dT_{max} or FS irrespective of whether exercise was started early or late after MI, despite an improvement in cell function.[15,17] Neither was FS in MI improved by exercise in our study. However, other indexes of cardiac function such as aortic blood flow (VTI_{Ao}) and regional amplitude and velocities of contraction were improved after exercise. In several clinical studies, alterations in wall motion (including wall thickening) measured by echocardiography were shown to be good predictors of subsequent cardiac events of morbidity and mortality[31,32] and interventions that halt, slow or reverse these ventricular dysfunctions should markedly improve clinical outcomes.[33] The higher exercise-induced improvement of amplitude and velocity of contraction in ENDO allowed partially to recovering a transmural non-uniformity. This may in turn contribute in the exercise-induced beneficial effect on cardiac function.

In view of the concern that late exercise may aggravate LV remodelling after a large MI and life expectancy, we investigated LV remodelling with or without exercise. Five weeks of exercise decreased LV end-diastolic and -systolic diameters, and did not aggravate LV remodelling. Our exercise protocol was a moderate endurance protocol, confirmed by the fact that Sham animals exercised at the same intensity did not show any change in any parameters investigated (data not shown). These observations are in agreement with a recent study reporting that 8 weeks of moderate exercise in mice with MI cardiomyopathy[14] and hypertrophic cardiomyopathy[34] reversed collagen content with little effect on cardiac hypertrophy. In our study, exercise did not induce a higher mortality consistent with previous studies with human patients.[16]

4.3 Exercise-induced effects on contractile cellular properties

The mechanisms for LV dysfunction after MI remain incompletely understood but have been proposed to be a consequence of cellular alterations and extracellular matrix remodelling.[1] Recent studies have shown that early exercise in mice after MI had no effect on LV remodelling but slightly attenuates global LV dysfunction mostly by improving myofilament function without Ca^{2+} signalling.[14] However, similar protocols performed in female Sprague–Dawley rat model showed a recovery of contraction function, Ca^{2+} handling and some indexes of improved myofilament Ca^{2+} sensitivity following early exercise after MI.[17]

In our study, cell shortening decreased after MI exclusively in ENDO cells, most probably due to both reduced Ca^{2+} release and decreased myofilament function. Exercise fully restored the ENDO cellular properties without affecting the EPI cells. The recovery of calcium transient after exercise was associated with changes in SERCA2a[17] and Na^+/Ca^{2+} exchanger[17] expression suggesting a recovery of the loading conditions of the sarcoplasmic reticulum. Further studies are needed to determine whether the exercise-induced improvement in systolic Ca^{2+} levels are due to changes in Ca^{2+} release properties through the ryanodine receptors.

Downloaded from cardiovascres.oxfordjournals.org at AstraZeneca R&D Lund on October 25, 2010

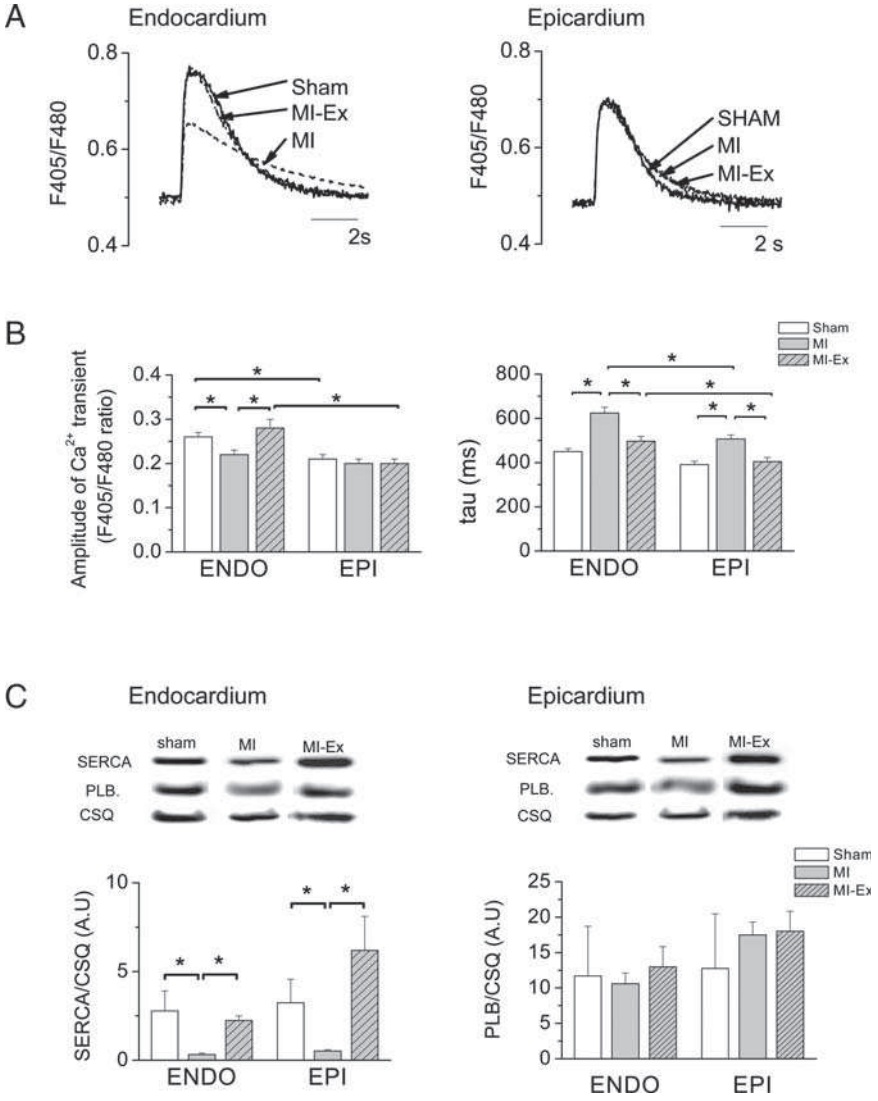

Figure 4 Calcium transient in isolated myocardial infarction (MI) and MI-exercise (MI-Ex) cardiomyocytes. (*A*) Ca^{2+} transient illustrations of endocardial (left trace) and epicardial (right trace) Sham, MI, and MI-Ex myocytes. (*B*) Average data of calcium transient amplitude and relaxation phase (tau). ($n = 55$–106 cells/5 hearts) (*C*) Immunoblot analysis of Ca^{2+}-handling proteins (SERCA and PLB) normalized with calsequestrin content ($n = 5$ hearts). *Adjusted $P < 0.05$.

Table 2 Regional mechanical properties of cardiomyocytes isolated from sham, myocardial infarcted (MI), and MI-exercised (MI-Ex) rats

	n	Sarcomere length, 1.9 μm				Sarcomere length, 2.3 μm				ΔpCa_{50}
		T_{pass}	T_{max}	pCa_{50}	n_H	T_{pass}	T_{max}	pCa_{50}	n_H	
Endocardium										
Sham	15	0.9 ± 0.2	47 ± 4	5.75 ± 0.02	4.1 ± 0.3	11.5 ± 0.9^{a}	50 ± 3	5.98 ± 0.02^{a}	4.7 ± 0.3	0.23 ± 0.01^{a}
MI	10	0.9 ± 0.3	40 ± 3	5.74 ± 0.03	4.6 ± 0.5	9.4 ± 1.2	47 ± 3	$5.88 \pm 0.03^{a,b,c}$	5.2 ± 0.5	$0.13 \pm 0.02^{b,c}$
MI-Ex	10	1.0 ± 0.2	45 ± 5	5.74 ± 0.03	4.7 ± 0.6	11.1 ± 1.9^{a}	46 ± 5	5.98 ± 0.02	5.1 ± 0.4	0.24 ± 0.02
Epicardium										
Sham	12	0.8 ± 0.1	36 ± 4	5.74 ± 0.01	4.4 ± 0.3	8.3 ± 0.8	38 ± 5	5.93 ± 0.01	4.6 ± 0.3	0.19 ± 0.01
MI	8	0.8 ± 0.3	35 ± 4	5.80 ± 0.01	5.0 ± 0.5	7.3 ± 1.5	40 ± 4	5.95 ± 0.01	5.4 ± 0.5	0.15 ± 0.02
MI-Ex	13	0.9 ± 0.3	38 ± 3	5.77 ± 0.01	4.8 ± 0.2	7.1 ± 0.5	40 ± 3	5.94 ± 0.01	5.2 ± 0.6	0.18 ± 0.02

Passive (T_{pass}) and maximal active (T_{max}) tensions in mN/mm^2 were measured at pCa9 and 4.5 and at 1.9 and 2.3 mm sarcomere length, respectively, on sub-epicardial (EPI) and sub-endocardial (ENDO) cells isolated from sham, MI, and MI-Ex hearts. pCa_{50} (pCa for half-maximal activation) and n_H (Hill coefficient) were calculated by fitting the force–pCa relation (see Materials and Methods). Values are means ± SEM (n = number of cells; five rats per group). [a]EPI vs. ENDO, [b]Sham vs. MI, [c]MI vs. MI-Ex; $P < 0.05$, two-way ANOVA.

Myofilament Ca^{2+} sensitivity was depressed at end-stage HF in the present study. Previous studies in single skinned myocytes have reported either increases[35] or decreases[3,4] in myofilament Ca^{2+} sensitivity both in human and experimental HF. The reasons for these different findings are not entirely clear. One explanation for these different findings

Downloaded from cardiovascres.oxfordjournals.org at AstraZeneca R&D Lund on October 25, 2010

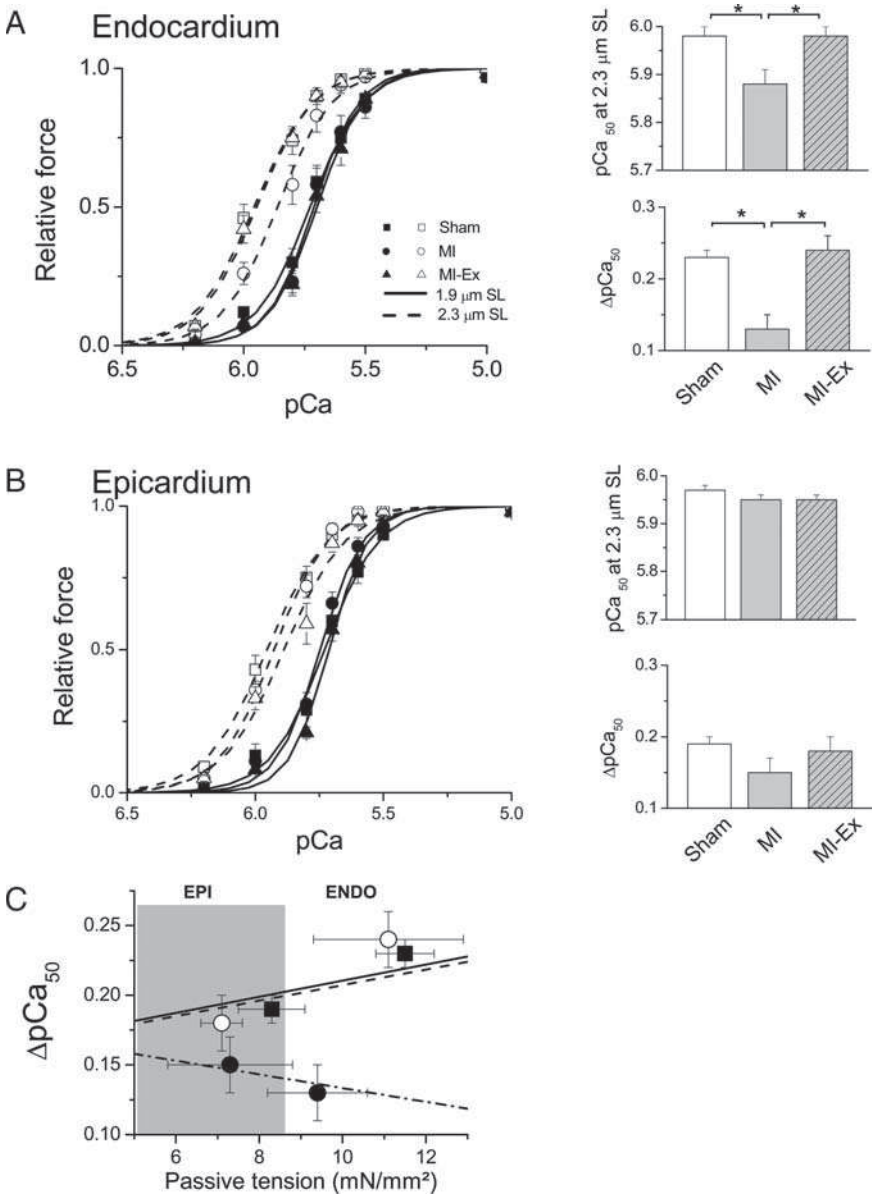

Figure 5 Effect of myocardial infarction (MI) and MI-exercise (MI-Ex) on myofilament properties in skinned cardiomyocytes: tension (normalized to maximal tension)-pCa curves of ENDO (*A*) and EPI (*B*) myocytes, measured at 1.9 (solid line, solid symbols) and at 2.3 μm (dashed line, open symbols) sarcomere length in Sham (square) MI (circle) and MI-Ex (triangle). (*A* and *B*, right) Myofilament Ca^{2+} sensitivity (pCa for half maximal activation) and the stretch-induced Ca^{2+} sensitization (ΔpCa_{50} difference in pCa_{50} obtained at 2.3 and 1.9 μm SL). (*C*) Correlation between ΔpCa_{50} and passive tension across the ventricle. Linear regressions were calculated on a scatter plot, including all individual data in Sham (solid line, square; $y = 0.15+0.005x$, $r = 0.51$ $P = 0.007$); MI (dash-dot line, solid circle, $y = 0.18–0.005x$, $r = -0.34$ $P = 0.16$); and MI-Ex (dashed line, open circle, $y = 0.15+0.005x$, $r = 0.34$ $P = 0.15$). *$P < 0.05$.

may relate to the different experimental preparations that were studied (multicellular vs. single myocyte skinned myocardium). Another explanation might be the level of neurohormonal stimulation present at the time of tissue preparation that will affect the balance between kinases and phosphatases. Indeed, most of the studies reported alterations of the level of phosphorylation of sarcomeric regulatory proteins that correlated with the changes in myofilament Ca^{2+} sensitivity. Finally, the origin of HF (ischaemic, pressure overload) and the stage of HF may also affect the results.[6]

HF in small rodents is associated with a shift in isomyosin synthesis from predominantly α-myosin towards β-myosin.[36] This shift observed during the LV remodelling has been proposed to improve myocardial work efficiency by generating cross-bridge force with a higher economy of energy consumption and thus maintaining contractility.[6] Similar shift can be observed in exercised animals.[24] In our study, β-MyHC content was increased by HF but was not affected by exercise. Thus, the beneficial effect of exercise on MI myocardial function is independent on myosin expression.

The level of MLC-2 phosphorylation affects myofilament Ca^{2+} sensitivity.[37] Increasing MLC-2 phosphorylation by incubating myofilaments with exogenous MLC Kinase (MLCK) increases myofilament Ca^{2+} sensitivity.[38–40] A decrease in MLC-2 phosphorylation has been described in failing human[41] and animal[3] hearts and has been associated with the observed decrease in myofilament Ca^{2+} sensitivity; similar results were obtained in ENDO MI myocytes of the present study. Thus, the increase in MLC-2 phosphorylation

Downloaded from cardiovascres.oxfordjournals.org at AstraZeneca R&D Lund on October 25, 2010

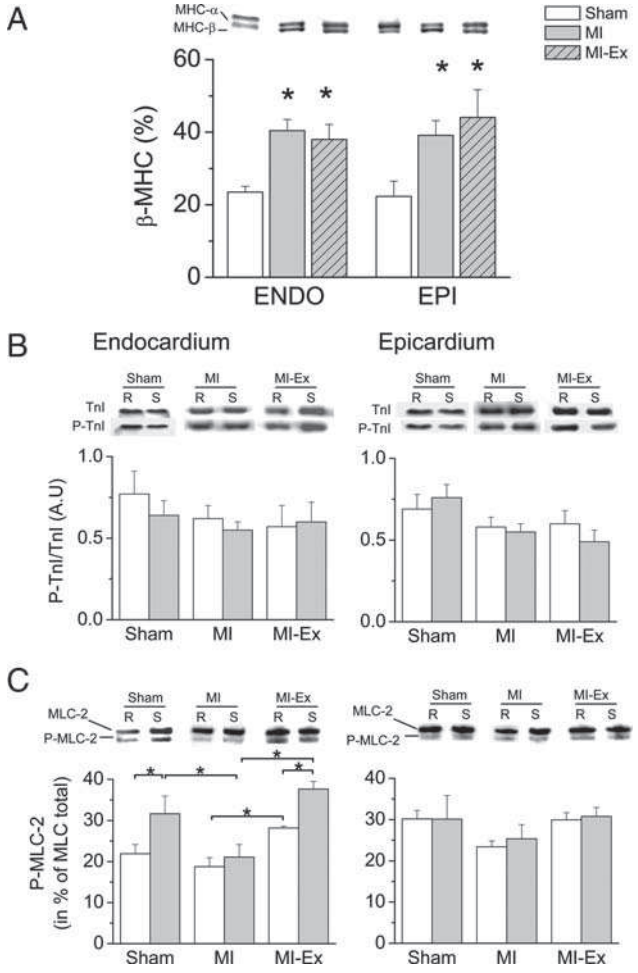

Figure 6 Effect of myocardial infarction and exercise on sarcomeric proteins: SDS–PAGE for α and β-MyHC isoforms; β-MyHC content was expressed in percentage of total MyHC in ENDO and EPI (*A*). Immunoblots with an anti-cardiac TnI and anti-cTnI phosphorylated by PKA (*B*), and with an anti-cardiac MLC-2 (*C*), on ENDO (left) and EPI (right) strips, in relax state (R, open bar) and after stretch (S, gray bar). *Adjusted $P < 0.05$.

in the ENDO tissue exclusively observed in the present study after exercise may by itself explain the improved myofilament Ca^{2+} sensitivity. The phosphorylation level of MLC-2 depends on the balance of activities between the MLCK and a protein phosphatase (PP).[40] MLCK activity is modulated by PKA and PKC phosphorylations, and Ca^{2+}–calmodulin interaction offering potential regulators for the exercise-induced effect on MLC-2 phosphorylation.[40,42] The normalization of Ca^{2+} transient after exercise in MI may contribute to increasing MLCK activity and thus MLC-2 phosphorylation. MLC-2 dephosphorylation is classically attributed to PP1. Studies suggest that PP1 activity and expression are increased in end-stage chronic heart failure (CHF) in dogs[43] but PP1 expression was found unchanged in rats with CHF.[44] In our study, alteration in PP1 activity after MI and/or exercise could account for the changes in MLC-2 phosphorylation and the lack of effect on TnI between MI and MI-Ex. However, more experiments are required to explore the kinase/phosphatase alteration after MI and exercise.

4.4 Limitations of the study

From the present study, we cannot draw any conclusions as to the effect of this protocol on life expectancy, since the animals were sacrificed at the end of the exercise protocol. In particular, future studies should determine how the improvement of the global and regional cardiac function and the normalization of the cellular dysfunctions post-MI at the end of the training could affect the occurrence of sudden cardiac death because of arrhythmic events. It would have been also interesting to obtain intraventricular pressure measurements that would have given more *in vivo* functional index, allowing to further explore the effect of exercise training on diastolic (dys)function in our model.

The present study indicates that exercise training started late after a large MI improved regional LV function and molecular phenotype, without any adverse effects on LV remodelling and survival during the protocol. The beneficial effects of exercise on cellular function have been proposed to restore β1-adrenergic signaling.[14] However, there is no sign here of such improvement that should affect the phosphorylation status of various proteins (TnI, PLB, titin-based passive tension). Future studies should be aimed at investigating whether this difference is due to the fact that exercise was performed in organisms in which the β-adrenergic signalling has been already extensively stimulated, suggesting other signalling pathways for exercise-induced beneficial effects. This is of particular interest since most patients with HF are treated with β-blockers. Another positive aspect of this study is that exercise preferentially restored the contractile properties of the tissue altered by the pathology (ENDO), allowing physiological cardiac contractile heterogeneity to be restored. Because of its relatively low cost, high availability and ease of use, exercise training is an intervention that could be accessible to most patients with HF.

Acknowledgements

Thanks are due to Patrice Bideaux, Guillermo Salazar and Christine Bernard-Crozier for technical assistance.

Conflict of interest: none declared.

Funding

This work was supported by the 'Association Française contre les Myopathies' and the Leducq Foundation. O.C. and A.L. are established investigators of CNRS.

References

1. Houser SR, Margulies KB. Is depressed myocyte contractility centrally involved in heart failure? *Circ Res* 2003;**92**:350–358.
2. Hajjar RJ, Gwathmey JK, Briggs GM, Morgan JP. Differential effect of DPI 201–106 on the sensitivity of the myofilaments to Ca2+ in intact and skinned trabeculae from control and myopathic human hearts. *J Clin Invest* 1988;**82**:1578–1584.
3. Cazorla O, Szilagyi S, Le Guennec JY, Vassort G, Lacampagne A. Transmural stretch-dependent regulation of contractile properties in rat heart and its alteration after myocardial infarction. *FASEB J* 2005;**19**:88–90.
4. Belin RJ, Sumandea MP, Kobayashi T, Walker LA, Rundell VL, Urboniene D *et al*. Left ventricular myofilament dysfunction in rat experimental hypertrophy and congestive heart failure. *Am J Physiol* 2006;**291**:H2344–H2353.
5. Ruf T, Schulte-Baukloh H, Ludemann J, Posival H, Beyersdorf F, Just H *et al*. Alterations of cross-bridge kinetics in human atrial and ventricular myocardium. *Cardiovasc Res* 1998;**40**:580–590.

Downloaded from cardiovascres.oxfordjournals.org at AstraZeneca R&D Lund on October 25, 2010

6. Daniels MC, Naya T, Rundell VL, de Tombe PP. Development of contractile dysfunction in rat heart failure: hierarchy of cellular events. *Am J Physiol* 2007;**293**:R284–R292.
7. Bogaert J, Rademakers FE. Regional nonuniformity of normal adult human left ventricle. *Am J Physiol* 2001;**280**:H610–H620.
8. Derumeaux G, Mulder P, Richard V, Chagraoui A, Nafeh C, Bauer F *et al*. Tissue Doppler imaging differentiates physiological from pathological pressure-overload left ventricular hypertrophy in rats. *Circulation* 2002;**105**:1602–1608.
9. Casillas JM, Gremeaux V, Damak S, Feki A, Perennou D. Exercise training for patients with cardiovascular disease. *Ann Readapt Med Phys* 2007;**50**: 403–418. 386–402.
10. Joshi SB. Exercise training in the management of cardiac failure and ischaemic heart disease. *Heart Lung Circ* 2007;**16**:S83–S87.
11. Palmer BM, Thayer AM, Snyder SM, Moore RL. Shortening and Ca2+ dynamics of left ventricular myocytes isolated from exercise-trained rats. *J Appl Physiol* 1998;**85**:2159–2168.
12. Hinken AC, Korte FS, McDonald KS. Porcine cardiac myocyte power output is increased after chronic exercise training. *J Appl Physiol* 2006; **101**:40–46.
13. Cohen MV. Coronary and collateral blood flows during exercise and myocardial vascular adaptations to training. *Exerc Sport Sci Rev* 1983;**11**: 55–98.
14. de Waard MC, van der Velden J, Bito V, Ozdemir S, Biesmans L, Boontje NM *et al*. Early exercise training normalizes myofilament function and attenuates left ventricular pump dysfunction in mice with a large myocardial infarction. *Circ Res* 2007;**100**:1079–1088.
15. Gaudron P, Hu K, Schamberger R, Budin M, Walter B, Ertl G. Effect of endurance training early or late after coronary artery occlusion on left ventricular remodeling, hemodynamics, and survival in rats with chronic transmural myocardial infarction. *Circulation* 1994;**89**:402–412.
16. Kubo N, Ohmura N, Nakada I, Yasu T, Katsuki T, Fujii M *et al*. Exercise at ventilatory threshold aggravates left ventricular remodeling in patients with extensive anterior acute myocardial infarction. *Am Heart J* 2004; **147**:113–120.
17. Wisloff U, Loennechen JP, Currie S, Smith GL, Ellingsen O. Aerobic exercise reduces cardiomyocyte hypertrophy and increases contractility, Ca2+ sensitivity and SERCA-2 in rat after myocardial infarction. *Cardiovasc Res* 2002;**54**:162–174.
18. Krenz M, Robbins J. Impact of beta-myosin heavy chain expression on cardiac function during stress. *JACC* 2004;**44**:2390–2397.
19. Trueblood NA, Inscore PR, Brenner D, Lugassy D, Apstein CS, Sawyer DB *et al*. Biphasic temporal pattern in exercise capacity after myocardial infarction in the rat: relationship to left ventricular remodeling. *Am J Physiol* 2005;**288**:H244–H249.
20. Turschner O, D'Hooge J, Dommke C, Claus P, Verbeken E, De Scheerder I *et al*. The sequential changes in myocardial thickness and thickening which occur during acute transmural infarction, infarct reperfusion and the resultant expression of reperfusion injury. *Eur Heart J* 2004;**25**: 794–803.
21. Reboul C, Tanguy S, Juan JM, Dauzat M, Obert P. Cardiac remodeling and functional adaptations consecutive to altitude training in rats: implications for sea level aerobic performance. *J Appl Physiol* 2005;**98**:83–92.
22. Borenstein N, Bruneval P, Behr L, Laborde F, Montarras D, Daures JP *et al*. An ovine model of chronic heart failure: echocardiographic and tissue Doppler imaging characterization. *J Card Surg* 2006;**21**:50–56.
23. Cazorla O, Lacampagne A, Fauconnier J, Vassort G. SR33805, a Ca2+ antagonist with length-dependent Ca2+ -sensitizing properties in cardiac myocytes. *Br J Pharmacol* 2003;**139**:99–108.
24. Cazorla O, Ait Mou Y, Goret L, Vassort G, Dauzat M, Lacampagne A *et al*. Effects of high-altitude exercise training on contractile function of rat skinned cardiomyocyte. *Cardiovasc Res* 2006;**71**:652–660.
25. Ashikaga H, Coppola BA, Hopenfeld B, Leifer ES, McVeigh ER, Omens JH. Transmural dispersion of myofiber mechanics: implications for electrical heterogeneity *in vivo*. *JACC* 2007;**49**:909–916.
26. Buchi M, Hess OM, Murakami T, Krayenbuehl HP. Left ventricular wall stress distribution in chronic pressure and volume overload: effect of normal and depressed contractility on regional stress-velocity relations. *Basic Res Cardiol* 1990;**85**:367–383.
27. Litwin SE, Katz SE, Morgan JP, Douglas PS. Serial echocardiographic assessment of left ventricular geometry and function after large myocardial infarction in the rat. *Circulation* 1994;**89**:345–354.
28. Konstam MA, Udelson JE, Sharpe N. Prevention and reversal of left ventricular remodeling: Summation. *J Card Fail* 2002;**8**:S506–S511.
29. Sullivan MJ, Higginbotham MB, Cobb FR. Exercise training in patients with severe left ventricular dysfunction. Hemodynamic and metabolic effects. *Circulation* 1988;**78**:506–515.
30. Giannuzzi P, Temporelli PL, Corra U, Gattone M, Giordano A, Tavazzi L. Attenuation of unfavorable remodeling by exercise training in postinfarction patients with left ventricular dysfunction: results of the Exercise in Left Ventricular Dysfunction (ELVD) trial. *Circulation* 1997;**96**:1790–1797.
31. Carluccio E, Tommasi S, Bentivoglio M, Buccolieri M, Prosciutti L, Corea L. Usefulness of the severity and extent of wall motion abnormalities as prognostic markers of an adverse outcome after a first myocardial infarction treated with thrombolytic therapy. *Am J Cardiol* 2000;**85**:411–415.
32. Moller JE, Egstrup K, Kober L, Poulsen SH, Nyvad O, Torp-Pedersen C. Prognostic importance of systolic and diastolic function after acute myocardial infarction. *Am Heart J* 2003;**145**:147–153.
33. Haykowsky MJ, Liang Y, Pechter D, Jones LW, McAlister FA, Clark AM. A meta-analysis of the effect of exercise training on left ventricular remodeling in heart failure patients: the benefit depends on the type of training performed. *JACC* 2007;**49**:2329–2336.
34. Konhilas JP, Watson PA, Maass A, Boucek DM, Horn T, Stauffer BL *et al*. Exercise can prevent and reverse the severity of hypertrophic cardiomyopathy. *Circ Res* 2006;**98**:540–548.
35. van der Velden J, Papp Z, Zaremba R, Boontje NM, de Jong JW, Owen VJ *et al*. Increased Ca2+-sensitivity of the contractile apparatus in end-stage human heart failure results from altered phosphorylation of contractile proteins. *Cardiovasc Res* 2003;**57**:37–47.
36. Swynghedauw B. Developmental and functional adaptation of contractile proteins in cardiac and skeletal muscles. *Physiol Rev* 1986;**66**:710–771.
37. Morano I. Tuning the human heart molecular motors by myosin light chains. *J Mol Med* 1999;**77**:544–555.
38. Clement O, Puceat M, Walsh MP, Vassort G. Protein kinase C enhances myosin light-chain kinase effects on force development and ATPase activity in rat single skinned cardiac cells. *Biochem J* 1992;**285**:311–317.
39. Olsson MC, Patel JR, Fitzsimons DP, Walker JW, Moss RL. Basal myosin light chain phosphorylation is a determinant of Ca2+ sensitivity of force and activation dependence of the kinetics of myocardial force development. *Am J Physiol* 2004;**287**:H2712–H2718.
40. Rajashree R, Blunt BC, Hofmann PA. Modulation of myosin phosphatase targeting subunit and protein phosphatase 1 in the heart. *Am J Physiol* 2005;**289**:H1736–H1743.
41. van der Velden J, Papp Z, Boontje NM, Zaremba R, de Jong JW, Janssen PML *et al*. The effect of myosin light chain 2 dephosphorylation on Ca2+-sensitivity of force is enhanced in failing human hearts. *Cardiovasc Res* 2003;**57**:505–514.
42. Grimm M, Mahnecke N, Soja F, El-Armouche A, Haas P, Treede H *et al*. The MLCK-mediated alpha1-adrenergic inotropic effect in atrial myocardium is negatively modulated by PKCepsilon signaling. *Br J Pharmacol* 2006; **148**:991–1000.
43. Gupta RC, Mishra S, Rastogi S, Imai M, Habib O, Sabbah HN. Cardiac SR-coupled PP1 activity and expression are increased and inhibitor 1 protein expression is decreased in failing hearts. *Am J Physiol* 2003; **285**:H2373–H2381.
44. Belin RJ, Sumandea MP, Allen EJ, Schoenfelt K, Wang H, Solaro RJ *et al*. Augmented protein kinase C-alpha-induced myofilament protein phosphorylation contributes to myofilament dysfunction in experimental congestive heart failure. *Circ Res* 2007;**101**:195–204.

Downloaded from cardiovascres.oxfordjournals.org at AstraZeneca R&D Lund on October 25, 2010

Annexe 2

Moderate exercise 1 prevents impaired Ca2+ handling in heart of CO exposed rat: implication for sensitivity to ischemia-reperfusion

C. Farah, G. Meyer, L. André, J. Boissière, S. Gayrard, O. Cazorla, S. Richard, F. Boucher, S. Tanguy, P. Obert, C. Reboul

Am J Physiol Heart Circ Physiol (October 1, 2010)

Articles in PresS. Am J Physiol Heart Circ Physiol (October 1, 2010). doi:10.1152/ajpheart.00835.2010

Moderate exercise prevents impaired Ca^{2+} handling in heart of CO exposed rat: implication for sensitivity to ischemia-reperfusion

C. Farah[1]*, G. Meyer[1]*, L. André[2], J. Boissière[1], S. Gayrard[1], O. Cazorla[2], S. Richard[2], F. Boucher[3], S. Tanguy[1], P. Obert[1], C. Reboul[1].

[1], Research Laboratory: EA 4278, Physiology and Physiopathology of Cardiovascular Adaptations to Exercise, Faculty of Sciences, Avignon University, F-84000 Avignon, France

[2], Research Laboratory: INSERM U637, Cardiovascular Physiopathology, MONTPELLIER1 University, Faculty of Medicine, F-34295 Montpellier, France

[3], Research Laboratory: CNRS UMR5525 PRETA-TIMC, F-38000 Grenoble University Joseph Fourier, Grenoble, France

*, both authors contributed equally to this work

Running Title: CO pollution and exercise cardioprotection

Words count: 3775

Contact information: Cyril.reboul@univ-avignon.fr

Phone number: 00.334.90.16.29.32

Fax number: 00.334.90.16.29.0

Copyright © 2010 by the American Physiological Society.

Introduction: Sustained urban carbon monoxide (CO) exposure exacerbates heart vulnerability to ischemia reperfusion via deleterious effects on the antioxidant status and Ca^{2+} homeostasis of cardiomyocytes. The aim of this work was to evaluate whether moderate exercise training prevents these effects. **Methods**: Wistar rats were randomly assigned to control group and to CO groups, living during 4 weeks in simulated urban CO pollution (30-100 ppm, 12 h/day) with (CO-Ex) or without exercise (CO-Sed). Exercise procedure began 4 weeks before CO exposure and was maintained twice a week in standard filtered air during CO exposure. On a first set of rats, myocardial ischemia (30 min) and reperfusion (120 min) were performed on isolated perfused rat hearts. On another set of rats, myocardial antioxidant status and Ca^{2+} handling were evaluated following environmental exposure. **Results and discussion**: Exercise training prevented CO-induced myocardial phenotypical changes. Indeed, exercise induced myocardial antioxidant status recovery in CO exposed rats, which is accompanied by normalization of SERCA-2a expression and then of Ca^{2+} handling. Importantly, in CO exposed rats, the normalization of cardiomyocytes phenotype with moderate exercise was associated with restored sensitivity of the myocardium to IR. Indeed, CO-Ex rats present a lower infarct size and a significant decrease of reperfusion arrhythmias when compared to their sedentary counterparts. To conclude, moderate exercise, by preventing CO-induced Ca^{2+} handling and myocardial antioxidant status alterations, reduces heart vulnerability to IR.

Keywords: Myocardial infarction, Environmental pollution, Endurance training, antioxidant status

1. Introduction

The severity of myocardial infarction results from a complex interplay between genetic, pathological and environmental factors (22, 27). Among environmental factors, numerous epidemiological studies have demonstrated that carbon monoxide (CO) pollution correlated with hospital admissions for cardiovascular diseases (3, 17), as well as cardiovascular mortality (28). We recently reported that sustained low level CO exposure, similar to that found in an urban environment, induced a pathological remodelling of the myocardium (1) rendering the heart more vulnerable to ischemia-reperfusion (IR) (18). This remodelling involves a marked alteration of enzymatic antioxidant status associated with marked changes in Ca^{2+} handling (1), promoting cardiomyocyte death and severe ventricular arrhythmias (18).

Today, amongst numerous cardioprotective strategies used to prevent deleterious myocardial remodelling associated with several pathological states, and/or to reduce the vulnerability of the heart to acute ischemic events, regular endurance exercise training is reported as one of the most practicable and sustainable methods (2, 7, 11, 25, 26). Although mechanisms responsible for exercise-induced cardioprotection remain unclear, many studies suggest that increased enzymatic antioxidant status plays an important role (7, 10, 35). In addition, exercise training is also reported to normalize Ca^{2+} homeostasis in the pathological myocardium (29, 32). Therefore, we have hypothesized that regular exercise training started prior to sustained CO exposure could prevent pathological cardiac remodelling and/or modulate heart vulnerability to IR.

The aim of this study was to evaluate potential cardioprotective effects of regular bouts of endurance training in an experimental rat model exposed to

simulated sustained urban CO pollution. Especially, we focused on the effects of exercise training on Ca^{2+} handling, myocardial enzymatic antioxidant status alterations and consequences on heart vulnerability to IR. The major results showed that regular bouts of endurance training prevented the pathological cardiac remodelling and the higher vulnerability to IR of the hearts of rats exposed to chronic CO.

2. Methods

All investigations complied with the *Guide for the Care and Use of Laboratory Animals* published by the US National Institutes of Health (NIH Publications No. 85-23, revised 1996) and with the approval of the French Ministry of Agriculture. All experiments have been approved by the local research ethics committee (Comité Régional d'Ethique).

2.1. Animals

Adult male Wistar rats (n=57; 384±3 g; Charles Rivers Laboratories) were randomly assigned to three experimental groups: 1) sedentary control group (Ctrl-Sed rats), 2) sedentary CO exposed group (CO-Sed rats), 3) trained CO exposed group (CO-Ex rats). All experimental groups were maintained on a 12:12 hour light-dark cycle and provided rat chow and water *ad libitum*.

2.2. Exercise training protocol

Moderate exercise training protocol was performed on a motor driven treadmill for 4 weeks, 5 days/week at a relative work rate corresponding to 50 % of maximal aerobic velocity (20 m/min; 40 min/day). During the 4 following weeks, corresponding to CO exposure period, to preserve exercise training benefits, exercise training was maintained in CO-Ex rats on a frequency of 2 days/week.

2.3. Carbon monoxide exposure

CO groups were exposed to simulated CO urban pollution for 4 weeks, 12 hours/day during the night phase. CO rats were housed in an airtight exposure container and exposure was performed as follows: i) During CO exposure, a CO concentration of 30 ppm was maintained in the airtight container and monitored with an aspirative CO analyzer (CHEMGARD Infrared Gas Monitor NEMA 4 Version, MSA), this initial concentration was completed with five 1 hour peaks at 100 ppm CO; ii) During ambient air exposure, animals were placed in the laboratory animal-house at a CO concentration of 0 ppm. Throughout this CO exposure period, Ctrl-Sed rats were confined in the laboratory animal-house and were subjected to the same restraint as the CO-Sed rats. At the end of the 4 weeks of CO exposure, the rats were housed for 24 hours in standard filtered air before euthanasia in order to avoid acute effects of CO on the myocardium.

2.4. Ca^{2+} handling in cardiomyocytes

In the first set of rats (n=4 rats/group; 10 myocytes/rat), evaluation of exercise training and CO exposure on excitation-contraction was performed on single ventricular cardiomyocytes isolated by enzymatic digestion (21). Unloaded cell shortening and Ca^{2+} concentration (Indo-1 dye) were measured using field stimulation (0.5 Hz, 22°C, 1.8 mM external Ca^{2+}). Sarcomere length (SL) and fluorescence (405 and 480 nm) were simultaneously recorded (IonOptix system, Hilton, USA) (1).

2.5. Regional myocardial ischemia-reperfusion protocol on isolated perfused heart

In a second set of rats (n=10/group), a regional myocardial IR protocol on isolated-perfused heart was performed (18). This model was chosen in order to abrogate the potential effects of CO exposure on hormonal, circulating and nervous parameters. The coronary occlusion-induced myocardial regional ischemia was maintained for 30 min. Subsequently, the heart was allowed to reperfuse during 120 min. Lactate dehydrogenase (LDH) release and incidence of ventricular fibrillation was evaluated during the reperfusion period. At the end of the perfusion, the hearts were divided into five slices perpendicular to the apex–base axis and Triphenyltetrazolium Chloride staining (TTC, 0.5 mg/ml for 20 min at 37°C) was used to assess myocardial tissue viability and to determine myocardial infarct size. Tissue slices were photographed; risk and infarcted area were then determined using a computer-based system (ImageJ, NIH, USA).

2.6. Biochemical assays

2.6.1. Heart antioxidant enzyme activity

In order to assess the effects of exercise training and/or CO exposure on the antioxidant capacity, heart enzymatic antioxidant status was measured in the third set of rats as previously described (n=5/group), (18). Superoxide dismutase (SOD), catalase (CAT) and glutathione peroxidase (GPx) enzymatic activities were evaluated.

2.6.2. Lactate dehydrogenase activity in coronary effluents

LDH activity, used as an index of cell membrane damage, was measured in coronary effluents at 5 min of reperfusion. LDH activity was measured spectrophotometrically using a LDH kit (LDH-P, BIOLABO SA, France).

2.6.3. Western blot analysis

Proteins were separated using 4-20 % SDS-PAGE and blotted onto a nitrocellulose membrane (Protran, Schleichen and Schuele, Dassel, Germany). Membranes were incubated overnight at 4°C with the SERCA-2a antibody (A010-20, Badrilla, UK), and levels were expressed relative to glyceraldehydes 3-phosphate dehydrogenase (GAPDH) content on the same membrane. Immunodetection was carried out using the ECL Plus system (Amersham Pharmacia, Little Chalfont Buckinghamshire, England).

2.7. Statistics

Data were analyzed using either one-way factorial or repeated measures ANOVA. When significant interactions were found, a Student-Newman-Keuls test was applied. Binomially distributed variables (such as incidence of ventricular fibrillations) were analyzed using a non parametric Yates' chi square test (Statview; Adept scientific, Letchworth, UK). A level of $p<0.05$ was considered statistically significant. Data are expressed as group means or group mean fractions of baseline ± S.E.

3. Results

3.1. Contraction and Ca^{2+} handling in single cells

Chronic exposure to CO pollution decreased SL shortening (Fig. 1 AB), increased diastolic cytosolic Ca^{2+} (Fig. 1 CD), and decreased the amplitude of the Ca^{2+} transient (Fig. 1 CE). In addition, the decay kinetics (tau) of the Ca^{2+} transient were impaired (Fig. 1 F), which was explained by a decrease in SERCA-2a expression in CO rats (Fig. 1 G). Exercise training prevented both SERCA-2a reduction (Fig. 1 G) and Ca^{2+} handling alterations (Fig. 1 DEF). Exercise training therefore preserved normal SL shortening, which was similar to that of rats living in standard filtered air (Fig. 1 AB).

3.2. Myocardial enzymatic antioxidant status.

After 4 weeks of sustained CO exposure, myocardial enzymatic antioxidant status was depressed. The SOD and GPx activities were reduced in CO-Sed rats compared to Ctrl-Sed rats (Fig. 2 AB). Exercise training prevented these deleterious effects as SOD and GPx activities did not differ between CO-Ex rats and Ctrl-Sed rats. In contrast, no effect from CO exposure or exercise training was reported on CAT activity (Fig. 2 C).

3.3. Infarct size and myocardial cells death.

Cardiac cells death induced by IR was aggravated by prolonged CO exposure (Fig. 3 AB). Indeed, infarct size was higher in CO rats than in controls. In addition, LDH release, measured in coronary effluents at the time of post-ischemic myocardial reperfusion and used as an index of cell membrane damage, was higher in CO exposed rats than in their counterparts. The promoting effect of CO exposure on myocardial necrosis was fully prevented by regular exercise as no difference in infarct size was observed between CO-Ex and Ctrl-Sed rats (Fig. 3 AB). Consistently, the same result was obtained regarding the effects of exercise on LDH release during post-ischemic reperfusion (Fig. 3 C).

3.4. Myocardial reperfusion arrhythmias.

Although no difference was observed in the incidence of VF (33 %, Ctrl-Sed *vs.* 50 % CO-Sed), chronic CO exposure was responsible for a marked increase in the severity of post-ischemic reperfusion VF. Indeed, sustained VF (Fig. 3 D) occurred in 25 % of CO-Sed rats, whereas this phenomenon was not observed in Ctrl-Sed rats (Fig. 3 E). Interestingly the pronounced deleterious effect of CO exposure on the severity of reperfusion arrhythmias was fully prevented by exercise training since no VF was reported in CO-Ex rats (Fig. 3 E).

4. Discussion

The major results of this study are that endurance training prevents the deleterious effects of sustained CO exposure on myocardial antioxidant status, cellular Ca^{2+} handling and myocardial vulnerability to IR injury.

4.1 CO exposure and cardioprotective effects of exercise training

In line with previous reports, including ours, we confirmed here deleterious effects of simulated urban CO exposure on enzymatic antioxidant status and cardiomyocyte Ca^{2+} handling (1, 4). Low and sustained levels of CO exposure promoted pathological cardiac remodelling with impaired Ca^{2+} handling due to increased diastolic Ca^{2+}, decreased Ca^{2+} transient and Ca^{2+} reuptake in the sarcoplasmic reticulum (SR) due to reduced SERCA-2a expression (1, 4). These changes are related to CO-induced oxidative stress (18, 37), being associated with altered redox (1) and enzymatic antioxidant statuses (1, 18).

One main result of the present study was that moderate exercise training conducted prior to CO exposure, successfully prevented the deleterious effects of CO exposure on myocardial enzymatic antioxidant activities (SOD and GPx). Even if the underlying mechanisms are not fully understood yet, exercise training is well-recognized today as one of the most efficient cardioprotective strategies, notably through the enhancement of myocardial antioxidant status (2, 7, 12, 15, 16). Consistently, exercise preserved antioxidant status and, thereby, prevented cytosolic Ca^{2+} overload and depressed Ca^{2+} transient in CO-trained rats, in line with various reports of beneficial effects of exercise training on Ca^{2+} handling in pathological population (21, 29, 32). Maintenance of normal SERCA-2a expression mainly

229 explained this benefit on Ca^{2+} homeostasis. Although direct effects of exercise
230 training on SERCA-2a expression could not be ruled out (21, 33), our results are
231 consistent with indirect effects mediated by the normalization of enzymatic
232 antioxidant status on this redox sensitive protein (8, 20, 31, 34).

233

234 4.2. Endurance training and sensitivity to IR consecutive to CO exposure

235 We recently reported that sustained CO-exposure increased the vulnerability
236 to IR (18). Although lower infarct sizes in CO rats were observed in this study
237 compared to the previous one (18), the present work confirms that CO exposure is
238 associated with increased severity of myocardial IR injuries, characterized by
239 exacerbated occurrence of sustained ventricular fibrillations and cardiomyocyte
240 death. These results are in line with the well-reported determinant role of oxidative
241 stress and Ca^{2+} overload in the severity of post-ischemic reperfusion arrhythmias,
242 cardiac dysfunction, and irreversible cardiomyocyte damages (5, 6, 22, 36). A major
243 result of our study was that endurance training, by preventing CO-induced cellular
244 alterations, fully prevented the worsened sensitivity of CO rats to IR. This is in
245 accordance with numerous studies supporting the successful cardioprotective effect
246 of exercise training against IR injuries (2, 7, 11, 25, 26). This beneficial effect has
247 been largely proposed to reflect improved myocardial enzymatic antioxidant status (7,
248 9, 25, 35). In our work, normalization of enzymatic antioxidant activities certainly
249 contributed to decrease the sensitivity of CO-rat hearts to IR. In addition, various
250 studies also reported the preservation of Ca^{2+} homeostasis as being a key factor for
251 improvement in ischemic heart disease tolerance (30). In particular, the functional
252 level of SERCA-2a is one of the factors that determines intracellular Ca^{2+} overload

following IR injuries (23, 30). Taken together, our results show that indirect effects (mediated by antioxidant effects) or/and direct beneficial effects of exercise on SERCA-2a expression play a major role to normalize heart vulnerability to IR in rats exposed to sustained CO.

Finally, it has to be noted that, in this work, no specific effect of low intensity exercise training was reported in Ctrl exercised rats when compared to Ctrl ones (data not shown). This result is not surprising since it is today well known that high intensity exercise training is more effective to induce adaptations in healthy rat hearts (13, 14). Therefore, one of the main findings of the present work is that an exercise training protocol, specifically design to follow the recommendation of the World Health Organisation (30 min 5 days per week at low intensity (24)), was shown to be efficient to prevent the development of a myocardial vulnerable phenotype in CO exposed rats.

Taken together, our results demonstrate that regular exercise training mainly prevents the toxicity of prolonged exposure to environmental CO due to urban pollution. These results point out the essential role of CO-induced cellular Ca^{2+} handling and antioxidant status alterations in the higher vulnerability of CO rats' myocardium to IR and the prevention of these alterations by exercise training. Endurance training, recognized as an efficient antioxidant strategy, seems to be a relevant cardioprotective approach capable of preventing higher cardiac vulnerability to ischemic stress. Given that exposure to air pollutants is an important health issue, responsible for 800,000 premature deaths worldwide each year and with increases in the risk of mortality from cardiovascular disease by 76% (19), such a workable preventive strategy is very attractive and deserves further interests.

5. Grants

This work was supported by a French National Research Agency grant (COMYOCARD).

6. Author Disclosure Statement.

No competing financial interests exist

7. Bibliography

1. **Andre L, Boissiere J, Reboul C, Perrier R, Zalvidea S, Meyer G, Thireau J, Tanguy S, Bideaux P, Hayot M, Boucher F, Obert P, Cazorla O, and Richard S.** Carbon Monoxide Pollution Promotes Cardiac Remodeling and Ventricular Arrhythmia in Healthy Rats. *Am J Respir Crit Care Med*, 2009.

2. **Ascensao A, Ferreira R, and Magalhaes J.** Exercise-induced cardioprotection--biochemical, morphological and functional evidence in whole tissue and isolated mitochondria. *Int J Cardiol* 117: 16-30, 2007.

3. **Burnett RT, Cakmak S, Brook JR, and Krewski D.** The role of particulate size and chemistry in the association between summertime ambient air pollution and hospitalization for cardiorespiratory diseases. *Environ Health Perspect* 105: 614-620, 1997.

4. **Bye A, Sorhaug S, Ceci M, Hoydal MA, Stolen T, Heinrich G, Tjonna AE, Najjar SM, Nilsen OG, Catalucci D, Grimaldi S, Contu R, Steinshamn S, Condorelli G, Smith GL, Ellingsen O, Waldum H, and Wisloff U.** Carbon monoxide levels experienced by heavy smokers impair aerobic capacity and cardiac contractility and induce pathological hypertrophy. *Inhal Toxicol* 20: 635-646, 2008.

5. **Dhalla NS, Temsah RM, and Netticadan T.** Role of oxidative stress in cardiovascular diseases. *J Hypertens* 18: 655-673, 2000.

6. **Dumitrescu C, Biondi R, Xia Y, Cardounel AJ, Druhan LJ, Ambrosio G, and Zweier JL.** Myocardial ischemia results in tetrahydrobiopterin (BH4) oxidation with impaired endothelial function ameliorated by BH4. *Proc Natl Acad Sci U S A* 104: 15081-15086, 2007.

7. **French JP, Hamilton KL, Quindry JC, Lee Y, Upchurch PA, and Powers SK.** Exercise-induced protection against myocardial apoptosis and necrosis: MnSOD, calcium-handling proteins, and calpain. *Faseb J* 22: 2862-2871, 2008.

8. **Grover AK, Samson SE, Robinson S, and Kwan CY.** Effects of peroxynitrite on sarcoplasmic reticulum Ca2+ pump in pig coronary artery smooth muscle. *Am J Physiol Cell Physiol* 284: C294-301, 2003.

9. **Hamilton KL, Quindry JC, French JP, Staib J, Hughes J, Mehta JL, and Powers SK.** MnSOD antisense treatment and exercise-induced protection against arrhythmias. *Free Radic Biol Med* 37: 1360-1368, 2004.

10. **Hamilton KL, Staib JL, Phillips T, Hess A, Lennon SL, and Powers SK.** Exercise, antioxidants, and HSP72: protection against myocardial ischemia/reperfusion. *Free Radic Biol Med* 34: 800-809, 2003.

11. **Kavazis AN.** Exercise preconditioning of the myocardium. *Sports Med* 39: 923-935, 2009.

12. **Kavazis AN, McClung JM, Hood DA, and Powers SK.** Exercise induces a cardiac mitochondrial phenotype that resists apoptotic stimuli. *Am J Physiol Heart Circ Physiol* 294: H928-935, 2008.

13. **Kemi OJ, Ellingsen O, Smith GL, and Wisloff U.** Exercise-induced changes in calcium handling in left ventricular cardiomyocytes. *Front Biosci* 13: 356-368, 2008.

14. **Kemi OJ and Wisloff U.** Mechanisms of exercise-induced improvements in the contractile apparatus of the mammalian myocardium. *Acta Physiol (Oxf)* 199: 425-439, 2010.

15. **Lennon SL, Quindry JC, French JP, Kim S, Mehta JL, and Powers SK.** Exercise and myocardial tolerance to ischaemia-reperfusion. *Acta Physiol Scand* 182: 161-169, 2004.

16. **Lew H and Quintanilha A.** Effects of endurance training and exercise on tissue antioxidative capacity and acetaminophen detoxification. *Eur J Drug Metab Pharmacokinet* 16: 59-68, 1991.

17. **Mann JK, Tager IB, Lurmann F, Segal M, Quesenberry CP, Jr., Lugg MM, Shan J, and Van Den Eeden SK.** Air pollution and hospital admissions for ischemic heart disease in persons with congestive heart failure or arrhythmia. *Environ Health Perspect* 110: 1247-1252, 2002.

18. **Meyer G, Andre L, Tanguy S, Boissiere J, Farah C, Lopez-Lauri F, Gayrard S, Richard S, Boucher F, Cazorla O, Obert P, and Reboul C.** Simulated urban carbon monoxide air pollution exacerbates rat heart ischemia-reperfusion injury. *Am J Physiol Heart Circ Physiol* 298: H1445-1453, 2010.

19. **Miller KA, Siscovick DS, Sheppard L, Shepherd K, Sullivan JH, Anderson GL, and Kaufman JD.** Long-term exposure to air pollution and incidence of cardiovascular events in women. *N Engl J Med* 356: 447-458, 2007.

20. **Morris TE and Sulakhe PV.** Sarcoplasmic reticulum Ca(2+)-pump dysfunction in rat cardiomyocytes briefly exposed to hydroxyl radicals. *Free Radic Biol Med* 22: 37-47, 1997.

21. **Mou YA, Reboul C, Andre L, Lacampagne A, and Cazorla O.** Late exercise training improves non-uniformity of transmural myocardial function in rats with ischaemic heart failure. *Cardiovasc Res* 81: 555-564, 2009.

22. **Murphy E and Steenbergen C.** Mechanisms underlying acute protection from cardiac ischemia-reperfusion injury. *Physiol Rev* 88: 581-609, 2008.

23. **Niwano K, Arai M, Koitabashi N, Watanabe A, Ikeda Y, Miyoshi H, and Kurabayashi M.** Lentiviral vector-mediated SERCA2 gene transfer protects against heart failure and left ventricular remodeling after myocardial infarction in rats. *Mol Ther* 16: 1026-1032, 2008.

24. **OMS and FIMS.** Committee on Physical Activity for Health. Exercise for Health. ***Journal of the World Health Organisation*** 73: 135-136, 1995.

25. **Powers SK, Demirel HA, Vincent HK, Coombes JS, Naito H, Hamilton KL, Shanely RA, and Jessup J.** Exercise training improves myocardial tolerance to in vivo ischemia-reperfusion in the rat. *Am J Physiol* 275: R1468-1477, 1998.

26. **Powers SK, Quindry JC, and Kavazis AN.** Exercise-induced cardioprotection against myocardial ischemia-reperfusion injury. *Free Radic Biol Med* 44: 193-201, 2008.

27. **Ruiz-Meana M and Garcia-Dorado D.** Translational cardiovascular medicine (II). Pathophysiology of ischemia-reperfusion injury: new therapeutic options for acute myocardial infarction. *Rev Esp Cardiol* 62: 199-209, 2009.

28. **Samoli E, Touloumi G, Schwartz J, Anderson HR, Schindler C, Forsberg B, Vigotti MA, Vonk J, Kosnik M, Skorkovsky J, and Katsouyanni K.** Short-term effects of carbon monoxide on mortality: an analysis within the APHEA project. *Environ Health Perspect* 115: 1578-1583, 2007.

29. **Stolen TO, Hoydal MA, Kemi OJ, Catalucci D, Ceci M, Aasum E, Larsen T, Rolim N, Condorelli G, Smith GL, and Wisloff U.** Interval training normalizes cardiomyocyte function, diastolic Ca2+ control, and SR Ca2+ release synchronicity in a mouse model of diabetic cardiomyopathy. *Circ Res* 105: 527-536, 2009.

30. **Talukder MA, Zweier JL, and Periasamy M.** Targeting calcium transport in ischaemic heart disease. *Cardiovasc Res* 84: 345-352, 2009.

31. **Viner RI, Krainev AG, Williams TD, Schoneich C, and Bigelow DJ.** Identification of oxidation-sensitive peptides within the cytoplasmic domain of the sarcoplasmic reticulum Ca2+-ATPase. *Biochemistry* 36: 7706-7716, 1997.

32. **Wisloff U, Loennechen JP, Currie S, Smith GL, and Ellingsen O.** Aerobic exercise reduces cardiomyocyte hypertrophy and increases contractility, Ca2+ sensitivity and SERCA-2 in rat after myocardial infarction. *Cardiovasc Res* 54: 162-174, 2002.

33. **Wisloff U, Loennechen JP, Falck G, Beisvag V, Currie S, Smith G, and Ellingsen O.** Increased contractility and calcium sensitivity in cardiac myocytes isolated from endurance trained rats. *Cardiovasc Res* 50: 495-508, 2001.

34. **Xu KY, Zweier JL, and Becker LC.** Hydroxyl radical inhibits sarcoplasmic reticulum Ca(2+)-ATPase function by direct attack on the ATP binding site. *Circ Res* 80: 76-81, 1997.

35. **Yamashita N, Hoshida S, Otsu K, Asahi M, Kuzuya T, and Hori M.** Exercise provides direct biphasic cardioprotection via manganese superoxide dismutase activation. *J Exp Med* 189: 1699-1706, 1999.

36. **Zhao X, Chen YR, He G, Zhang A, Druhan LJ, Strauch AR, and Zweier JL.** Endothelial nitric oxide synthase (NOS3) knockout decreases NOS2 induction, limiting hyperoxygenation and conferring protection in the postischemic heart. *Am J Physiol Heart Circ Physiol* 292: H1541-1550, 2007.

37. **Zuckerbraun BS, Chin BY, Bilban M, d'Avila JC, Rao J, Billiar TR, and Otterbein LE.** Carbon monoxide signals via inhibition of cytochrome c oxidase and generation of mitochondrial reactive oxygen species. *Faseb J* 21: 1099-1106, 2007.

401 **Legends to figures**

402

403 **Fig. 1.** Effects of exercise training and CO exposure on sarcomere length (SL)
404 shortening and Ca^{2+} handling in cardiomyocytes. A, Representative contraction of
405 intact cardiomyocytes measured by sarcomere shortening at 0.5 Hz. B, Amplitude of
406 sarcomere length shortening. Data are presented as percentage of baseline. C,
407 Representative Ca^{2+} transient during cardiomyocyte excitation-contraction. D,
408 Diastolic intracellular Ca^{2+}. E, Ca^{2+} transient amplitude. F, Ca^{2+} reuptake kinetics
409 (Tau). G, Cardiac expression of SERCA-2a. The GAPDH blot (37KDa) was used as a
410 loading control to normalize SERCA-2a protein expression. Data are presented as
411 mean ± S.E. (n=5 per group, one way ANOVA; §, $p<0.05$ Ctrl-Sed *vs*. CO-Sed, *,
412 $p<0.05$ CO-Sed *vs*. CO-Ex).

413

414

415 **Fig. 2**. Effects of exercise training and CO exposure on myocardial antioxidant
416 enzyme activities. A, Superoxide dismutase (SOD) activity; B, Glutathione peroxidase
417 (GPx) activity; C, Catalase (CAT) activity. Activities are expressed in U/mg of protein.
418 Data are presented as mean ± S.E. (n=5 per group, one way ANOVA; §, $p<0.05$ Ctrl-
419 Sed *vs*. CO-Sed, *, $p<0.05$ CO-Sed *vs*. CO-Ex).

420

421

422 **Fig. 3.** Effects of exercise training and CO exposure on IR-induced cellular death and
423 post-ischemic ventricular fibrillations. A, Representative sections of area at risk and
424 infarct size of rat hearts stained respectively with Evans Blue and triphenyltetrazolium
425 chloride (TTC) after 30 min regional ischemia and 120 min reperfusion from isolated

426 heart experiments in each experimental group. B, Infarct sizes expressed as
427 percentage of area at risk. Data are presented as mean ± S.E. (Ctrl-Sed n=7, CO-
428 Sed n=6, CO-Ex- n=6, one way ANOVA; §, $p<0.05$ Ctrl-Sed vs CO-Sed, *, $p<0.05$
429 CO-Sed vs CO-Ex). C, LDH activity observed in coronary effluents at 5 min of
430 reperfusion and used as a marker of cell death. Data are presented as mean ±
431 S.E.(Ctrl-Sed n=9, CO-Sed n=7, CO-Ex n=10, one way ANOVA; §, $p<0.05$ Ctrl-Sed
432 *vs*. CO-Sed, *, $p<0.05$ CO-Sed *vs*. CO-Ex). D, Representative plot of ventricular
433 fibrillation (VF). E, Incidence of ventricular fibrillations occurring during the 5 first
434 minutes of reperfusion. Data are presented as percentage of rats per experimental
435 group. (Ctrl-Sed n=6, CO-Sed n=8, CO-Ex n=9, non parametric Yates' chi square
436 test; §, $p<0.05$ Ctrl-Sed *vs.* CO-Sed, *, $p<0.05$ CO-Sed *vs*. CO-Ex).
437

Fig. 1

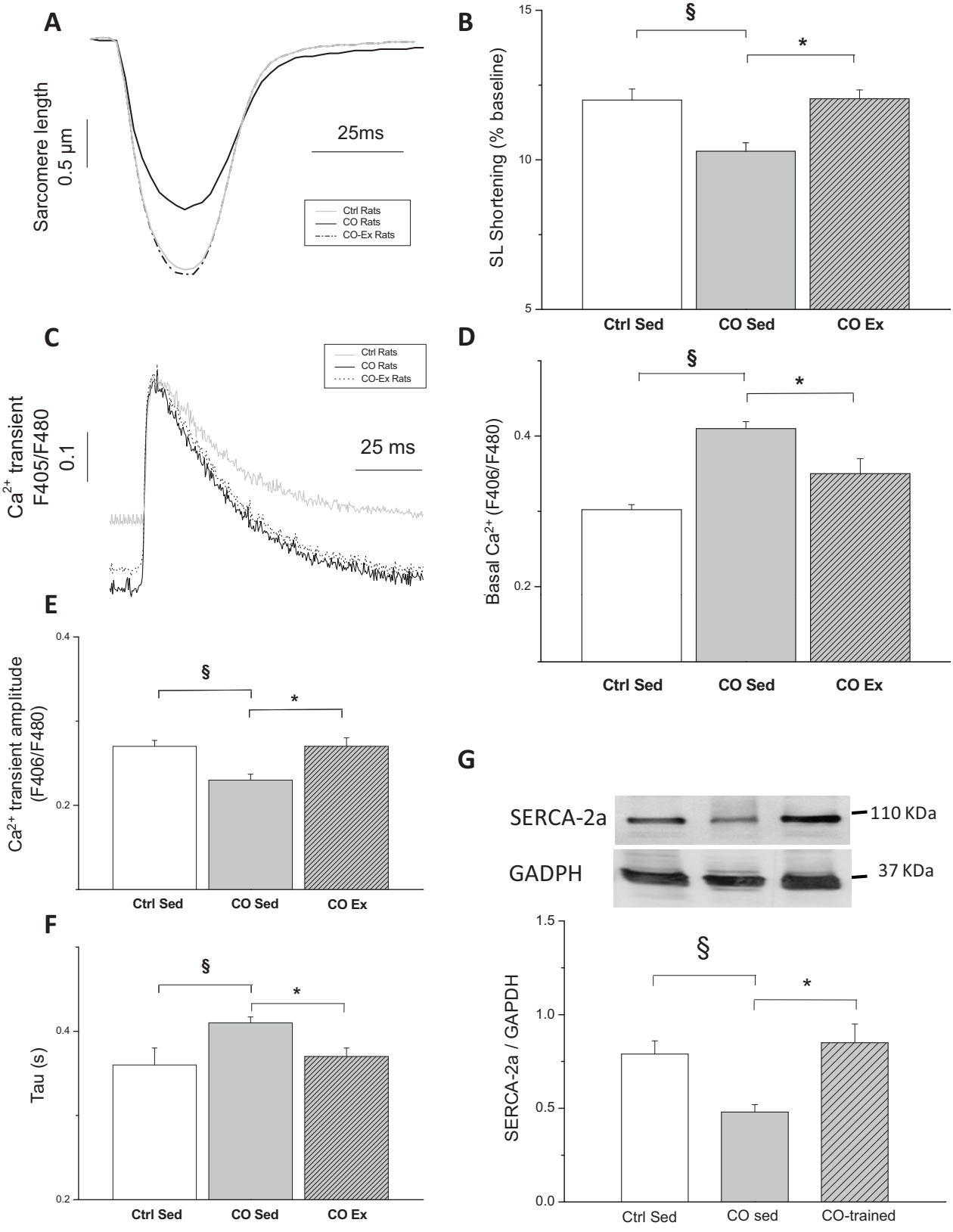
A
Sarcomere length
0.5 µm
25ms
Ctrl Rats
CO Rats
CO-Ex Rats
B
SL Shortening (% baseline)
15
10
5
§
*
Ctrl Sed
CO Sed
CO Ex
C
Ca2+ transient
F405/F480
0.1
25 ms
Ctrl Rats
CO Rats
CO-Ex Rats
D
Basal Ca2+ (F406/F480)
0.4
0.2
§
*
Ctrl Sed
CO Sed
CO Ex
E
Ca2+ transient amplitude
(F406/F480)
0.4
0.2
§
*
Ctrl Sed
CO Sed
CO Ex
F
Tau (s)
0.4
0.2
§
*
Ctrl Sed
CO Sed
CO Ex
G
SERCA-2a
110 KDa
GADPH
37 KDa
SERCA-2a / GAPDH
1.5
1.0
0.5
0.0
§
*
Ctrl Sed
CO sed
CO-trained

Fig. 2

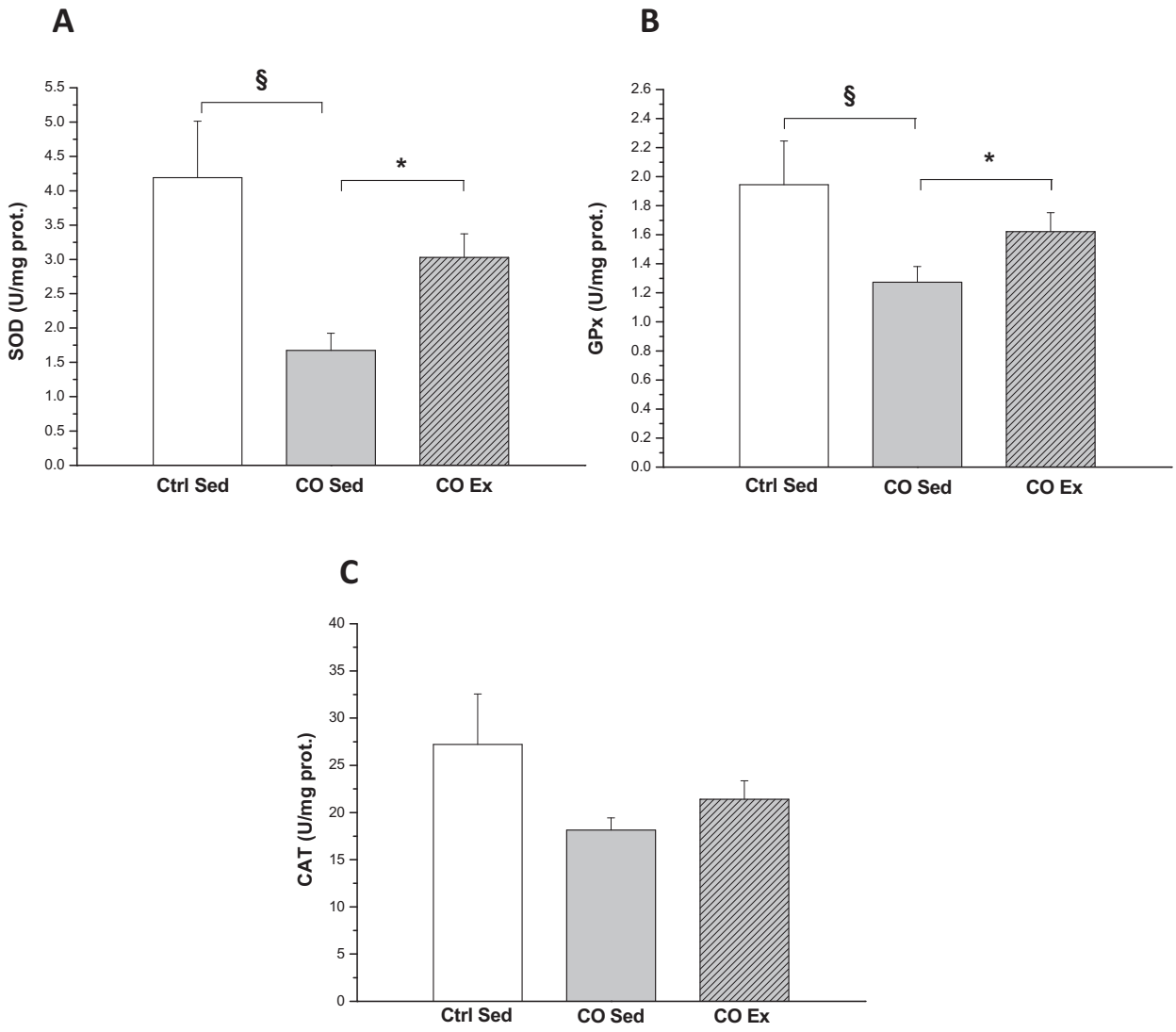
A
§
*
SOD (U/mg prot.)
5.5
5.0
4.5
4.0
3.5
3.0
2.5
2.0
1.5
1.0
0.5
0.0
Ctrl Sed
CO Sed
CO Ex
B
§
*
GPx (U/mg prot.)
2.6
2.4
2.2
2.0
1.8
1.6
1.4
1.2
1.0
0.8
0.6
0.4
0.2
0.0
Ctrl Sed
CO Sed
CO Ex
C
CAT (U/mg prot.)
40
35
30
25
20
15
10
5
0
Ctrl Sed
CO Sed
CO Ex

Fig. 3

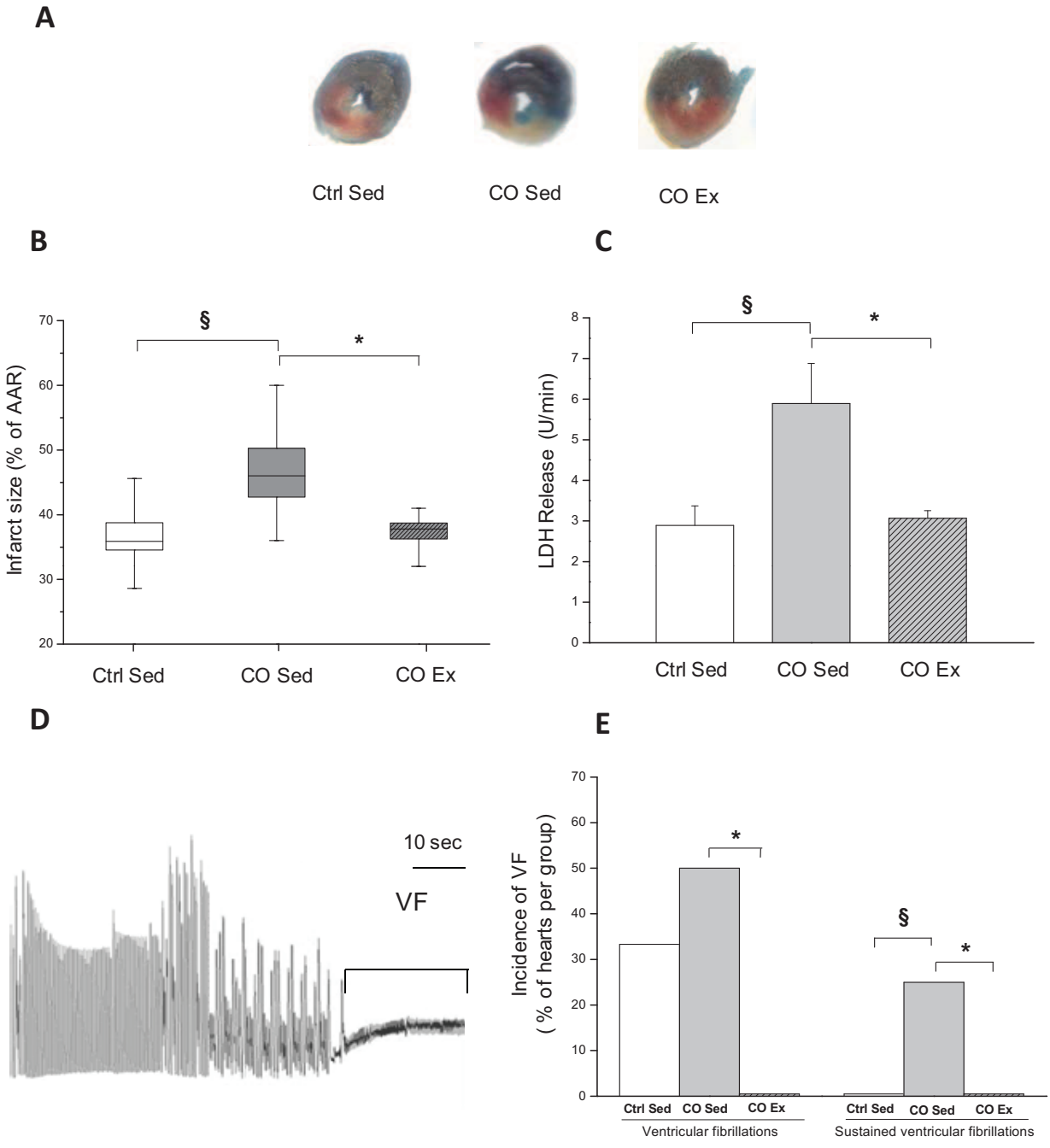
A
Ctrl Sed
CO Sed
CO Ex
B
Infarct size (% of AAR)
§
*
Ctrl Sed
CO Sed
CO Ex
C
LDH Release (U/min)
§
*
Ctrl Sed
CO Sed
CO Ex
D
10 sec
VF
E
Incidence of VF
(% of hearts per group)
*
§
*
Ctrl Sed
CO Sed
CO Ex
Ventricular fibrillations
Ctrl Sed
CO Sed
CO Ex
Sustained ventricular fibrillations

Bibliographie

1. Capewell SB, Ford EA. Cardiovascular risk factor trends and potential for reducing coronary heart disease mortality in the United States of America. Publication OMS *Bull World Health Organ* 2010;88:120–130
2. Knisley SB, Baynham TC. Line stimulation parallel to myofibers enhances regional uniformity of transmembrane voltage changes in rabbit hearts. *Circ Res.* 1997;81(2):229-241.
3. Frolkis JP, Pothier CE, Blackstone EH, et al. Frequent ventricular ectopy after exercise as a predictor of death. *N Engl J Med.* 2003;348(9):781-790.
4. Feigl EO. Coronary physiology. *Physiol Rev.* 1983;63(1):1-205.
5. Ingwall JS. Energy metabolism in heart failure and remodelling. *Cardiovasc Res.* 2009;81(3):412-419.
6. Ingwall JS, Weiss RG. Is the failing heart energy starved? On using chemical energy to support cardiac function. *Circ Res.* 2004;95(2):135-145.
7. Bremer J. Carnitine--metabolism and functions. *Physiol Rev.* 1983;63(4):1420-1480.
8. Bers DM, Ziolo MT. When is cAMP not cAMP? Effects of compartmentalization. *Circ Res.* 2001;89(5):373-375.
9. Sommer JR. Ultrastructural considerations concerning cardiac muscle. *J Mol Cell Cardiol.* 1982;14 Suppl 3:77-83.
10. Gordon AM, Homsher E, Regnier M. Regulation of contraction in striated muscle. *Physiol Rev.* 2000;80(2):853-924.
11. Gregorio CC, Fowler VM. Mechanisms of thin filament assembly in embryonic chick cardiac myocytes: tropomodulin requires tropomyosin for assembly. *J Cell Biol.* 1995;129(3):683-695.
12. Maruyama K. Connectin, an elastic protein from myofibrils. *J Biochem.* 1976;80(2):405-407.
13. Labeit S, Kolmerer B. Titins: giant proteins in charge of muscle ultrastructure and elasticity. *Science.* 1995;270(5234):293-296.
14. Granzier H, Labeit S. Cardiac titin: an adjustable multi-functional spring. *J Physiol.* 2002;541(Pt 2):335-342.
15. Bers DM. Cardiac excitation-contraction coupling. *Nature.* 2002;415(6868):198-205.
16. Schaub MC, Hefti MA, Zaugg M. Integration of calcium with the signaling network in cardiac myocytes. *J Mol Cell Cardiol.* 2006;41(2):183-214.
17. Solaro RJ, Van Eyk J. Altered interactions among thin filament proteins modulate cardiac function. *J Mol Cell Cardiol.* 1996;28(2):217-230.
18. Fuchs F, Wang YP. Length-dependence of actin-myosin interaction in skinned cardiac muscle fibers in rigor. *J Mol Cell Cardiol.* 1997;29(12):3267-3274.
19. Gunning P, O'Neill G, Hardeman E. Tropomyosin-based regulation of the actin cytoskeleton in time and space. *Physiol Rev.* 2008;88(1):1-35.
20. de Tombe PP. Cardiac myofilaments: mechanics and regulation. *J Biomech.* 2003;36(5):721-730.
21. Cazorla O, Szilagyi S, Le Guennec JY, et al. Transmural stretch-dependent regulation of contractile properties in rat heart and its alteration after myocardial infarction. *Faseb J.* 2005;19(1):88-90.
22. Contreras L, Gomez-Puertas P, Iijima M, et al. Ca2+ Activation kinetics of the two aspartate-glutamate mitochondrial carriers, aralar and citrin: role in the heart malate-aspartate NADH shuttle. *J Biol Chem.* 2007;282(10):7098-7106.
23. McCormack JG, Halestrap AP, Denton RM. Role of calcium ions in regulation of mammalian intramitochondrial metabolism. *Physiol Rev.* 1990;70(2):391-425.
24. Territo PR, Mootha VK, French SA, et al. Ca(2+) activation of heart mitochondrial oxidative phosphorylation: role of the F(0)/F(1)-ATPase. *Am J Physiol Cell Physiol.* 2000;278(2):C423-435.

25. Moreno SN, Mason RP, Docampo R. Ca2+ and Mg2+-enhanced reduction of arsenazo III to its anion free radical metabolite and generation of superoxide anion by an outer mitochondrial membrane azoreductase. *J Biol Chem.* 1984;259(23):14609-14616.

26. Denton RM, McCormack JG. Ca2+ as a second messenger within mitochondria of the heart and other tissues. *Annu Rev Physiol.* 1990;52:451-466.

27. Balaban RS. Cardiac energy metabolism homeostasis: role of cytosolic calcium. *J Mol Cell Cardiol.* 2002;34(10):1259-1271.

28. Hansford RG, Castro F. Role of Ca2+ in pyruvate dehydrogenase interconversion in brain mitochondria and synaptosomes. *Biochem J.* 1985;227(1):129-136.

29. Brandes R, Bers DM. Simultaneous measurements of mitochondrial NADH and Ca(2+) during increased work in intact rat heart trabeculae. *Biophys J.* 2002;83(2):587-604.

30. Liu T, O'Rourke B. Regulation of mitochondrial Ca2+ and its effects on energetics and redox balance in normal and failing heart. *J Bioenerg Biomembr.* 2009;41(2):127-132.

31. Liu X, Kim CN, Yang J, et al. Induction of apoptotic program in cell-free extracts: requirement for dATP and cytochrome c. *Cell.* 1996;86(1):147-157.

32. Newmeyer DD, Farschon DM, Reed JC. Cell-free apoptosis in Xenopus egg extracts: inhibition by Bcl-2 and requirement for an organelle fraction enriched in mitochondria. *Cell.* 1994;79(2):353-364.

33. Liu T, O'Rourke B. Enhancing mitochondrial Ca2+ uptake in myocytes from failing hearts restores energy supply and demand matching. *Circ Res.* 2008;103(3):279-288.

34. Xu W, Liu Y, Wang S, et al. Cytoprotective role of Ca2+- activated K+ channels in the cardiac inner mitochondrial membrane. *Science.* 2002;298(5595):1029-1033.

35. Maack C, Cortassa S, Aon MA, et al. Elevated cytosolic Na+ decreases mitochondrial Ca2+ uptake during excitation-contraction coupling and impairs energetic adaptation in cardiac myocytes. *Circ Res.* 2006;99(2):172-182.

36. O'Rourke B, Blatter LA. Mitochondrial Ca2+ uptake: tortoise or hare? *J Mol Cell Cardiol.* 2009;46(6):767-774.

37. Gunter TE, Yule DI, Gunter KK, et al. Calcium and mitochondria. *FEBS Lett.* 2004;567(1):96-102.

38. Pacher P, Szabo C. Role of poly(ADP-ribose) polymerase 1 (PARP-1) in cardiovascular diseases: the therapeutic potential of PARP inhibitors. *Cardiovasc Drug Rev.* 2007;25(3):235-260.

39. McCord JM. Oxygen-derived free radicals in postischemic tissue injury. *N Engl J Med.* 1985;312(3):159-163.

40. Halliwell B, Gutteridge JM. Role of free radicals and catalytic metal ions in human disease: an overview. *Methods Enzymol.* 1990;186:1-85.

41. Dhaunsi GS, Gulati S, Singh AK, et al. Demonstration of Cu-Zn superoxide dismutase in rat liver peroxisomes. Biochemical and immunochemical evidence. *J Biol Chem.* 1992;267(10):6870-6873.

42. Kirkman HN, Gaetani GF. Mammalian catalase: a venerable enzyme with new mysteries. *Trends Biochem Sci.* 2007;32(1):44-50.

43. Brigelius-Flohe R. Tissue-specific functions of individual glutathione peroxidases. *Free Radic Biol Med.* 1999;27(9-10):951-965.

44. Liu H, Colavitti R, Rovira, II, et al. Redox-dependent transcriptional regulation. *Circ Res.* 2005;97(10):967-974.

45. Reid MB. Nitric oxide, reactive oxygen species, and skeletal muscle contraction. *Med Sci Sports Exerc.* 2001;33(3):371-376.

46. Pitkanen S, Robinson BH. Mitochondrial complex I deficiency leads to increased production of superoxide radicals and induction of superoxide dismutase. *J Clin Invest.* 1996;98(2):345-351.

47. Luo X, Pitkanen S, Kassovska-Bratinova S, et al. Excessive formation of hydroxyl radicals and aldehydic lipid peroxidation products in cultured skin fibroblasts from patients with complex I deficiency. *J Clin Invest.* 1997;99(12):2877-2882.

48. Ide T, Tsutsui H, Kinugawa S, et al. Mitochondrial electron transport complex I is a potential source of oxygen free radicals in the failing myocardium. *Circ Res.* 1999;85(4):357-363.

49. Bogaert J, Rademakers FE. Regional nonuniformity of normal adult human left ventricle. *Am J Physiol Heart Circ Physiol.* 2001;280(2):H610-620.

50. Mou YA, Reboul C, Andre L, et al. Late exercise training improves non-uniformity of transmural myocardial function in rats with ischaemic heart failure. *Cardiovasc Res.* 2009;81(3):555-564.

51. Dilly KW, Rossow CF, Votaw VS, et al. Mechanisms underlying variations in excitation-contraction coupling across the mouse left ventricular free wall. *J Physiol.* 2006;572(Pt 1):227-241.

52. Ashikaga H, Coppola BA, Hopenfeld B, et al. Transmural dispersion of myofiber mechanics: implications for electrical heterogeneity in vivo. *J Am Coll Cardiol.* 2007;49(8):909-916.

53. Weiss HR, Neubauer JA, Lipp JA, et al. Quantitative determination of regional oxygen consumption in the dog heart. *Circ Res.* 1978;42(3):394-401.

54. Kainulainen H, Komulainen J, Leinonen A, et al. Regional differences of substrate oxidation capacity in rat hearts: effects of extra load and endurance training. *Basic Res Cardiol.* 1990;85(6):630-639.

55. Stewart S, MacIntyre K, Hole DJ, et al. More 'malignant' than cancer? Five-year survival following a first admission for heart failure. *Eur J Heart Fail.* 2001;3(3):315-322.

56. Hunt SA, Baker DW, Chin MH, et al. ACC/AHA guidelines for the evaluation and management of chronic heart failure in the adult: executive summary. A report of the American College of Cardiology/American Heart Association Task Force on Practice Guidelines (Committee to revise the 1995 Guidelines for the Evaluation and Management of Heart Failure). *J Am Coll Cardiol.* 2001;38(7):2101-2113.

57. Hunt SA. ACC/AHA 2005 guideline update for the diagnosis and management of chronic heart failure in the adult: a report of the American College of Cardiology/American Heart Association Task Force on Practice Guidelines (Writing Committee to Update the 2001 Guidelines for the Evaluation and Management of Heart Failure). *J Am Coll Cardiol.* 2005;46(6):e1-82.

58. Delahaye F, de Gevigney G, Gaillard S, et al. [Epidemiology and economic impact of heart failure in France]. *Arch Mal Coeur Vaiss.* 1998;91(11):1307-1314.

59. Swynghedauw B. Molecular mechanisms of myocardial remodeling. *Physiol Rev.* 1999;79(1):215-262.

60. Cranefield PF, Aronson RS. Torsades de pointes and early afterdepolarizations. *Cardiovasc Drugs Ther.* 1991;5(2):531-537.

61. Tomaselli GF, Beuckelmann DJ, Calkins HG, et al. Sudden cardiac death in heart failure. The role of abnormal repolarization. *Circulation.* 1994;90(5):2534-2539.

62. Janse MJ. Electrophysiological changes in heart failure and their relationship to arrhythmogenesis. *Cardiovasc Res.* 2004;61(2):208-217.

63. Richard S, Leclercq F, Lemaire S, et al. Ca2+ currents in compensated hypertrophy and heart failure. *Cardiovasc Res.* 1998;37(2):300-311.

64. Aimond F, Beck L, Gautier P, et al. Cellular and in vivo electrophysiological effects of dronedarone in normal and postmyocardial infarcted rats. *J Pharmacol Exp Ther.* 2000;292(1):415-424.

65. Qin D, Zhang ZH, Caref EB, et al. Cellular and ionic basis of arrhythmias in postinfarction remodeled ventricular myocardium. *Circ Res.* 1996;79(3):461-473.

66. Furukawa T, Bassett AL, Furukawa N, et al. The ionic mechanism of reperfusion-induced early afterdepolarizations in feline left ventricular hypertrophy. *J Clin Invest.* 1993;91(4):1521-1531.

67. Lehnart SE, Wehrens XH, Marks AR. Defective ryanodine receptor interdomain interactions may contribute to intracellular Ca2+ leak: a novel therapeutic target in heart failure. *Circulation.* 2005;111(25):3342-3346.

68. Yano M, Ikeda Y, Matsuzaki M. Altered intracellular Ca2+ handling in heart failure. *J Clin Invest.* 2005;115(3):556-564.

69. Marx SO, Reiken S, Hisamatsu Y, et al. PKA phosphorylation dissociates FKBP12.6 from the calcium release channel (ryanodine receptor): defective regulation in failing hearts. *Cell.* 2000;101(4):365-376.

70. Terentyev D, Gyorke I, Belevych AE, et al. Redox modification of ryanodine receptors contributes to sarcoplasmic reticulum Ca2+ leak in chronic heart failure. *Circ Res.* 2008;103(12):1466-1472.

71. Yano M, Okuda S, Oda T, et al. Correction of defective interdomain interaction within ryanodine receptor by antioxidant is a new therapeutic strategy against heart failure. *Circulation.* 2005;112(23):3633-3643.

72. Zissimopoulos S, Docrat N, Lai FA. Redox sensitivity of the ryanodine receptor interaction with FK506-binding protein. *J Biol Chem.* 2007;282(10):6976-6983.

73. Marston SB, de Tombe PP. Troponin phosphorylation and myofilament Ca2+-sensitivity in heart failure: increased or decreased? *J Mol Cell Cardiol.* 2008;45(5):603-607.

74. Liggett SB. Beta-adrenergic receptors in the failing heart: the good, the bad, and the unknown. *J Clin Invest.* 2001;107(8):947-948.

75. He ZH, Bottinelli R, Pellegrino MA, et al. ATP consumption and efficiency of human single muscle fibers with different myosin isoform composition. *Biophys J.* 2000;79(2):945-961.

76. Javadpour MM, Tardiff JC, Pinz I, et al. Decreased energetics in murine hearts bearing the R92Q mutation in cardiac troponin T. *J Clin Invest.* 2003;112(5):768-775.

77. Spindler M, Saupe KW, Christe ME, et al. Diastolic dysfunction and altered energetics in the alphaMHC403/+ mouse model of familial hypertrophic cardiomyopathy. *J Clin Invest.* 1998;101(8):1775-1783.

78. Ertz-Berger BR, He H, Dowell C, et al. Changes in the chemical and dynamic properties of cardiac troponin T cause discrete cardiomyopathies in transgenic mice. *Proc Natl Acad Sci U S A.* 2005;102(50):18219-18224.

79. Maytum R, Geeves MA, Lehrer SS. A modulatory role for the troponin T tail domain in thin filament regulation. *J Biol Chem.* 2002;277(33):29774-29780.

80. Crilley JG, Boehm EA, Blair E, et al. Hypertrophic cardiomyopathy due to sarcomeric gene mutations is characterized by impaired energy metabolism irrespective of the degree of hypertrophy. *J Am Coll Cardiol.* 2003;41(10):1776-1782.

81. Tian R, Christe ME, Spindler M, et al. Role of MgADP in the development of diastolic dysfunction in the intact beating rat heart. *J Clin Invest.* 1997;99(4):745-751.

82. Neubauer S, Horn M, Cramer M, et al. Myocardial phosphocreatine-to-ATP ratio is a predictor of mortality in patients with dilated cardiomyopathy. *Circulation.* 1997;96(7):2190-2196.

83. Murakami Y, Zhang Y, Cho YK, et al. Myocardial oxygenation during high work states in hearts with postinfarction remodeling. *Circulation.* 1999;99(7):942-948.

84. Sanbe A, Tanonaka K, Kobayasi R, et al. Effects of long-term therapy with ACE inhibitors, captopril, enalapril and trandolapril, on myocardial energy metabolism in rats with heart failure following myocardial infarction. *J Mol Cell Cardiol.* 1995;27(10):2209-2222.

85. Ide T, Tsutsui H, Hayashidani S, et al. Mitochondrial DNA damage and dysfunction associated with oxidative stress in failing hearts after myocardial infarction. *Circ Res.* 2001;88(5):529-535.

86. Scheubel RJ, Tostlebe M, Simm A, et al. Dysfunction of mitochondrial respiratory chain complex I in human failing myocardium is not due to disturbed mitochondrial gene expression. *J Am Coll Cardiol.* 2002;40(12):2174-2181.

87. Hill MF, Singal PK. Right and left myocardial antioxidant responses during heart failure subsequent to myocardial infarction. *Circulation.* 1997;96(7):2414-2420.
88. Dai L, Brookes PS, Darley-Usmar VM, et al. Bioenergetics in cardiac hypertrophy: mitochondrial respiration as a pathological target of NO*. *Am J Physiol Heart Circ Physiol.* 2001;281(6):H2261-2269.
89. van der Vusse GJ, Glatz JF, Stam HC, et al. Fatty acid homeostasis in the normoxic and ischemic heart. *Physiol Rev.* 1992;72(4):881-940.
90. Remondino A, Rosenblatt-Velin N, Montessuit C, et al. Altered expression of proteins of metabolic regulation during remodeling of the left ventricle after myocardial infarction. *J Mol Cell Cardiol.* 2000;32(11):2025-2034.
91. Allard MF, Emanuel PG, Russell JA, et al. Preischemic glycogen reduction or glycolytic inhibition improves postischemic recovery of hypertrophied rat hearts. *Am J Physiol.* 1994;267(1 Pt 2):H66-74.
92. Hotchkiss RS, Karl IE. Reevaluation of the role of cellular hypoxia and bioenergetic failure in sepsis. *Jama.* 1992;267(11):1503-1510.
93. van den Heuvel AF, van Veldhuisen DJ, van der Wall EE, et al. Regional myocardial blood flow reserve impairment and metabolic changes suggesting myocardial ischemia in patients with idiopathic dilated cardiomyopathy. *J Am Coll Cardiol.* 2000;35(1):19-28.
94. Karim SM, Rhee AY, Given AM, et al. Vascular reactivity in heart failure: role of myosin light chain phosphatase. *Circ Res.* 2004;95(6):612-618.
95. Hajri T, Ibrahimi A, Coburn CT, et al. Defective fatty acid uptake in the spontaneously hypertensive rat is a primary determinant of altered glucose metabolism, hyperinsulinemia, and myocardial hypertrophy. *J Biol Chem.* 2001;276(26):23661-23666.
96. Peters A, Liu E, Verrier RL, et al. Air pollution and incidence of cardiac arrhythmia. *Epidemiology.* 2000;11(1):11-17.
97. Peters A, Dockery DW, Muller JE, et al. Increased particulate air pollution and the triggering of myocardial infarction. *Circulation.* 2001;103(23):2810-2815.
98. von Klot S, Peters A, Aalto P, et al. Ambient air pollution is associated with increased risk of hospital cardiac readmissions of myocardial infarction survivors in five European cities. *Circulation.* 2005;112(20):3073-3079.
99. Peel JL, Metzger KB, Klein M, et al. Ambient air pollution and cardiovascular emergency department visits in potentially sensitive groups. *Am J Epidemiol.* 2007;165(6):625-633.
100. Zanobetti A, Schwartz J. Particulate air pollution, progression, and survival after myocardial infarction. *Environ Health Perspect.* 2007;115(5):769-775.
101. Wellenius GA, Batalha JR, Diaz EA, et al. Cardiac effects of carbon monoxide and ambient particles in a rat model of myocardial infarction. *Toxicol Sci.* 2004;80(2):367-376.
102. Henry CR, Satran D, Lindgren B, et al. Myocardial injury and long-term mortality following moderate to severe carbon monoxide poisoning. *Jama.* 2006;295(4):398-402.
103. Brook RD, Franklin B, Cascio W, et al. Air pollution and cardiovascular disease: a statement for healthcare professionals from the Expert Panel on Population and Prevention Science of the American Heart Association. *Circulation.* 2004;109(21):2655-2671.
104. Samoli E, Touloumi G, Schwartz J, et al. Short-term effects of carbon monoxide on mortality: an analysis within the APHEA project. *Environ Health Perspect.* 2007;115(11):1578-1583.
105. Morris RD, Naumova EN, Munasinghe RL. Ambient air pollution and hospitalization for congestive heart failure among elderly people in seven large US cities. *Am J Public Health.* 1995;85(10):1361-1365.
106. Dales R. Ambient carbon monoxide may influence heart rate variability in subjects with coronary artery disease. *J Occup Environ Med.* 2004;46(12):1217-1221.
107. Mirza A, Eder V, Rochefort GY, et al. CO inhalation at dose corresponding to tobacco smoke worsens cardiac remodeling after experimental myocardial infarction in rats. *Toxicol Sci.* 2005;85(2):976-982.

108. Sheps DS, Herbst MC, Hinderliter AL, et al. Production of arrhythmias by elevated carboxyhemoglobin in patients with coronary artery disease. *Ann Intern Med.* 1990;113(5):343-351.
109. Wright GR, Jewczyk S, Onrot J, et al. Carbon monoxide in the urban atmosphere: hazards to the pedestrian and the street-worker. *Arch Environ Health.* 1975;30(3):123-129.
110. Stern FB, Halperin WE, Hornung RW, et al. Heart disease mortality among bridge and tunnel officers exposed to carbon monoxide. *Am J Epidemiol.* 1988;128(6):1276-1288.
111. Sorhaug S, Steinshamn S, Nilsen OG, et al. Chronic inhalation of carbon monoxide: effects on the respiratory and cardiovascular system at doses corresponding to tobacco smoking. *Toxicology.* 2006;228(2-3):280-290.
112. Gandini C, Castoldi AF, Candura SM, et al. Carbon monoxide cardiotoxicity. *J Toxicol Clin Toxicol.* 2001;39(1):35-44.
113. Ernst A, Zibrak JD. Carbon monoxide poisoning. *N Engl J Med.* 1998;339(22):1603-1608.
114. Piantadosi CA. Carbon monoxide poisoning. *N Engl J Med.* 2002;347(14):1054-1055.
115. Zuckerbraun BS, Chin BY, Bilban M, et al. Carbon monoxide signals via inhibition of cytochrome c oxidase and generation of mitochondrial reactive oxygen species. *Faseb J.* 2007;21(4):1099-1106.
116. Allred EN, Bleecker ER, Chaitman BR, et al. Acute effects of carbon monoxide exposure on individuals with coronary artery disease. *Res Rep Health Eff Inst.* 1989(25):1-79.
117. Weaver LK, Hopkins RO, Elliott G. Carbon monoxide poisoning. *N Engl J Med.* 1999;340(16):1290; author reply 1292.
118. Tenhunen R, Marver HS, Schmid R. Microsomal heme oxygenase. Characterization of the enzyme. *J Biol Chem.* 1969;244(23):6388-6394.
119. Doherty S. Carbon monoxide poisoning. *J Accid Emerg Med.* 2000;17(2):154.
120. Rudra CB, Williams MA, Sheppard L, et al. Relation of whole blood carboxyhemoglobin concentration to ambient carbon monoxide exposure estimated using regression. *Am J Epidemiol.*171(8):942-951.
121. Kardinaal AF, Aro A, Kark JD, et al. Association between beta-carotene and acute myocardial infarction depends on polyunsaturated fatty acid status. The EURAMIC Study. European Study on Antioxidants, Myocardial Infarction, and Cancer of the Breast. *Arterioscler Thromb Vasc Biol.* 1995;15(6):726-732.
122. Khaw KT, Bingham S, Welch A, et al. Relation between plasma ascorbic acid and mortality in men and women in EPIC-Norfolk prospective study: a prospective population study. European Prospective Investigation into Cancer and Nutrition. *Lancet.* 2001;357(9257):657-663.
123. Kardinaal AF, Kok FJ, Ringstad J, et al. Antioxidants in adipose tissue and risk of myocardial infarction: the EURAMIC Study. *Lancet.* 1993;342(8884):1379-1384.
124. Steinberg D, Witztum JL. Is the oxidative modification hypothesis relevant to human atherosclerosis? Do the antioxidant trials conducted to date refute the hypothesis? *Circulation.* 2002;105(17):2107-2111.
125. Bourraindeloup M, Adamy C, Candiani G, et al. N-acetylcysteine treatment normalizes serum tumor necrosis factor-alpha level and hinders the progression of cardiac injury in hypertensive rats. *Circulation.* 2004;110(14):2003-2009.
126. George J, Carr E, Davies J, et al. High-dose allopurinol improves endothelial function by profoundly reducing vascular oxidative stress and not by lowering uric acid. *Circulation.* 2006;114(23):2508-2516.
127. Cailleret M, Amadou A, Andrieu-Abadie N, et al. N-acetylcysteine prevents the deleterious effect of tumor necrosis factor-(alpha) on calcium transients and contraction in adult rat cardiomyocytes. *Circulation.* 2004;109(3):406-411.
128. Belardinelli R, Georgiou D, Scocco V, et al. Low intensity exercise training in patients with chronic heart failure. *J Am Coll Cardiol.* 1995;26(4):975-982.

129. Wilson JR, Groves J, Rayos G. Circulatory status and response to cardiac rehabilitation in patients with heart failure. *Circulation.* 1996;94(7):1567-1572.
130. Hambrecht R, Gielen S, Linke A, et al. Effects of exercise training on left ventricular function and peripheral resistance in patients with chronic heart failure: A randomized trial. *Jama.* 2000;283(23):3095-3101.
131. Kemi OJ, Haram PM, Wisloff U, et al. Aerobic fitness is associated with cardiomyocyte contractile capacity and endothelial function in exercise training and detraining. *Circulation.* 2004;109(23):2897-2904.
132. Wisloff U, Loennechen JP, Currie S, et al. Aerobic exercise reduces cardiomyocyte hypertrophy and increases contractility, Ca2+ sensitivity and SERCA-2 in rat after myocardial infarction. *Cardiovasc Res.* 2002;54(1):162-174.
133. Wisloff U, Stoylen A, Loennechen JP, et al. Superior cardiovascular effect of aerobic interval training versus moderate continuous training in heart failure patients: a randomized study. *Circulation.* 2007;115(24):3086-3094.
134. Belardinelli R, Georgiou D, Cianci G, et al. Randomized, controlled trial of long-term moderate exercise training in chronic heart failure: effects on functional capacity, quality of life, and clinical outcome. *Circulation.* 1999;99(9):1173-1182.
135. Flynn KE, Pina IL, Whellan DJ, et al. Effects of exercise training on health status in patients with chronic heart failure: HF-ACTION randomized controlled trial. *Jama.* 2009;301(14):1451-1459.
136. Wisloff U, Najjar SM, Ellingsen O, et al. Cardiovascular risk factors emerge after artificial selection for low aerobic capacity. *Science.* 2005;307(5708):418-420.
137. Opie LH, Knuuti J. The adrenergic-fatty acid load in heart failure. *J Am Coll Cardiol.* 2009;54(18):1637-1646.
138. Finkelstein MM, Jerrett M, Sears MR. Environmental inequality and circulatory disease mortality gradients. *J Epidemiol Community Health.* 2005;59(6):481-487.
139. Picht E, Zima AV, Blatter LA, et al. SparkMaster: automated calcium spark analysis with ImageJ. *Am J Physiol Cell Physiol.* 2007;293(3):C1073-1081.
140. Wharton DC. Purification of electron-transfer components from Pseudomonas. *Methods Enzymol.* 1978;53:646-661.
141. Beers RF, Jr., Sizer IW. A spectrophotometric method for measuring the breakdown of hydrogen peroxide by catalase. *J Biol Chem.* 1952;195(1):133-140.
142. Marklund S. Spectrophotometric study of spontaneous disproportionation of superoxide anion radical and sensitive direct assay for superoxide dismutase. *J Biol Chem.* 1976;251(23):7504-7507.
143. Cohn JN, Archibald DG, Ziesche S, et al. Effect of vasodilator therapy on mortality in chronic congestive heart failure. Results of a Veterans Administration Cooperative Study. *N Engl J Med.* 1986;314(24):1547-1552.
144. Wehrens XH, Lehnart SE, Huang F, et al. FKBP12.6 deficiency and defective calcium release channel (ryanodine receptor) function linked to exercise-induced sudden cardiac death. *Cell.* 2003;113(7):829-840.
145. Farr MA, Basson CT. Sparking the failing heart. *N Engl J Med.* 2004;351(2):185-187.
146. de Lamirande E, O'Flaherty C. Sperm activation: role of reactive oxygen species and kinases. *Biochim Biophys Acta.* 2008;1784(1):106-115.
147. Andre L, Boissiere J, Reboul C, et al. Carbon Monoxide Pollution Promotes Cardiac Remodeling and Ventricular Arrhythmia in Healthy Rats. *Am J Respir Crit Care Med.* 2009.
148. Cazorla O, Ait Mou Y, Goret L, et al. Effects of high-altitude exercise training on contractile function of rat skinned cardiomyocyte. *Cardiovasc Res.* 2006;71(4):652-660.
149. Cohn JN, Levine TB, Olivari MT, et al. Plasma norepinephrine as a guide to prognosis in patients with chronic congestive heart failure. *N Engl J Med.* 1984;311(13):819-823.

150. Stolen KQ, Kemppainen J, Ukkonen H, et al. Exercise training improves biventricular oxidative metabolism and left ventricular efficiency in patients with dilated cardiomyopathy. *J Am Coll Cardiol.* 2003;41(3):460-467.
151. Roveda F, Middlekauff HR, Rondon MU, et al. The effects of exercise training on sympathetic neural activation in advanced heart failure: a randomized controlled trial. *J Am Coll Cardiol.* 2003;42(5):854-860.
152. Leosco D, Rengo G, Iaccarino G, et al. Exercise promotes angiogenesis and improves beta-adrenergic receptor signalling in the post-ischaemic failing rat heart. *Cardiovasc Res.* 2008;78(2):385-394.
153. Nishiyama Y, Maeda H, Tanaka M, et al. Effect of physical training on corrected QT dispersion in patients with nonischemic heart failure. *Circ J.* 2004;68(10):946-949.
154. Deligiannis A. Exercise rehabilitation and skeletal muscle benefits in hemodialysis patients. *Clin Nephrol.* 2004;61 Suppl 1:S46-50.
155. Ait Mou Y, Reboul C, Andre L, et al. Late exercise training improves non-uniformity of transmural myocardial function in rats with ischaemic heart failure. *Cardiovasc Res.* 2009;81(3):555-564.
156. Fauconnier J, Andersson DC, Zhang SJ, et al. Effects of palmitate on Ca(2+) handling in adult control and ob/ob cardiomyocytes: impact of mitochondrial reactive oxygen species. *Diabetes.* 2007;56(4):1136-1142.
157. Bradford MM. A rapid and sensitive method for the quantitation of microgram quantities of protein utilizing the principle of protein-dye binding. *Anal Biochem.* 1976;72:248-254.
158. Srere PA. An eclectic view of metabolic regulation: control of citrate synthase activity. *Adv Enzyme Regul.* 1970;9:221-233.
159. Janssen AJ, Trijbels FJ, Sengers RC, et al. Spectrophotometric assay for complex I of the respiratory chain in tissue samples and cultured fibroblasts. *Clin Chem.* 2007;53(4):729-734.
160. Akar FG, Aon MA, Tomaselli GF, et al. The mitochondrial origin of postischemic arrhythmias. *J Clin Invest.* 2005;115(12):3527-3535.
161. Stanley WC, Recchia FA, Lopaschuk GD. Myocardial substrate metabolism in the normal and failing heart. *Physiol Rev.* 2005;85(3):1093-1129.
162. Hare JM, Mangal B, Brown J, et al. Impact of oxypurinol in patients with symptomatic heart failure. Results of the OPT-CHF study. *J Am Coll Cardiol.* 2008;51(24):2301-2309.
163. Parodi O, De Maria R, Oltrona L, et al. Myocardial blood flow distribution in patients with ischemic heart disease or dilated cardiomyopathy undergoing heart transplantation. *Circulation.* 1993;88(2):509-522.
164. Bers DM. Calcium cycling and signaling in cardiac myocytes. *Annu Rev Physiol.* 2008;70:23-49.
165. Xie LH, Chen F, Karagueuzian HS, et al. Oxidative-stress-induced afterdepolarizations and calmodulin kinase II signaling. *Circ Res.* 2009;104(1):79-86.
166. Zima AV, Blatter LA. Redox regulation of cardiac calcium channels and transporters. *Cardiovasc Res.* 2006;71(2):310-321.
167. Hove-Madsen L, Llach A, Bayes-Genis A, et al. Atrial fibrillation is associated with increased spontaneous calcium release from the sarcoplasmic reticulum in human atrial myocytes. *Circulation.* 2004;110(11):1358-1363.
168. Ali A, Malik FS, Dinshaw H, et al. Reduction in QT dispersion with rheolytic thrombectomy in acute myocardial infarction: evidence of electrial stability with reperfusion therapy. *Catheter Cardiovasc Interv.* 2001;52(1):56-58.
169. Neubauer S. The failing heart--an engine out of fuel. *N Engl J Med.* 2007;356(11):1140-1151.
170. Gielen S, Hambrecht R. Effects of exercise training on vascular function and myocardial perfusion. *Cardiol Clin.* 2001;19(3):357-368.
171. Green DR, Reed JC. Mitochondria and apoptosis. *Science.* 1998;281(5381):1309-1312.
172. Belardinelli R. Exercise training in chronic heart failure: how to harmonize oxidative stress, sympathetic outflow, and angiotensin II. *Circulation.* 2007;115(24):3042-3044.

173. Ennezat PV, Malendowicz SL, Testa M, et al. Physical training in patients with chronic heart failure enhances the expression of genes encoding antioxidative enzymes. *J Am Coll Cardiol.* 2001;38(1):194-198.
174. Giordano FJ. Oxygen, oxidative stress, hypoxia, and heart failure. *J Clin Invest.* 2005;115(3):500-508.
175. Bolli R, Marban E. Molecular and cellular mechanisms of myocardial stunning. *Physiol Rev.* 1999;79(2):609-634.
176. Takimoto E, Kass DA. Role of oxidative stress in cardiac hypertrophy and remodeling. *Hypertension.* 2007;49(2):241-248.
177. Ter Keurs HE, Boyden PA. Calcium and arrhythmogenesis. *Physiol Rev.* 2007;87(2):457-506.
178. Yan Y, Liu J, Wei C, et al. Bidirectional regulation of Ca2+ sparks by mitochondria-derived reactive oxygen species in cardiac myocytes. *Cardiovasc Res.* 2008;77(2):432-441.
179. Bellinger AM, Reiken S, Carlson C, et al. Hypernitrosylated ryanodine receptor calcium release channels are leaky in dystrophic muscle. *Nat Med.* 2009;15(3):325-330.
180. O'Connor CM, Whellan DJ, Lee KL, et al. Efficacy and safety of exercise training in patients with chronic heart failure: HF-ACTION randomized controlled trial. *Jama.* 2009;301(14):1439-1450.
181. Fauconnier J, Lacampagne A, Rauzier JM, et al. Ca2+-dependent reduction of IK1 in rat ventricular cells: a novel paradigm for arrhythmia in heart failure? *Cardiovasc Res.* 2005;68(2):204-212.
182. Roman RJ. P-450 metabolites of arachidonic acid in the control of cardiovascular function. *Physiol Rev.* 2002;82(1):131-185.
183. Thom SR, Fisher D, Xu YA, et al. Adaptive responses and apoptosis in endothelial cells exposed to carbon monoxide. *Proc Natl Acad Sci U S A.* 2000;97(3):1305-1310.